Thermochemical gasification of local lignocellulosic biomass via fixed-bed and fluidized-bed reactors

Shiplu Sarker

Thermochemical gasification of local lignocellulosic biomass via fixed-bed and fluidized-bed reactors

Doctoral dissertation
Submitted in partial fulfillment of the requirements for the degree of Doctor of Philosophy (PhD)

Doctoral Dissertation 131

University of Agder
Faculty of Engineering and Science
2016

Doctoral Dissertations at the University of Agder 131

ISSN: 1504-9272
ISBN: 978-82-7117-824-6

Printed by the Printing Office, University of Agder
Kristiansand

To my parents

Life is the art of drawing sufficient conclusions from insufficient premises

-Samuel Butler

Abstract

The government in Norway aims to double the bioenergy use from 14 TWh to 28 TWh between the year 2008 and 2020. This calls for major changes in the current energy practice and an increase in the biomass based energy applications in the total energy mix. One effort to this end is the replacement of existing space heating oil burners with heat from biomass combustion. However, this strategy alone could not be able to adequately meet the target of further bioenergy expansion. Neither will it help in achieving the Kyoto aim of reducing CO_2 emission. So an alternative such as gasification could be a part of the solution. Gasification offers many advantages, but a major concern towards this technology is the logistics. A highly efficient gasification process would mean very little to a technical viability if efficient biomass supply is not guaranteed. Thus maintaining a smooth biomass supply to the conversion plant is important in perspective of which local lignocellulosic biomass could be an interesting option. In terms of the availability of lignocellulosic biomass, Norway is strategically well placed due thanks to its abundant forest reserves. Norway and forest are the two sides of the same coin which makes this country ever attractive in developing and practicing local bioenergy research, which is partly why this study is conducted.

The main objective of the present project was to utilize local forest crops birch, oak and spruce and energy crops like poplar and willow as feedstocks for lab-scale fixed bed downdraft gasification. Further to evaluate the gasification performance interaction with biomass characteristics and process parameters, experimental work consisted of series of gasification tests was optimized over a range of air equivalence ratio (ER) between 0.19 and 0.45. The key results in terms of gas lower heating value (LHV), gas yield, cold gas efficiency (CGE) and carbon conversion efficiency (CCE) indicated that the producer gas obtained from all types of woodchips species gasification exhibited a great potential to be utilized for further downstream applications.

Besides wood, in many places of the world the lion’s share of the biomass is contributed from herbaceous biomass. Hence this research also focused on two

local herbaceous biomasses, alfalfa and wheat straw (in pellets) from Spain and one local herbaceous biomass common reed (in briquettes) from Norway for investigating gasification via two fluidized bed configurations being pilot-scale and lab-scale, and one fixed-bed downdraft gasifier respectively. Pilot-scale 4.7 kg/h air-blown gasification of sole alfalfa pellets was carried out at a variable ER between 0.25 and 0.30. The resulting bed temperature was ca 780 °C and the maximum producer gas lower heating value (LHV) was ca 4.2 MJ/Nm^3 which suits for combined heat and power application. Pilot-scale test also yielded producer gas composition rich in H_2 composition (around 13 % dry basis vol.), indicating the potential of this gas to be utilized for hydrogen production.

In addition to the pilot-scale tests, a series of lab-scale fluidized bed gasification on alfalfa and wheat straw pellets were conducted for a wide range of ER (0.20-0.35) achieved by varying both fuel and air input. The optimized gasification performance attained for the two feedstocks differed in respect to the operational ER with a higher ER (0.35) for alfalfa and a lower ER (0.30) for wheat straw respectively. At the optimum condition, the gas produced from both the feedstocks exhibited a good LHV value above 4.1 MJ/Nm^3 which can be recommended for engine or, turbine application. However, owing to the poor H_2 composition of 4 %, this technology may not suit downstream H_2 production.

The fixed bed gasification on common reed briquettes on the other hand is a very recent addition to the current project which is not fully developed yet. Therefore the preliminary results obtained from a solitary test run were not representative. The measured parameters so far indicated that the gas LHV, bed temperature and ER range of 2.9 MJ/Nm^3, 498 °C and 0.35-0.86 respectively can be achieved.

Last but not the least, a techno-economic modeling considering a producer gas generator in a 100 % renewable energy hybrid plant was performed for a standalone household in Grimstad by using HOMER (a commercial hybrid energy optimization tool). The results showed that producer gas generator together with the other renewable energy options is capable of fulfilling the annual electricity demand of a remote household with a constraint of a producer

gas price less than 0.1$/$Nm^3$. This system also provided environmental gain worth ~22,000 kg/year of CO_2 equivalent savings.

All in all, the influence of diverse local biomass feedstock on diverse gasification techniques is proved to be feasible in aspects of technology, economy and sustainability.

Preface

This thesis work was carried out at the Faculty of Engineering and Science, University of Agder, Grimstad, Norway during the years between 2012 and 2015. At its different phases the contributions and supports from several people were substantial without which this study would never be possible. I gratefully acknowledge all those kind souls.

I would like to express my sincere and heartiest appreciation to my supervisor Prof. Henrik Kofoed Nielsen who from the beginning till the end provided vital supports and guidance to smoothly conduct the scientific work and hence to formulate this thesis. He has been positive and bearing enduring faith on me that helped to keep focused even at the period of hardship. I am deeply indebted to him.

Special thanks will go to the personnel of the Faculty of Engineering and Science, whose involvement was imperative in the course of my career at this department. I gratefully note the head of the department Mr. Rein Terje Thorstensen, financial secretary Mrs. Sissel Stenersen and PhD advisor Mrs. Emma Elizabeth Horneman for taking care of my financial, personal and administrative issues. I also greatly appreciate Dr. Turid Knutsen, Dr. Paul Arentzen, Mr. Steve Schading and Mr. Johan Olav Brakestad for their substantial help in developing technical aspects of this project. I would like to take the opportunity to acknowledge many others who implicitly or, explicitly engaged at various aspects of my work. I would highly appreciate the efforts of the scientific and technical staffs of the Chemical Engineering laboratory of University of Zaragoza (UNIZAR) for providing assistance and to participate into critical discussions. It's a privilege to be a part of a very knowledgeable scientific community at UNIZAR where I endeavored a sojourn for about six months courtesy to BRISK (Biofuel Research Infrastructure for Sharing Knowledge, European Commission 7^{th} framework program) which is also highly acknowledged.

Beyond the academia, I made some good friends whose social engagement would always revitalize my passion for delivering the level best at work. I especially remember and thank my colleagues who I met in the social events such as coffee breaks, lunch breaks, outings etc. These all were the important sources of energy at my work.

Finally, my warmest thanks go to my family whose relentless support and patience gave me the confidence and strength. The encouraging words of my parents, the paradise smile of my daughter (Semantica Sarker) and the unconditional love of my wife Sharmistha Sarker were the wisdoms making my life easy at work. I owe a great deal and no words are enough to express my heartiest gratitude to all of them.

Grimstad, July 2015
Shiplu Sarker

List of publications

The outcome of this PhD study is mainly overviewed by the five international journal publications where the author of this dissertation is the major contributor. The publications are referred to by roman numerals.

I Sarker S, Nielsen HK. Preliminary fixed-bed downdraft gasification of birch woodchips. *International Journal of Environmental Science and Technology* 2015*; 12 (7): 2119-2126*

II Sarker S, Bimbela F, Sánchez JL, Nielsen HK. Characterization and pilot scale fluidized bed gasification of herbaceous biomass: A case study on alfalfa pellets. *Energy Conversion and Management* 2015; *91: 451-458*

III Sarker S, Arauzo J, Nielsen HK. Semi-continuous feeding and gasification of alfalfa and wheat straw pellets in a lab-scale fluidized bed reactor. *Energy Conversion and Management* 2015; *99: 50-61*

IV Sarker S, Nielsen HK. Assessing the gasification potential of five woodchips species by employing a lab-scale fixed-bed downdraft reactor. *Energy Conversion and Management* 2015*; 103: 801-813*

V Sarker S. Feasibility analysis of a renewable hybrid energy system with producer gas generator fulfilling remote household electricity demand in Southern Norway. *Renewable Energy* 2016; 87:772-781

Other relevant publications not included in this thesis are listed below:

1. Sarker S, Nielsen HK. Erratum to: Preliminary fixed-bed downdraft gasification of birch wood chips. *International Journal of*

Environmental Science and Technology (published online, July 2015)

2. Sarker S, Nielsen HK, Knutsen T, Tokheim LA. Characterization of biomass by employing thermogravimetric analysis and lab-scale gasifiers. *4th International Symposium on Gasification and its Applications* (iSGA4), 2014, *Vienna, Austria.* (Conference proceedings)

3. Sarker S, Nielsen HK. Preliminary gasification of biomass and utilization of producer gas to electricity. *World Sustainable Energy Days (WSED), Wels, Austria*, 2013. (Conference proceedings)

4. Sarker S. Thermochemical characterization and fixed-bed downdraft gasification of selected biomass. (Journal paper: work in progress for submission)

Table of Contents

Abstract VII
Preface X
List of publications XII
List of Figures XVI
List of Tables XIX
1 Introduction 1
1.1 Motivation 1
1.2 Hypothesis and objectives 2
1.3 Thesis organization 3
1.4 Scientific contribution of the thesis 4
2 Background of biomass and gasification 5
2.1 Biomass 5
2.2 Biomass classification 5
2.3 Lignocellulosic biomass 6
2.4 Selection of biomass 8
2.5 Biomass application 10
2.6 Energetic utilization of biomass 11
2.7 Thermochemical conversion of biomass 12
2.7.1 Pyrolysis 12
2.7.2 Combustion 12
2.7.3 Gasification 13
2.7.4 Hydrothermal upgrading and hydro-thermal liquefaction 18
3 Materials and experimental methods 19
3.1 Feedstock and its preparation 19
3.1.1 Woody biomasses (Paper I and IV) 19
3.1.2 Herbaceous biomasses (Paper II and III) 21
3.2 Biomass characterization 23
3.2.1 Physiochemical analysis 23
3.2.2 Thermogravimetric analysis 27
3.3 Fixed-bed downdraft gasification experiment 29
3.3.1 Gasification system 29
3.3.2 Test protocol 31
3.3.3 Analytical measurement 33
3.3.4 Mass balance 34
3.4 Bubbling fluidized bed gasification 34
3.4.1 Pilot-scale bubbling fluidized bed gasification 35
3.4.2 Lab-scale bubbling fluidized bed gasification 39
3.5 Techno-economic analysis of a producer gas generator in a standalone renewable hybrid plant 42
3.5.1 Model set-up 43
3.5.2 Load data and energy sources 44
3.5.3 Emission parameters 45

4 Results and discussions 47
4.1 Biomass characterization 47
4.1.1 Physiochemical analysis 47
4.1.2 Thermogravimetric analysis 50
4.2 Fixed-bed downdraft gasification 55
4.2.1 Gasification of woody forest crops 56
4.2.2 Preliminary gasification of common reed briquettes 64
4.2.3 Mass balance 67
4.3 Pilot-scale fluidized bed gasification experiment 67
4.3.1 Gasification performance of alfalfa pellets 68
4.4 Small-scale fluidized bed gasification 73
4.4.1 Comparison of gasification between alfalfa and wheat straw pellets: semi-continuous feeding 73
4.5 Techno-economic analysis of a gasification plant based renewable hybrid energy system 83
4.5.1 System performance: simulation and optimization 83
4.5.2 Sensitivity analysis 84
5 Conclusions and future recommendations 87
5.1 Fixed-bed downdraft gasification of woody biomass 87
5.2 Fluidized bed gasification of herbaceous biomass 89
5.3 Techno-economic evaluation of renewable hybrid plant operating with producer gas generator 90
5.4 Future recommendation 91
References 93
Appended papers 102
Paper I 103
Paper II 113
Paper III 123
Paper IV 137
Paper V 175

List of Figures

Figure 1.1: Thesis organization 3
Figure 2.1: Lignocellulose structures of biomass, adapted from (Potters et al., 2010) 7
Figure 2.2: Ternary diagram of the selected biomasses (yellow dots: woody feedstocks; red dots: herbaceous feedstocks; FC: Fixed carbon; VM: Volatile matters) 9
Figure 2.3: Biomass energy conversion pathways (modified from (Maghanaki et al., 2013)) 11
Figure 2.4: A generalized scheme representing the steps of biomass gasification 13
Figure 2.5: Some important gasification reactions (Basu, 2010) 15
Figure 2.6: Producer gas applications 17
Figure 3.1: Harvesting, collection and pre-treatment of biomass; a) & b): willow (Dømmesmoen, Grimstad), c) & d): common reed (Hisøy, Arendal) 20
Figure 3.2: Some available options for biomass pre-treatment; a): batch dryer, b): hammer mill, c): briquetting press 21
Figure 3.3: Biomass pellets and briquettes for gasification tests (a): alfalfa pellets, b): wheat straw pellets, c): common reed briquettes 22
Figure 3.4: Heating microscope used for analyzing melting behavior of ash at University of Agder 26
Figure 3.5: A generalized scheme of the actual fixed-bed downdraft gasification system 29
Figure 3.6: Flow diagram of the gas sampling unit 30
Figure 3.7: Gas cooling and conditioning devices 31
Figure 3.8: Pilot scale gasification system at University of Zaragoza, Spain 36
Figure 3.9: Close view of some important sections in gasification system (c) control panel for displaying operational parameters e) μ-GC standalone PC storing gas data; the rest of the figures are marked) 37
Figure 3.10: Real-time tar sampling 39
Figure 3.11: A generalized scheme of the actual lab-scale bubbling fluidized bed gasification system 40
Figure 3.12: Simulation set-up and modeling steps 45

Figure 4.1: Characteristic temperatures during ash melting test of herbaceous biomass samples in oxidizing atmosphere. DT is deformation temperature, HT hemisphere and FT flow temperature 49
Figure 4.2: TGA plots of two classes of biomass (top: wood; bottom: herbaceous) 51
Figure 4.3: DTG plots of two classes of biomass (top: wood; bottom: herbaceous) 52
Figure 4.4: logβ vs. 1/T plots for kinetic analysis of TGA data 54
Figure 4.5: Effect of ER on gas compositions and gasification performance of forest crops 59
Figure 4.6: Effect of ER on gas compositions and gasification performance of energy crops 60
Figure 4.7: Effect of bed temperature on gas compositions and gasification performance of forest crops 62
Figure 4.8: Effect of bed temperature on gas compositions and gasification performance of energy crops 63
Figure 4.9: Evolution of gas composition and air and fuel feed over time on stream 66
Figure 4.10: Evolution of various temperatures for different zones over time on stream 66
Figure 4.11: Effect of ER on operational parameters of pilot plant gasification 69
Figure 4.12: Various temperature profiles and sensors location; left: evolution of temperatures over time, right: location of temperature probes (except T_7) along the reactor 70
Figure 4.13: Evaluation of gas compositions and LHV as an effect of ER for alfalfa 74
Figure 4.14: Evaluation of gas compositions and LHV as an effect of ER for wheat straw 75
Figure 4.15: Average performance parameters from the gasification of alfalfa 76
Figure 4.16: Average performance parameters from the gasification of wheat straw 77
Figure 4.17: Evolution of temperature profiles at various ER (left: alfalfa, right: wheat straw) 78
Figure 4.18: Influence of ER on tar composition from alfalfa 79
Figure 4.19: Influence of ER on tar composition from wheat straw (ER = 0.20 & 0.25) 80

Figure 4.20: Influence of ER on tar composition from wheat straw (ER = 0.30 & 0.35) 81
Figure 5.1: Comparison of fixed-bed downdraft gasification performance among different woodchips species (error bars representing the deviation from the average of all runs) 88
Figure 5.2: Comparison of gasification performance of alfalfa between Pilot-scale and lab-scale plant at ER = 0.30 (error bars representing the deviation from the average of all runs).....90

List of Tables

Table 2.1: Variation in gasification properties among the existing gasification technologies, modified from (Belgiorno et al., 2003) 16
Table 2.2: Producer gas cleaning methods, modified from (Hasler et al., 1998). 17
Table 3.1: Technical specifications and list of various components in the Fixed-bed gasification system and their usage 32
Table 3.2: Variation in batch feeding corresponding to ER 41
Table 4.1: Proximate, ultimate and LHV analysis of the studied feedstocks 47
Table 4.2: Kinetic analysis results for the selected biomass based on Flynn-Wall-Ozawa method 54
Table 4.3: Variation in structural composition between herbaceous and woody biomass 55
Table 4.4: Comparison of average gasification results between two different tests on birch woodchips 57
Table 4.5: Summary results obtained from the preliminary test of common reed briquettes 65
Table 4.6: Economics and emission parameters among the different modeled energy plants 84
Table 4.7: Sensitivity analysis of the optimum hybrid plant (Bio/PV/wind/battery/converter) as an effect of producer gas unit price 85

1 Introduction

1.1 Motivation

Three familiar developments such as continuously depleting fossil fuels, rapidly rising energy demand and the progressively increasing greenhouse gas emissions best describe the world's energy outlook at present. With the population growth, the energy consumption is proportionally rising and expected to increase 56 % by the year 2040 (Sieminski, 2013) compared to the year 2000. Moreover, greenhouse gases (GHG), particularly CO_2 emission, have already exceeded its safe limit and accelerated to ca. 400 ppm (González et al., 2015), owing mainly to the excessive use of fossil fuels. Escalated emissions are also observed from other potential gases (e.g., CH_4, N_2O, etc.). Against this backdrop, it is thus a common consensus among scientists that an urgent replacement of fossil fuels with renewable energy would be necessary so that the incumbent environmental challenges are safely negotiated and the energy security is sustainably achieved. There exist various forms of renewable energy such as wind, solar, hydro, biomass, geothermal, tidal and wave energy which all can be incorporated in a sustainable development of energy exploitation. However, the availability of wind and solar is not completely reliable and is characterized with seasonal variability (Chow et al., 2003); further, expansion of large hydro power is limited due to the detrimental societal and environmental impact (Abbasi & Abbasi, 2011); and the technology toward extracting energy from tidal power is still in the early days (Sleiti, 2015). Therefore biomass can emerge as one of the most interesting renewable energy options, because of its diverse usage, storability and wide spread availability, to serve as a reliable alternative to future energy.

Over the centuries, ever since human beings learnt to make fire by using wood, biomass for producing energy has been in use. Since then biomass utilization has been catapulted and diversified in various directions through a number of conversion pathways such as biochemical and thermochemical (McKendry,

2002b). Although biological conversion has shown a tremendous success in the recent past primarily towards producing engine fuels (bioethanol and biogas), this conversion lacks in several areas such as: requirement of long processing time, enzymatic pretreatment (only for starch and celluloses for bioethanol production), low product yield, etc. (Brown, 2011; Maurya et al., 2015). In addition, a conflict between food vs. feed as a result of utilizing conventional biomasses (mainly grain and oilseed crops, and grasses) for producing liquid biofuel exists. A significant effort is thus placed on thermochemical conversion, particularly towards gasification which allows to transform all forms of biomass (through partial oxidation) to high energy content gas that subject to downstream applications can yield further products such as heat, electricity and chemicals. Within gasification, lignocellulosic biomass, i.e., agricultural and biological waste, residues and wood etc. is greatly favored. This biomass is abundant, non-competing with agricultural lands and suitable for high temperature treatment and therefore is considered as key material to contribute towards bioenergy under which the motivation of this work is deeply rooted. Further, a special emphasis is also placed on local lignocellulosic biomass which in the scenario of producing decentralized power is even more appealing since this mode of application can fulfill the energy demand of a given community independently without requiring the access to national grid electricity.

1.2 Hypothesis and objectives

The overall hypothesis of the thesis was that by regulating the input parameters, the gasification performance of various woody (birch, oak, spruce, willow and poplar) and herbaceous (alfalfa, wheat straw and common reed) biomasses can be widely varied and the resulting optimized conditions can be used as reference for future local bioenergy research.

Broadly, the aim was to gain insight of the local lignocellulosic biomasses in terms of their potential of fixed and fluidized bed gasification. The overall objectives can further be broken into the following steps of work:

- Characterization of selected biomass for thermochemical conversion
- Investigating the feasibility of selected woody biomass for gasification
- Examining the potential of local herbaceous biomass for gasification
- Determining the techno-economic feasibility of gasification application

1.3 Thesis organization

The thesis organization is presented in Figure 1.1. Overall the thesis consists of five chapters. The study motivation, hypothesis, objectives and the thesis organization are outlined in Chapter 1. Chapter 2 gives the background of biomass and its suitability of gasification. Chapter 3 deals with materials and methods and covers background, pre-treatment and characterization (proximate, ultimate, TGA, fusion temperature, kinetics, etc.) of selected feedstocks; experimental set-up, test protocol, analytical procedures of fixed and fluidized bed gasification; and, modeling set-up of techno-economic analysis using HOMER.

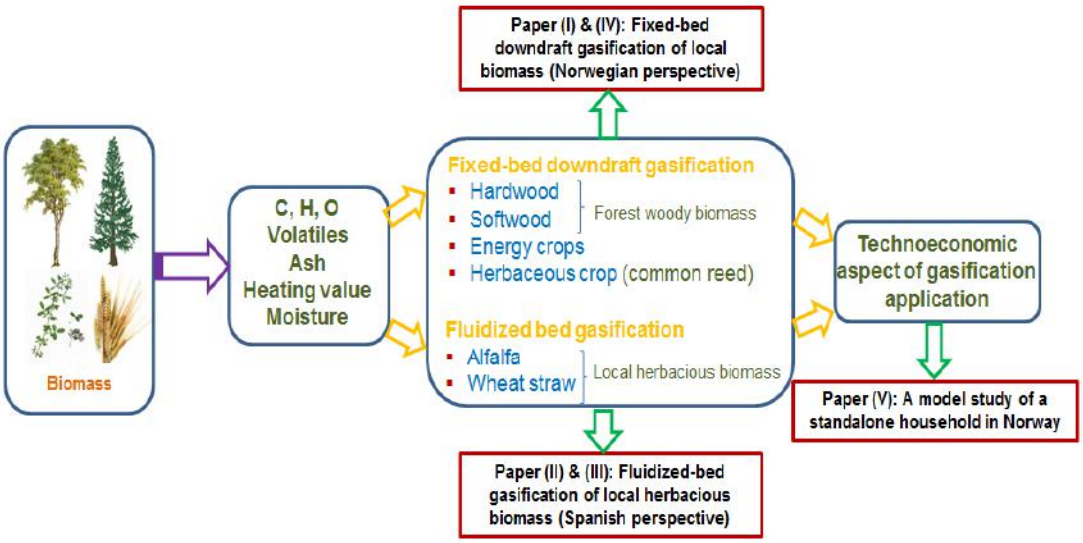

Figure 1.1: Thesis organization

Chapter 4 is devoted to describing results and discussions. In this chapter, the obtained results from fixed and fluidized bed gasification on woody and

herbaceous biomasses are discussed in light of operational parameters, quality of biomasses and to the performance of gasification. The feedstocks characteristics results are also presented and finally the techno-economic analysis covering simulation, optimization and sensitivity assessment of a gasification based hybrid plant model are given. In Chapter 5, the major conclusions drawn from this project are stated and the recommendations and future research possibilities are proposed.

1.4 Scientific contribution of the thesis

The scientific contribution of this research work can be summarized below:

- Thermal characterization and kinetics modeling of the selected biomass was performed and some of the results were compared against the gasification tests using lab scale fixed bed and fluidized bed gasifiers (paper III).
- Gasification performance of five local woody biomasses (birch, oak, spruce, poplar and willow) on fixed-bed downdraft gasification was optimized for a number of operating conditions (paper IV).
- Alfalfa pellets were successfully gasified in a continuous feeding pilot scale fluidized bed reactor and gasification performance was optimized under a range of operating conditions (paper II).
- Alfalfa pellets were further gasified in a semi-continuous lab-scale fluidized bed reactor and the gasification performance was optimized under a wide range of operating conditions. Same processing steps were repeated for wheat straw pellets and the obtained results between the two feedstocks were compared (paper III).
- A preliminary test investigating the feasibility of local herbaceous biomass (common reed) using fixed-bed downdraft reactor was conducted and the results were discussed. Also, the scope of future research was suggested.
- Modeling work assessing the techno-economic viability of a gasification generator based renewable hybrid energy plant satisfying a standalone household electricity demand in Grimstad was established by using simulation tool HOMER (paper V).

2 Background of biomass and gasification

2.1 Biomass

Biomass has been a major source of energy for humans since historic times and it has been estimated that biomass resources cover approximately 10 % of the total global primary energy supply (REN 21, 2015). Every year a vast amount of biomass grows through photosynthetic reactions out of which approximately 200 billion tons are annually available for energy conversion (McKendry, 2002a). All the plants that capture sunlight for photosynthesis are called biomass. A generally acceptable definition of biomass by EU directive 2001/77/EC (RES-E) is: *"Biomass shall mean the biodegradable fraction of products, waste and residues from agriculture (including vegetal and animal substances), forestry and related industries, as well as the biodegradable fraction of industrial and municipal waste."* The amount of CO_2 released during the combustion of biomass is almost equal to the amount of CO_2 utilized for plant growth. This justifies the reason why biomass is considered a renewable source. In a broader term, biomass includes all the living species-plants and animals that are now alive or was a short time ago (Basu, 2010). Fossil-fuels, in fact, are also the product of organic materials (plants and living species) which after exposing millions of years of transformation leading to fuels. Unlike biomass, they however do not reproduce and thereby are not renewables.

2.2 Biomass classification

In terms of origin, the type of biomass varies, which with reference to (Cuadros et al., 2013), can be classified as:

- **Natural biomass**: It is the biomass that occurs spontaneously in nature without human intervention (i.e.; resources generated in the natural pruning of a forest, some woody and herbaceous biomasses, etc.)

- **Residual biomass**: It is the biomass generated by human activity. Residual biomass can be distinguished between dry residual biomass (which comes from resources generated in agricultural and forestry activities in agribusiness and wood processing industries) and wet waste biomass such as biodegradable discharges formed by urban and industrial wastewater, livestock wastes (usually manure) and the residues from urban solids.

- **Energy crops:** They are the crops (such as sunflower, sugar cane, maize, beet, thistle, willow, poplar, switch grass, etc.) grown on agriculture and forestry land, dedicated exclusively to the production of non-food biomass for energy production. They are divided into woody and herbaceous.

- **Marine biomass**: The aquatic biomass resources namely algae, sea weeds, etc. are part of this group. Marine biomass is increasingly gaining popularity as feedstock for energy conversion.

In this work, the conversion of lignocellulosic biomass mainly the forest crops, energy crops, herbaceous crops and agricultural wastes will be discussed.

2.3 Lignocellulosic biomass

Lignocellulosic, being cellulose, hemicellulose and lignin are the three main components of biomass. Unlike carbohydrates or starch, lignocellulose is not easily digestible by humans and therefore its utilization to energy production does not pose a great threat to the world's food supply (Lim et al., 2012). The lignocellulosic plant biomass consists of a complex cell wall composed of micro-fibrils network of celluloses on which layers of hemicelluloses and lignin are subsequently deposited. Of all the compounds forming the lignocellulosic

materials, almost half are cellulose and around 5 - 30 % is lignin (McKendry, 2002a). The bond between cellulose and lignin can occur directly or, through hemicelluloses as shown in Figure 2.1. For a plant biomass, cellulose and hemicellulose give structure while lignin glues them together. The properties of these components as of relevance are briefly discussed below:

Cellulose

Cellulose is a linear polysaccharide crystalline polymer consists of thousands of monomeric units of anhydro-D-glucose units with a β-(1→4) linkage (Mohan et al., 2006; Pasangulapati et al., 2012) which allows the micro-fibril structure to develop a stronger inter and intra-molecular hydrogen bonding. During thermal conversion, cellulose degrades to a moderate temperature between 240 °C and 350 °C and yields volatiles, tar and char (Robbins et al., 2012).

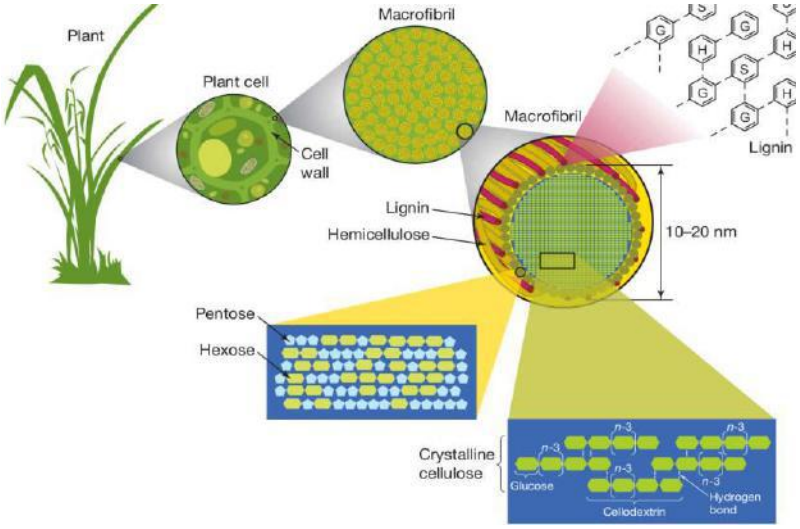

Figure 2.1: Lignocellulose structures of biomass, adapted from (Potters et al., 2010)

Hemicellulose

Unlike celluloses, hemicelluloses have less branched chains polymerization and have therefore crystalline regions. Furthermore, hydrogen bonds are less

effective, making this polysaccharide more accessible to attack by chemical reagents. Hemicellulose is thermo-chemically unstable and decomposed between temperature 200 °C and 260 °C resulting volatiles and less tar and char than those from cellulose (Robbins et al., 2012).

Lignin

Lignin acts as a gluing material and gives elasticity and mechanical strength to the biomass. It is a complex three dimensional branched polymer of phenyl-propane consisting with 4-propylene phenol, 4-propylene-2-methoxy phenol, 4-propylene-2.5-dimethoxyphenol (Bridgwater & Boocock, 1996). These phenyl-propane units are cross linked between themselves and insoluble both in water and sulfuric acid (Basu, 2010; Klass, 1998), making them thermally more stable than cellulose (Ramiah, 1970). As highly stable, lignin degrades over a broad range of temperature, typically, between 280 °C and 500 °C and yields a higher amount of char than those of cellulose and hemicellulose (Serapiglia et al., 2009).

Besides cellulose, hemicellulose and lignin, biomass also contains secondary components called water and organic solvent solubles and insolubles. Fatty acids, alcohols, phenols etc. are water or organic solvent soluble components, while ashes, starches, proteins etc. are insolubles (Basu, 2010).

2.4 Selection of biomass

Thousands of biomass can be identified as feedstocks for gasification. These huge resources represent varying characteristics which under a single framework of study is difficult to apprehend. Hence a common approach to select biomass for gasification is to develop interest to a particular group or, a number of feedstocks that in-terms of physical and chemical properties (moisture, volatiles, ash, carbon, hydrogen and oxygen, etc.) are attractive and can potentially meet the desired characteristics of producer gas (high heating value, less tars and particulates etc.) and its intended application (Vaezi et al., 2012). Since the

present study emphasizes on generating producer gas that is potentially applicable to generate distributed power, the feedstocks available around the local areas were selected. Moreover, to meet the economic, environmental and sustainability requirement, the biomass having negligible environmental, technical and societal impact was considered. To this end, lignocellulosic biomasses appear to be a good option and hence these biomasses from among various distinctive families were undertaken as feedstocks given below:

- Long rotation forest crops (birch, oak, spruce)
- Short rotation woody energy crops (poplar and willow)
- Herbaceous biomass (alfalfa, wheat straw and common reed)

Knowing the physical or chemical properties, the suitability of a solid fuel for thermal conversion can be predicted by locating it on a ternary diagram, which has been a popular approach for many years. Thus the current fuels, based on the given proximate analysis data in literatures (Boateng et al., 2008; Demirbas, 2004; Phyllis2), are plotted in a ternary diagram (Figure 2.2) below.

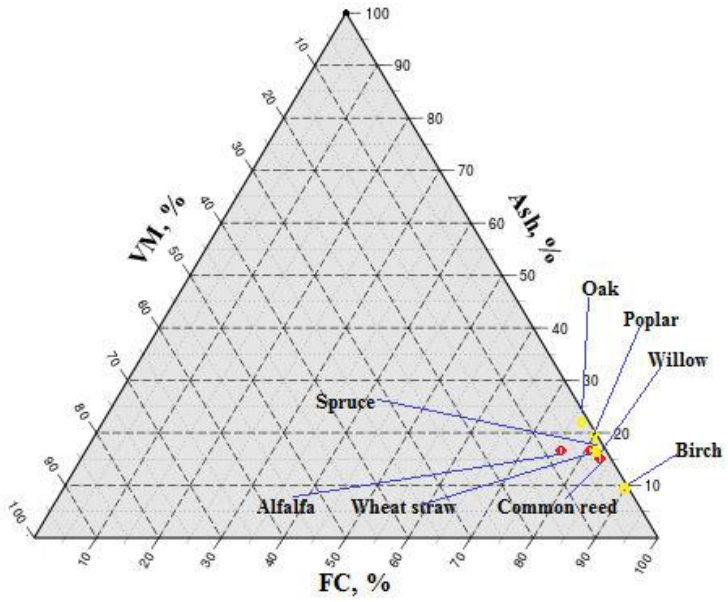

Figure 2.2: Ternary diagram of the selected biomasses (yellow dots: woody feedstocks; red dots: herbaceous feedstocks; FC: Fixed carbon; VM: Volatile matters)

As seen (Figure 2.2), based on literature, the selected biomasses used in the current project have high volatile matter (>70 %) and fixed carbon contents which are the desirable properties for gasification (Basu, 2010). Alfalfa has ash content over 5 % which albeit high is fairly typical for herbaceous biomass considered for gasification.

2.5 Biomass application

Several conversion methods exist for the use of biomass as fuel for thermal energy production, electricity production, or as raw material for the production of liquid and gaseous biofuel:

- **Thermal energy production**: Thermal energy or heat is mainly obtained via direct combustion of forest biomass and waste from agriculture, wood processing industries and solid wastes from municipalities. The heat generated is mainly used both for domestic and industrial needs.

- **Electricity production**: Electricity is also obtained primarily by the combustion of different types of biomass such as those utilized for the production of thermal energy, but biogas and syngas produced via anaerobic digestion and gasification respectively are also in practice. The electricity yield employing biomass is not very high due to the inherent fuel characteristics such as high moisture.

- **Liquid biofuels production**: There are mainly two types of liquid biofuels: bioethanol, which is generally produced from fermentation with yeast of starch and sugary crops, such as sugar cane, sugar beet, corn and grain, etc., and biodiesel, which is produced from vegetable oil crops, such as sunflower, rape, etc., and animal fats. Liquid biofuels can be utilized for propulsion, heat and power.

- **Gaseous biofuels production:** In this application, gaseous biofuels are produced by an anaerobic biological process using primarily wet waste

biomasses. This gas consists largely of methane having a reasonably good calorific value that can either be used for generating both electricity and heat, or for transportation fuels through direct utilization. Gaseous biofuels can also be produced via gasification, generating energy rich fuel gas composed largely of hydro-carbon gases, CO, CO_2, H_2 and H_2O.

2.6 *Energetic utilization of biomass*

Energy from biomass can be obtained by means of a number of processes, e.g.; biochemical, thermochemical, etc., some of which are outlined in Figure 2.3.

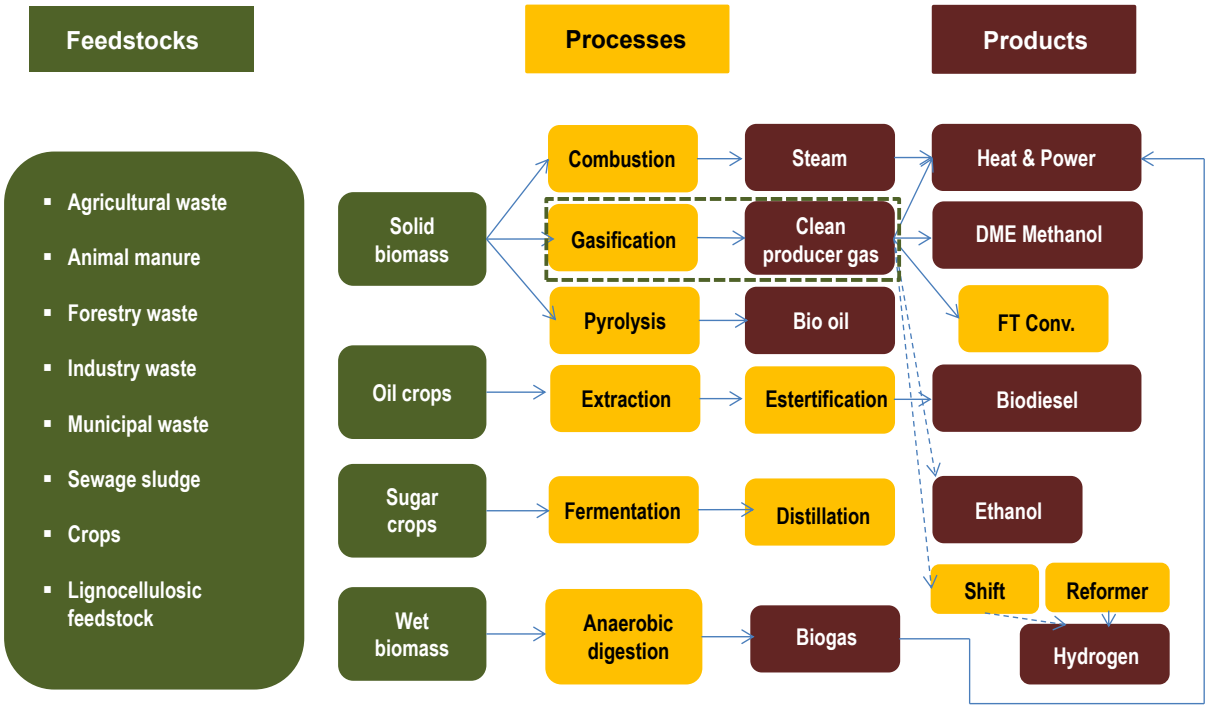

Figure 2.3: Biomass energy conversion pathways (modified from (Maghanaki et al., 2013))

The present work focuses on the energy use of biomass through thermochemical conversion; hence only this process is overviewed in the following sub-sections.

2.7 Thermochemical conversion of biomass

Thermochemical conversion means transforming biomass by a series of chemical reactions using heat. During thermochemical conversion, normally three types of processes namely pyrolysis, combustion and gasification are distinguished by the amount of oxygen supplied. This is briefly discussed below.

2.7.1 Pyrolysis

Pyrolysis can be defined as the decomposition of biomass by heat in absence of an oxidizing agent, resulting in the production of solid carbonaceous materials (soot or char), liquids and gases through four thermal stages (Basu, 2010), e.g.; drying (ca. 100 °C), initial stage (ca. 100-300 °C), intermediate stage (> 200 °C) and final stage (ca. 300-900 ºC). Some of the pyrolysis reactions start at around 300 °C (InnoFireWood's, 2015) but the reactions become more rapid and progressive in the temperature ranging between ca. 400 and ca. 700 °C (Sharma et al., 2015). Depending on the temperature and residence time, ranging from few seconds to days, pyrolysis can be differed and accordingly, the type of yields. Slow pyrolysis with low heating rate results in solid char as a main product, while fast pyrolysis as a result of high heating rates produces mainly liquid oils (Tanger et al., 2013).

2.7.2 Combustion

Perhaps the most commonly used thermal conversion is combustion. In theory, combustion is an exothermal process (> 1000 °C) completely oxidizing the organic matter of biomass with enough oxygen (oxygen amount higher than stoichiometric) to sustain thermal reactions yielding carbon dioxide, water, ashes and heat. Despite the apparent simplicity, combustion is a complex process from a technological point of view, where high reaction rates end into a large amounts of heat and many different products. Any type of biomass (under a certain level of moisture) can be effectively combusted to generate heat. However, to produce

electricity via a Rankine cycle, 100 % biomass combustion is still challenging and co-combustion with coal is practiced for that matter. So far, maximum throughput of 10 % biomass (Van Loo & Koppejan, 2008) is achieved across the existing plants undertaken co-combustion of biomass and fossil fuel.

2.7.3 Gasification

Gasification is a complex thermochemical process in which normally a carbonaceous feedstock is heated (i.e.; allothermal, autothermal, etc.) to high temperature by partial oxidation of feedstock with the help of an oxidation medium such as air, steam, CO_2, oxygen, or combination of these (Kumar et al., 2009). Through series of chemical reactions (McKendry, 2002a) the process generates producer gas which typically consists of CO, CO_2, H_2, CH_4, H_2O and C_nH_n etc.(Hindsgaul et al., 2000).

Thermochemical gasification usually occurs at temperatures of ca. 800-1000 ^{0}C and involves following processing steps (Boerrigter & Rauch, 2006; Rollinson & Karmakar, 2015) which are shortly described and illustrated by Figure 2.4 below.

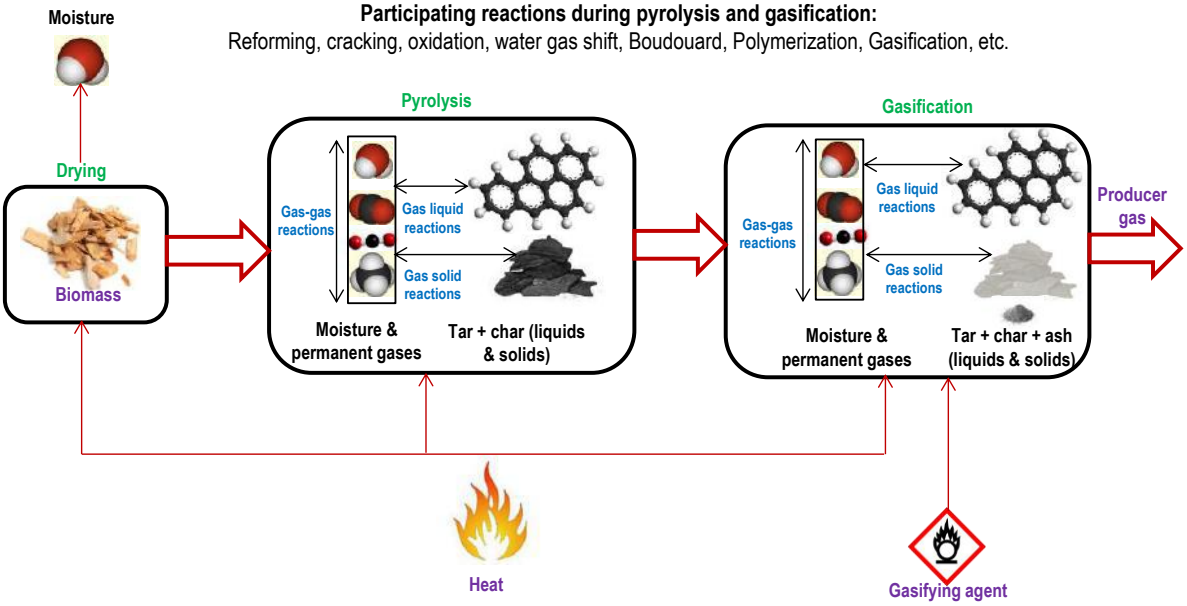

Figure 2.4: A generalized scheme representing the steps of biomass gasification

- **Heating and drying (ca. 0-250 °C)**: In this step (100-200 °C) the moisture from the biomass is removed with the help of heat (Puig-Arnavat et al., 2010). Low moisture in biomass means less heat for drying and thus higher gasification efficiency (Hughes & Larson, 1997).

- **Thermal decomposition or, pyrolysis (ca. 250-500 °C)**: Pyrolysis is a thermal degradation process occurred in oxygen scarce environment, decomposing biomass into combined solids, liquids and gases.

- **Reduction and gas phase reactions (ca. 800-1100 °C)**: In reduction, primarily the char is converted into gas through heterogeneous gas-solid reactions while the resulted gaseous products from pyrolysis are gasified completely to form the permanent gases (CO, CO_2, H_2, CH_4 etc.). The reactions in this step are generally endothermic and thus require sufficient heat to occur.

- **Combustion (ca. 800-1100 °C)**: Through combustion in general the oxidation of char takes place. Char oxidation is exothermic in nature and provides necessary heat for sustaining endothermic gasification reactions. In directly heated gasifiers, ignition is first started up most frequently with char combustion which produces the necessary heat to establish the other steps of thermal conversion. Besides char, gases and liquids can also participate into combustion, yielding gases composed of: CO and CO_2, etc.

A number of important reactions (Basu, 2010) taking place during gasification is shown in Figure 2.5.

The arrows in these reactions indicate that the reactions are in equilibrium and can move in any directions, depending on temperature, pressure and concentration of the reacting species. Moreover, as seen (in Figure 2.5), the product gas from the gasification is a mixture of gas components like carbon monoxide, carbon dioxide, methane, hydrogen and water vapor.

1. *Boudouard reaction*: $C + CO_2 \leftrightarrow 2CO;\ \Delta H = +172\ kJ/mol$
2. *Combustion reaction*: $C + O_2 \leftrightarrow CO_2;\ \Delta H = -408.8\ kJ/mol$
3. *Carbon partial reaction*: $2C + O_2 \leftrightarrow 2CO;\ \Delta H = -246.4\ kJ/mol$
4. *Dry reforming reaction*: $CH_4 + CO_2 \leftrightarrow 2CO + 2H_2;\ \Delta H = -793\ kJ/mol$
5. *Hydrogasification*: $C + 2H_2 \leftrightarrow CH_4;\ \Delta H = +75\ kJ/mol$
6. *Methanation*: $CO + 3H_2 \leftrightarrow CH_4 + H_2O;\ \Delta H = -227\ kJ/mol$
7. *Steam reforming*: $CH_4 + H_2O \leftrightarrow CO + 3H_2;\ \Delta H = +206\ kJ/mol$
8. *Water − gas reaction*: $C + H_2O \leftrightarrow CO + H_2;\ \Delta H = +131\ kJ/mol$
9. *Water − gas shift reaction*: $CO + H_2O \leftrightarrow CO_2 + H_2;\ \Delta H = +41.98\ kJ/mol$
10. *Partial oxidation (exothermic)*: $CO + 0.5O_2 \leftrightarrow CO_2;\ \Delta H = -111\ kJ/mol$

Figure 2.5: Some important gasification reactions (Basu, 2010)

Gasification reactors

Biomass gasification can be performed using a number of reactors which on the basis of transport process are generally categorized as: fixed bed, fluidized bed, entrained bed and plasma reactors (Basu, 2010). Within this classification, the choice of the reactors is primarily depended on physio-chemical properties of biomass and the desired scale (or size) of conversion. Typically, fluidized bed reactors are more frequently available for medium to large scale application, in contrast to fixed bed reactors which are particularly suited for small scale applications with some exceptions. Unlike these two reactors, entrained flow and plasma reactors are primarily devoted to treat (usually at temperature > 1500 °C) aggressive and difficult fuels, which by conventional reactors otherwise would be difficult to deal with.

Regardless of the types and configurations, the gasification reactors usually operate at high temperature (ca. 1000-1200°C) and follow the four processing steps as described in section 2.7.3. The variation in gasification properties of existing gasification technologies are illustrated in Table 2.1.

Table 2.1: Variation in gasification properties among the existing gasification technologies, modified from (Belgiorno et al., 2003)

Properties	Fixed bed		Fluidized bed		Entrained bed
	Updraft	Downdraft	Bubbling	Circulating	
Oxidant requirement	Low	Low	Moderate	Moderate	High
Coarse feedstock input	Very good	Very good	Good	Good	Poor
Fine feedstock input	Limited	Limited	Good	Good	Excellent
Reaction zone temperature	High	High	Medium	High	Very high
Applicability range	Medium	Low	High	High	Very high
Producer gas LHV	Poor	Poor	Poor	Fair	Poor
Tar content	Very high	Very low	Medium	Medium	Negligible
Particulates content	Very low	High	High	High	Low
Cold gas efficiency	Excellent	Good	Good	Excellent	Good
Carbon conversion efficiency	Good	Good	Fair	Very good	Good
Thermal efficiency	Excellent	Very good	Good	Very good	Good

Gasification product and its utilization

The producer gas is the main product obtained from biomass gasification and char, tar and ash are the least desirable by-products. Coupled with high quality producer gas, minimum generation of tar and char ensures high gasification efficiency. However, raw gas generated often includes impurities in the form of tars (or, tarry liquids), solids, particulates, alkali materials, sulfur materials and others which need to be cleaned before it can be directed to the intended downstream applications. Producer gas cleaning can be achieved by employing a variety of techniques summarized in Table 2.2.

The cleaned producer gas depending on composition and quality can be used for a range of applications, like production of biofuels or direct utilization in internal combustion engines, turbines and boilers, etc. (Ahrenfeldt et al., 2013; Clausen et al., 2010). Figure 2.6 shows the various possibilities of producer gas usage.

Table 2.2: Producer gas cleaning methods, modified from (Hasler et al., 1998)

Treatment categories	Cold gas cleaning		Thermal treatment	
	Devices	Temperature [°C]	Devices	Temperature [°C]
Tar reduction	Sand bed filter, rotational wash tower, rotational atomizer, wet electrostatic precipitator (WESP)	10-20, 50-60, < 100, 40-50	Fabric filter, catalytic tar cracker	~ 200, 900
Alkalis & NH_3 abatement	Sand bed filter	10-20	Catalysts: absorbed on bauxites, dolomites/nickels	~ 650-750, ~900
H_2S removal	Sand bed filter, rotational atomizer	10-20, < 100	Catalysts: absorption on metal oxides	~300-500
HCl reduction	Sand bed filter, rotational atomizer, wet scrubber	10-20, < 100, ~50		
Particulates abatement	Sand bed filter, rotational wash tower, rotational atomizer, wet electrostatic	10-20, 50-60, < 100, 40-50	Fabric filter, Hot electrostatic precipitator (HSEP)	~ 200, ~500

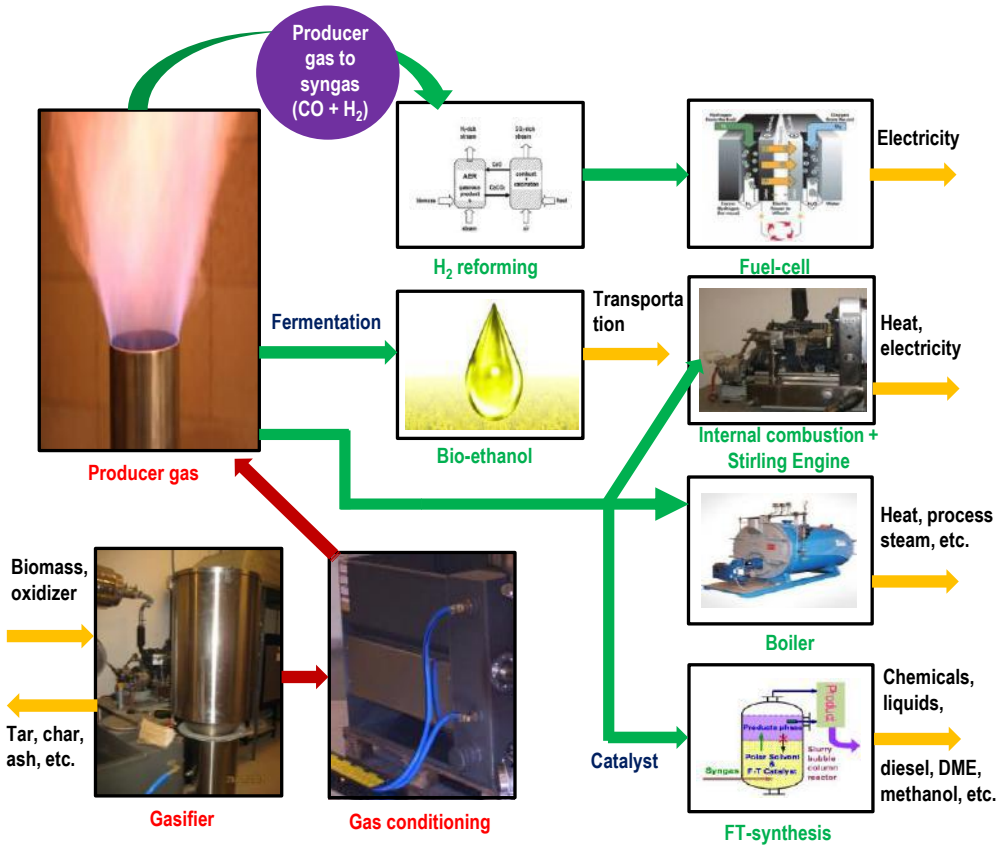

Figure 2.6: Producer gas applications

2.7.4 Hydrothermal upgrading and hydro-thermal liquefaction

Hydrothermal upgrading (HTU) and hydro-thermal liquefaction (HTL) are the other thermochemical processes. However, in contradiction to gasification, in these processes wet biomass is transformed into bio-oil at elevated temperature (ca. 150 to 370 °C) and pressure (ca. 4 to 22 MPa) within the sub-critical and super-critical zones of water (Brown, 2011). High pressure maintains liquid state and thus facilitates biomass slurries to be converted into useful products at high temperature. Generally, HTL uses higher temperature and pressure than those of HTU. Both of these techniques, however, are expensive and still in the demonstration scale.

3 Materials and experimental methods

In order to investigate the gasification potential of different biomass across different gasification technologies, the present work used various woody and herbaceous biomasses in fixed and fluidized bed reactors. Moreover, a modeling study concerning the utilization of producer gas in a renewable hybrid energy plant powering a remote household was also aimed. To this end, thus the various aspects of feedstock preparation, experimental set-up, analytical measurement and modeling technique are given in the following sub-sections.

3.1 Feedstock and its preparation

3.1.1 Woody biomasses (Paper I and IV)

Forest crops: birch (*Betula pendula),* oak (*Quercus petraea)* and spruce (*Picea abies),* and energy crops: poplar (*Populus trichocarpa)* and willow (*Salix* sp.) representative of two categories of local biomass were considered as feedstocks for gasification using fixed-bed downdraft reactor. The forest crops (birch, oak and spruce) were harvested from a local forest at Dømmesmoen, Grimstad (coordinate: 58° 21’ 8.6” N, 8° 34’ 32.78” E), while the energy crops (poplar and willow) were cultivated and harvested from an agricultural land (area: ~0.3 ha) located in proximity to Dømmesmoen, Grimstad. The variation in classification, age and harvesting periods of different woody biomasses is reflected to Table 1 of paper IV. Further, Figure 3.1 below illustrates some snapshots of different harvesting and pre-treatment phases of local biomasses in Southern Norway.

Woody biomasses for gasification tests were prepared by following the three processing steps, e.g.; harvesting, drying and in field wood chipping. Harvesting of the forest crops was achieved by using a chain saw while the energy crops were harvested by means of a brush saw. After harvesting, woody biomasses of

all types were dried in two different techniques: natural drying (outdoor) and artificial drying (indoor by using a batch dryer).

Figure 3.1: Harvesting, collection and pre-treatment of biomass; a) & b): willow (Dømmesmoen, Grimstad), c) & d): common reed (Hisøy, Arendal)

The woody energy crops (poplar and willow) received natural drying. After harvest in late winter, trees were left exposed on-field for a particular period to allow moisture evaporation followed by chipping, storing (some of these steps are shown in the Figure 3.1 above), and further in-house drying. These altogether contributed to decrease overall moisture from > 50 % to < 15 %. The forest crops (birch, oak and spruce) were chipped in the forest and afterwards dried (at ca. 60 °C air temperature) in a batch dryer (Figure 3.2a).

In the biomass dryer, an electrical heating element of about 2.4 kW capacity provides necessary heat while a blower (Lindab CK 160 °C, Sweden) with a rating of ca. 4 kW transmits the hot air throughout the feedstocks placed inside the drying chamber. A batch of ca. 80 kg wet biomass was loaded for each drying

instance that remains for about 40 h, after which a desired level of moisture was generally achieved. Generally, moisture content down to 3 % could be attained as a result of batch drying by using the current dryer.

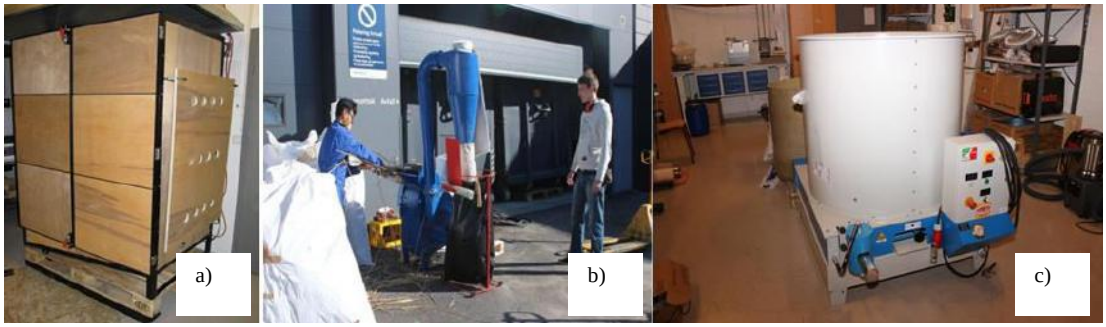

Figure 3.2: Some available options for biomass pre-treatment; a): batch dryer, b): hammer mill, c): briquetting press

Prior to gasification tests, woody biomass of all types was chipped to a size between ca. 2 and 50 mm by employing a disc chipper (NHS 7201E 4, Denmark). Once produced, the woodchips were stored in big fertilizer bags. Dried woodchips were sieved through a 10 x 10 mm mesh screen (chicken mesh) in order to reduce fine particles. The chips which passed through the screen were removed while the remaining was used for conducting experiments.

3.1.2 Herbaceous biomasses (Paper II and III)

As herbaceous biomass crops, alfalfa (*Medicago sativa* L.) and wheat straw (*Triticum aestivum* L.) was selected as feedstocks for fluidized bed gasification. These biomasses were locally grown and harvested from around the area of Ebro valley, Spain. Alfalfa was grown and harvested from the surroundings of Pina de Ebro, 40 km Southeast of Zaragoza (Aragón, Spain) and wheat straw was harvested from Tordesillas, 70 km south of Valladolid (Castilla y León, Spain). In addition to alfalfa and wheat straw, one other herbaceous biomass namely common reed (*Phragmites autralis*) was selected for fixed-bed downdraft

gasification in Grimstad. Common reed (CR) was harvested (Figure 3.1) from a field at Hisøy located ca. 20 km Northeast of Grimstad.

Herbaceous biomasses for gasification were prepared by following the processes harvesting, drying and pelletizing or, briquetting. For alfalfa and wheat straw harvesting was followed by combined drying and pelletizing (detailed in paper II & III) resulting in pellets of approximately 6 mm Ø x 25 mm and 8 mm Ø x 20 mm size respectively. Common reed, on the other hand, was naturally dried in-field to moisture level of ca. 10 % before manual harvest by a scythe and then hammer milled (ARP- safe APS, Denmark, Figure 3.2b) with a screen size of 5 mm before briquetting to 45 mm ∅ briquettes by employing a piston press briquetting machine (Mythos 45, Comafer, Italy, Figure 3.2c). Due to the pelletizing and briquetting, the density of the herbaceous feedstocks greatly enhanced allowing improved fuel feeding to the gasification reactors. The images of the produced pellets and briquettes are shown in Figure 3.3.

Figure 3.3: Biomass pellets and briquettes for gasification tests (a): alfalfa pellets, b): wheat straw pellets, c): common reed briquettes

Approximately 100 kg pellets of alfalfa and wheat straw pellets was supplied to the gasification facility at UNIZAR by Molinos Afau S.L. (Zaragoza, Spain), while approximately 50 kg of common reed briquettes were produced by using in-house briquetting machine. After receipt, pellets and briquettes were stored at room condition for further usage.

3.2 Biomass characterization

In order to understand the differences in gasification properties, it is relevant to know biomass characteristics. Characterization can be achieved by using several methods, such as analytical (proximate, ultimate, chemical etc.) (Basu, 2010), structural (cellulose, hemicellulose and lignin) and graphical (Van-krevelen diagram, ternary diagram, etc.). Due to the relevance of the current project, only analytical and thermal analyses are briefly discussed in this thesis.

3.2.1 Physiochemical analysis

Proximate analysis

Proximate analysis is an important method used for physical characterization related to thermogravimetric analysis. It gives biomass composition as ratios of moisture content (MC), volatile matter (VM), fixed carbon (FC) and ash. The proximate analysis results of the present biomasses are presented in Table 4.1 (section 4.1.1). For a detailed discussion, the readers are however referred to paper I through IV, enclosed in the appendix.

Moisture

Moisture is an important property of biomass. Average moisture content of biomass can vary between 3 % and 90 % (Vassilev et al., 2010). In general, high moisture in biomass can negatively influence thermo-chemical conversion such as production of char, tar, ash and efficiency, but the presence of some can show positive contribution towards gasification (Acharjee et al., 2011). In the current work, moisture was mainly determined based on oven dried method by following the standards ASTM D-871-72 (Materials, 1975) (paper II) and EN 14774: 2009 (EN14774:2009, 2009a) (paper III & IV). In a special instance (paper I), moisture analyzer (Metler Toledo LJ16, Switzerland) was used to evaluate the moisture content of birch.

Volatiles

Volatiles are normally released when biomass is heated between the temperatures 150 and 500 °C. Biomass typically contains 70 to 90 % volatiles (Basu, 2010), which albeit high makes it more reactive than conventional fossil fuels. Volatiles in this work were evaluated based on the protocol EN 15148:2009 (EN15148:2009, 2009).

Ash

Ash is an inorganic solid left after fuel combustion. List of inorganic materials that compose ash include Ca, Na, K, Si, P, Al, Fe, Mg, Cl, S etc. Ash composition in biomass is fairly diverse and influenced by the type of feedstock, soil, climate and cultivation (Van Loo & Koppejan, 2008). Usually, ash in woody biomass is rich in alkali compounds (Na, K, Ca, Mg), while in herbaceous biomass (straw, reed, rice husk etc.) the ash in addition is rich in silicon (Umamaheswaran & Batra, 2008) content. The presence of the type of alkali materials can dictate ash melting temperature which eventually can cause process difficulties due to the fouling and slagging in units for high temperature combustion or, gasification, e.g.; turbine, engine, boiler etc. (Wang et al., 2008). Likewise, silicon can also be responsible for process failure as a result of agglomeration to the conversion units. Ash thus needs to be carefully accounted concerning thermochemical application.

Ash in biomass can be measured by following a range of standards and procedures. In the present work, the protocols CEN/TS15403 (CEN/TS15403, 2006), EN 15403:2011(EN15403:2011, 2011) and EN 14775:2009 (EN14774:2009, 2009b) were primarily used. Herbaceous biomass alfalfa was analyzed according to the standard EN 15403:2011 (EN15403:2011, 2011) (paper II), while an external lab Eurofins Environmental Testing Sweden AB utilized protocol CEN/TS15403 (CEN/TS15403, 2006) for measuring the ash content of birch (paper I), and EN 14775:2009 (EN14774:2009, 2009b) for measuring all the woody biomasses (birch, oak, spruce, poplar and willow).

Heating value

Heating value is another important fuel property directly linked to process and conversion efficiency. Owing to the low density and higher atomic ratio (O:C and H:C), heating value of biomass is in generally lower compared to that of fossil fuels. Typically, two types of heating values are reported: higher heating value (HHV) and lower heating value (LHV) which between themselves is differed depending on the inclusion and exclusion of latent heat of water vapor. The measurement of LHV does not take latent heat of water vapor into account and thus lower in magnitude than that of HHV. To determine the heating value of fuels, a number of techniques, i.e.; empirical (Pieratti, 2011) and analytical, can be employed.

In this project, an analytical method involving in-house bomb calorimeter (IKA C 2000, Germany) was used for herbaceous biomasses (alfalfa and wheat straw) which further were compared to the empirical correlation (Gaur & Reed, 1995) below (eq. 1). LHV of all the woody biomasses including common reed, on the other hand, were measured by an external lab Eurofins AB, Gothenburg, Sweden, according to the standard SS-EN 14918/15400 ISO 1928.

$$HHV = 0.3491 * C + 1.1783 * H + 0.1005 * S - 0.0151 * N - 0.1034 * O - 0.0211 * Ash \ [MJ/kg, d.b.] \quad (1)$$

where,
C, H, S, N and O are in [%] of carbon, hydrogen, sulfur, nitrogen and oxygen respectively.

$$LHV = HHV (1- w/100) - 2.444 * (w/100) - 2.444 * (H/100) * 8.936 * (1-(w/100)) \ [MJ/kg, w.b.] \quad (2)$$

where,
2.444 is the enthalpy difference between gaseous and liquid water at 25°C; 8.936 is the molar ratio between H_2O and H_2 and w is the moisture content of the fuel in wt % (d.b.).

Ultimate analysis

The elemental composition of the studied biomass was determined by ultimate analysis using an in-house elemental analyzer, Leco TrueSpec Micro (USA) for herbaceous biomass alfalfa and wheat straw and by an external analyzer (Eurofins Environmental testing AB, Gothenburg, Sweden) for the rest of the samples. To conduct ultimate analysis, there exists several modes of instrumental set-up i.e.; C-H-N, C-H-N-S or, oxygen mode, which can be chosen depending on the desired analysis elements (García et al., 2012). In this work, C-H-N-S mode was applied and thus the oxygen was evaluated by difference. The protocols used for the measurement of each elements and the obtained results are stated in the footnote of Table 4.1 (section 4.1.1).

Ash melting behavior analysis

Besides ash content, ash fusion temperature was measured by employing a heating microscope with a Rhodium furnace (HR18) set-up developed by Hesse Instruments, Germany, as shown in Figure 3.4.

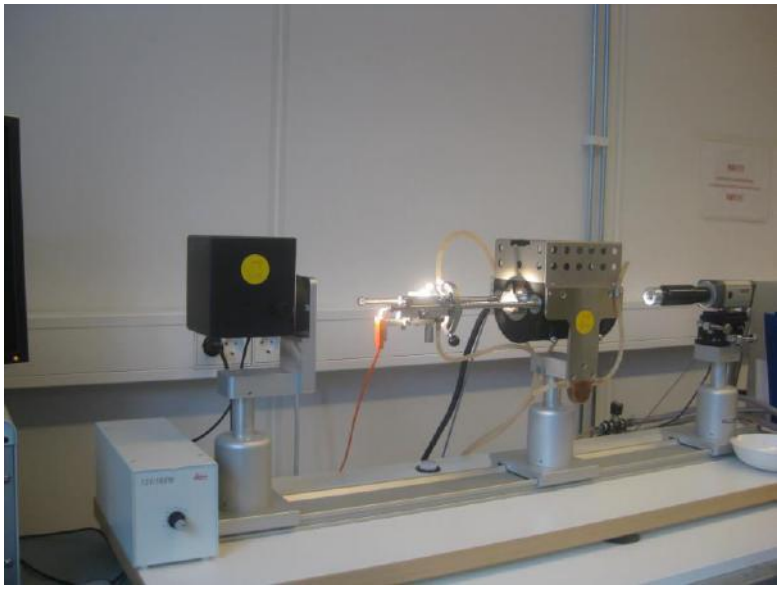

Figure 3.4: Heating microscope used for analyzing melting behavior of ash at University of Agder

The sample preparation for the analysis was conducted as according to the standard CEN/TS 15370-1:2006 (CEN/TS15370-1:2006, 2006), which is detailed in paper III. By this analysis, important temperatures such as shrinking temperature (ST), deformation temperature (DT), hemisphere temperature (HT) and flow temperature (FT) was measured and reported for further interpretation.

3.2.2 Thermogravimetric analysis

Thermogravimetric analysis gives quantitative evaluation of thermal decomposition of biomass over time as a result of chemical reactions (Carrier et al., 2011) occurred in presence of air or, inert environment or both. Simple experimental set-up that includes a precision balance and a furnace allowing constant (isothermal or static) or linear temperature rise, or the combination of both, can produce thermogravimetric analysis (TGA). Typical TGA curve shows a relation between mass versus temperature or time while a differential thermogravimetric (DTG) curve illustrates a relation between mass-loss rate and temperature or time. Both of these curves can provide a good basis for understanding the physical and structural properties of biomass and hence are important in this context.

TGA instruments and methods

In the present study, both TGA and DTG analyses were performed that investigated the thermal behavior of woody and herbaceous biomasses under a controlled heating so that obtained results can be used to compare gasification results of fixed bed and fluid-bed (chapter 4 & 5) experiments.

To carry out thermogravimetry tests, two different TGA instruments were used. For alfalfa and wheat straw, Thermal analyzer NETZCH STA 449 F3 Jupiter (Germany), was used; while for woody feedstocks (birch and willow), Thermal analyzer TA Instruments Q500 (USA), was employed.

Herbaceous samples (approximately 17-35 mg weight and < 5 mm particle size) were heated (at a heating rate of 10 °C/min) from room temperature until 950 °C

in three stages of heating (room to 110 °C, 110 °C to 600 °C, 600 °C to 950 °C) with variable dwelling using nitrogen as carrier gas. The heating program and the test protocol are detailed in paper III.

Wood samples (approx. 10-25 mg weight and < 5 mm particle size) were first heated from room temperature to 110 °C at 3 °C/min and kept at that temperature (110 °C) for 30 min so that moisture was evaporated. Samples were further heated and pyrolyzed to 900 °C at a heating rate of 20 °C/min and kept at the final temperature for 45 min to allow volatiles to be released. At pyrolysis stage, nitrogen was used as carrier gas with a flow rate of 100 normal mL/min. The samples were switched to combustion 20 minutes after holding at temperature 900 °C with air as oxidizing agent flowing at the same rate as of N_2 (during pyrolysis). To achieve repeatability, duplicate analysis of each sample was conducted.

Kinetics

The TGA and DTG results were further analyzed for kinetics. The knowledge gained from TGA kinetics help interpreting gasification and thus included in the present context. Kinetics of TGA data can be primarily obtained by the modeling techniques namely differential and integral (White et al., 2011), which are further classified as:

- Non-isothermal modeling (The differential method), and
- The Flynn-Wall-Ozawa modeling (Integral iso-conversional method)

The present work utilized the integral iso-conversional method or the Flynn-Wall-Ozawa (FWO) method. FWO involves the measurement of temperatures corresponding to fixed values of conversion fraction (α) from experiments at different heating rates (β), which is determined from the equation below:

$$log\beta = log\left[\frac{AE}{g(\alpha)R}\right] - 2.315 - 0.457\frac{E}{RT} \quad (3)$$

where,

A is pre-exponential factor, [1/s]

T is pyrolysis/gasification temperature [K]
E is activation energy in [kJ/mol]
R is the universal gas constant = 8.314 [Jg/mol K]

3.3 Fixed-bed downdraft gasification experiment

3.3.1 Gasification system

Once the feedstocks were prepared, woodchips and common reed briquettes were gasified by using an air-blown lab-scale fixed-bed downdraft gasifier.

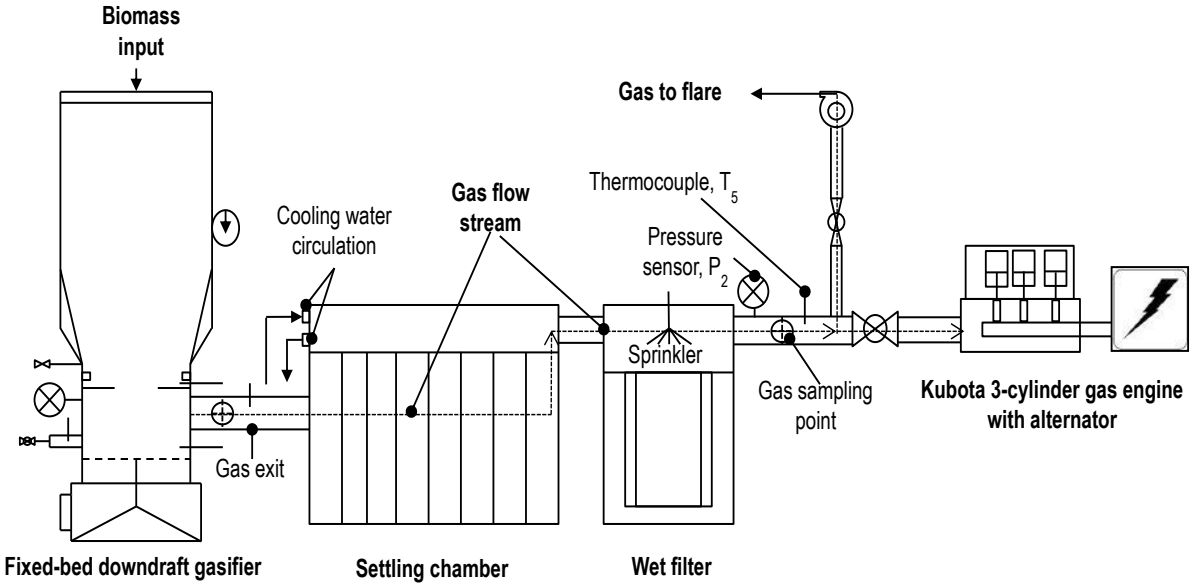

Figure 3.5: A generalized scheme of the actual fixed-bed downdraft gasification system

The gasifier (Victory Gasworks, Washington, USA) was a part of a gasification system (as shown in Figure 3.5) which, besides the reactor, composed of hopper, gas cooling and conditioning filters, heat exchangers, several pressure and temperature sensors, tar sampling point, ash handling chamber, U-scale (placed underneath the entire gasification system), flaring point, power generation unit

and gas sampling unit (Figure 3.6) that further employed series of devices to enable continuous measurement of evolved gas and data logging (via a LabVIEW module).

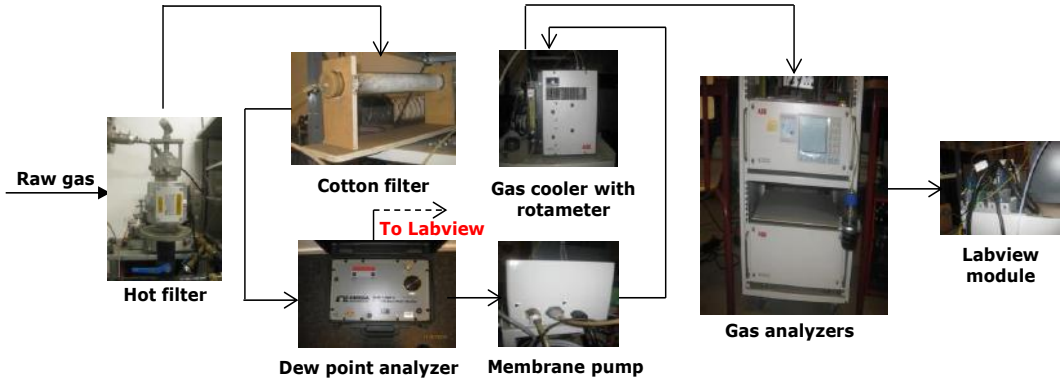

Figure 3.6: Flow diagram of the gas sampling unit

The gas produced as a result of gasification exited at the side of the gasifier and immediately cooled and conditioned. A close view of the gas cooling and conditioning devices is shown by Figure 3.7.

Clean tap water flow of ~2.8 kg/min was continuously supplied through the heat exchanger to cool the produced gas while hanging ribbons in the settling chamber and glass wool in the dry filter captured soot and particles. After cooling and conditioning, the gas was either directed to flare or engine depending on the needs. Noticeably, due to the lack of representative data, engine test results are not reported in this thesis although some successful runs were achieved.

The operation of the gasification system along with the gas sampling unit is discussed at length in paper I & paper IV. Here, only a short overview is presented. Further, the description of lists of individual parts composing the entire gasification unit is illustrated by Table 3.1 below.

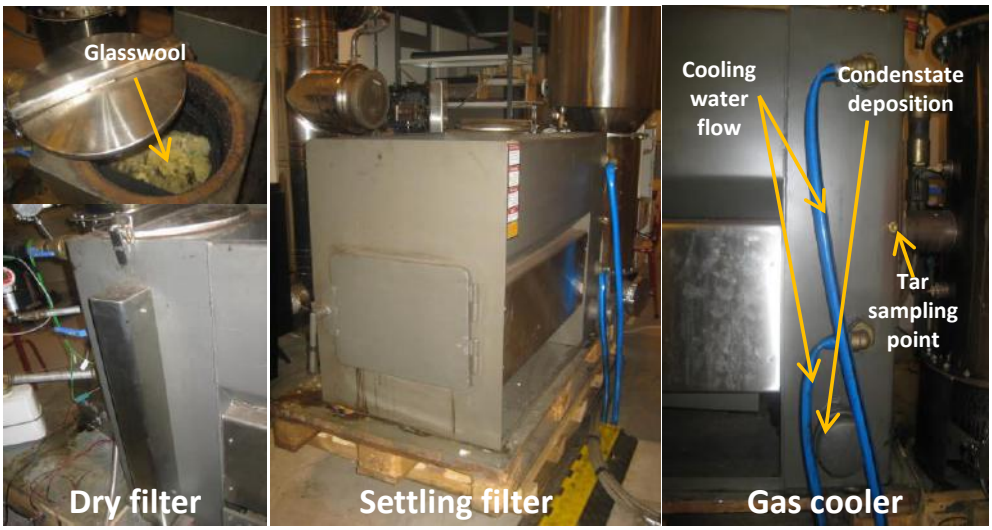

Figure 3.7: Gas cooling and conditioning devices

3.3.2 Test protocol

During start up, the gasifier was fed (batch fed, i.e.; fed only once) with charcoal (ca. 2 kg) and successively woodchips (7-12 kg) until a hopper height of ~ 0.2 m (from tip). The hopper lid was closed and air supply valve was opened allowing air to enter through the center of the reactor via 6 air supply nozzles (located just above an exchangeable restriction ring, 100 mm ∅). A draft fan, located downstream of the producer gas exit, created suction which caused the air to flow through the reactor. After feeding, the gasifier was ignited resulting the combustion of charcoal (generating necessary heat for gasification) followed by thermal conversion of input fuels.

Once ignition started, process achieved stabilization after slightly over half an hour which continued for another 5 - 6 h to allow data collection and process optimization. Periodic vibration of a shaker, placed at the side of the hopper, and reciprocal oscillation of a grate, located at the bottom of the reactor, assisting downward movement of the fuel as well as discharge of ash through perforated openings of the grate.

Table 3.1: Technical specifications and list of various components in the Fixed-bed gasification system and their usage

Item	Specification	Use
Gasifier		
Hopper	Material: AISI 304 & 316, Size: 0.5 mϕ, 0.13 m^3	Solid feeding (fuel + charcoal)
Reactor	Material: AISI 304 & 316, Size: 0.26 mϕ x 0.60 m	Thermochemical conversion
Restriction ring	100 mmϕ	Allowing concentrated high-temperature zone
Grate	0.26 mϕ, perforated	Fuel movement and ash disposal
Shaker motor		Avoiding bridging and chanelling
Air supply system		
Variable speed induced fan	Ventur SC 10A 055T (0.55 kW, 400 V), Sweden	Creating draft
Nozzle	Six pieces; size: ~ 5 mmϕ; position: 0.2 m height of the reactor (above the restriction ring)	Supplying gasification agent
Air diaphragm meter	0.04 - 6 m^3/h (BK-G4, Elster, Germany)	Registering air input
Filtration and cleaning system		
Gas-water heat exchanger		Gas cooling, tar + particulate collection
Settling chamber	Dry filter with hanging ribbons	Reducing raw gas particulates
Dry filter	Standard glass wool for insulation	Further raw gas cleaning
Ash chamber		Collecting residual char+ash
Instrumentation		
Balancing scale	DINI ARGEO, Italy; capacity: 1500 kg max.	Tracking weight change during fuel conversion
Temperature sensors (T_1 through T_5)	K-type (T1: downstream gas, T2: reduction, T3: gas exit, T4: combustion, T5: air inlet)	Measuring temperature at various zones
Pressure sensors (P_1 and P_2)	DCM/SN Diff, Fema, Germany (P_1: before filter, P_2: after filter)	Evaluating pressure difference before and after filtration
Sampling point at hot gas exit	Brass septum connector	Tar sampling based on SPA protocol
Gas sampling equipment		
Hot filter	Material: ceramic, FE2, ABB, Germany; working temperature: 150 °C	Reducing particulates from sampled gas
Cotton filter	Made of twist filter	Reducing aerosols from the sampling gas
Dew-point analyzer (chilled mirror)	Omega, RHB-1500, USA	Determining the gas moisture
Membrane pump	4N, ABB, France	Providing flow in the sampling line
Gas cooler	SCC-C, ABB, Germany	Drying the sampling gas at c. 3 °C
Non-dispersive infrared sensor	Advance optima, AO2020 (URAS 26); ABB, Germany	Analyzing CO, CO_2 & CH_4
Thermal conductivity detector	Advance optima, AO2020 (CALDOS 27); ABB, Germany	Analyzing H_2
Paramagnetic analyzer	Advance optima, AO2020 (MAGNUS 206); ABB, Germany	Analyzing O_2
Lab view module	National Instruments	Extracting real-time measurement to a stand alone PC for record and further analysis
Power generation unit		
Reciprocating Internal Combustion Engine	Kubota DG972-E2 (USA), Verticle 4-cycle (3-cylinder) liquid cool natural gas, 17.6 kW	Producing heat and power by using the producer gas

Once stabilization was achieved, the gasification performance was optimized by varying air supply between the range 3 and 8 m^3/h (by regulating the speed of the draft fan). The change in air supply simultaneously resulted in the change in feed flow, typically between the range 1.7 and 2.4 kg/h, the combined impact of which is usually expressed by a term called equivalence ratio (ER) - a ratio between actual air and stoichiometric air. The various aspects of gasification were analyzed with respect to this ratio which was calculated by following the equations stated elsewhere in paper IV. Moreover, the several other process parameters such as lower heating value (LHV), gas yield (Vg), cold gas efficiency (CGE) and carbon conversion efficiency (CCE) were calculated based on the equations given elsewhere in paper II & paper III. The further two process parameters namely tar (with liquids and particulates) and char were also determined analytically by accounting condensate from the gas cooler and the char residue left in the ash bin respectively. Residual char was further muffled at 550 °C (muffle furnace, Nabertherm P330) for approximately 20 h to precisely estimate the ratio between char and ash.

3.3.3 Analytical measurement

Temperature and pressure

To allow R&D, the gasification system was featured with a number of sensors and instruments located at raw gas line and sampling gas line respectively. In the raw gas stream, five K type thermocouples were used to determine the temperature profile at various gasification zones (located 150 mm apart along the reactor height), air input and gas exit respectively. Two pressure sensors measured the differential pressure before and after the gas filtration while air diaphragm meter registered the volumetric air input through the gasifier.

Gas sampling unit

During the gasification experiment, parts of the raw gas were continuously diverted through a gas sampling line (Figure 3.6) where further measuring instruments were located. Sample gas was first cleaned from particles by a hot

ceramic filter then passed through a diaphragm pump, a cotton filter, a chilled mirror dew point analyzer (for the measurement of gas moisture), a gas cooler and finally though different analyzer sensors measuring gas composition in terms of five principle components CO, CO_2, CH_4, H_2 and O_2 respectively. All the instruments were further connected to a stand-alone PC through a Labview (National Instruments, USA) module to facilitate data collection and storage. It is to be noted that cotton filter (indicated in Figure 3.6) was a new addition to the gas sampling line after the work for paper I was completed. Hence that device did not reflect to the gas sampling figure (Figure 3) of that publication. Additionally, wet teflon filter was replaced with a dry glass wool filter, the description of which logically was non-existent in the experimental section of paper I. Besides cotton filter and dry filter, a strategic sampling point (Figure 3.7) located at the hot gas exit was added to allow gas sampling for compositional analysis of tar, which complies with the SPA protocol detailed elsewhere at (Brage et al., 1997) and paper IV.

3.3.4 Mass balance

During gasification, the total weight of the gasification system was continuously monitored and to identify the measurement sensitivity and system reliability, the mass balance was conducted by considering the material inputs and outputs. For accounting inputs, dry air, biomass and moisture from both air and biomass were used, while for outputs, dry producer gas, dry char, tar, condensates, and moisture in the gas and char were considered. However, the particulates accumulated in the settling filter were not included in the total output calculations. The mass balance equations given elsewhere in the study by (Rao et al., 2004) was used as reference for the present calculation.

3.4 Bubbling fluidized bed gasification

To process local herbaceous biomasses from Spain, i.e.; alfalfa and wheat straw, two different bubbling fluidized bed (BFB) gasifier configurations namely a pilot

plant and a lab-scale plant was used. The pilot plant was mainly employed to treat alfalfa pellets while both alfalfa and wheat straw pellets were used for lab-scale gasification. The experimental set-up of the two gasification systems is succinctly discussed in the forthcoming sub-sections.

3.4.1 Pilot-scale bubbling fluidized bed gasification

Gasification system

The pilot scale atmospheric BFB gasification system at University of Zaragoza, Spain consisted of a feeding system, fluidized bed reactor, gas cleaning, tar sampling, ash disposal and gas measuring equipment including with a number of pressure and temperature sensors. The detailed description of the individual segment of the gasification system can be found elsewhere in paper II. Here, only their key features are given. The entire gasification unit is illustrated by Figure 3.8. Additionally, some of the important sections of the gasification system are shown by Figure 3.9.

The pilot scale gasifier operated with air as gasifying agent and processed biomass with a throughput capacity of approximately 10 kg/h (GPT, 2015). The reactor was made of AISI 310 refractory stainless steel with a diameter and height of 0.36 m and 3.5 m respectively, stepped vertically in two sections called bed and freeboard.

Along the height of the reactor seven temperature sensors (T_1-T_7) were spaced equally apart (140 mm) around the bed (T_2-T_6) and one each located at the bottom (T_1) and at the freeboard respectively (see figure 1, paper II). Additionally, two pressure sensors were positioned around the bed, spaced 0.115 m apart along the reactor height. To minimize heat loss and to reduce operational risk the entire reactor was covered from top to bottom with glass wool insulation blanket of 0.3 m thickness on the reactor's outer wall.

Air utilized for gasification was supplied to the bottom of the reactor through air nozzles and regulated by a mass flow controller operating between the range of

0.5 Nm^3/h and 100 Nm^3/h. Biomass and bed-material (silica-sand, avg. size: 367 μm) was continuously fed to the reactor via two augers attached to the corresponding hoppers of 40 kg each (one each for biomass and bed-material respectively).

Figure 3.8: Pilot scale gasification system at University of Zaragoza, Spain

Augers were independently driven by variable speed control motors and calibrated for a desired feeding rate before the start of a particular experiment.

The resulting raw gas from the gasification was conditioned and cleaned by a series of devices (such as cyclone, wet scrubber and char bin) located at various gas streams and solid recovery points respectively (refer figure 1, paper II). The cyclone removed the particles from the producer gas, wet scrubbers stripped condensable tars and cooled the gases while ash and char bin collected the solid residues left after the gasification tests. The solid and liquid residues obtained after each gasification operation were measured to account mass balance.

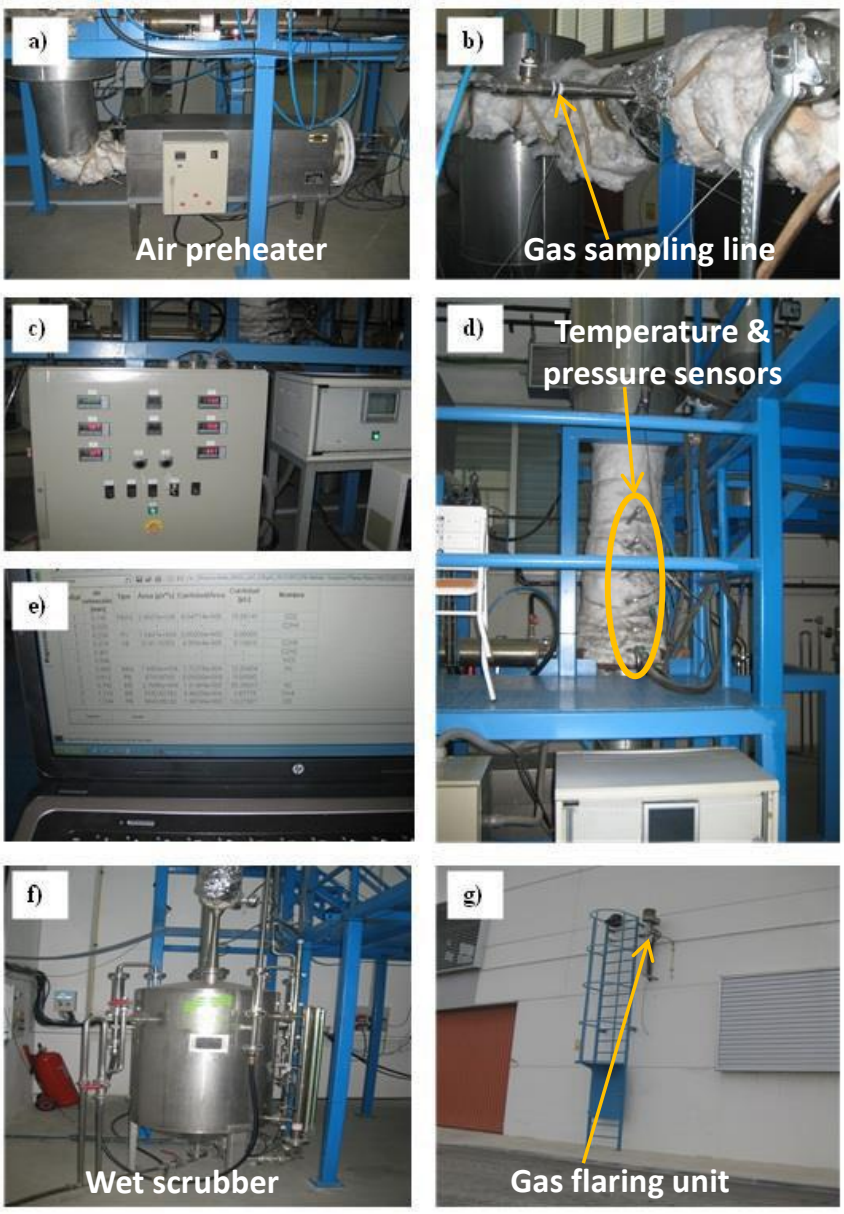

Figure 3.9: Close view of some important sections in gasification system (c) control panel for displaying operational parameters e) μ-GC standalone PC storing gas data; the rest of the figures are marked)

Test protocol

Test protocol of the current gasification facility followed several operational phases identified as pre-heating, combustion and gasification. During pre-

heating, hot air from an air-preheater (Figure 3.9a) was delivered to the reactor to increase bed temperature around 450 – 500 °C which was achieved approximately 3 h after start-up. As soon as the bed temperature reached to ca. 500 °C, a small amount of biomass was combusted, contributing to further increase temperature to a desired ca. 800 °C in about 20 to 30 min. The high temperature at this point set the gasifier in an auto-thermal regime at which gasification was initiated. Gasification was usually achieved by adjusting air flow rate (4.16 to 4.99 Nm^3/h), but keeping fuel flow rate constant at 4.7 kg/h. Present gasification tests were primarily investigated for two different stints characterized with two different values of equivalence ratio, namely 0.25 and 0.30. Each stint lasted for about 3 h during which stable data in terms of gas quality were collected and analyzed. After the end of an experimental run, the solid and liquid residues were recovered and accounted for mass balance. Further, to determine the proportional distribution of char and ash, the collected solid residues were muffled as according to the standard CEN/TS 15403:2006 (CEN/TS15403, 2006) and by-differenced. The expressions used to calculate various gasification parameters such as ER, gas LHV, gas yield, CGE and CCE are given in paper II (eq. 1 through 4).

Analytical measurement

Part of the gas from the main gas stream was diverted through a sampling line (Figure 3.9b) containing options for tar measurement and gas compositional analysis. By such analyses, performance of gasification was monitored continuously. The gas passing through the main exit was mixed with propane and flared outside the gasification unit (Figure 3.9g).

Tar measurement

The tar sampling section was located close to the gas exit in the gas sampling line, which served both as tar recovery and sampling gas cleaning. The entry of the gas sampling line was kept heated by an electric heating element (ca. 400 °C) to avoid tar condensation before the tar train. In the tar train, the sampling gas was first cooled through two cold condensers (~ 0.75 L each, filled with ice) from where tar was recovered and measured (Figure 3.10). Afterwards, the gas

was further cleaned by a cotton filter and then directed to the gas analysis system through a flow meter monitoring the quantity of the gas sampled. Fractions of the tar recovered from the condensers were analyzed for composition by using a GC-MS (Gas chromatography mass spectrometry) (Agilient 7890 A, USA).

Gas analysis

Gas quality, in terms of composition, was analyzed every two minutes by means of a micro-gas chromatograph (Agilient 3000A μGC, Model G2801A, USA) located downstream of the gas sampling line. The μGC consisted of two modules (Plot U and Molsieve 5A) which were calibrated for measuring different gas species prior experiments. Plot U determined gas components CO_2, C_2H_4, C_2H_6, C_2H_2 and H_2S while Molsieve analyzed gas species in terms of H_2, N_2, CH_4, CO and O_2 respectively. μGC data were recorded in a standalone PC (Figure 3.9e) for data analysis and interpretation.

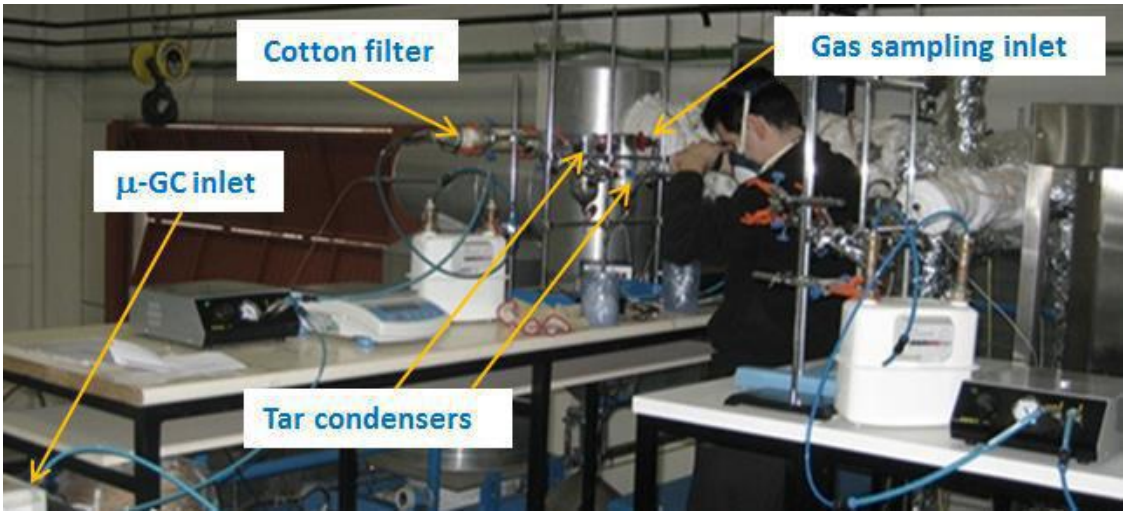

Figure 3.10: Real-time tar sampling

3.4.2 Lab-scale bubbling fluidized bed gasification

Likewise the pilot plant, a small scale BFB gasification facility also consisted of units for feeding, gas conditioning, gas analyzing, solid removal and gas and tar

sampling. The extended discussions of each of these components are presented in paper III. Below, only the important aspects are briefly covered.

Gasification system

The gasification facility (situated at UNIZAR) and its essential components are depicted by Figure 3.11.

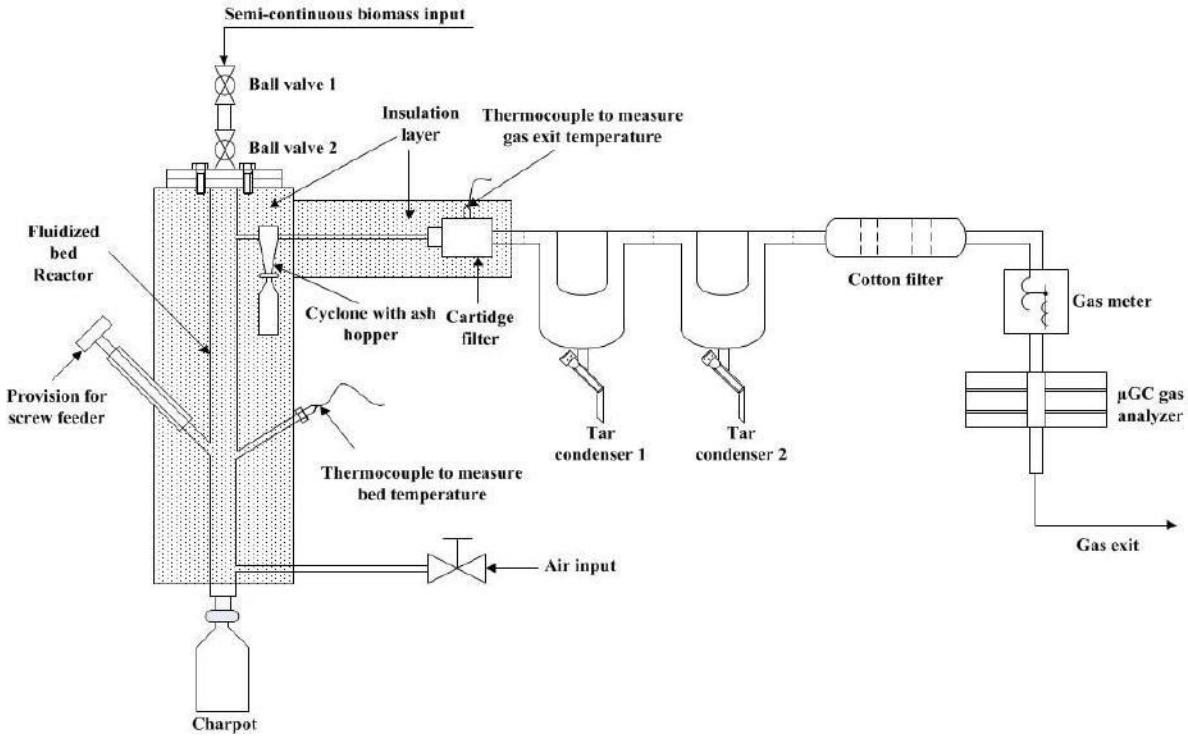

Figure 3.11: A generalized scheme of the actual lab-scale bubbling fluidized bed gasification system

The reactor is a fluidized bed gasifier made of AISI 310 refractory austenitic stainless steel cylindrical pipe with an inner diameter and height of 0.04 m and 1.5 m respectively. The entire reactor, including a cyclone and an ash hopper (located at the gas exit and the bottom of the reactor respectively), was enclosed to an electrical furnace providing start-up heat. At different access points (furnace, fluid bed, cyclone and gas exit) of the reactor, the temperature was monitored via a set of K-type thermocouples. The fluidized bed in the reactor

was made of silica sand constituted around 150 mm of static depth above the distributor plate (located close to the bottom of the reactor). The reactor operated with atmospheric pressure and air as gasifying agents, introduced at the bottom of the reactor in the range between 0.16 Nm^3/h and 0.25 Nm^3/h controlled via a flow controller system. The fuel feeding was achieved by directly introducing the fuel pellets (9-15 g) at the top of the reactor once in every three minutes (semi-continuous feeding) through a two-valve assembly. The operational procedure of the two-valve assembly together with the feeding strategy is described in detail in paper III. Here, only the feeding strategy corresponding to each ER is summarized in Table 3.2.

Table 3.2: Variation in batch feeding corresponding to ER

	Alfalfa pellets			**Wheat straw pellets**			
Equivalence ratio	0.23	0.30	0.35	0.20	0.25	0.30	0.35
Feed, gram per 3 min	10	10	10	15	12	9	9

The gas produced after gasification was cleaned by employing standard equipment: cyclone, char pot and hot filter (cartridge filter) where the char pot collected the unconverted char, the hot filter removed particulates and kept exit gas hot at ca. 400 °C (to avoid tar condensation in the gas stream). In the lab-scale installation, all the gas produced was used for sampling and hence no separate sampling train was required.

Test protocol

At gasification start-up, the furnace was electrically heated from room temperature up to a desired gasification temperature of ca. 850 °C, achieved in 3 - 4 h. A gasifying agent was introduced during pre-heating and continued until the end of the gasification so that necessary fluidization bubbling was kept. As soon as the gasification temperature was achieved, the semi-continuous manual biomass feeding was started after 10-20 min of which the gasification stability in terms of temperature (± 10° C) and gas quality (LHV: ±0.5 MJ/Nm^3) were

reached. After stabilization, gas sampling was started and lasted for about 45-60 min to facilitate operational data collection for further analysis. The operational parameters such as ER, gas LHV, CGE and CCE were determined by following the equations stated elsewhere in paper II & paper III. It is to be noted that the feeding scheme for two different fuels was different primarily to compensate the size of the pellets during manual feeding as well as to maintain theoretical minimum fluidization velocity (1.6 cm/s). Since the ER was the primary parameter varied and was aimed to keep between the range 0.20 and 0.35, accordingly, the air flow and the fuel feeding adjusted. For alfalfa, only the air flow was varied between the range of 0.16 Nm^3/h and 0.25 Nm^3/h, while for wheat straw pellets both air (0.21 Nm^3/h and 0.25 Nm^3/h) and feed flow (0.18 kg/h and 0.30 kg/h) were varied. Once a gasification test corresponding to fixed ER values ended, the solid residues and tar were collected and analyzed.

Analytical measurement

Analytical measurement of lab-scale plant such as quantitative and qualitative evaluation of tar, producer gas, ash, char, temperature etc. is fairly comparable to that of the pilot-plant. For pertinent discussion, readers are thus referred to the section 3.4.1 and paper III.

3.5 Techno-economic analysis of a producer gas generator in a standalone renewable hybrid plant

Including the optimization of gasification performance by using fixed bed downdraft and fluidized bed gasifier experiments, this research work aimed to evaluate techno-economic feasibility of a gasification-based renewable hybrid energy plant. To do so, an approach here was to develop a series of concepts for renewable hybrid energy plants with an option of producer gas generator, wind, photovoltaic, natural gas generator and diesel generator which potentially is able to meet a typical annual electricity demand of a standalone house located in Grimstad, Norway. Commercially, many simulation tools such as HOMER

(HOMER), Hybrid2 (HYBRID2, 2012), HOGA (HOGA, 2012) etc. provide options to build and optimize hybrid energy plants in terms of technical and economic feasibility. Among these tools, for convenience, HOMER (Hybrid Optimization Modeling Software) was chosen in this study.

By HOMER, the series of plant configurations using producer gas generator, wind, solar, natural gas generator and diesel generator was first optimized based on net present cost (NPC). Then a sensitivity analysis as a result of varying producer gas/fossil fuel price was performed to investigate the impact of fuel cost on the performance of hybrid system. Last, the best combination of sources forming the optimized hybrid plant in terms of technical and economic feasibility was chosen and proposed.

3.5.1 Model set-up

Based on the standard demographic data provided by the Statistical bureau, Norway (SSB, 2015), it was identified that a 2 kWe of base load power plant would be adequate to meet standalone electricity demand of a house remotely located in Grimstad. Considering this, first an energy model (see Figure 2, paper V) was built based on natural gas[*] or, diesel power generator (DG) of 2 kW capacity (for specifications see Table 3, paper V) each to power a remote house. Then a feasibility analysis of this model was performed in aspects of NPC, emissions and sensitivity of the fuel price.

In the next step, the natural gas/diesel generator was replaced by a producer gas generator and two other renewable sources such as photovoltaic (PV) (for specifications refer to Table 4, paper V) and wind (specifications: Table 4, paper V) to construct a hybrid plant facilitating the same amount of power as that of a fossil generator alone. For PV module simulation, the capacity of the device was allowed to vary between the range 1 and 3 kW and the annual variation of both temperature and solar irradiation was taken into account. The wind energy model, on the other hand, was simulated for the maximum wind turbine capacity

[*] Natural gas is scarce in Norway and hence propane is instead used in real applications. However, due to complexities of modeling propane sources in HOMER, natural gas (characteristically close to propane) resource was assumed as an available option for the present economic analysis.

of 1 kW. Besides PV and wind, battery and capacitor (for specifications, see Table 6 & 7, paper V) were also added to the model to facilitate power storage and power conversion. Power storage enhances energy reliability whereas power conversion transforms power according to the need of the end users. In the simulations, scenarios with or without battery, or capacitor were considered to evaluate their impact on the optimum configurations.

Once system configurations utilizing different renewable sources were completed, feasibility analysis followed by sensitivity analysis was performed. This resulted in a list of system configurations in the increasing order of NPC and levelized cost of energy (LCOE) from which an optimum renewable energy system was determined and proposed.

During the model set up, a range of energy-economic and system data used are shortly discussed in the forthcoming sub-sections and detailed in paper V, while the simulation steps are indicated by Figure 3.12 below.

3.5.2 Load data and energy sources

Load data (as shown in Figure 1, paper V) for the Grimstad household was presented with reference to the information provided by Statistics Bureau (SSB, 2015). According to this data, a single household in southern Norway consumes average 54 kWh/day of electricity with a peak load of 2.8 kW. Both mono and hybrid system models were developed in such a way that this demand was reliably met.

In regards to the energy sources, producer gas, natural gas, solar irradiation and average wind speed for the local condition were considered. The producer gas was assumed to be supplied from fixed-bed downdraft gasifier of the current project. Hence the production and price of the producer gas was considered to be influenced by the processing of biomass and the operating cost of the gasifier.

The solar radiation data for the studied site was extracted from the NASA meteorological dataset (NASA, 2015). Based on the data from NASA (NASA, 2015), the annual average solar radiation and clearness index of 2.84

kWh/m^2/day and 0.489 was assumed for the simulation (also shown in Figure 4, paper V). Moreover, the influence of annual ambient temperature was also included and shown by Figure 5, paper V.

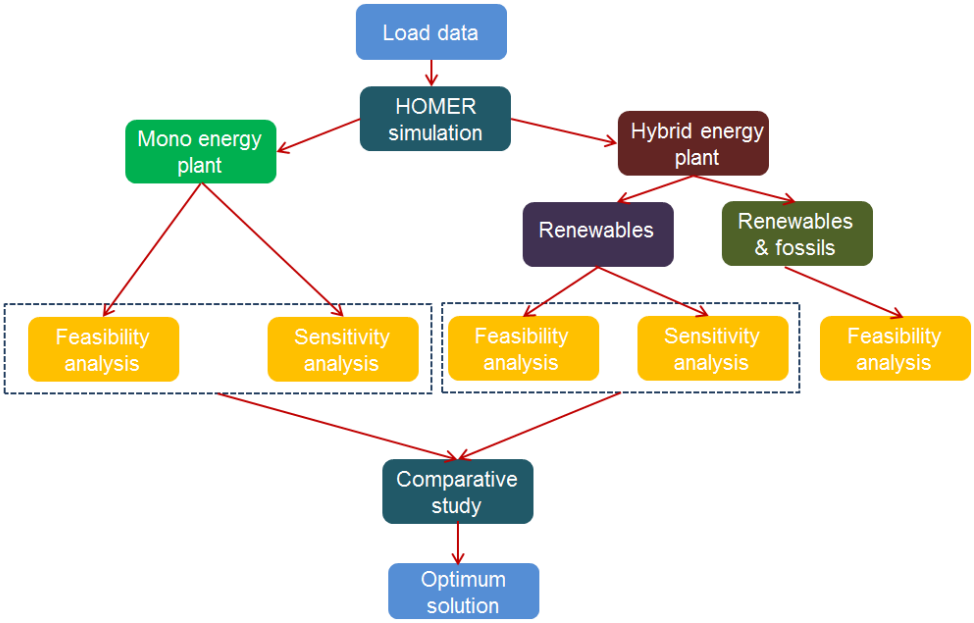

Figure 3.12: Simulation set-up and modeling steps

Likewise solar data, wind energy data were also adapted from the NASA meteorological dataset (NASA, 2015). Surrounded by the coast of the Skagerrak sea, the wind varying between the range 2.7 and 7.2 m/s throughout the year, is a potential renewable source of Grimstad. The monthly average wind profile in Grimstad can be viewed from Figure 6, paper V.

3.5.3 Emission parameters

In addition to energy and economic feasibility, HOMER also evaluates the viability of a model energy system in terms of emissions. Basically, six pollutants CO_2, CO, unburned hydrocarbon (UHC), particulate matter (PM), SO_2 and NO_x are accounted. In the present simulations, the annual CO_2 equivalent

emissions from all the modeled plants were calculated and compared in evaluating system performance corresponding to the environmental impacts.

4 Results and discussions

4.1 Biomass characterization

4.1.1 Physiochemical analysis

Results obtained from proximate and ultimate analyses are tabulated in Table 4.1 and the ash fusion temperature analysis results of herbaceous feedstocks are illustrated by Figure 4.1.

Table 4.1: Proximate, ultimate and LHV analysis of the studied feedstocks

Properties	**Proximate analysis**							
	Woody biomass					Herbaceous biomass		
	Birch	Oak	Spruce	Poplar	Willow	Alfalfa	Wheat straw	Common reed
Moisture, % w.b.	9.15	8.47	9.05	11.38	8.6	8	7.5	7.9
Volatiles;% d.b.	82.2	82.9	82.6	83.9	80.7	74.4	78.8	81.8
Ash, % d.b.	0.5	1.4	0.7	0.9	1.3	15.5	5.2	3.1
Fixed carbon, % d.b.	17.15	15.59	16.56	15	17.87	10.03	15.91	15
LHV, MJ/kg (d.b.)	20.0	18.9	20.3	19.7	19.8	16.7	18.4	17.7
LHV, MJ/kg (daf)	20.1	19.2	20.4	19.9	20.1	19.8	19.4	18.3
Elements (%)	**Ultimate analysis**							
	Woody biomass					Herbacious biomass		
	Birch	Oak	Spruce	Poplar	Willow	Alfalfa	Wheat straw	Common reed
Carbon (C)*	50.4	48.9	50.7	49.4	49.9	41.6	46.2	47.5
Hydrogen (H)*	5.6	6.0	6.0	6.0	5.9	4.9	5.4	5.6
Oxygen (O)**	43.4	43.5	42.4	43.5	42.4	33.9	42.6	43.3
Nitrogen (N)*	0.12	0.2	0.1	0.2	0.53	2.39	0.38	0.3
Sulfur (S)***	0.017	0.0	0.0	0.0	0.038	0.25	0.06	0.04
Chlorine (Cl)****	0.019	<0.011	<0.011	<0.011	<0.011	1.43	0.15	0.11

Analysis standard

*:EN 15104:2011; **: EN14918:2010; ***: SS 187177:1991; ****: EN 15289/15408; d.b.: dry base; daf: dry & ash free

Proximate analysis

Moisture content

Moisture content of all the biomasses ranged from ca. 8 % to 11 %. In general, the reasonably low moisture from the biomasses in the current laboratories suits well to the requirement of gasification principles.

Ash

Ash content in the two groups of biomasses i.e.; woody and herbaceous, were significantly different with the obvious highest from herbaceous and the lowest from woody feedstocks respectively. Among herbaceous biomasses, alfalfa resulted in ca. 16 % (d.b.) ash (paper II & III, Table 3.1), and wheat straw resulted in ca. 5 % (d.b.) (paper II and Table 4.1) ash respectively. The ash level of alfalfa in the present study is slightly higher than that of the past study (Boateng et al., 2008), but this did not reflect to the gasification difficulties in terms of agglomeration, sintering etc., as bed temperature was kept below the melting point of ash. Ash in the woodchips, on the other hand, ranged from 0.5 % to 1.4 % with the highest from oak and the lowest from birch respectively (paper IV and Table 4.1). Among the forest and the energy crops, generally, the latter showed a slightly higher ash content than that of the former, presumably because of the higher bark proportion in their wood due to the higher surface to volume ratio for the shoots compared to the bigger trees (Serapiglia et al., 2013).

Volatile combustible matter

The volatiles of all the biomasses ranged from ca. 74 % to ca. 84 % (Table 4.1) with expectedly higher values in wood than that of herbaceous ones. The obtained results in general showed a good agreement with the past study by (Boateng et al., 2008; Demirbas, 2004; Jenkins et al., 1998) for similar biomasses. As a rule of thumb, the higher the volatiles, the better the gasification, as fuel combustibility is enhanced (Basu, 2010).

Heating value

The LHV of all the investigated biomass is presented in Table 4.1. With some negligible exception, the observed values ranged from ~17 MJ/kg to ~20 MJ/kg (d. b.) which generally showed an inverse relationship to that of the level of ash. Expectedly, the actual woody biomasses owing to their higher carbon content resulted in higher LHV (Moka, 2012) than herbaceous ones (Table 4.1). However, in case of dry and ash free analysis, the LHV of all the samples was found fairy similar (Table 4.1), meaning the combustible part of the biomasses has fairly the equal LHV regardless the type.

Ultimate analysis

Ultimate analysis revealed that the chemical compositions of woodchips were superior in terms of C and H and inferior in terms of Cl, S and N to herbaceous biomass. C and H positively contribute to the quality of producer gas from gasification and hence their high value is desirable. Conversely, Cl, S and N, are the ash indicating elements and thus their high value in herbaceous biomass is less suitable to gasification. Based on these facts, woody feedstocks had the chemical characteristics more favorable towards gasification.

Ash fusion temperature analysis

The ash fusion temperature analysis results for herbaceous biomasses are illustrated by Figure 4.1.

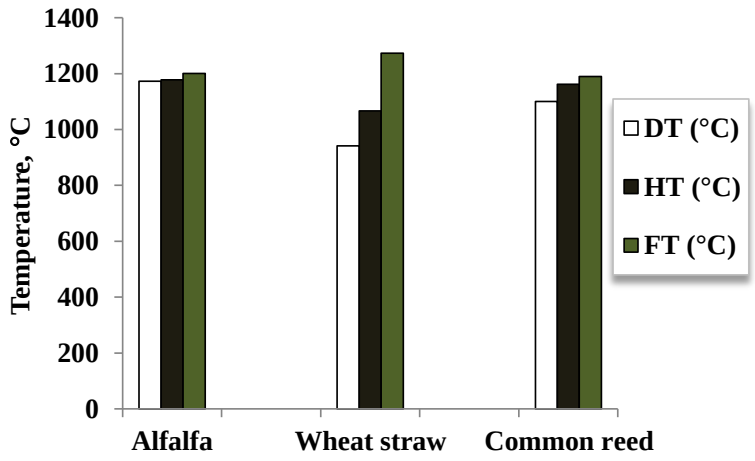

Figure 4.1: Characteristic temperatures during ash melting test of herbaceous biomass samples in oxidizing atmosphere. DT is deformation temperature, HT hemisphere and FT flow temperature

As can be seen, alfalfa resulted in the highest DT and HT, while wheat straw resulted in the highest FT. Common reed yielded lower DT and HT than those of alfalfa, but the FT between these two samples was fairly similar. Ash melting temperature is generally a function of the composition of various metals and

oxides present in biomass ash (Li et al., 2013). Generally, the higher the presence of alkali metals (such as K), the lower the melting temperature of ash (Wang et al., 2008). However, this could differ if the proportionate composition of other metals/minerals varies. It is worthwhile to note that the correlation between ash melting temperature and composition is not covered in the scope of the present research and hence melting temperature from the present results cannot be utilized to predict composition of ash. Nevertheless, from the present analysis it is clear that at reactor bed temperature exceeding ca. 1200 °C, wheat straw ash is less likely to start melting compared to that of alfalfa and common reed. It is worthwhile to note that agglomeration as a result of ash melting and such was not encountered in the present gasification experiments.

4.1.2 Thermogravimetric analysis

TGA and DTG plots

The weight loss curves of birch and willow for a heating rate of 20 K/min to 900 °C, and of alfalfa and wheat straw for a constant heating rate of 10 K/min 600 °C is shown by Figure 4.2. The samples showed three steps of mass loss, occurring at the stages of moisture evaporation, devolatilization and finally char conversion to ash. Although moisture evaporation for all the feedstock resulted in similar amount of degraded mass, distinctive differences exhibited due to the devolatilization and char conversion. Expectedly, a greater extent of mass loss was obtained from woody feedstocks during devolatilization and char conversion stages due to the presence of higher level of volatiles and less amount of ash (Table 4.1). However, the onset of devolatilization from the woody biomass was delayed and occurred at ca. 200° C in contrast to ca. 170° C from herbaceous feedstock (see Fig. 4.3). This was presumably due to the difference in the structural composition. Wood in general contains higher level of cellulose (Shahzadi et al., 2014) which may in turn contribute to increase thermal stability and as such the start of devolatilization at a relatively higher temperature.

As far as differential thermogravimetric, DTG profiles (Figure 4.3) are concerned, maximum rate of weight loss for all the investigated biomass fell

between the range ca. 293 ° C and ca. 380 °C. For the woody biomass, especially for birch, the peak was identified at the highest of ca. 378° C.

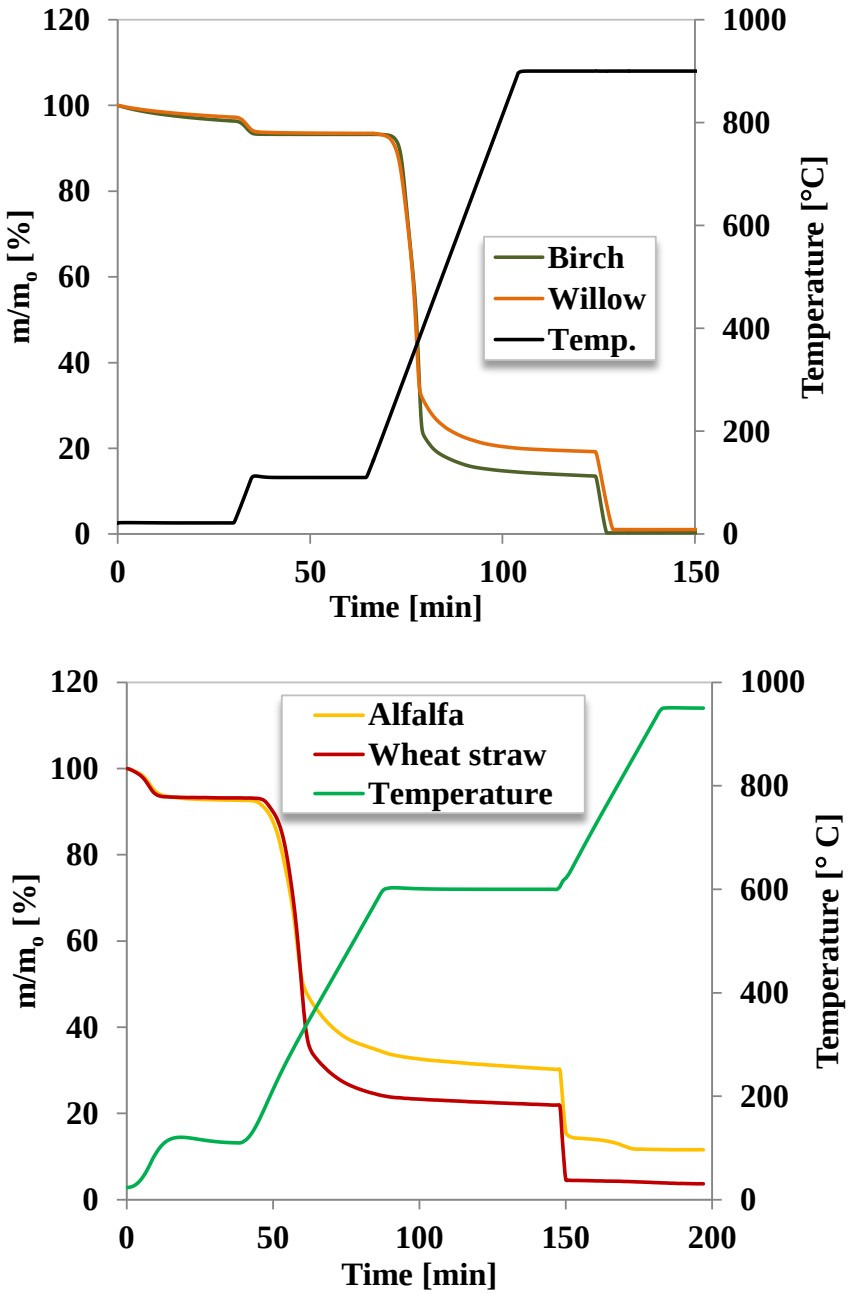

Figure 4.2: TGA plots of two classes of biomass (top: wood; bottom: herbaceous)

Moreover, this biomass showed a second peak at around 316° C, which was expected, due to the partial degradation of hemicellulose; as theoretically this component decomposes at a lower temperature than that of cellulose (Varhegyi et al., 1989).

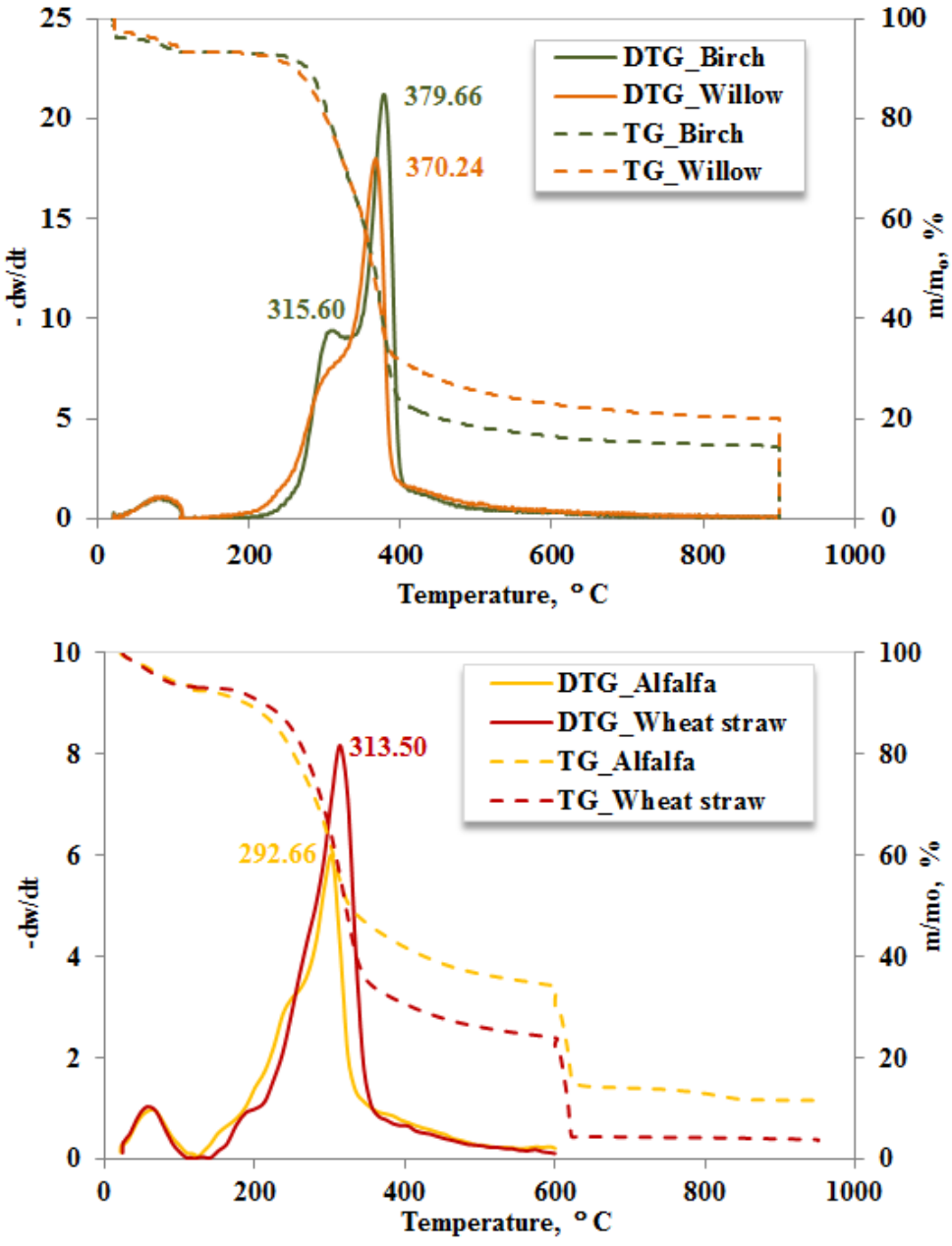

Figure 4.3: DTG plots of two classes of biomass (top: wood; bottom: herbaceous)

Despite woody biomass of the same class (hardwood), this peak however was not distinctive from willow. The shoulder-like hemicellulose peak for birch was also observed in a past study by (Shen et al., 2009). Additionally, that study (Shen et al., 2009) also encountered no-shoulder hemicellulose peak from softwood comparing to that of hardwood due to the difference in the degree of hemicellulose decomposition between these two wood species (Ramiah, 1970). The reduced hemicellulose peak from the present willow might have been a result of its higher ash content compared to that of birch (Table 4.1).

In regards to the DTG curves for the samples of herbaceous biomass, wheat straw exhibited a peak at a slightly higher temperature than that of alfalfa. However, the second peak characterizing hemicellulose degradation was not discernible from this feedstock (Pasangulapati et al., 2012) although an evidence of slight evolution was noticed from alfalfa. The hemicellulose decomposition is likely to be influenced by the presence of inorganic components like alkali metals such as potassium and sodium which perhaps contributed to diminishing the appearance of hemicellulose shoulder from the DTG curve of wheat straw (Greenhalf et al., 2012). However, since the analysis of alkali metals was outside the scope of this work such relationship cannot be precisely compared. It is also noticed from DTG plots that both woody and herbaceous biomass degraded over a broad range of temperature probably due to the presence of lignin (Shahzadi et al., 2014), which by far is the most thermally stable structural components of biomass. Noticeably, part of the DTG curve covering the stage of combustion (illustrating char conversion) has not been discussed here, since char combustion was already mentioned along with TGA results above. By using eq. (3) from Section 3.2.2 the logβ vs. 1/T plots for the feedstocks alfalfa, wheat straw, birch and willow is shown in Figure 4.4.

Based on these plots and using the data of the slopes of eq. (3) (Chapter 3), obtained kinetic analysis data from devolatilization is summarized in Table 4.2. As can be seen (Table 4.2), the conversion ranges of kinetic data for the two herbaceous and woody biomass types differed with the lower range for herbaceous biomass, 0-40 % and the higher range for the woody biomass, 0-60 % respectively. This was due to the fact that mass conversion rate of the herbaceous

biomasses was much faster beyond 40% degradation, leading to unstable kinetic data beyond that range. The activation energy (E), on the other hand, varied between the ranges from 52 to 106 kJ/mol., being lower for herbaceous and higher for woody biomass respectively.

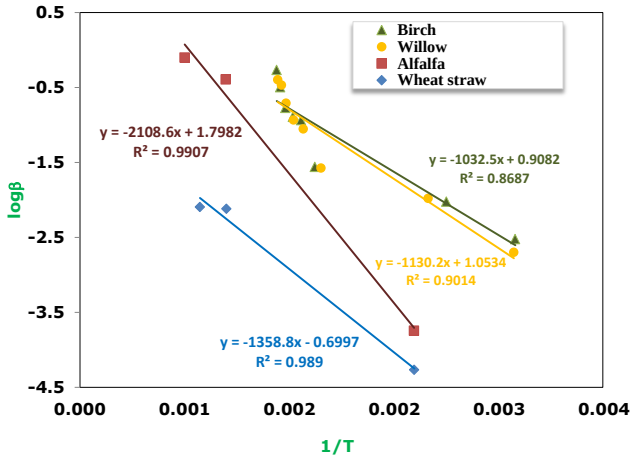

Figure 4.4: logβ vs. 1/T plots for kinetic analysis of TGA data

Table 4.2: Kinetic analysis results for the selected biomass based on Flynn-Wall-Ozawa method

Feedstock	E, kJ/mol	A, [s^{-1}]	r^2	Conversion range, %	Temperature range, K
Birch	106.06	6.23E+27	0.8687	0-60 %	294-651
Willow	102.23	2.21E+17	0.9014	0-60 %	294-647
Alfalfa	52.44	2.01E+06	0.9907	0-40 %	294-575
Wheat straw	85.23	7.75E+09	0.9890	0-40 %	294-578

Activation energy of 106 kJ/mol. for birch was in good agreement with the study by Shen et al. (Shen et al., 2009) while for wheat straw, the activation energy was dramatically different than that of by (Cai & Bi, 2009). The past work, however, used a different conversion range (10-85 %). Literature studies devoted to examine the activation energy of alfalfa and willow are scarce and hence clear

comparison of these feedstocks cannot be made. One property that perhaps further explains activation energy is structural composition which due to the relevance is depicted in Table 4.3, referring the data presented in paper II & IV and in Phyllis database (Phyllis2) for wheat straw.

Between the two group of biomass, herbaceous biomass in general contained less lignin and somewhat lower cellulose which potentially was the reason contributing to the variation in activation energy (see Tables 4.2 & 4.3). Theoretically, higher presence of which would potentially enhance activation energy as lignin is thermally stable at higher temperature. Further, the degradation behavior of hemicellulose might also influence the magnitude of activation energy.

Table 4.3: Variation in structural composition between herbaceous and woody biomass

Feedstock	Cellulose*, %	Hemicellulose*, %	Lignin*, %
Alfalfa	30.0	13.0	15.0
Wheat straw	37.9	26.8	18.3
Birch	40.6	29.6	26.3
Willow	38.5	17.6	26.3

* Phyllis 2 database

From the DTG analysis curves in Figure 4.3, it can be recalled that hemicellulose peaks for the herbaceous biomasses were not distinctive compared to those for the woody feedstocks and therefore the dissimilarity in activation energy between these two biomass types.

4.2 Fixed-bed downdraft gasification

Summary results of the biomasses regarding downdraft gasification are discussed in the forthcoming sub-sections. For elaborated discussions, readers are however referred to the published papers (I & IV), attached at the end of this thesis.

4.2.1 Gasification of woody forest crops

Gasification of birch (paper I & IV)

Birch was the first forest crop used in this study. The preliminary test on this biomass was complemented with more tests at the later stage with a modified experimental set-up. Primarily, the design in regards to the draft fan, grate and gas purification filters were altered and as a result, the obtained parameters differed. The results of both these tests were individually discussed in paper I & IV. Below, only the comparison of their performance is briefly discussed.

Performance comparison: preliminary test (paper I) vs. recent tests (paper IV)
The summarized results from paper I (Sarker & Nielsen, 2014) in terms of important gas compositions, ER, LHV, Vg, Q_{air}, m_{feed}, CGE, and bed temperature is shown in Table 4.4.

From Table 4.4 it appears that the preliminary gasification was immature, especially because of the fact that the gas LHV, bed temperature and air flow were lower than the acceptable range of typical gasification. For example, it is known that gas LHV less than 4 MJ/Nm^3 is not suitable for downstream utilization (Arjharn et al., 2012). Also, low H_2 and low CO in the gas composition reduce the possibility of using gas either for Fischer-Tropsch synthesis (Buragohain et al., 2010) or, for fuel cell conversion (Buragohain et al., 2010). The low bed temperature and simultaneously the low CO_2 most likely was a result of limited exothermic combustion reactions (providing heat for gasification). This further explains that the endothermic Boudouard, water-gas and shift reactions (Figure 2.5) could not fully establish, and as such, the low ratio of H_2, CO and CH_4 in the producer gas composition. Imbalanced interaction between exothermic and endothermic reactions possibly contributed to technical difficulties in the form of bridging, abrupt change in air flow resistance and degraded quality of the producer gas and therefore revealed poor gasification performance in the preliminary test.

Table 4.4: Comparison of average gasification results between two different tests on birch woodchips

Properties	Preliminary test	Recent tests (avg. of 3 runs)
Test year	2013	2014-2015
Average air flow rate, Nm^3/h	1.8	3.8
Biomass feed rate, kg/h (as received)	0.7	2.1
ER range	ca. 0.25-0.80	ca. 0.19-0.80
Total operation time, min/run	ca. 350	ca. 320
Average gas composition		
CO, % wt.	12.3	19.2
CO_2, % wt.	5.5	9.9
H_2, % wt.	6.7	11.1
CH_4, % wt.	0.5	2.1
LHV, MJ/Nm^3	2.4	4.4
Avg. bed temperature, °C	434	634
Avg. gas yield, Nm^3/kg	2.92	2.1
CGE, %	35.5	44.5
Char yield, g/kg	N.D.	131.6
Tar +liquid yield, g/kg	N.D.	16.6
Ash yield, g/kg	N.D.	16.2

Nevertheless, the experience gained from this experiment provided a good foundation to incorporate future modification in various areas i.e.; air supply fan, grate movement pattern, wet filter, etc. which eventually resulted in improved gasification performance for the later runs reported in paper IV.

Concerning later tests, the gasification performance was evaluated based on three similar runs with identical feedstocks. The gasification tests were primarily conducted for a varied ER ranging between 0.19 and 0.80, which affected the evolution trend of different operational parameters (Table 4.4). The average gas composition by volume $\%_{\text{dry base}}$ for the four main gas species CO, CO_2, H_2 and CH_4 were 19.2 ± 0.62, 9.93 ± 0.40, 11.07 ± 0.80 and 2.07 ± 0.25 respectively. These values, especially the amount of combustible components demonstrated a

good potential to producer gas downstream utilization as the gas LHV reached to mean 4.37 ± 0.15 MJ/Nm^3. The average air flow, fuel flow and bed temperature reached to 3.83 ± 0.26 Nm^3/h, 2.06 ± 0.09 kg/h and 634 ± 46 °C respectively and were significantly higher than those obtained from the preliminary operation. These values may have improved thermal decomposition and as such enhanced performance in regards to CGE (44.5 ± 0.53 %), char (131.6 ± 99.79 g/kg), tar (16.64 ± 8.92 g/Nm^3) and ash (16.2 ± 9.56 g/kg), which to some extent comply with the literature (Sheth & Babu, 2009) for similar biomass. Moreover, the optimum ER range (0.37-0.43) coincides with the past study (Zainal et al., 2002) on gasification of woody biomass. It can therefore be concluded that gasification of birch under the present reactor configuration is feasible and suitable to contribute to local bioenergy expansion.

Gasification of forest and energy crops (paper IV)

Gasification tests using forest crops birch, oak and spruce and energy crops SRC poplar and willow were performed under a similar experimental condition for a variable ER between 0.19 and 0.80. The ER affected the evolution of number of process parameters: producer gas compositions, LHV, Vg, CGE, CCE etc., which in light of each experimented feedstock are discussed and illustrated by Figures 4.5 through 4.8 below.

Effect of ER on producer gas compositions

Producer gas from the gasification of woody feedstock, mainly composed of the major species CO, CO_2, H_2, CH_4 and N_2 whose distribution varied as input feedstocks and process conditions, varied.

As the ER gradually increased, the evolution of different gas species differed and exhibited different tendencies (see Figures 4.5 & 4.6). CO for example showed a varying upward and downward trend for most of the biomass except poplar for which the trend was increasing throughout (statistically insignificant; $p = 0.05$). The CO trend increased between ER 0.32 and 0.50, and thereafter decreased. Expectedly, due to the influence of Boudouard reaction (Sarker et al., 2015), the evolution of CO_2 was inverse (downward and upward) to that of CO. Likewise

CO, the other combustible species such as CH_4 and H_2 showed varying tendencies with ER as the feedstock differed (see section 3.2.1, paper IV).

Effect of feedstock on gas composition

Woody energy crops in general yielded a lower average CH_4 and higher H_2 than those of forest crops. This may primarily be due to the enhanced reforming reactions at an expense of CH_4 (Ni et al., 2006), or, due to the enhanced endothermic water gas and shift reactions (Sarker et al., 2015). For CH_4 alone, willow contributed higher values than that of poplar likely due to the enhanced methanation. Among all the biomasses, spruce by far had the lowest average H_2 which was likely due to the compromised water-gas reaction (Purdon, 2010).

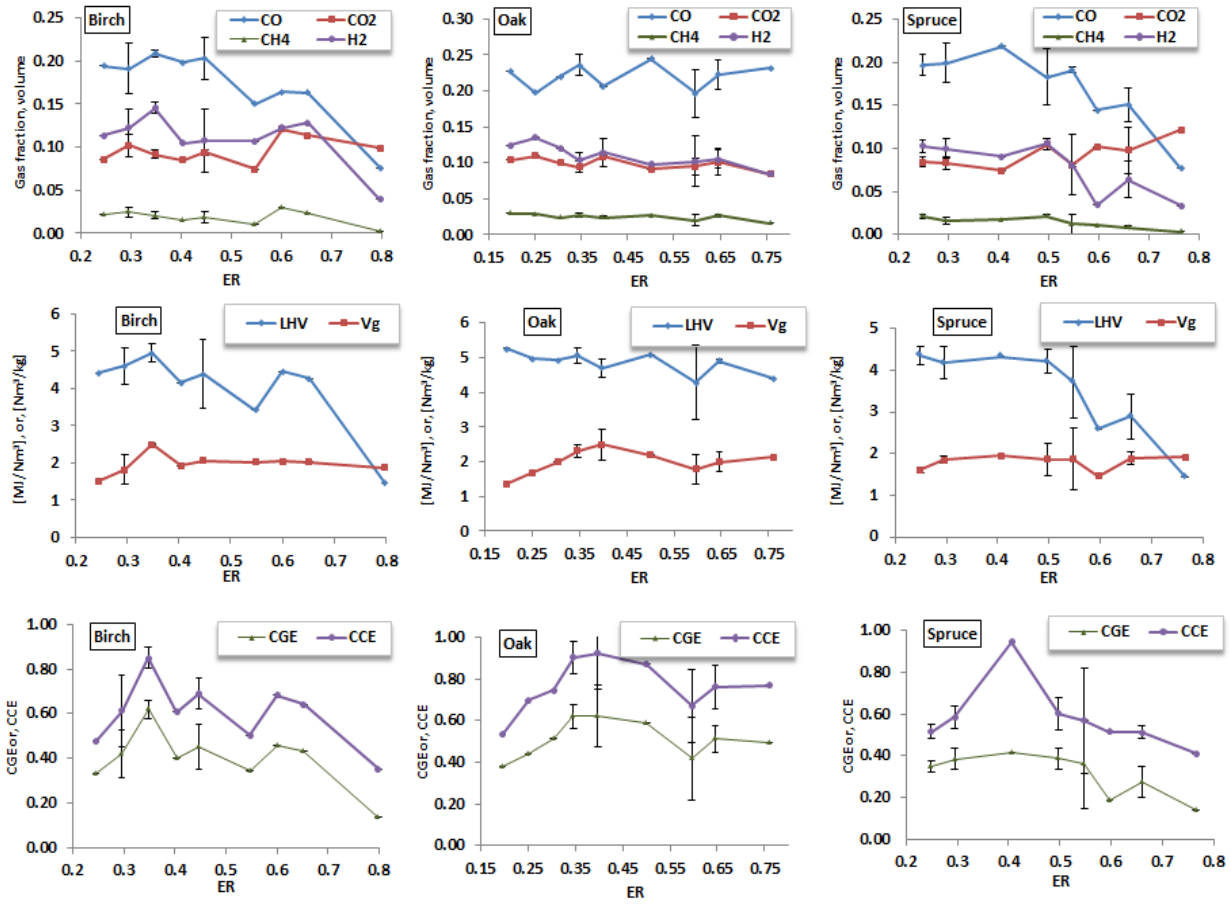

Figure 4.5: Effect of ER on gas compositions and gasification performance of forest crops

The balance of the mentioned reactions maybe influenced by the bigger forest woodchips with thicker bark in contradiction to much smaller chips from young shoots from willow and poplar.

Effect of ER on performance of gasification

As the ER varied, the gas compositions and the gasification performance in regards to gas LHV, gas yield (Vg), CGE and CCE were affected as the ER. The relationship between these parameters and ER are detailed in paper IV. Below, only their key points are discussed.

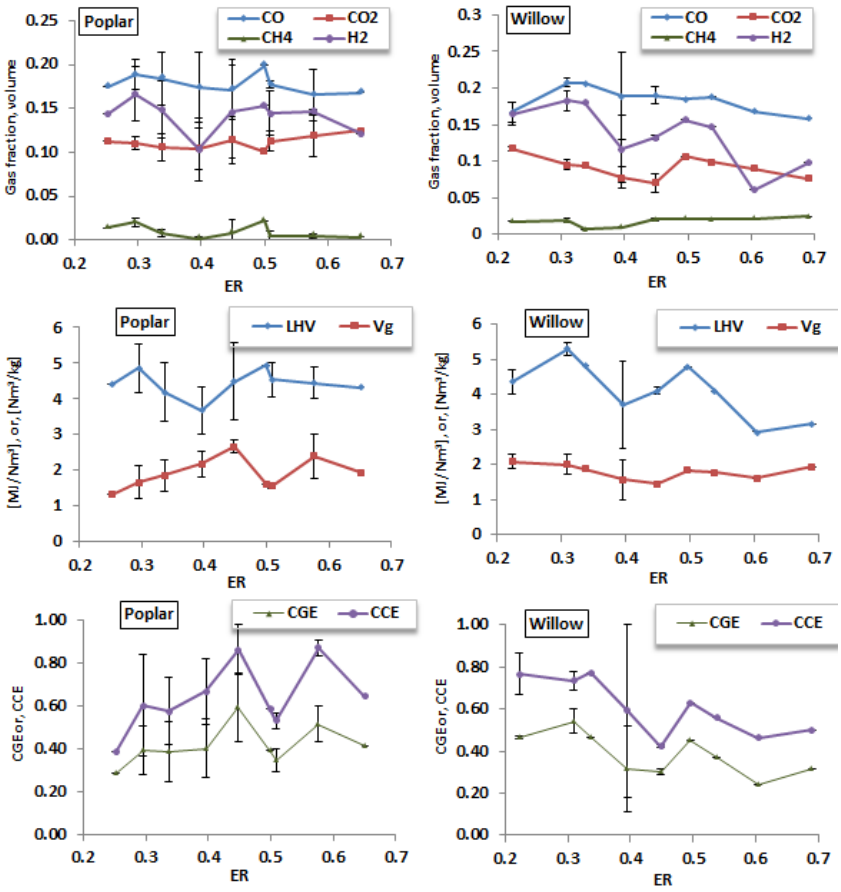

Figure 4.6: Effect of ER on gas compositions and gasification performance of energy crops

First, in terms of the producer gas LHV for forest crops (birch, oak and spruce), the trend was increasing and decreasing (with ER) with mean value ranging between ca. 4.0 MJ/Nm^3 and ca. 4.5 MJ/Nm^3. Spruce yielded the lowest average LHV (ca. 4.0 MJ/Nm^3) corresponding to the highest (of 4.5 MJ/Nm^3) from oak, while birch showed a somewhat similar (~2 % lower) yield to that of oak. Since spruce had the lowest average yield of H_2 and CH_4 (see Figure 5, paper IV) this biomass produced the lowest average LHV. On the other hand, the production of total combustible gases between birch and oak was pretty similar and thus the similar yield in terms of average producer gas LHV.

Between the energy crops, the average gas LHV from poplar was found higher than that of willow presumably because of the increased level of average CO and H_2. Interestingly, in this group of biomass, the higher CH_4 yield from willow (Figure 4.6) could not compensate for the concurrent decrease in CO and H_2 and therefore obtained at lower gas LHV than that of poplar.Noticeably, among the individual gas species measured, CH_4 has the highest LHV and thus a little variation of this component could lead to a greater variation in gas LHV.

Second, in terms of mean gas yield (Vg) most of the feedstocks (except spruce) followed the similar increasing and decreasing tendencies to that of gas LHV as the ER stepwise rose. Generally, the average Vg for the studied woodchips varied between 1.76 Nm^3/kg and 2.17 Nm^3/kg, with the highest from oak and the lowest from spruce respectively. The lower H_2 content in the producer gas from spruce was thought to decrease gas yield while higher combustible quantities might be the reason why oak resulted higher amount of producer gas. Theoretically, the factors such as devolatilization, air input, fuel input and type, fuel moisture, etc. dictate the gas yield from gasification. Typically, at optimized ER, the strength of devolatilization increases (Gómez-Barea et al., 2005) and accordingly, the increased quantities of producer gas.

Third, the trend of the efficiencies (CGE and CCE) was expectedly influenced by the combined effect of gas LHV and Vg. Average CGE of all biomasses ranged between ca 35 % and ca 45 % while CCE averaged between 62 % and 72 % respectively. These values (CGE and CCE) assess the main performance of

gasification in respect to all the measured input and output parameters. In addition, LHV and Vg are also closely linked to the factors such as bed temperature, char yield, tar yield, etc. The interrelationships between these parameters are however not discussed here and covered in the following sub-section (also in section 3.3, paper IV), as of relevance.

In short, the optimized ER at which the gasification performance in respect to various process parameters (gas compositions, gas yield, gas LHV, CGE and CCE) of all the woodchips maximized ranged between 0.29 and 0.45 which are in good agreement with a past study (Zainal et al., 2002) related to gasification of wood.

Effect of bed temperature on performance of gasification

Together with the ER, bed temperature is also an important parameter affecting gasification. The bed temperature is correlated to the ER (see Figure 4.7).

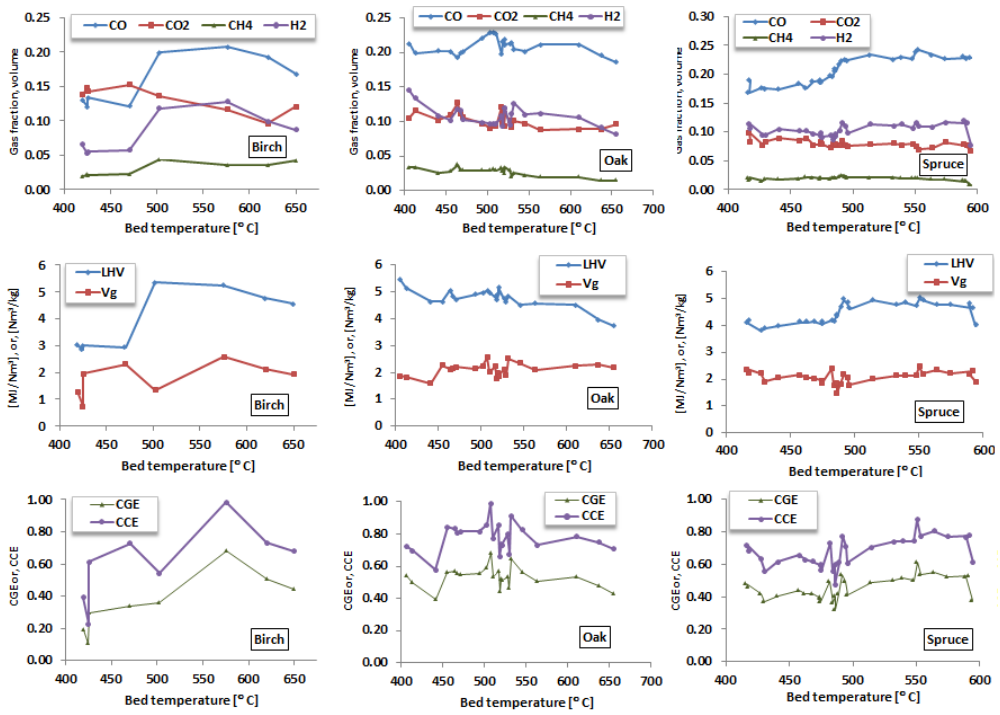

Figure 4.7: Effect of bed temperature on gas compositions and gasification performance of forest crops

Noticeably, the measured bed temperature for the present experiment might not reflect exact temperature during operation as temperature sensor was positioned slightly away from the reactor bed. Nevertheless, for simplicity the temperature correction was not performed and measured temperature is considered as bed temperature. In general, the maximum bed temperature for all the fuels ranged between ca. 600 °C and ca. 770 °C with the highest from willow and the lowest from spruce respectively. Among the forest crops, birch and oak achieved the maximum bed temperature of 700 °C corresponding to 600 °C for spruce. Energy crops in general exhibited higher bed temperature than that of forest crops, being ca. 750 °C for poplar and ca. 770 °C for willow respectively.

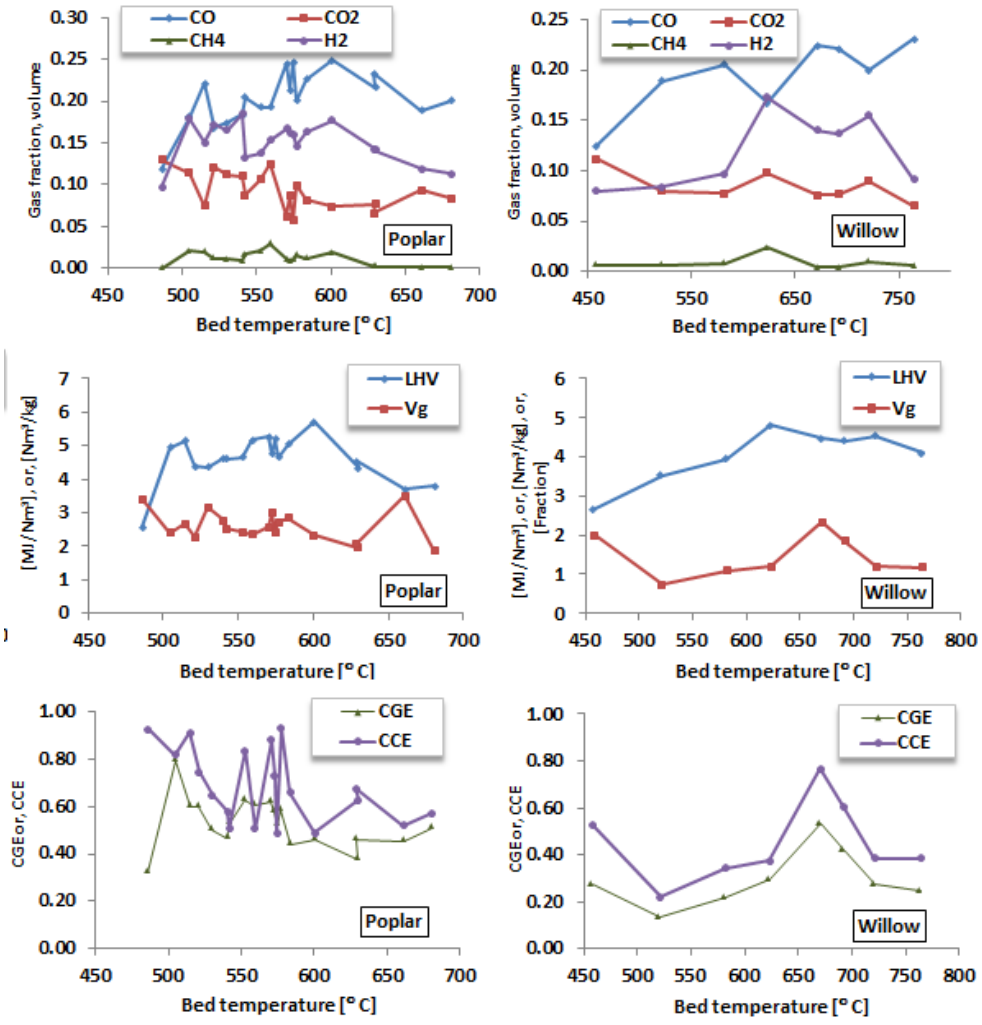

Figure 4.8: Effect of bed temperature on gas compositions and gasification performance of energy crops

With the evolution of these temperatures, the process parameters varied and exhibited different trends. For example, the average gas LHV, regardless of the type of biomass, showed a simultaneous increasing and decreasing trend as the bed temperature increased (Figures 4.7 & 4.8).

This is consistent with the theory: the higher the bed temperature, the higher the exothermic oxidation reactions and lower the production of combustible gas, and thus lower the gas LHV. The average gas yield (Vg), on the other hand, did not show any clear trend. Apparently, Vg for most of the crops tended to optimize within the bed temperature of 550 °C and 600 °C beyond which the trend was either increasing or decreasing. The higher gas yield at higher bed temperature is a result of combustion reactions as for birch while the lower gas yield at higher bed temperature was caused due to the dilution of gas with enhanced N_2 (as for oak, spruce and energy crops). With the concurrent effect of gas LHV and Vg, the average CGE for all the biomasses resulted in a varying upward and downward trend. Noticeably, among all the crops, spruce yielded the lowest average CGE owing to its combined lowest average gas LHV and gas yield, while oak resulted in the highest average CGE due to the contrasting reasons to that of spruce. Likewise CGE, average CCE followed the similar increasing and decreasing tendency with bed temperature, although the absolute value for willow reached its maximum at a higher bed temperature 700 °C than that of the rest of the crops. This might have been caused by the difference in physical properties such as bulk density, proportion of bark in wood, etc.

4.2.2 Preliminary gasification of common reed briquettes

In addition to the gasification of woodchips, a fixed bed downdraft gasifier was recently (date: 02.07.2015) tested on common reed briquettes (Figure 4.8). The sole experiment ran for about 330 minutes and followed the same test procedure as of woodchips experiments (see section 4.2.1). The operational data, i.e.; gas composition, temperature, ER, air flow, fuel flow etc. evolved as a result of the gasification test. This is summarized in Table 4.5. Additionally, the time-averaged (each 10 minutes) evolution of gas composition and air flow is presented by Figure 4.9.

As can be seen (Figure 4.9), throughout the experimental run (~5 h) the evolution of the gas data was not stable and characterized with distinctive peaks and troughs throughout. This may have been due to the process abnormalities linked to the phenomena of bridging, unsteady production of charcoal, deposition of ash around air flow nozzles, etc. The evolved gas species (dry basis) obtained from the experiments can be seen in Table 4.5.

Table 4.5: Summary results obtained from the preliminary test of common reed briquettes

Properties	Values
Test date	02.07.2015
Average air flow rate, Nm^3/h	4.3
Biomass feed rate, kg/h	1.3
ER range	0.35-0.86
Total operation time, hrs.	ca 330
Average gas composition	
CO, % wt.	11.5
CO_2, % wt.	13.6
H_2, % wt.	7.3
CH_4, % wt.	0.7
LHV, MJ/Nm^3 (wt.)	2.5
Avg. bed temperature, °C	498
Avg. gas yield, Nm^3/kg	3.9
CGE, %	54.6
Char yield, g/kg (wt.)	60.7

This gas LHV, as far as engine or turbine application is considered, is substantially lower than the desirable minimum 4 MJ/Nm^3 (Arjharn et al., 2012) and thus is not recommended for further application of such. Observing the profiles of different temperatures (Figure 4.10), on the other hand, the average bed temperature ca 498 °C was found unsatisfactory and thus not completely representative to gasification. This can also be confirmed from a past study

(Dogru, 2004), where bed temperature for an optimum gasification of non-woody biomass using fixed-bed downdraft gasifier was found to range between 1000 and 1100 °C.

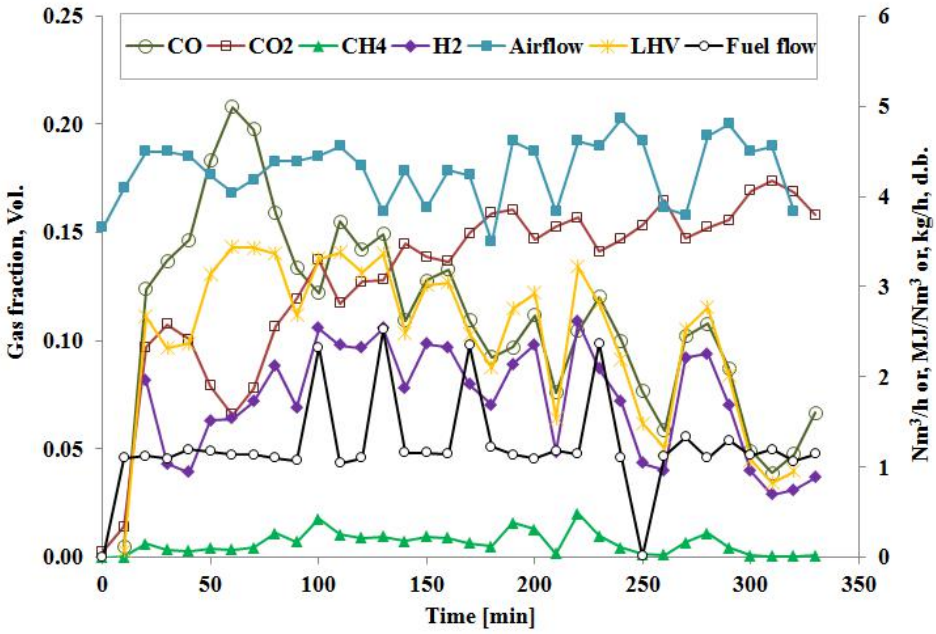

Figure 4.9: Evolution of gas composition and air and fuel feed over time on stream

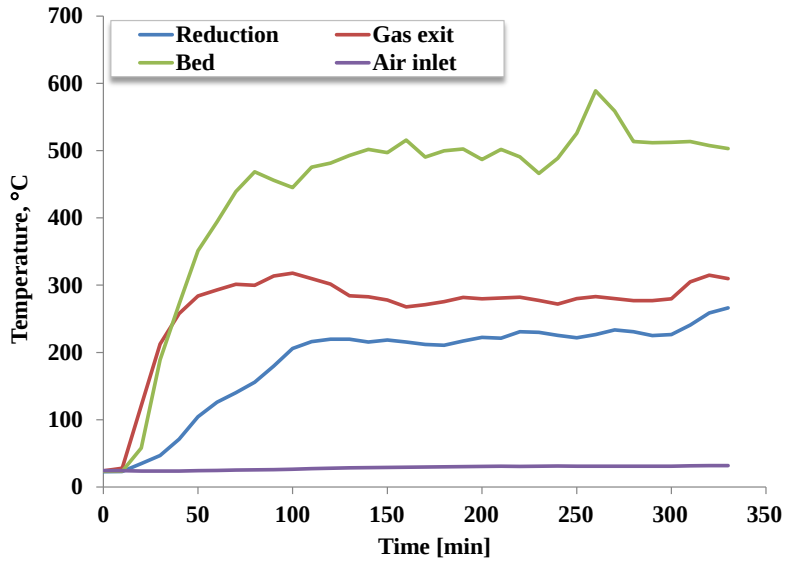

Figure 4.10: Evolution of various temperatures for different zones over time on stream

From the above discussion, it is thus obvious that the preliminary test requires extended research. Nevertheless, as yet, some of the positive findings that encourage future research are:

- LHV maximized to 3.5 MJ/Nm^3 corresponding to ER = 0.45
- CGE reasonably averaged and maximized at 55 % and ~83 % respectively
- Operational time moderately reached to 330 min
- Char yield reasonably amounted to 60 g/kg

4.2.3 Mass balance

As stated in paper IV, mass balance accuracy of maximum ca. 95 % was achieved from all the woodchips gasification tests reported in this work. However, in many cases a reasonable balance closure could not be attained, presumably due to the gas leakages, particulates accumulation in the settling filter and uncaptured tars. The possible sources of minor errors as discussed in paper IV could alternatively be the reason of major errors for the insensible mass balances. One or two cases mass balance went over 100 % accuracy which may sometimes be expected (Siedlecki et al., 2011).

4.3 Pilot-scale fluidized bed gasification experiment

As already mentioned, only alfalfa and wheat straw were selected as local herbaceous biomasses for fluidized bed gasification. Compared to wheat straw, the fluidized-bed gasification on alfalfa is relatively scarce. Hence, the current work focused on evaluating gasification potential of alfalfa across two different gasifier configurations. Additionally, a novel feeding system enabling direct feeding of both biomass pellets to a small scale unit was emphasized. The following sub-sections briefly overview the results obtained from the gasification tests using pilot and lab scale reactors. The results are further discussed at length in paper II & III, annexed at the end of this thesis.

4.3.1 Gasification performance of alfalfa pellets

As a local herbaceous crop, alfalfa is widely available around the area of Ebro river valley and exhibits wealth of possibilities for being converted into energy through gasification as well being used as fodder crop. Considering this, a part of this thesis is devoted to examine the potential of alfalfa as a feedstock for pilot scale fluidized bed gasification. The gasification approach involved was to vary one of the basic parameters such as ER and to observe the corresponding effect on a range of other operational parameters namely gas yield, gas LHV, CGE, CCE etc. which is discussed below.

Producer gas quality: composition, LHV and yield

The producer gas resulting from the gasification of alfalfa pellets, mainly composed of the gas species CO, H_2, CO_2, N_2, CH_4, C_2H_4, C_2H_6 the evolution of which as an effect of ER at 0.25 and 0.30 was investigated. As the results from paper II revealed, these gases did not present much of a variation as the ER varied. Two reasons might attribute to this fact. First, the ER change might have occurred between a very narrow margin which perhaps was not indicative enough to observe the changes in gas composition; and second, due to the feedstock properties (low volatile, high ash, etc.) the conversion behavior was probably not influenced by the region of the narrow variation in ER, and hence the less impact on evolved gas. Generally herbaceous biomass produces the best quality gas, while the operational ER is kept low, primarily between the range 0.20 and 0.36 (Alauddin et al., 2010).

Observing the trend of gas components as depicted by Figure 4.11, the CO yield showed an upward tendency in contrast to that of CO_2, H_2 and CH_4 dropped as the ER increased. The increase in CO possibly indicates the increasing extent of Boudouard reaction, while the concurrent drop in H_2 and CO_2 presumably implies the compromised water-gas shift reaction at higher ER. The other minor species such as C_2H_4 and C_2H_6 remained fairly unaffected despite the modified ER (data presented in paper II).

The producer gas composition is an excellent indicator for the producer gas quality based on which further gas utilization may be recommended. For example, the effect of total combustible quantity in the producer gas influences the quantity of gas LHV, which is indicative to judge the suitability of gas for specific downstream application. In the present case, increasing ER contributed to increase the overall combustible composition of gas from ca 25.3 % to 26.0 %, which directly affected the gas LHV that slightly increased from ~4.19 MJ/Nm^3 to ~4.21 MJ/Nm^3. This implies that enhancing ER improved the quality of produced gas which may in turn increase the usefulness of gas for further energy conversion via engine or, turbine.

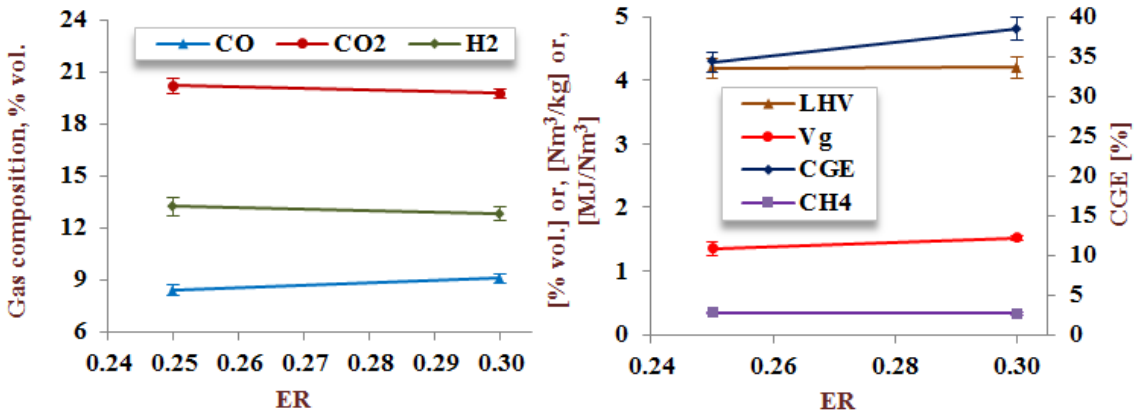

Figure 4.11: Effect of ER on operational parameters of pilot plant gasification

Additionally, the producer gas components are also of interest depending on their amount. For example producer gas high in CH_4 content may suit for bio-methanation (van der Meijden et al., 2009). Similarly high mixture of CO/H_2 (Carpenter et al., 2010) favors further processing of producer gas into hydrogen, biodiesel, SNG (synthetic natural gas) application.

Another parameter representing the characteristics of the producer gas is the yield. Theoretically, the higher the ER the higher the bed temperature (T_2, as indicated in Figure 5.4) and consequently, the higher the gas yield as a result of strengthening combustion, reforming, devolatilization etc. In the present case, the

severity of reforming reaction perhaps increased as a result of decreased production of CH_4 at escalated ER and thus the increase in gas yield. The increased gas yield in general improves the performance of gasification. However, if the quantitative increase does not translate to the qualitative increase in terms of gas LHV, less energy is available from gas for further utilization. This can be evidenced when a large proportion of a given amount of producer gas consists of incombustible species, i.e.; N_2, CO_2, etc., than those of the combustible species contributing to LHV.

Temperature profile, tar and char yield

The temperature profiles evolved from five equidistant sensors (T_2-T_6) are shown in Figure 4.12. One distant sensor (T_7) located at the far top of the freeboard is not covered in Figure 4.12. The position of the equidistant sensors along the gasifier is also displayed by an image embedded to Figure 4.12.

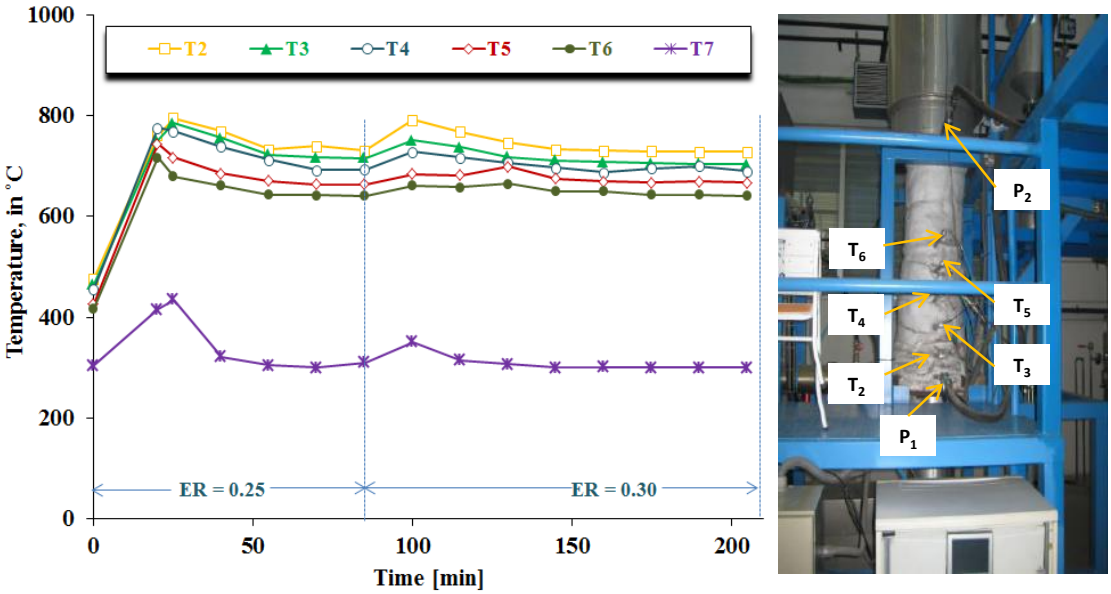

Figure 4.12: Various temperature profiles and sensors location; left: evolution of temperatures over time, right: location of temperature probes (except T_7) along the reactor

As can be seen, the average temperatures of all the probes were slightly higher or constant in case of higher ER. Besides the short period of start-up and changeover of ER from 0.25 to 0.30, the temperature profiles shown by all the sensors were rather stable throughout. The temperatures, especially the temperatures around the bed (T_2-T_6) dictated various parameters of the gasification the effect of which is broadly discussed in paper II. Reiterating some of the key points from that discussion: the higher the bed temperature the higher the combustible species CO, CH_4, C_2H_4 and higher the gas yield, gas LHV and CGE as opposed to the lower H_2 and CO_2, due to the interactions and extent of several thermochemical reactions namely Boudouard, water-gas shift, combustion etc., as explained further in paper II.

Two other parameters influencing the quality of gasification are tar and char. High production of tar and char cost both energy and efficiency, and hence their high yield is least desirable in gasification. Typically, high gasification temperature leads to reduced tar and char production through enhanced reforming and shift reactions (Aznar et al., 2006). The effect of ER and the derived bed temperature on tar and char production could not be concluded from the present study because of the two reasons, namely: each experiment was conducted at two subsequent ERs; and char and tar were collected at the end of an experiment representing the effect of total ER range instead of an individual ER. It is evident that the total tar yielded after all runs averaged at 1.12 ± 0.04 g/Nm^3. This value is in agreement with the previous study on fixed bed gasification of the similar feedstock, but surprisingly low for the actual conventional fluidized bed gasification used in our experiment without catalyst. For example, a fluidized bed gasification study carried out by Ref. (Narvaez et al., 1996) reported that for an optimum operational ER, the tar yield ranged between 3 and 7 g/m^3. Also, Turn et al. (Turn et al., 1998) found the resulted tar yield from bagasse and banagrass to lie between 12 g/m^3 and 19 g/m^3. Unlike, the lower tar yield from the present study is not clearly known.

While the tar yield showed a significant deviation from the literature values at the similar gasification condition, char yield (281.7 ± 28 g/kg) showed a slightly higher value than that of the past study by Ref. (Aznar et al., 2006). For a typical

fluidized bed gasification, char yield is expected to keep in the range between 10 % and 20 % mass (Xiao et al., 2007) of the feed input compared to ours at 28 %. This, however, can exhibit a signification deviation depending on process characteristics in relation to fuel conversion, extent of gasification reactions, bed temperature etc.

In addition to gravimetric analysis, tar was also studied for compositional analysis, the results of which are presented in paper II. As reported, approximately 12 tar compounds representing various groups of phenols, pyridine, benzenamine and heavy tar quinoline, indole etc. were detected. Phenols are secondary tar, primarily deriving from lignin decomposition (Li et al., 2015) and generally appear when the gasification temperature exceeds 500 °C. Moreover, their production peaks at around 700 – 800 °C at the expense of primary tar (comprising of alcohols, ketones, aldehydes etc.) (Basu, 2010). Since the gasification tests of alfalfa occurred between the temperatures 700 and 800 °C, the higher abundance of phenols was expected. It was also noticed that a few of the tar compounds identified were nitrogen containing molecules (amino-pyridine, benzonitrile, benzenamine, etc.) which were thought to be originated from fuel nitrogen. As alfalfa contained high nitrogen in its chemical composition this result is logically justified.

Gasification efficiencies

The effectiveness of gasification is generally expressed by the two common terms called cold gas efficiency (CGE) and carbon conversion efficiency (CCE). These efficiencies determine the performance of a given gasification plant based on input biomass and output products. Overall, the CGE from present alfalfa feedstock was low (~39 %) and below that of typical lignocellulosic biomass (Alauddin et al., 2010). The combined effect of low combustible gas quantity especially the low CO, gas and char yield was primarily the reason for low CGE. Moreover, some technical issues such as gas leakage and dimension of gasifier are also reported to negatively influence CGE (Gómez-Barea et al., 2005). Coupled with CGE, the CCE - representing the degree of utilization of carbon was also low and found as average ca 60 % for the ER at 0.30 (CCE data is not

presented in paper II). The low CCE was possibly a result of the low amount of gas CO (~8 % to ~9 % throughout ER) and high amount of char in the gasification by-products. Generally, CCE value can be enhanced by minimizing the production of tar and char and by increasing the carbonaceous species in the producer gas. Additionally, increasing the freeboard height of reactor leads to increase in residence time of fuel during gasification which could also contribute to increase the value of CCE, as mentioned in the study by (Gómez-Barea et al., 2005).

4.4 Small-scale fluidized bed gasification

4.4.1 Comparison of gasification between alfalfa and wheat straw pellets: semi-continuous feeding

In the small scale configuration, alfalfa and wheat straw pellets were considered as feedstocks for gasification. Likewise pilot plant test, here the ER, was allowed to vary by modifying the air and fuel flow and correspondingly the trend of other operational parameters (gas composition, gas LHV, gas yield, CGE and CCE) between the two different feedstocks were compared. The obtained gasification results are extensively discussed in paper III. In the forthcoming sub-sections some of the key features are only presented.

Effect of ER on producer gas compositions and gas LHV

Typical gas species found in producer gas of alfalfa and wheat straw were CO, CO_2, H_2, CH_4, C_2H_4, C_2H_6, C_2H_2 and N_2 the evolution of which was continuously monitored and the average data are illustrated by Figure 4.13 & 4.14.

As the results showed in paper III, with the rise in ER, the total combustible quantities, i.e.; total percent amount of CO, H_2, CH_4, C_2H_4, C_2H_6 and C_2H_2 for alfalfa linearly increased from 19.8 % (ER = 0.23) to 22.3 % (ER = 0.35) in

contrast to wheat straw which decreased from 22.8% (ER = 0.20) to 17.4 % (ER = 0.35) with some variations in between.

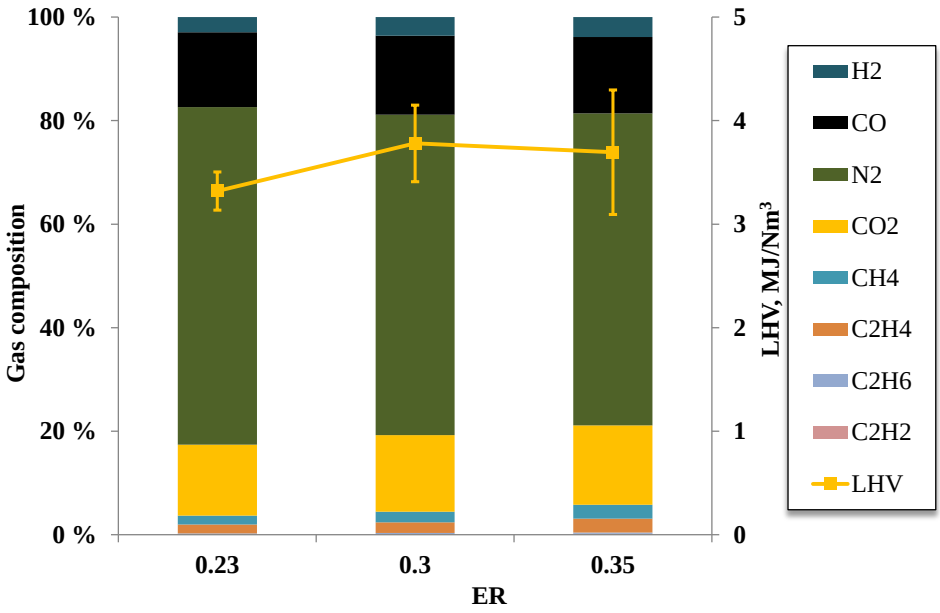

Figure 4.13: Evaluation of gas compositions and LHV as an effect of ER for alfalfa

Among the gas components identified from both the biomass, expectedly, CO_2 increased throughout, while the other components showed varied patterns (detailed in paper III).

In general, the average gas LHV from alfalfa peaked when ER maximized at 0.35 due to the increase in total combustibles. On the other hand, for wheat straw, at ER=0.30, the combustible components CO and H_2 dropped, but the light hydrocarbons (CH_4, C_2H_4, C_2H_6 and C_2H_2) increased, which as theoretically have a stronger influence on gas LHV than the rest of the combustible components, the average gas LHV increased (from 3.97 MJ/Nm^3 to 4.1 MJ/Nm^3). However, ER exceeding 0.30 reduced the total combustibles from wheat straw due to enhanced combustion, resulting in reduced average gas LHV.

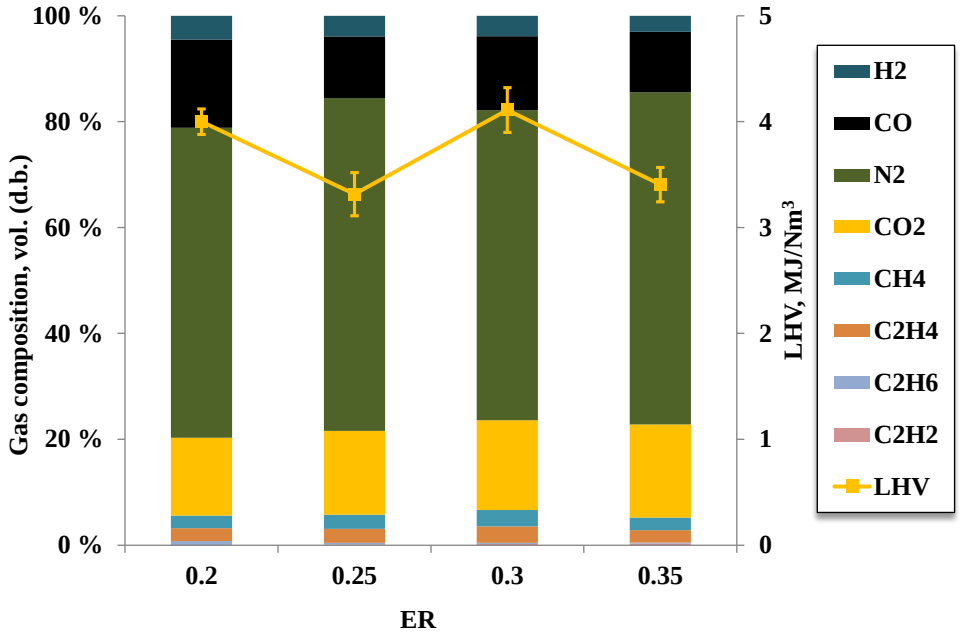

Figure 4.14: Evaluation of gas compositions and LHV as an effect of ER for wheat straw

Effect of ER on gasification performance

The gasification performance results of alfalfa and wheat straw in terms of gas yield, char yield, tar yield, CGE and CCE are presented in detail in paper III and summarized in the Figures 4.15 and 4.16 below.

As can be seen in Figure 4.15, the gas yield and gas LHV from alfalfa increased with ER and maximized when ER reached to the highest 0.35. The combined effect of these two parameters reflected to CGE and CCE which correspondingly increased and displayed similar patterns as those of LHV and gas yield. The increase in gas yield for alfalfa was perhaps due to the enhanced reforming and tar cracking, as implied by the quantitative decrease in char and tar. Clearly, the continued increase in air supply contributed to the continued enhancement of gasification performance, allowing to increase ER further. However, due to the constraint in regards to feeding, as well as the possibility of losing fluidization, the ER was not possible to exceed the level of 0.35 which eventually appeared to be optimum under the conditions investigated in the present experiments.

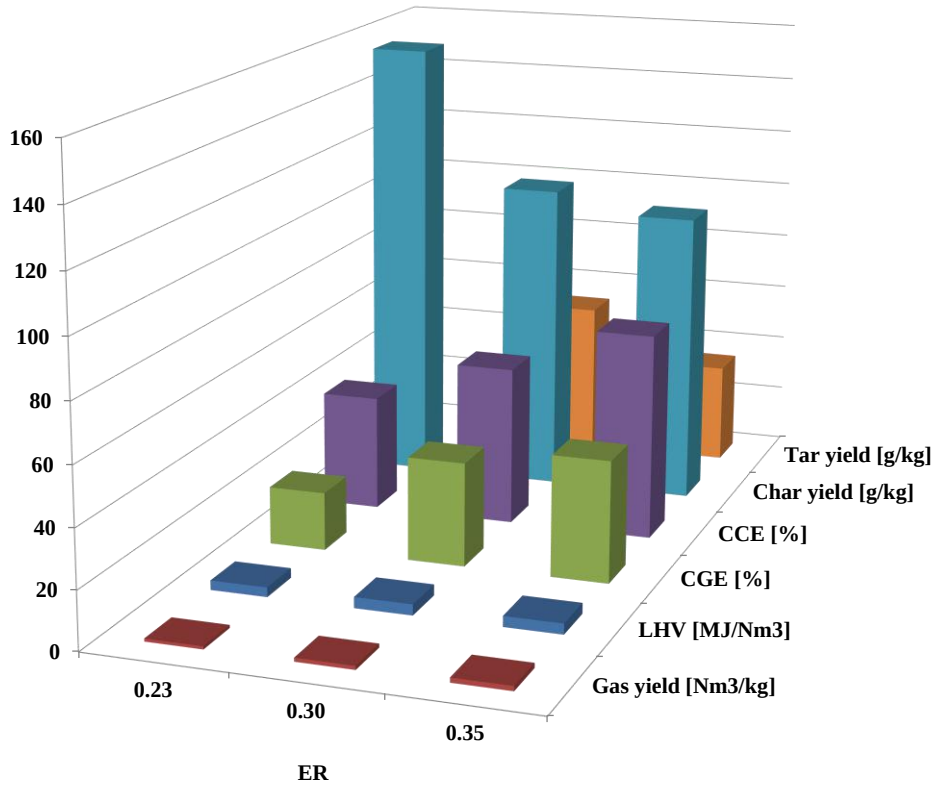

Figure 4.15: Average performance parameters from the gasification of alfalfa

As far as the wheat straw is concerned, first, the rise in ER between 0.20 and 0.25 contributed to increase the quantity of the producer gas, but the quality (LHV, tar, char, CGE and CCE) dropped or remained unaffected (Figure 4.16). The increased gas yield with the rise in ER was likely due to enhanced devolatilization (Gómez-Barea et al., 2005). Further, as the ER increased up to 0.30, there was a dramatic improvement in all the major parameters of gasification, including efficiencies, LHV, gas quality, gas yield and tar yield, apart from char which showed a higher yield. The interplay of several chemical reactions such as reforming, water gas shift, devolatilization, etc. perhaps favored gasification and as such the improvement in process parameters at ER = 0.30. However, the increase in char is surprising. One explanation for this could be the influence of higher contribution of ash and particulates in char than the char alone. Finally, maximizing the ER at highest 0.35 was not reflective to the

performance of gasification for which most of the parameters degraded, except gas yield and CCE. The gas yield at this level of ER was mainly boosted by the enhanced quantity of CO_2 which ultimately contributed to raising the quantity of carbonaceous gas, and eventually the CCE.

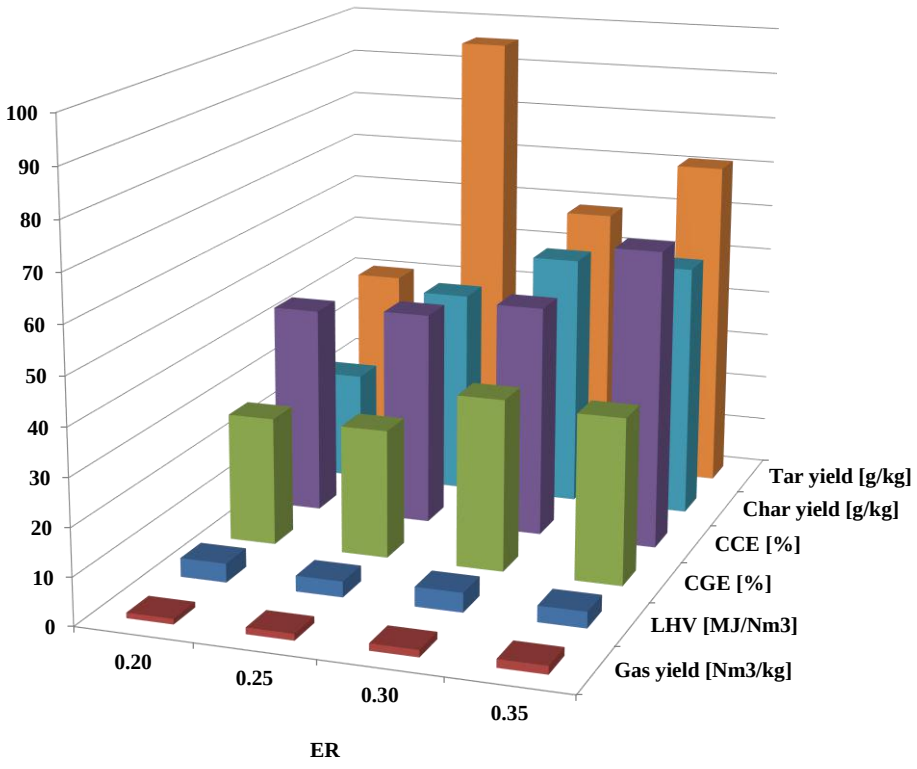

Figure 4.16: Average performance parameters from the gasification of wheat straw

It can thus be concluded that the variation in the optimized ER was mainly due to the dissimilarities in physical and chemical properties between the two feedstocks (Table 4.1), as the gasification condition was kept fairly similar.

Effect of ER on bed temperature

Like other process parameters, the evolution of bed temperature was also observed as a result of modified ER which is demonstrated by Figure 4.17. Typically, the higher the level of ER is the higher the bed temperature. Although this trend followed in the present case of gasification, the bed temperature did not

profoundly vary and hovered between the range 868° C and 873° C for both feedstocks as ER modulating between 0.20 and 0.35.

In regards to alfalfa, the highest bed temperature of ~873° C was achieved at ER = 0.35 at which gasification performance optimized in respect to the most of the operational parameters, including the increased conversion of char and tar. This is clearly the effect of increased supply of oxygen contributing to increase the severity of reforming and cracking.

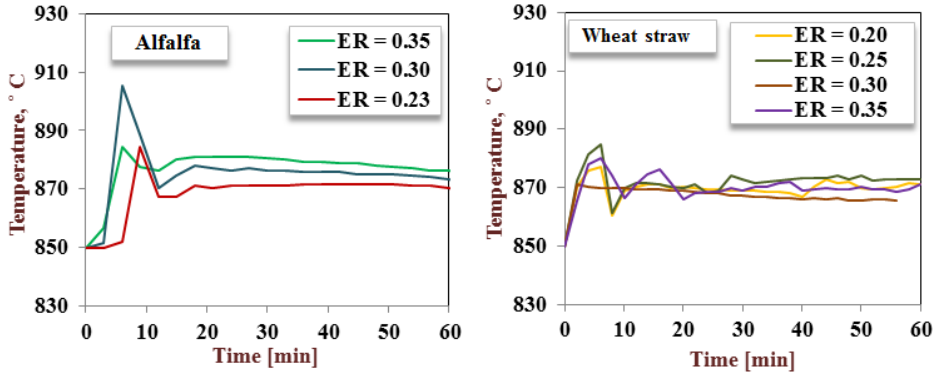

Figure 4.17: Evolution of temperature profiles at various ER (left: alfalfa, right: wheat straw)

As far as wheat straw is concerned, the trend of temperature was upward as with ER. However, the process performance waned significantly as the bed temperature exceeded 869 °C (corresponding to the ER > 0.30) primarily owing to the decreased level of gas LHV and increasing content of volumetric tar. At higher bed temperature, as the strength of combustion increased, the gas LHV degraded, while the accelerated deposition of tar might have resulted in the contribution of heavier tar molecules at an expense of primary and secondary tar.

Compositional analysis of tar

The influence of each ER change on composition of tar from both alfalfa and wheat straw is presented in Figure 4.18 and 4.19.

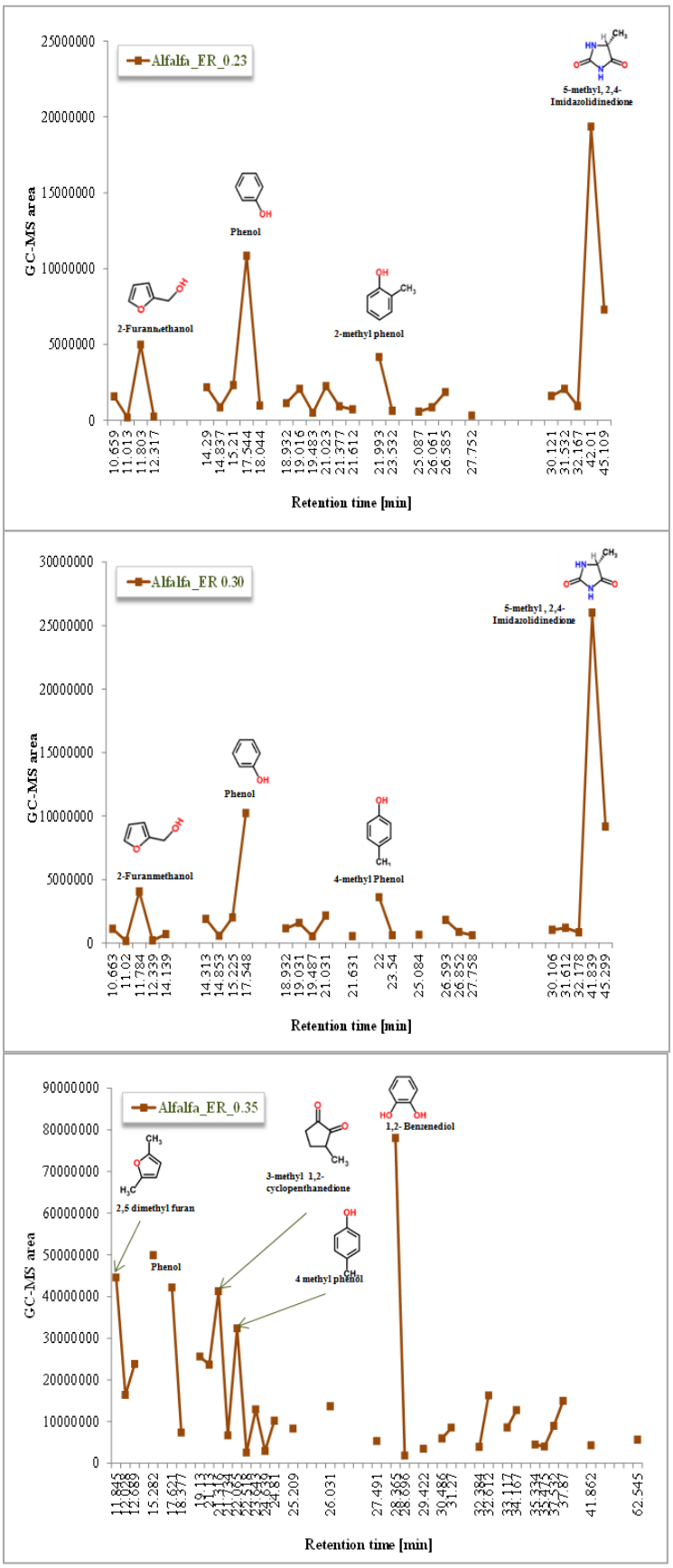

Figure 4.18: Influence of ER on tar composition from alfalfa

Noticeably, for all operational ER and both feedstocks, phenols are the most abundant tar compounds observed from the analyzed samples. Phenols are secondary tar typically derived from the decomposition of lignin (Li et al., 2015) and potentially stable over a wide range of operating temperature. In addition to phenols, tertiary tar 5-methyl, 2,4-Imidazolidinedione and nitrogen containing species methenamine, benezenamine, etc. were also identified in the peaks detected from the GC-MS.

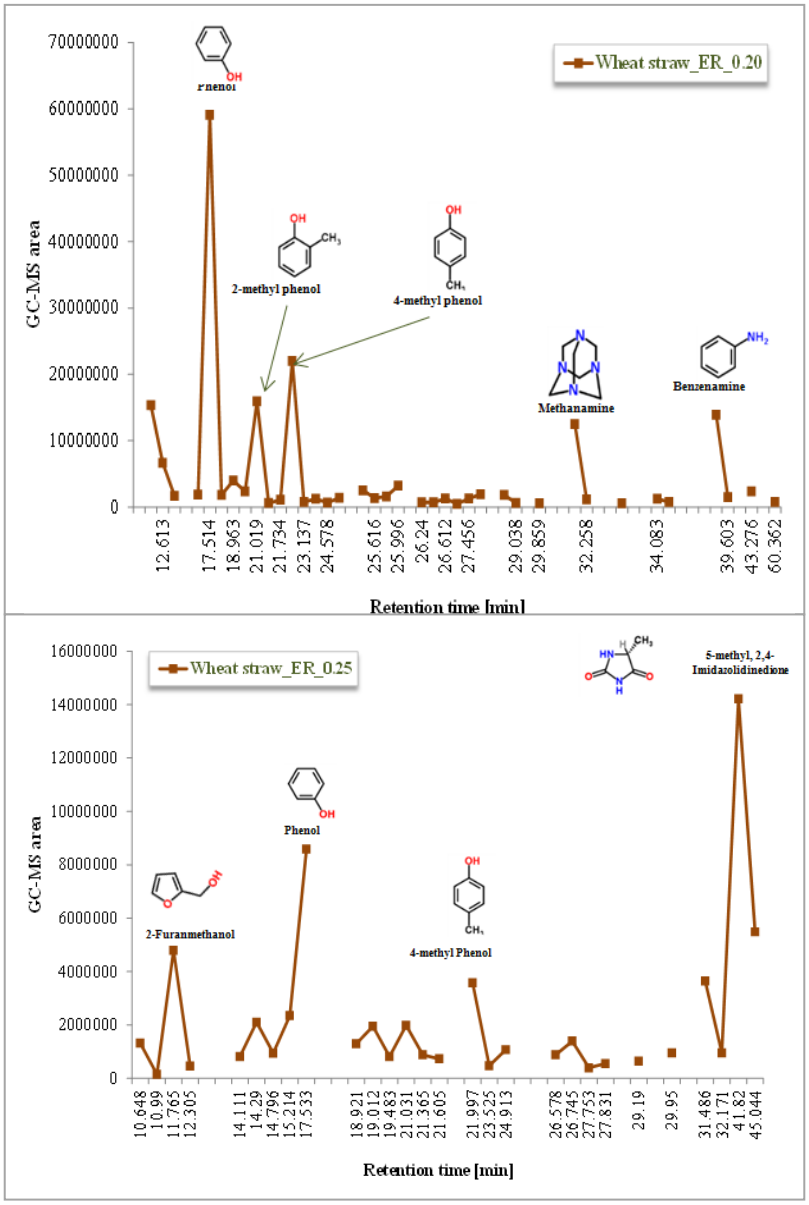

Figure 4.19: Influence of ER on tar composition from wheat straw (ER = 0.20 & 0.25)

The tertiary tars generally appear at an expense of primary and secondary tar at a relatively higher temperature (ca. 650° C) and potentially last around the temperature exceeding 900 °C (Basu, 2010), while the nitrogen in N_2-containing tars are mainly originated either from fuel or, from gasification agent or, from both (Li et al., 2015).

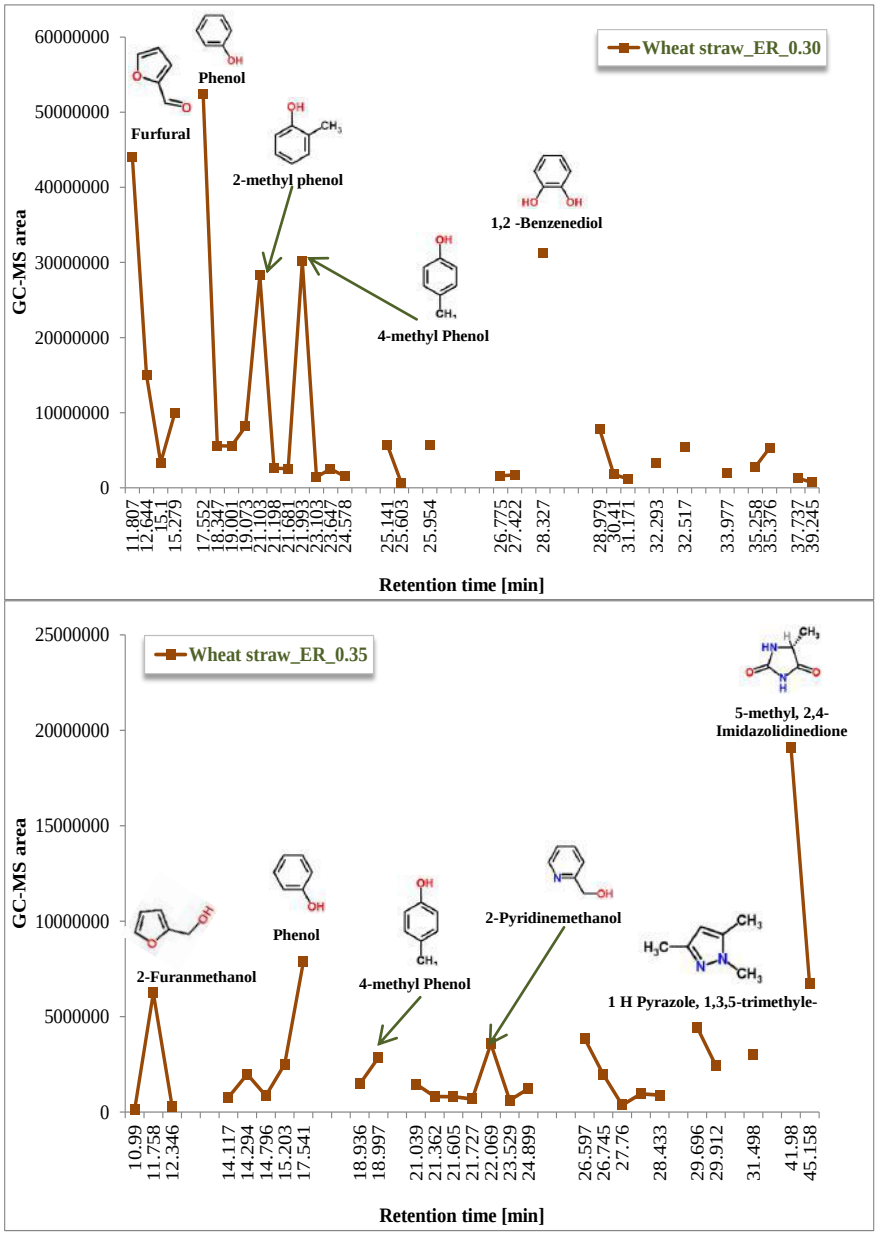

Figure 4.20: Influence of ER on tar composition from wheat straw (ER = 0.30 & 0.35)

Particularly for alfalfa, at the individual ER 0.23 and 0.30 (Figure 4.18), the tar compounds identified were pretty comparable where the highest peak resulting from tertiary tar 5-methyl, 2,4-Imidazolidinedion. As the ER increased further up to maximum 0.35, phenols were still the major contributors in the tar spectra with increasing abundance primarily from the derivatives of methyl. However, the tertiary tar 5-methyl, 2,4-Imidazolidinedione greatly diminished at this stage while the appearance of phenol 1,2-benzenediol became stronger.

Clearly, the higher the ER, the higher was the presence of secondary and tertiary tars in the samples from the tests of alfalfa.

Likewise alfalfa, the tar compositions identified from the samples of wheat straw represented similar abundance frequencies in terms of phenol and its derivatives, see Figure 4.19. Moreover, at the lower ER (between 0.20 and 0.25) some nitrogen containing tars such as 2-Pyridinemethanol and 1 H Pyrazole, 1,3,5-trimethyle- were detected, which however tended to degrade as the ER rose further at 0.30. At ER = 0.30, the presence of furan (furfural) was identified, which is expected due to the chemical composition of agricultural waste (Budinova et al., 2003).

Including phenols and the various forms of tertiary tars, at ER = 0.35, the nitrogen containing tars reappeared. Since wheat straw contains negligible amounts of nitrogen in its chemical composition, the nitrogen containing tars are primarily thought to originate from air, which was used as gasifying agent for the present gasification tests. In paper III it was stated that the content of volumetric tar rose when the ER rose from 0.30 to 0.35. Thus according to the tar results for ER = 0.35 in Figure 4.20, the hypothesis extra tar might have contributed to the development of tertiary tars seems to be validated now.

4.5 Techno-economic analysis of a gasification plant based renewable hybrid energy system

The techno-economic analysis using HOMER followed three steps of methodology, i.e.; simulation, optimization and sensitivity, the results of which are briefly presented below.

4.5.1 System performance: simulation and optimization

To determine system performance, both simulation and optimization results for mono and hybrid energy plants were used.

First, in regards to the mono energy plant, the optimized system consisted of a diesel generator (DG) or, a natural gas generator (NG) with a rated capacity of 2.5 kW, two units of batteries and one capacitor of 1 kW capacities respectively. By keeping the fuel price as realistic as possible, the economic viability of the mono energy plant was assessed based on the diesel and natural gas price of 0.8 \$/L and 0.6 \$/m^3 respectively (EIA, 2015).

The results revealed that according to both economic and environmental aspects, an NG system is preferable over DG. Optimum net present cost (NPC) and LCOE of NG system was found to be 90,420 \$ and 0.365 \$/kWh both of which were ca. 12 % less than those of a DG system. Moreover, the CO_2 equivalent emission from the former was 17 % less than that of the latter, indicating a clear environmental advantage in regards to greenhouse gas emission. Comparison of different economics and emission parameters between the mono and hybrid energy plants are illustrated by Table 4.6.

Second, in regards to the hybrid energy plant, as much as five energy components namely PV, wind turbine, diesel/natural gas/producer gas generator, battery and capacitor with various combinations were used. The simulation results produced total eight possible power plant configurations out of which

three were composed solely of renewable sources. Among the renewable hybrid plants, which was the interest of the present investigation, Bio / PV / wind / battery / capacitor were found optimum based on lowest NPC and LCOE at 72,232 $/year and 0.306 $/kWh. According to the simulation this plant is able to produce total 19,886 kWh/year of electricity, with a contribution of 15628 kWh/year (ca. 79 %) from the producer gas generator, 2886 kWh/year (ca. 15 %) from the wind turbine and the rest (1366 kWh/year) from the PV arrays respectively. Comparing to the total energy demand of a selected single household, the total electricity generated by the optimized plant closely satisfies the demand. Apart from the feasibility in terms of meeting energy demand, renewable hybrid plants are also advantageous in terms of fulfilling the commitment towards the environment. For example, if the mono-energy plant running with fossil diesel is replaced with the current optimized hybrid plant of Bio/PV/wind configuration, the annual CO_2 reduction of 22,626 kg could be achieved.

Table 4.6: Economics and emission parameters among the different modeled energy plants

Plant configuration	Total NPC ($)	COE ($/kWh)	Emissions (CO_2),	Diesel unit cost ($/L)	Natural gas cost ($/m^3)	Wood gas unit cost ($/m^3)
Mono energy plant						
Disel generator	101,254	0.408	22,626	0.8	-	-
Natural gas generator	90,420	0.365	19,302	-	0.6	-
Hybrid energy plant						
Bio/PV/wind/battery/converter	72,232	0.306	26,894*	-	-	0.1
Bio/wind/battery/converter	77,949	0.332	27,390*	-	-	0.1
Bio/PV/battery/converter	79,589	0.341	28,453*	-	-	0.1
Bio/PV/diesel/battery/converter	83,210	0.336	28,325	0.8	-	0.1
NG/PV/battery/converter	77,947	0.334	13,509	-	0.6	-
Bio/PV/NG	77,230	0.312	27,589	-	0.6	0.1
NG/wind/battery/converter	74,382	0.300	15,164	-	0.6	-
Bio/wind/NG/battery/converter	75,101	0.303	25,778	-	0.6	0.1

*: No net environmental impact

4.5.2 Sensitivity analysis

Sensitivity for both types of plant configuration was evaluated based on fluctuated fuel prices so that the international price uncertainties can be

considered into the modeling. For a mono energy system with a diesel generator (DG) it was found that due to the fuel price varying from 0.1 $/L to 1 $/L (in space of 0.1 $/L), the NPC varied almost linearly between the range $ 26,300 and $122,669 corresponding to the LCOE of 0.106 $/kWh and 0.495 $/kWh respectively. Additionally, the growth rate of LCOE was found much faster than that of NPC when the diesel cost exceeded to 0.52 $/L. Mono energy systems for natural gas (NG) for the similar interval of price variation (0.1 $/$m^3$ to 1$/$m^3$) resulted in the LCOE and NPC to vary between the range 0.113 $/kWh and 0.566 $/kWh, and $28,063 and $140,312 respectively. Since the simulation and sensitivity parameter was kept identical, the higher NPC and LCOE of natural gas generator were thought to be caused by the difference in the efficiency of the generator, chosen to 20.4 % for NG and 23.8 % for DG respectively.

The sensitivity of the hybrid energy plants was mainly assessed with respect to the variable producer gas price between 0.1 $/$m^3$ and 1$/$m^3$. The simulation results of which are summarized in Table 4.7.

Table 4.7: Sensitivity analysis of the optimum hybrid plant (Bio/PV/wind/battery/converter) as an effect of producer gas unit price

Wood gas ($/$m^3$)	Total NPC ($)	COE ($/kWh)
0.1	72,232	0.306
0.2	128,489	0.544
0.3	184,746	0.782
0.4	241,002	1.020
0.5	297,258	1.259
0.6	353,515	1.497
0.7	409,553	1.734
0.8	465,494	1.971
0.9	521,436	2.208
1.0	577,378	2.444

Expectedly, the value of NPC and LCOE was affected by the increasing producer gas price. More interestingly, each step of increase in fuel price hugely

contributed to the increase in cost values. The NPC ranged between $72,232 and $ 5,77,378 corresponding to the LCOE between 0.306 $/kWh and 2.444 $/kWh. With the 9 steps increase in producer gas price both the NPC and LCOE showed overall 8 times increase from the values at start.

In conclusion, hybrid plants with PV/wind and an option of producer gas generator in terms of economics is competitive over mono fossil energy plants under the constraint of producer gas unit price keeping below 0.1 $/$m^3$.

5 Conclusions and future recommendations

The major conclusions drawn from the each phase of the current research work and the potential future perspective is given below.

5.1 Fixed-bed downdraft gasification of woody biomass

The experiments with fixed-bed downdraft gasification revealed that a maximum benefit of the present technology in terms of reasonable gas composition could be achieved with a wide range of equivalence ratio (0.29 to 0.45). Some of the key findings of fixed-bed downdraft gasification of five different woodchips is illustrated by Figure 5.1 and listed in bullet points below:

- Average gasification performance obtained from the hardwood forest crops birch and oak closely agreed in terms of the major operational parameters: LHV and Vg, but oak gave better CGE and CCE compared to those of birch.
- Gasification performance of softwood spruce was found little inferior to that of hardwoods in regards to LHV, Vg, CGE and CCE yield.
- Between two woody energy crops, the gasification performance of poplar in aspects of important process parameters was revealed superior to those of willow.
- Woody energy crops provided better reactor bed temperature and higher H_2 yield compared to the preliminary experiment with common reed briquettes.
- The gasification performance of the five studied woodchips species was ranked as: oak > birch > poplar > willow > spruce, when the given operational conditions in terms of ER varied from 0.19 to 0.80.

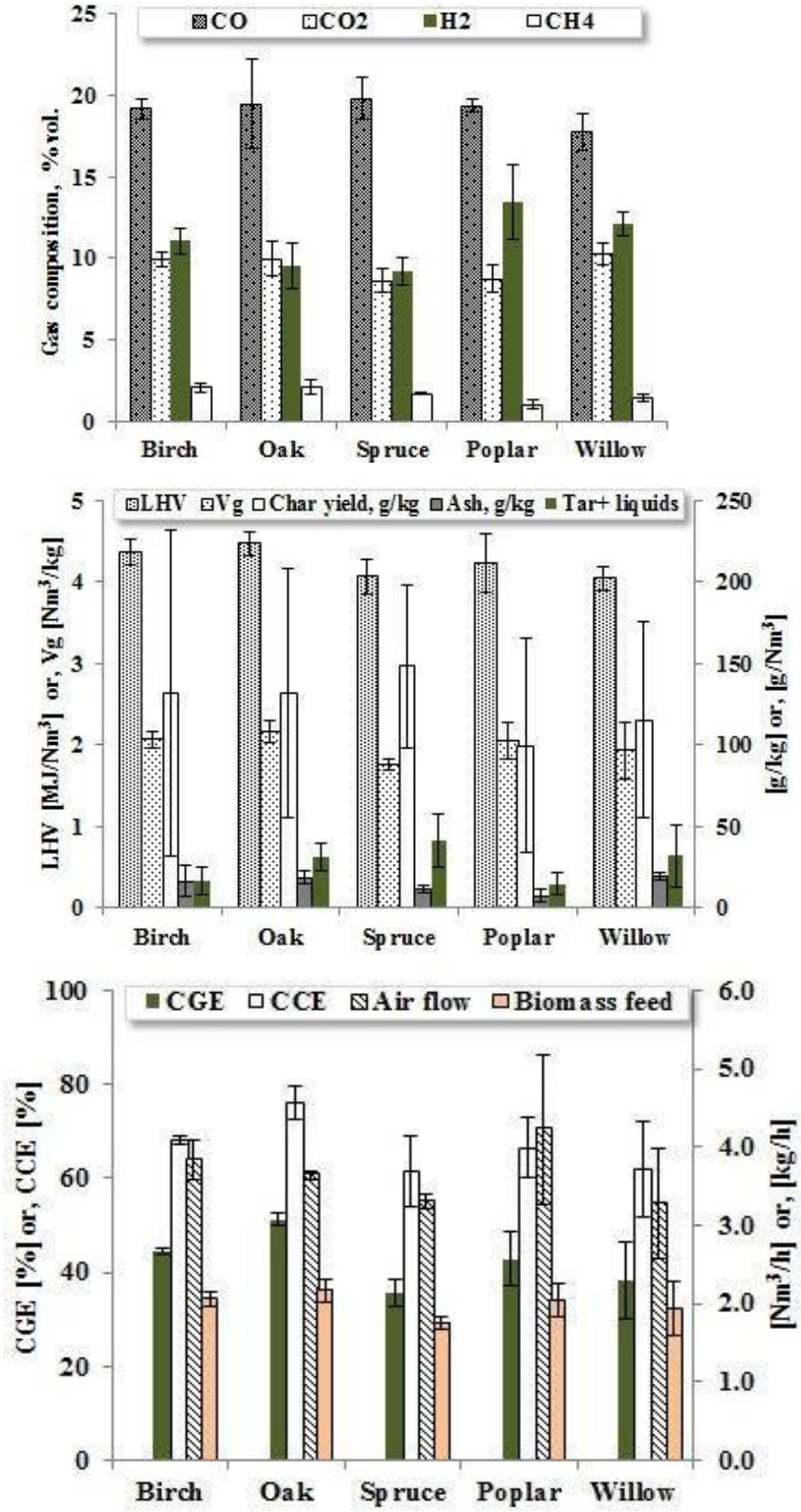

Figure 5.1: Comparison of fixed-bed downdraft gasification performance among different woodchips species (error bars representing the deviation from the average of all runs)

Overall, the small scale gasification of all the woody feedstocks showed a good potential for being converted into useful gas and ultimately to contribute to the local bioenergy expansion which in the long-run is beneficial both for securing environment goals and for achieving energy sustainability.

5.2 Fluidized bed gasification of herbaceous biomass

In the present fluidized bed gasification study, two novel initiatives was undertaken: the fodder crop alfalfa was investigated in a pilot-plant gasifier, and herbaceous biomass pellets were directly fed to a lab-scale fluidized bed reactor.

From the pilot scale test runs, gasification of alfalfa was found feasible over the selected ER range of 0.25-0.30. Further, quantitative analysis revealed that the obtained producer gas had a high H_2 content (of 13 % dry basis vol.) which is promising for this gas to utilize for hydrogen production. Moreover, the producer gas had a reasonably high LHV value of ca. 4.2 MJ/Nm^{3}which could also be a plus for recommending this technology for CHP applications based on combustion engine or turbine. In-regards to the lab scale gasification, the same feedstock (alfalfa), nevertheless, demonstrated different results, where CO yield was found higher than that of H_2. Dissimilarities also existed in the other process parameters: Vg, LHV and CGE, as displayed in Figure 5.2 for ER = 0.30. Overall, the gasification characteristics of alfalfa were influenced by the type of feeding and the type of the gasifiers.

Lab scale gasification tests of alfalfa and wheat straw uncovered that both the feedstocks yielded similar producer gas characteristics with a potential of gas utilization to the CHP application, since average gas LHV kept within the range of 4 MJ/Nm^3. This value, however, is somewhat lower than that of the pilot scale, see Figure 5.2. Over the ER ranges used, gasification performance of alfalfa optimized at ER = 0.35 as opposed to wheat straw at ER = 0.30. Throughout the operational ranges, the major drawbacks of using this technology

were the low yield of H_2, CGE and CCE due to high production of tar, particulates and char. This could perhaps be improved by conducting further studies on biomass residence time and redesign of gasifier which is beyond the scope of this work.

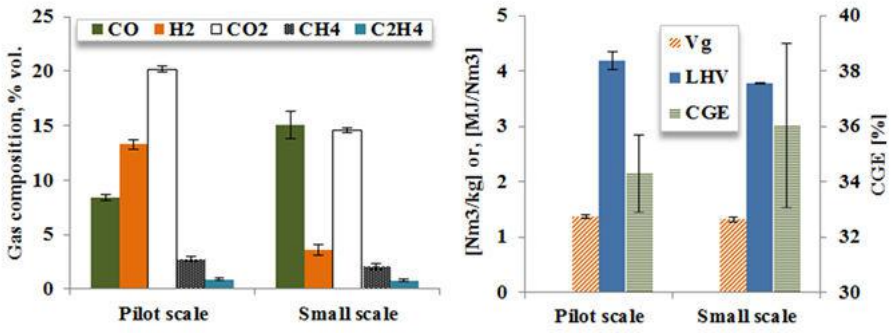

Figure 5.2: Comparison of gasification performance of alfalfa between Pilot-scale and lab-scale plant at ER = 0.30 (error bars representing the deviation from the average of all runs)

All in all, the results obtained from both the gasification units are expected to pave the way for promoting gasification in regards to other potential local herbaceous biomass for which further optimization of operational conditions may be recommended.

5.3 Techno-economic evaluation of renewable hybrid plant operating with producer gas generator

Prior to market penetration of a new technology, a techno-economic evaluation is needed. There is no exception for gasification plants. In the present research, the techno-economic evaluation of a producer gas generator operating with a fixed bed downdraft gasifier on woodchips in a renewable hybrid plant was assessed for operational feasibility in terms of technology, economy and environment. The model case considered was an arbitrary standalone house in Grimstad municipality utilizing average electricity complying with the average demand

within the community. The results showed that a renewable hybrid plant consisting of producer gas generator (2 kW), PV (1 kW), wind (1 kW), battery (1 unit) and capacitor (1kW) is optimum in terms of net present cost (NPC), levelized cost of energy (LCOE) and an environmental gain worth 22,626 kg/year. CO_2 savings, under the constraint that producer gas production price does not exceed the cost 0.1 $/m^3.

Since a gasification plant in a renewable hybrid energy configuration gives obvious economic and environmental advantages, the current finding is interesting as far as application of fixed-bed downdraft gasifier in a local renewable hybrid plant is concerned.

5.4 Future recommendation

The present thesis has addressed a few challenges within the area of local bioenergy exploitation by suggesting optimized process parameters for diverse biomass feedstocks in two contemporary gasification configurations. However, based on the author's experience and understanding, some of the crucial aspects still remain to be investigated, potentially forming the topics for future research.

First, prior to gasification, all the biomasses were thoroughly examined for physical and chemical quality by employing thermogravimetry, ultimate analysis, ash melting behavior and so on, whereas the structural analysis values were obtained from the existing literature results. Knowing the precise structural composition of a specific biomass from a specific site would be more representative in assessing the current results in the context of distribution of primary biomass components. Especially, the thermogravimetric graphs could be better explained and the gasification phenomenon would probably be better predicted. Nonetheless, because the study is solely based on the constraint of theoretical structural values, there is a window of opportunity to develop future perspectives in this regard.

Second, this thesis lacks with information of ash composition. Compositional analysis of ash allows to understanding the contribution of specific materials on behavior of sintered ash. Since the current research did not experience any melting or agglomerated ash during the gasification tests, determining ash composition was perhaps not an essential requirement to fulfill the objectives of the end interest. However, in global perspective, the priori knowledge on compositional ash helps determining the suitability of a particular biomass for a particular thermochemical conversion application for which a substantial part of the relevant future work may be devoted.

Third, in regards to the compositional analysis of tar, this study is not comprehensive. No doubt tar is an important parameter of the gasification study whose estimation is the key not only to know the gasification technology but also to develop process parameters regarding the technology. Two methods namely tar condensation and SPA, were employed to report the compositional tar. The compositional analysis using offline condensation produced successful tar characterization results with GC-MS for herbaceous biomass. However, the attempts in regards to the SPA sampling for woody biomass were not completely successful and representative, except a few samples of oak. Thus to propel the current research a step ahead, developing a sampling protocol allowing to collect representative samples suiting the successful SPA analysis where a wide scope clearly exists is imperative.

Finally, the fixed-bed downdraft gasification of herbaceous biomass (common reed) is still underdeveloped. From the operational experience, it is well established that the present fixed-bed gasification system is feasibly suited for woody biomass for a wide range of operating conditions. However, to increase the fuel flexibility, this gasification reactor should also be made tolerant for herbaceous biomass which can very well be a topic for future work.

References

Abbasi, T., Abbasi, S.A. 2011. Small hydro and the environmental implications of its extensive utilization. *Renewable and Sustainable Energy Reviews*, **15**(4), 2134-2143.

Acharjee, T.C., Coronella, C.J., Vasquez, V.R. 2011. Effect of thermal pretreatment on equilibrium moisture content of lignocellulosic biomass. *Bioresource technology*, **102**(7), 4849-4854.

Ahrenfeldt, J., Thomsen, T.P., Henriksen, U., Clausen, L.R. 2013. Biomass gasification cogeneration – A review of state of the art technology and near future perspectives. *Applied Thermal Engineering*, **50**(2), 1407-1417.

Alauddin, Z.A.B.Z., Lahijani, P., Mohammadi, M., Mohamed, A.R. 2010. Gasification of lignocellulosic biomass in fluidized beds for renewable energy development: A review. *Renewable and Sustainable Energy Reviews*, **14**(9), 2852-2862.

Arjharn, W., Hinsui, T., Liplap, P., Raghavan, G. 2012. Evaluation of electricity production from different biomass feedstocks using a pilot-scale downdraft gasifier. *Journal of Biobased Materials and Bioenergy*, **6**(3), 309-318.

Aznar, M.P., Caballero, M.A., Sancho, J.A., Francés, E. 2006. Plastic waste elimination by co-gasification with coal and biomass in fluidized bed with air in pilot plant. *Fuel Processing Technology*, **87**(5), 409-420.

Barrio, M. 2002. Experimental investigation of small-scale gasification of woody biomass. in: *Department of thermal energy and hydropower*, Vol. Doctor of Philosophy, The Norwegian University of Science and Technology. 7491, Trondheim, Norway, pp. 236.

Basu, P. 2010. *Biomass gasification and pyrolysis: practical design and theory*. Academic press., pp. 376

Belgiorno, V., De Feo, G., Della Rocca, C., Napoli, R.M.A. 2003. Energy from gasification of solid wastes. *Waste Management*, **23**(1), 1-15.

Boateng, A.A., Mullen, C.A., Goldberg, N., Hicks, K.B., Jung, H.-J.G., Lamb, J.F. 2008. Production of bio-oil from alfalfa stems by fluidized-bed fast

pyrolysis. *Industrial & engineering chemistry research*, **47**(12), 4115-4122.

Boerrigter, H., Rauch, R. 2006. Review of applications of gases from biomass gasification. *ECN Biomassa, Kolen en Milieuonderzoek*, **20**.

Brage, C., Yu, Q., Chen, G., Sjöström, K. 1997. Use of amino phase adsorbent for biomass tar sampling and separation. *Fuel*, **76**(2), 137-142.

Bridgwater, A.V., Boocock, D.G.B. 1996. *Developments in Thermochemical Biomass Conversion*. Springer, p. 1-1647.

Brown, R.C. (Ed.) 2011. Thermochemical Processing of Biomass Conversion into Fuels, Chemicals and Power, John Wiley & Sons Ltd., pp. 330.

Budinova, T., Savova, D., Petrov, N., Razvigorova, M., Minkova, V., Ciliz, N., Apak, E., Ekinci, E. 2003. Mercury adsorption by different modifications of furfural adsorbent. *Industrial & engineering chemistry research*, **42**(10), 2223-2229.

Buragohain, B., Mahanta, P., Moholkar, V.S. 2010. Thermodynamic optimization of biomass gasification for decentralized power generation and Fischer–Tropsch synthesis. *Energy*, **35**(6), 2557-2579.

Cai, J., Bi, L. 2009. Kinetic analysis of wheat straw pyrolysis using isoconversional methods. *Journal of thermal analysis and calorimetry*, **98**(1), 325-330.

Carpenter, D.L., Bain, R.L., Davis, R.E., Dutta, A., Feik, C.J., Gaston, K.R., Jablonski, W., Phillips, S.D., Nimlos, M.R. 2010. Pilot-scale gasification of corn stover, switchgrass, wheat straw, and wood: 1. Parametric study and comparison with literature. *Industrial & Engineering Chemistry Research*, **49**(4), 1859-1871.

Carrier, M., Loppinet-Serani, A., Denux, D., Lasnier, J.-M., Ham-Pichavant, F., Cansell, F., Aymonier, C. 2011. Thermogravimetric analysis as a new method to determine the lignocellulosic composition of biomass. *Biomass and Bioenergy*, **35**(1), 298-307.

CEN/TS15370-1:2006. 2006. Solid biofuels - Method for the determination of ash melting behaviour - Part 1: Characteristic temperatures method, European Committee for Standardization.

CEN/TS15403. 2006. Methods for determination of ash content European Committee for Standardization.

Chow, J., Kopp, R.J., Portney, P.R. 2003. Energy resources and global development. *Science*, **302**(5650), 1528-1531.

Clausen, L.R., Elmegaard, B., Houbak, N. 2010. Technoeconomic analysis of a low CO 2 emission dimethyl ether (DME) plant based on gasification of torrefied biomass. *Energy*, **35**(12), 4831-4842.

Cuadros F., González-González A., Ruiz-Celma A.,López-Rodriguez F., Garcia-Sanz-Calcedo J.,Garcia J. A., and Mena A., 2013. Challenges of Biomass in a Development Model Based on Renewable Energies. in: *Without bounds: A scientific canvas of nonlinearity and complex dynamics*, eBook, Springer, USA. p. 748.

Demirbas, A. 2004. Combustion characteristics of different biomass fuels. *Progress in Energy and Combustion Science*, **30**(2), 219-230.

Dogru, M. 2004. Gasification of leather residues—Part I. Experimental study via a pilot scale air blown downdraft gasifier. *Energy Sources*, **26**(1), 35-44.

EIA. 2015. Independent Statistics & Analysis. U.S. Energy Information Administration

EN14774:2009. 2009a. Solid biofuels, determination of moisture content European Committee for Standardization, pp. 12.

EN14774:2009. 2009b. Solid recovered fuels, determination of ash content European Committee for Standardization.

EN15403:2011. 2011. Solid recovered fuels, determination of ash content European Committee for Standardization, pp. 16.

García, R., Pizarro, C., Lavín, A.G., Bueno, J.L. 2012. Characterization of Spanish biomass wastes for energy use. *Bioresource Technology*, **103**(1), 249-258.

Gaur, S., Reed, T.B. 1995. An atlas of thermal data for biomass and other fuels. National Renewable Energy Lab., Golden, CO (United States).NREL/TB 433-7965

Gómez-Barea, A., Arjona, R., Ollero, P. 2005. Pilot-plant gasification of olive stone: a technical assessment. *Energy & fuels*, **19**(2), 598-605.

González, A., Riba, J.-R., Puig, R., Navarro, P. 2015. Review of micro- and small-scale technologies to produce electricity and heat from Mediterranean forests′ wood chips. *Renewable and Sustainable Energy Reviews*, **43**(0), 143-155.

GPT, T.-C.P.G. 2015. Pilot scale fluid bed gasification plant.<https:// http://gpt.unizar.es/facilities/pilot-scale-fluid-bed-gasification-plant>. Last accessed: 29.08.2015

Greenhalf, C.E., Nowakowski, D.J., Bridgwater, A.V., Titiloye, J., Yates, N., Riche, A., Shield, I. 2012. Thermochemical characterisation of straws and high yielding perennial grasses. *Industrial Crops and Products*, **36**(1), 449-459.

Hasler, P., Bühler, R., Nussbaumer, T. 1998. Evaluation of gas cleaning technologies for biomass gasification. *Biomass for Energy and Industry: 10th European Conference and Technology Exihibition*., Würzburg, Germany.<http://hoga-renewable.es.tl/>. Last accessed: 29.08.2015.

Hindsgaul, C., Schramm, J., Gratz, L., Henriksen, U., Dall Bentzen, J. 2000. Physical and chemical characterization of particles in producer gas from wood chips. *Bioresource Technology*, **73**(2), 147-155.

HOGA. 2012. Hybrid renewable optimization by generic algorithms, Vol. 2015. Spain: University of Zaragoza.

HOMER. Hybrid optimization model for electric renewables, Vol. 2012, CO, USA: HOMER energy.

Hughes, W.E., Larson, E.D. 1997. Effect of fuel moisture content on biomass-IGCC performance. *ASME 1997 International Gas Turbine and Aeroengine Congress and Exhibition*. American Society of Mechanical Engineers. pp. V002T05A001-V002T05A001.

HYBRID2. 2012. The hybrid power system simulation model, Vol. 2015. MA, USA: Renewable Energy Research Laboratory (RERL).

InnoFireWood's. 2015. Burning of Wood.< http://virtual.vtt.fi/virtual/innofirewood/stateoftheart/database/burning/burning.html>. Last accessed: 01.09.2015

Jenkins, B.M., Baxter, L.L., Miles Jr, T.R., Miles, T.R. 1998. Combustion properties of biomass. *Fuel Processing Technology*, **54**(1–3), 17-46.

Klass, D.L. 1998. *Biomass for renewable energy, fuels, and chemicals*. Academic press.p.193-212.

Kumar, A., Jones, D.D., Hanna, M.A. 2009. Thermochemical biomass gasification: a review of the current status of the technology. *Energies*, **2**(3), 556-581.

Li, L., Huang, S., Wu, S., Wu, Y., Gao, J., Gu, J., Qin, X. 2015. Fuel properties and chemical compositions of the tar produced from a 5 MW industrial biomass gasification power generation plant. *Journal of the Energy Institute*, **88**(2), 126-135.

Li, Q.H., Zhang, Y.G., Meng, A.H., Li, L., Li, G.X. 2013. Study on ash fusion temperature using original and simulated biomass ashes. *Fuel Processing Technology*, **107**, 107-112.

Lim, J.S., Abdul Manan, Z., Wan Alwi, S.R., Hashim, H. 2012. A review on utilisation of biomass from rice industry as a source of renewable energy. *Renewable and Sustainable Energy Reviews*, **16**(5), 3084-3094.

Maghanaki, M.M., Ghobadian, B., Najafi, G., Galogah, R.J. 2013. Potential of biogas production in Iran. *Renewable and Sustainable Energy Reviews*, **28**(2013), 702-714.

Materials, A.s.f.T.a. 1975. Standard Test Method for Moisture Analysis of Particular Wood Fuels, part 21, ASTM International, West Conshohocken, PA, 2013.

Maurya, D.P., Singla, A., Negi, S. 2015. An overview of key pretreatment processes for biological conversion of lignocellulosic biomass to bioethanol. *3 Biotech*, 1-13.

McKendry, P. 2002a. Energy production from biomass (part 1): overview of biomass. *Bioresource technology*, **83**(1), 37-46.

McKendry, P. 2002b. Energy production from biomass (part 2): conversion technologies. *Bioresource technology*, **83**(1), 47-54.

Mohan, D., Pittman, C.U., Steele, P.H. 2006. Pyrolysis of Wood/Biomass for Bio-oil: A Critical Review. *Energy & Fuels*, **20**(3), 848-889.

Moka, V.K. 2012. Estimation of calorific value of biomass from its elementary components by regression analysis., Bachelor thesis, NIT, Rourkela, India. < http://ethesis.nitrkl.ac.in/3376/1/thesis.pdf>.Last accessed: 10.03.2016

Narvaez, I., Orio, A., Aznar, M.P., Corella, J. 1996. Biomass gasification with air in an atmospheric bubbling fluidized bed. Effect of six operational variables on the quality of the produced raw gas. *Industrial & Engineering Chemistry Research*, **35**(7), 2110-2120.

NASA. 2015. Surface meteorology and Solar Energy-Location, NASA, USA. < https://eosweb.larc.nasa.gov/sse/>. Last accessed: 29.08.2015.

Ni, M., Leung, D.Y.C., Leung, M.K.H., Sumathy, K. 2006. An overview of hydrogen production from biomass. *Fuel Processing Technology*, **87**(5), 461-472.

Pasangulapati, V., Ramachandriya, K.D., Kumar, A., Wilkins, M.R., Jones, C.L., Huhnke, R.L. 2012. Effects of cellulose, hemicellulose and lignin on thermochemical conversion characteristics of the selected biomass. *Bioresource Technology*, **114**(0), 663-669.

Phyllis2. ECN, The Netherlands. < https://www.ecn.nl/phyllis2/>. Last accessed: 29.08.2015.

Pieratti, E. 2011. Biomass gasification in small scale plants: experimental and modeling analysis. in: *Department of Civil and Environment*, Vol. Doctor of Philosophy, Università Delgi Studi Di Trento. Trento, Italy, pp. 159.

Potters, G., Van Goethem, D., Schutte, F. 2010. Promising biofuel resources: lignocellulose and algae. *Nature Education*, **3**(9), 14.

Puig-Arnavat, M., Bruno, J.C., Coronas, A. 2010. Review and analysis of biomass gasification models. *Renewable and Sustainable Energy Reviews*, **14**(9), 2841-2851.

Purdon, M.J. 2010. Softwood gasification in a small scale downdraft gasifier, Master thesis, Humboldt State University, USA. < http://humboldt-dspace.calstate.edu/handle/2148/665>.Last accessed: 29.08.2015.

Ramiah, M. 1970. Thermogravimetric and differential thermal analysis of cellulose, hemicellulose, and lignin. *Journal of Applied Polymer Science*, **14**(5), 1323-1337.

Rao, M.S., Singh, S.P., Sodha, M.S., Dubey, A.K., Shyam, M. 2004. Stoichiometric, mass, energy and exergy balance analysis of countercurrent fixed-bed gasification of post-consumer residues. *Biomass and Bioenergy*, **27**(2), 155-171.

REN 21. 2015. Renewables 2015. Global status report.< http://www.ren21.net/status-of-renewables/global-status-report/>.Last accessed: 01.09.2015.

Robbins, M.P., Evans, G., Valentine, J., Donnison, I.S., Allison, G.G. 2012. New opportunities for the exploitation of energy crops by thermochemical conversion in Northern Europe and the UK. *Progress in Energy and Combustion Science*, **38**(2), 138-155.

Rollinson, A.N., Karmakar, M.K. 2015. On the reactivity of various biomass species with CO2 using a standardised methodology for fixed-bed gasification. *Chemical Engineering Science*, **128**(0), 82-91.

Sarker, S., Arauzo, J., Nielsen, H.K. 2015. Semi-continuous feeding and gasification of alfalfa and wheat straw pellets in a lab-scale fluidized bed reactor. *Energy Conversion and Management*, **99**, 50-61.

Sarker, S., Nielsen, H. 2014. Preliminary fixed-bed downdraft gasification of birch woodchips. *International Journal of Environmental Science and Technology*, 1-8.

Serapiglia, M., Cameron, K., Stipanovic, A., Abrahamson, L., Volk, T., Smart, L. 2013. Yield and Woody Biomass Traits of Novel Shrub Willow Hybrids at Two Contrasting Sites. *BioEnergy Research*, **6**(2), 533-546.

Serapiglia, M.J., Cameron, K.D., Stipanovic, A.J., Smart, L.B. 2009. Analysis of biomass composition using high-resolution thermogravimetric analysis and percent bark content for the selection of shrub willow bioenergy crop varieties. *BioEnergy Research*, **2**(1-2), 1-9.

Shahzadi, T., Mehmood, S., Irshad, M., Anwar, Z., Afroz, A., Zeeshan, N., Rashid, U., Sughra, K. 2014. Advances in lignocellulosic biotechnology: A brief review on lignocellulosic biomass and cellulases. *Advances in Bioscience and Biotechnology*, **2014**.

Sharma, A., Pareek, V., Zhang, D. 2015. Biomass pyrolysis—A review of modelling, process parameters and catalytic studies. *Renewable and Sustainable Energy Reviews*, **50**, 1081-1096.

Shen, D.K., Gu, S., Luo, K.H., Bridgwater, A.V., Fang, M.X. 2009. Kinetic study on thermal decomposition of woods in oxidative environment. *Fuel*, **88**(6), 1024-1030.

Sheth, P.N., Babu, B.V. 2009. Experimental studies on producer gas generation from wood waste in a downdraft biomass gasifier. *Bioresource Technology*, **100**(12), 3127-3133.

Siedlecki, M., De Jong, W., Verkooijen, A.H. 2011. Fluidized bed gasification as a mature and reliable technology for the production of bio-syngas and applied in the production of liquid transportation fuels—a review. *Energies*, **4**(3), 389-434.

Sieminski, A. 2013. International energy outlook 2013. *US Energy Information Administration (EIA) Report Number: DOE/EIA-0484*. < http://www.eia.gov/forecasts/ieo/pdf/0484(2013).pdf>. Last accessed: 01.09.2015.

Sleiti, A. 2015. Overview of Tidal Power Technology. *Energy Sources, Part B: Economics, Planning, and Policy*, **10**(1), 8-13.

SSB. 2015. Statistisk Sentralbyrå. 2015 ed. Table: 10314: Net consumption of electricity, by consumer group (GWh) (M), < https://www.ssb.no/statistikkbanken/SelectVarVal/saveselections.asp>. Last accessed: 29.08.2015

Tanger, P., Field, J.L., Jahn, C.E., DeFoort, M.W., Leach, J.E. 2013. Biomass for thermochemical conversion: targets and challenges. *Frontiers in plant science*, **4:**218.doi: 10/3389/fpls.2013.00218

Turn, S.Q., Kinoshita, C.M., Ishimura, D.M., Zhou, J. 1998. The fate of inorganic constituents of biomass in fluidized bed gasification. *Fuel*, **77**(3), 135-146.

Umamaheswaran, K., Batra, V.S. 2008. Physico-chemical characterisation of Indian biomass ashes. *Fuel*, **87**(6), 628-638.

Vaezi, M., Passandideh-Fard, M., Moghiman, M., Charmchi, M. 2012. On a methodology for selecting biomass materials for gasification purposes. *Fuel Processing Technology*, **98**(0), 74-81.

van der Meijden, C., Veringa, H., Vreugdenhil, B., van der Drift, A., Zwart, R., Smit, R. 2009. Production of bio-methane from woody biomass. *Bio-methane World Gas Conference. Buenos Aires*.p.1-8.

Van Loo, S., Koppejan, J., 2008. *The handbook of biomass combustion and co-firing*. Earthscan, London.pp.441.

Varhegyi, G., Antal Jr, M.J., Szekely, T., Szabo, P. 1989. Kinetics of the thermal decomposition of cellulose, hemicellulose, and sugarcane bagasse. *Energy & Fuels*, **3**(3), 329-335.

Vassilev, S.V., Baxter, D., Andersen, L.K., Vassileva, C.G. 2010. An overview of the chemical composition of biomass. *Fuel*, **89**(5), 913-933.

Wang, L., Weller, C.L., Jones, D.D., Hanna, M.A. 2008. Contemporary issues in thermal gasification of biomass and its application to electricity and fuel production. *Biomass and Bioenergy*, **32**(7), 573-581.

White, J.E., Catallo, W.J., Legendre, B.L. 2011. Biomass pyrolysis kinetics: a comparative critical review with relevant agricultural residue case studies. *Journal of Analytical and Applied Pyrolysis*, **91**(1), 1-33.

Xiao, R., Jin, B., Zhou, H., Zhong, Z., Zhang, M. 2007. Air gasification of polypropylene plastic waste in fluidized bed gasifier. *Energy Conversion and Management*, **48**(3), 778-786.

Zainal, Z.A., Rifau, A., Quadir, G.A., Seetharamu, K.N. 2002. Experimental investigation of a downdraft biomass gasifier. *Biomass and Bioenergy*, **23**(4), 283-289.

Appended papers

Paper I

Preliminary Fixed-bed downdraft gasification of birch woodchips

Shiplu Sarker, Henrik Kofoed Nielsen

Published in **International Journal of Environmental Science and Technology**, 2015, 12(7) : 2119-2126

Journal information (ISI web of science):

Publisher: **Springer**
Impact factor: **2.19** (2014)
Rank: **86/221** (Environmental Sciences)

Int. J. Environ. Sci. Technol. (2015) 12:2119–2126
DOI 10.1007/s13762-014-0618-8

ORIGINAL PAPER

Preliminary fixed-bed downdraft gasification of birch woodchips

S. Sarker · H. K. Nielsen

Received: 16 March 2013 / Revised: 17 March 2014 / Accepted: 10 May 2014 / Published online: 3 June 2014

Abstract This paper investigated the possibilities of using birch wood chips for fixed-bed downdraft gasification. The preliminary air gasification resulted producer gas with an average composition of 11.5 % CO, 5.4 % CO_2, 5.9 % H_2, 0.38 % CH_4 corresponding to a mean lower heating value of about 2 MJ/kg. The approximate size of woodchips used for gasification was around 11.5 mm for a maximum solid throughput of 0.65 kg/h. The obtained equivalence ratio (ratio between actual air fuel ratio and stoichometric air fuel ratio) as a result of air and biomass feed was close to 0.45 which was stable throughout the test. Producer gas left the gasifier at ca. 150 °C and was diverted for flaring owing to the level of low energy content. Despite availability, the option for gas to generate heat and electricity via integrated gas engine has not been utilized in the present case and remained for further ongoing research.

Keywords Birch wood · Fixed-bed · Downdraft · Gasification · Producer gas

Introduction

The global energy is running the risk of scarcity and phase out of fossil fuel in the coming future (Shafiee and Topal 2009; Zainal et al. 2002). This will cause the utilization of various energy sources including with the renewables in all aspects of societies and industries. Mobilizing energy sectors toward sustainable and renewable technologies are a revolutionary stride expected to yield pronounced benefits in the context of energy security, reliability and environmental emissions (Ahmed et al. 2011). Gasification of biomass is one promising candidate to successfully achieve this transformation. By gasification, solid biomass gets converted into combustible gas with a typical composition of CO, CO_2, H_2, CH_4, N_2 and a trace amount of inert components (Hindsgaul et al. 2000; Barman et al. 2012), which has enormous potential to be utilized into range of applications (Brown and Brown 2013; Gautam 2010). Biomass with many different types is viable for gasification, but wood is particularly preferred due to its characteristics superior over coal and many grassy biomass as exemplified by high volatiles, low sulfur and low ash content (Janajreh and Al Shrah 2013; Shul'ga et al. 2012). Graphically, the convenient properties of wood in respect of other solid fuels has been depicted in popular Van krevelen diagram and cited by number of researchers (Janajreh and Al Shrah 2013; Basu 2010; Barrio 2002). Considering that, present work is based on one class of wood such as birch (*Betula Pendula*), as a feedstock for gasification.

Birch is abundant in northern European climate (Grønli 1996), but predominantly used for household applications as firewood to meet the heat demand. So far, utilizing birch for combustion contributed to a number of emissions leading to environmental and health hazards (Hedberg et al. 2002). These drawbacks pose a great concern triggering in search for alternative that could sustainably be applied for energy production. Gasification in that direction consequently emerged as a viable solution to diminish much of the issues associated with combustion. Unlike combustion which requires equal or higher amount of stoichiometric air, gasification occurs at oxygen scarce

S. Sarker (✉) · H. K. Nielsen
Faculty of Engineering and Sciences, University of Agder, 4898 Grimstad, Norway
e-mail: shiplu.sarker@uia.no

condition and hence contributes to a significant reduction in pollutant emissions. For this study, therefore, gasification of birch woodchips is proposed which to date has not been exploited to the knowledge of the authors.

In general, thermochemical conversion of biomass is performed into three different types of gasifiers commonly known as fixed-bed, fluid-bed and entrained flow reactors (Kotowicz et al. 2013; Couto et al. 2013). Fixed-bed reactors are further categorized into updraft, downdraft and cross-draft gasifiers based on the way feedstock and gas move through the system. Within the fixed-bed reactors, downdraft technologies offer several advantages that include: simplicity in construction (Wei 2010), suitability for small scale applications (Asadullah 2014) and the possibilities of generating less tar (McKendry 2002; Son et al. 2011; Chopra and Jain 2007) as a result of hot gas passing through the high-temperature zone of the reactor. Based on these premises, the present work investigated air gasification of fixed-bed downdraft gasifier utilizing wood as feedstock.

Experimental investigation of fixed-bed downdraft gasification of woodchips has been explored in many contemporary works. Lenis et al. (Lenis et al. 2013), for example, focused on five different wood species (*Acacia mangium, Eucalyptus* sp., *Pinus* sp., *Pinus patula* and *Gmelina arborea*) for which first the gasification model was formulated which was further validated in a lab scale reactor. Lee et al. (2013) developed their studies based on fixed-bed air gasification and further to electricity generation via spark ignition internal combustion (IC) engine using pine and red oak as feeding materials. Fixed-bed downdraft gasification of woodchips with air as gasifying agent was performed by a comprehensive research conducted by Zainal et al. (2002) who established the effect of operational parameters on the quality and quantity of producer gas. Published research (Yoon et al. 2011) also included the influence of several parameters on fixed-bed gasification of woodchips (German Conifer) using air and steam mixtures as the gasifying medium.

In line with those previous contributions, biomass energy research group at University of Agder is facilitating the fundamental components necessary for gasification and subsequently for energy production. This paper only reports the preliminary work which was devoted to examine the possibilities of utilizing birch wood chips for fixed-bed gasification with air as gasifying agent.

Materials and methods

Date and location of the study: 08/08/2013, University of Agder, Grimstad, Norway.

Feedstock

Birch wood was cut down by a chain saw and further chipped by a disk chipper (NHS 720 IE 4, Denmark) with a nominal cutting length of about 11.5 mm during the winter 2012–2013 at Grimstad, Norway. Produced wood chips were then placed indoor, stacked with a 20 cm thick layer for natural drying, which was promoted by repeated mixing with shovel. The photograph of birch woodchips is illustrated in Fig. 1.

Characterization of birch woodchips

Birch woodchips was characterized for moisture, proximate, ultimate and heating value analysis prior to gasification. Moisture was determined in situ gravimetrically with a moisture analyzer (Metler Toledo LJ16, Switzerland) programmed for 105 °C temperature. By this instrument, total weight loss of a sample is measured with corresponding increase in temperature until no further weight measurement at the set temperature. Volatiles were determined by the external lab Eurofins Environmental Testing Sweden AB according to the protocol EN 15148/15402. Ash was measured complying with the standard CEN/TS 15403, whereas fixed carbon was evaluated by difference. Calorific value of feedstock was measured in situ employing bomb calorimeter (LECO AC 500, USA) that followed the standard CEN/TS 14918/15400 ISO. Likewise volatiles, elemental analysis of birch wood was also conducted externally by Eurofins Environmental Testing Sweden AB according to the protocol EN 15104/15407 for carbon, hydrogen, oxygen and nitrogen and according to the protocol EN 15289/15408 for chlorine (Cl) and sulfur (S). The characterization of birch woodchips in respect of proximate and ultimate analysis is presented in Table 3.

Fig. 1 Birch woodchips used for gasification

Fig. 2 Flaring of fixed-bed downdraft gasifier integrated with a natural gas engine (University of Agder)

Table 1 Specifications of the gasification unit: source Victory Gasworks

Item	Description
Gasifier	Victory super CHP
Type	Air blown downdraft gasifier
Input	~1.13 kg/kWh
Maximum speed	4–90 m^3/h (adjustable)
Output with engine	5–15 kW_e, 3 kW hot water
Operating temperature	1,050–1,250 °C

Table 2 Specifications of the gas engine: source Kubota Engine America Corporation

Item	Description
Engine	Kubota DG972-E2
Type	Vertical 4-cycle liquid cool natural gas
No. of cylinders	3
Maximum speed	3,600 rpm
Volume	0.962 m^3
Output (natural gas)	17.6 kW

Experimental setup

Gasifier and engine

The experimental setup consists of a fixed-bed downdraft Victory gasifier unit with integrated hopper, producer gas cooling and cleaning system. The specification of gasifier is given by the Table 1, whereas Fig. 2 shows the structure of the gasifier system. The gasification unit comprises with a 0.13-m^3 cone structure feeding hopper above the reactor.

Main body of this structure is made from a 500-mm outer diameter steel pipe with an internal air jacket and refractory insulation in reaction zone. Total height of the gasifier including with the hopper is around 1.7 m. The inclined shape of the hopper ensures the smooth gravitational flow of feeding material into the throat for better gasification and tar reduction. Biomass is fed from the top, while the air is induced through six nozzles above an exchangeable restriction ring (100 mm). Nozzles are equidistantly located around the circumference of pipe above the throat of the gasifier. To provide a sufficient draft necessary for the air to pass through the system, a fan is located at the end of gas exit and powered by a battery bank charged by a gas engine (for this experimental set up). In a typical case, producer gas exiting from gasifier runs the engine and gets converted into heat and electricity which is subsequently stored in a lead-acid battery for further usage (Fig. 2).

Biomass as moves downward from the top of the gasifier is dried and devolatilized by the heat carried from the combustion zone. High-temperature gas from the combustion zone is gasified by the gas and solid phase reactions and exits from the bottom of the gasifier. After passing the gasifier, the producer gas is cooled in a gas–water heat exchanger, resulting in condensation of a portion of water vapor. Additional gas cleaning is achieved in a settling chamber filled with hanging ribbons while final cooling and filtration is conducted by a water sprayed Teflon filter screen sieve. While leaving the gasifier, the producer gas also comes into contact with the glowing char and the ashes and as a result provides the additional cleaning effect. Char produced through the thermochemical reaction is also

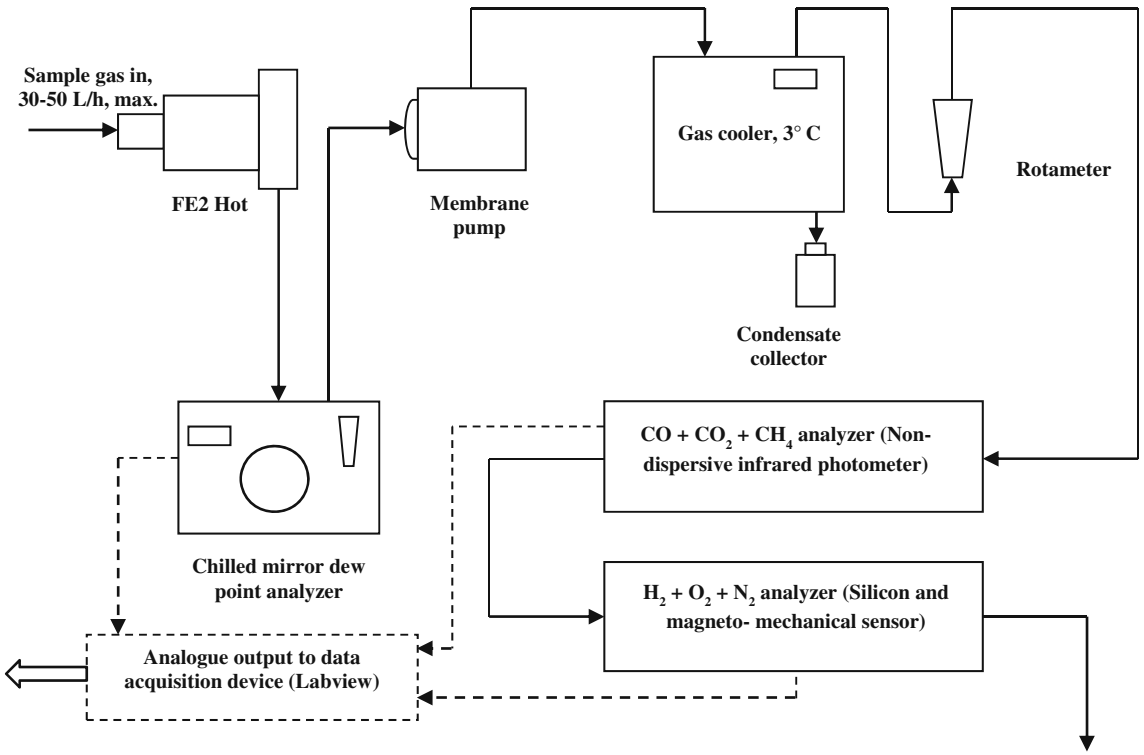

Fig. 3 Components used in gas sampling and data acquisition

gasified by high temperature (~900–1,000 K) (Jayah et al. 2003) and generates necessary heat to propagate the gasification steps throughout the reactor. Ash, the final solid product of gasification with a very little value for combustion and gasification, is collected from the grate, positioned beneath the combustion chamber. Cleaned producer gas is by-passed for flaring to identify the quality before diverting to the gas engine. Flame in the flare turns from bright yellow to bluish (corresponding to the high energy content gas) once the producer gas is ready for consumption in the gas engine.

The gasifier is also featured with a vibrating mechanism, a shaker, driven by an electric motor to generate the vibration motions at a regular interval. Such vibrations reduce the risk for channeling and bridging of biomass inside the gasifier and sustain the continuous downward movement of feedstock. The grate is reciprocally rotated by adjustable intervals for a smoother and easier ash discharge.

Further downstream, the gasifier is coupled with a 0.962 L three cylinder natural gas engine rated with 17.6 kW mechanical power. The engine is capable to run at a wide range of speed up to 3,600 rpm. In the present case, the engine generates electricity in two DC generators with a total capacity of 5 kW. The electricity is stored in the battery which with the help of an inverter subsequently transforms DC power into AC which is further utilized by an adjustable load of 5.3 kW (electric heaters). The specifications of engine as per Kubota Engine America Coroporation is illustrated in Table 2.

Gas sampling

In order to measure and monitor the composition of the producer gas, a part of the gas is bypassed at a maximum flow rate of 50 L/h through the state-of-the art gas sampling facility consisting with hot filter, dew point analyzer, membrane pump, rotameter, gas cooler and gas analyzers as demonstrated in Fig. 3. In the first step, dust particles are removed from gas by the hot filter (FE2, ABB, Germany) operating at a temperature of around 150 °C. The relatively cleaned gas is then flown through a dew point analyzer (Omega, RHB-1500, USA) for determining the dew point, necessary for evaluating dryness of the gas. Subsequently, gas is partially dried by supplying through a gas cooler (SCC-C Sample gas cooler, ABB, Germany), maintaining about 3 °C temperature at outlet. Flow into the sampling line is maintained by a diaphragm pump (Membrane pump 4 N, ABB, France) and controlled by a rotameter (0–50 L/h), governing the flow at a desired level. After cleaning and drying via hot filter and gas cooler, the gas is finally sent to the analyzers. In principle, gas analyzer detects the gas composition within the flow range of 20–40 L/h which is monitored by the rotameter located into the flow line. Two analyzer units (Advance optima, AO2020; ABB, Germany) mounting three different sensors

(URAS 26, CALDOS 27 and MAGNOS 206) measure various composition of producer gas. Gas analyzer unit 1 houses analyzer component URAS 26, working with the principle of non-dispersive infrared photometer and measures percent composition of CO, CO_2 and CH_4 in the producer gas. Analyzer unit 2 contains two sensors CALDOS 27 and MAGNOS 206 and determines the percent amount of H_2 and O_2 in the sample gas content. Sensor CALDOS 27 uses the concept of high thermal conductivity of H_2 for gas measurement, while paramagnetic nature of oxygen is utilized in MAGNOS 206 to analyze oxygen in the sample gas flow.

Analytical

Produced gas composition after gasification was evaluated in situ by the ABB gas analyzers as specified in "Gas sampling" section, whereas the lower heating value was calculated based on the procedure set by ISO 6976. Temperature at different locations of gasifier, air and gas was measured by the number of K-type thermocouples mounted in and around the gasifier. Two pressure sensors (Smart DCM/SN Diff, Fema, Germany) measure the pressure difference in the process as a result of filtration (hot and wet) and obstruction in the gas and biomass. Figure 4 shows the location of four temperature sensors: T_1 (at reduction), T_2 (gas exit), T_3 (combustion) and T_5 (air inlet) and one pressure sensor, p_1 within the gasifier. T_4 (filtered gas) and p_2 are located in the downstream of the gas flow and therefore are not covered in Fig. 4. Degradation of feed during gasification was monitored by a scale (Dini Argeo, DGT PK, Italy) installed beneath the gasifier assembly. The values registered in the scale, gas analyzers, temperature sensors, pressure sensors and dew point analyzer were acquired through Labview data acquisition software (National Instruments, LabVIEW 2010, USA) for further interpretation. Screen shot of Labview programming is given in the "Appendix".

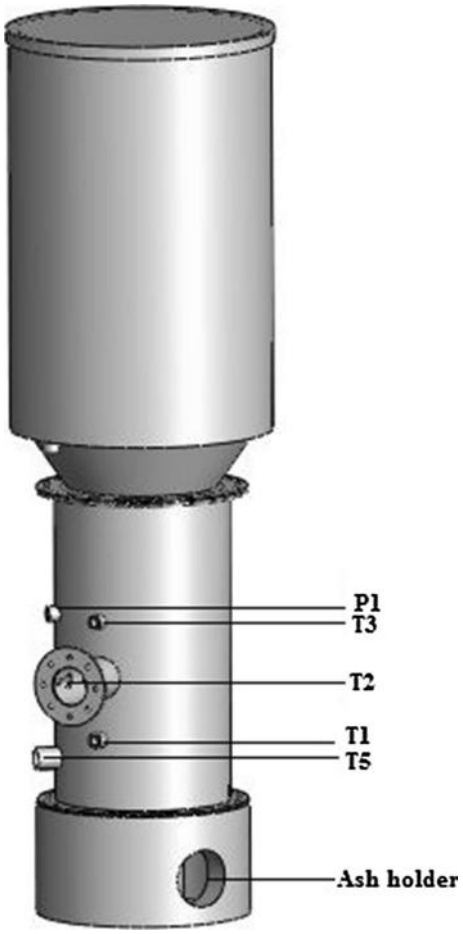

Fig. 4 Pressure and temperature sensors along the gasifier

Results and discussion

Feedstock characterization

Results of feedstock characterization (Table 3) demonstrated that the level of moisture in birch woodchips is acceptably low which in terms of gasification is very attractive (Atnaw et al. 2014; Gautam 2010). Additionally, birch has low ash, low sulfur, low chlorine and high calorific value and high volatile matter content as reflected in Table 3. Woody biomass exhibiting such composition possibly yields less or no tar in the produced gas within the operating scale that does not exceed 30 kW as evidenced by (Son et al. 2011; Warren et al. 1995). Moreover, low ash offers substantial advantages in reducing the potential of slagging and slow biomass conversion, as discussed by (Rajvanshi 1986). High carbon content (50.4 %) furthermore suggests why the calorific value of this biomass is rather high (Moka 2012). Knowing the physical and chemical composition of biomass is of great importance to understand the gasification phenomena associated with reaction chemistry, gas composition and tar characteristics further can be extrapolated for energy and mass balance of the entire system.

Gasification of birch wood chips

Among the range of operations, trial run of gasifier with 100 % birch wood chips (moisture content 15.2 %) that carried on August 8, 2013, was most interesting in terms of fuel gas composition and calorific value. The experiment continued for about 6 h during which period several experimental parameters such as characteristics of producer gas, gas flow, temperature and pressure at different

Table 3 Proximate and ultimate analysis of birch woodchips

Proximate analysis (dry basis)	
Moisture, %	7
Volatiles, %	82.2
Fixed carbon, %	10.45
Ash, %	0.35
LHV (MJ/kg)	17.9
Ultimate analysis (dry basis)	
Carbon, %	50.4
Hydrogen, %	5.6
Oxygen, %	43.4
Nitrogen, %	0.12
Sulfur, %	0.017
Chlorine, %	0.019

locations and biomass feed degradation pattern are measured and illustrated in Fig. 5 through 7.

Figure 5 demonstrates the evolution of producer gas composition and its corresponding LHV (Lower heating value) throughout the test period. Among the combustible species of generated gas, CO was found highest with an average of 11.8 %, followed by hydrogen (5.9 %) and methane (0.38 %). Gas LHV, a direct function of combustible components, reached to a peak at approximately 2.5 MJ/kg when reasonably higher CO and H_2 were produced after some 4 h of operation. However, the trend was varying to a great degree, characterized by few unstable periods close to second, third and fifth h of operation. These phenomena are perhaps attributed to a several factors such as bridging, abrupt change in temperature (Zainal et al. 2002), instability in air supply (Reed et al. 1988). In fact, the decrease in airflow during the unstable periods was clearly observed and evidenced by Fig. 6. Generally, the decrease in battery voltage causes the decrease in fan speed which ultimately reflects in air flow and in turn in gas pressure, biomass conversion, temperature and gas characteristics, as indicated by Fig. 5 through 7. While other parameters were influenced, airflow resulted an average equivalence ratio (ER) of 0.45 which is arguably high for gasification. By and large, downdraft gasification was proved to perform better when operated within the range of 0.25 ER (Reed et al. 1988). The study of (Zainal et al. 2002), however, showed the successful operation even with an ER up to 0.43. Likewise equivalence ratio, mean cold gas efficiency for this experiment was relatively low, approximately to 54 %. Typical cold gas efficiency for fixed-bed downdraft gasifier lies in the range between 65 and 75 % as reported by (Knoef et al. 2012). Cold gas efficiency for this work could probably be improved by increasing airflow eventually contributing to the reaction chemistry between gas and solid components, causing high composition of combustible species in the producer gas.

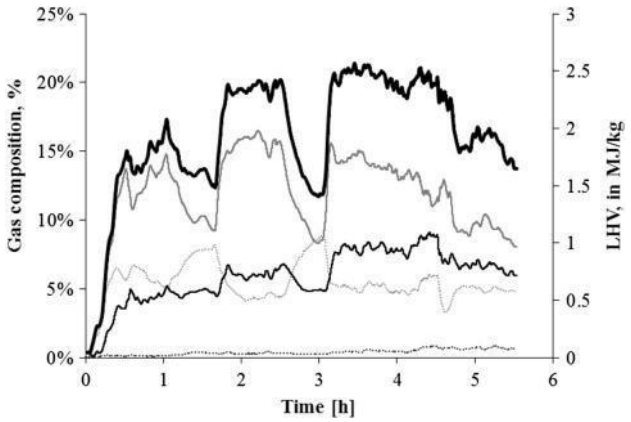

Fig. 5 Composition of producer gas and its corresponding calorific value: LHV (*Thick solid black line*); CO (*Solid gray line*); CO_2 (*Dotted gray line*); H_2 (*Thin solid black line*); CH_4 (*Dotted black line*)

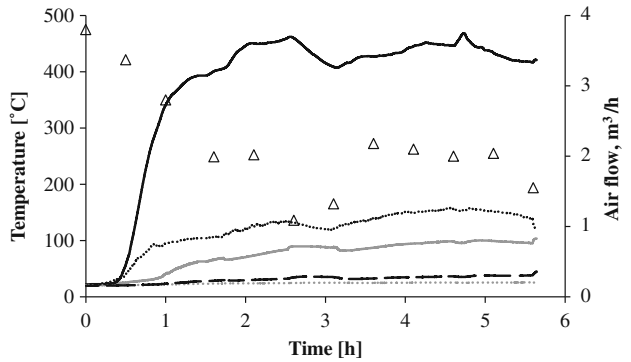

Fig. 6 Temperature at different gasifier locations and airflow: T_1, reduction (*Solid gray*); T_2, raw gas exit (*Dotted black*); T_3, combustion (*Solid black*); T_4, filtered gas exit (*Dotted gray*); T_5, air inlet (*Dashed black*); airflow (*empty triangles*)

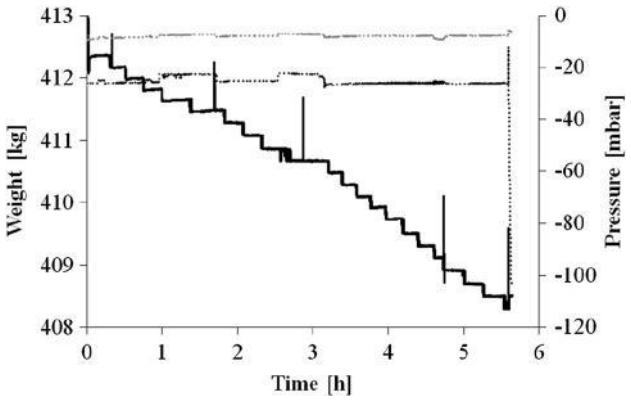

Fig. 7 Biomass degradation and pressure gradient during gasification of birch wood: Weight reduction (*Solid black line*); p1, pressure before filtration (*Dotted black line*); p2, pressure after filtration (*Dotted gray line*)

Principally, air is the only external input that can be varied while gasifier is under operation and thus leaving a wide scope for further investigation at a numerous air inputs.

The basic idea of this preliminary study was to evaluate the performance of measurement system that generates necessary operational and technical data from gasification. So observing the nature and relation between parameters as illustrated by Fig. 5 through 7 would provide a solid basis for further improvement in technical and theoretical aspects which include optimization of process parameters, evaluation of tar, experimentation on power production.

Conclusion

This study revealed the performance of a downdraft fixed-bed gasifier for producing high energy gas by utilizing birch woodchips as a feedstock. In the preliminary run, the LHV of the producer gas reached to maximum 2.5 MJ/kg with a corresponding ER of 0.45. The average product gas composition (11.5 % CO, 5.4 % CO_2, 5.9 % H_2, 0.38 % CH_4) and the cold gas efficiency (54 %) were nevertheless found low, suggesting a wide scope of performing more research on birch wood gasification. The present research thus is ongoing and yet to discover the heat and electricity potential of wood gas by incorporating gas engine as a downstream energy conversion unit.

Acknowledgments The authors greatly acknowledge the PhD funding and the facilities of University of Agder together with J.B.Ugland AS to conduct this research. Assistance from a number of people during biomass harvesting and pre-treatment is also highly noted.

Appendix

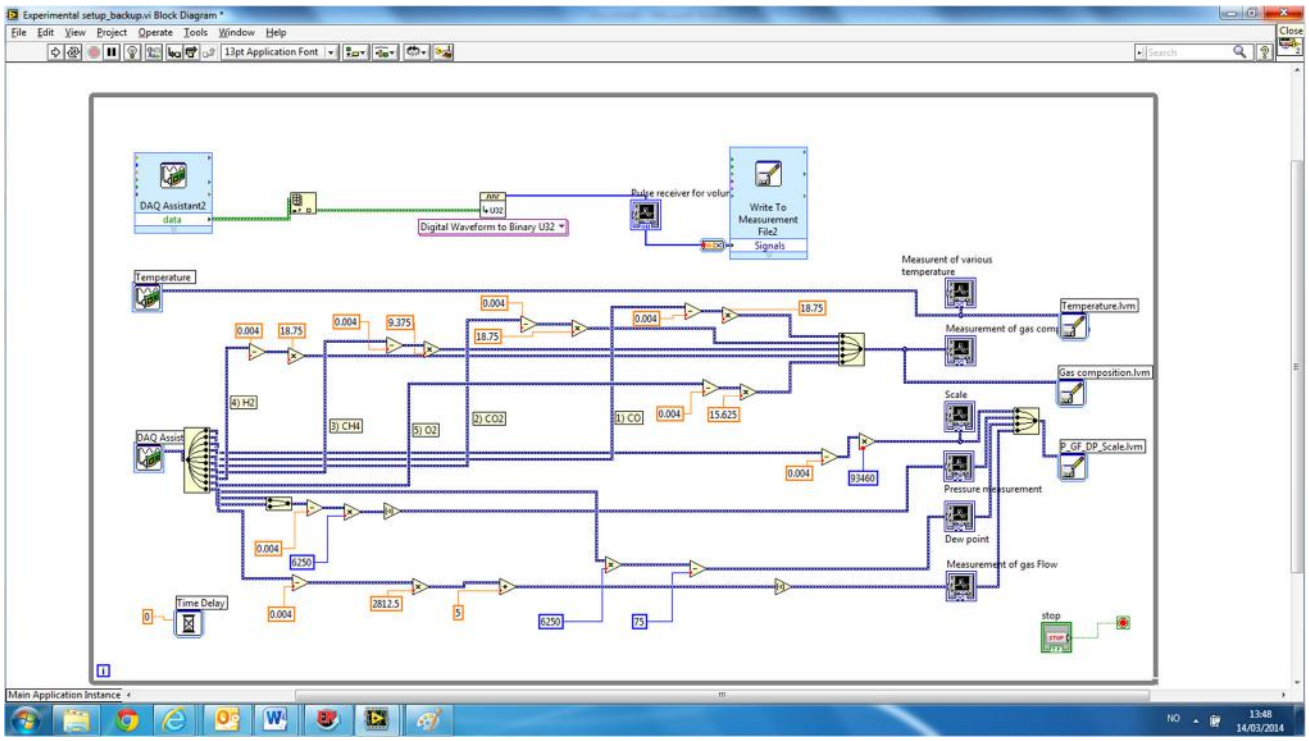

References

Ahmed I, Nipattummakul N, Gupta A (2011) Characteristics of syngas from co-gasification of polyethylene and woodchips. Appl Energy 88(1):165–174

Asadullah M (2014) Barriers of commercial power generation using biomass gasification gas: a review. Renew Sustain Energy Rev 29:201–215

Atnaw SM, Sulaiman SA, Yusup S (2014) Influence of fuel moisture content and reactor temperature on the calorific value of syngas resulted from gasification of oil palm fronds. Sci World J. doi:10.1155/2014/121908

Barman NS, Ghosh S, De S (2012) Gasification of biomass in a fixed bed downdraft gasifier—a realistic model including tar. Bioresour Technol 107:505–511

Barrio M (2002) Experimental investigation of small-scale gasification of woody biomass. PhD dissertation, Norwegian University of Science and Technology, Trondheim, Norway

Basu P (2010) Biomass gasification and pyrolysis: practical design and theory. Academic press, USA

Brown RC, Brown TR (2013) Biorenewable resources: engineering new products from agriculture. John Wiley & Sons, USA

Chopra S, Jain AK (2007) A review of fixed bed gasification systems for biomass. Agric Eng Int: CIGR J 9:1–26

Couto N, Rouboa A, Silva V, Monteiro E, Bouziane K (2013) Influence of the biomass gasification processes on the final composition of syngas. Energy Proced 36:596–606

Gautam G (2010) Parametric study of a commercial-scale biomass downdraft gasifier: experiments and equilibrium modeling. Dissertation, Auburn University, USA

Grønli MG (1996) A theoretical and experimental study of the thermal degradation of biomass. Dissertation, Norwegian University of Science and Technology, Trondheim, Norway

Hedberg E, Kristensson A, Ohlsson M, Johansson C, Johansson P-Å, Swietlicki E, Vesely V, Wideqvist U, Westerholm R (2002) Chemical and physical characterization of emissions from birch wood combustion in a wood stove. Atmos Environ 36(30):4823–4837

Hindsgaul C, Schramm J, Gratz L, Henriksen U, Dall Bentzen J (2000) Physical and chemical characterization of particles in producer gas from wood chips. Bioresour Technol 73(2):147–155

Janajreh I, Al Shrah M (2013) Numerical and experimental investigation of downdraft gasification of wood chips. Energy Convers Manag 65:783–792

Jayah T, Aye L, Fuller R, Stewart D (2003) Computer simulation of a downdraft wood gasifier for tea drying. Biomass Bioenergy 25(4):459–469

Knoef HAM, Ahrenfeldt J, Angrill LS, Group NOvT-NOBT (2012) Handbook biomass gasification. BTG Biomass Technology Group, Netherlands

Kotowicz J, Sobolewski A, Iluk T (2013) Energetic analysis of a system integrated with biomass gasification. Energy 52:265–278

Lee U, Balu E, Chung J (2013) An experimental evaluation of an integrated biomass gasification and power generation system for distributed power applications. Appl Energy 101:699–708

Lenis Y, Osorio L, Pérez J (2013) Fixed bed gasification of wood species with potential as energy crops in Colombia: the effect of the physicochemical properties. Energy Sources, Part A: Recovery, Util Environ Eff 35(17):1608–1617

McKendry P (2002) Energy production from biomass (part 3): gasification technologies. Bioresour Technol 83(1):55–63

Moka VK (2012) Estimation of calorific value of biomass from its elementary components by regression analysis. BTech thesis, NIT Rourkela, India

Rajvanshi AK (1986) Biomass gasification. Altern Energy Agric 2:83–102

Reed T, Reed TB, Das A, Das A (1988) Handbook of biomass downdraft gasifier engine systems. Biomass Energy Foundation, USA

Shafiee S, Topal E (2009) When will fossil fuel reserves be diminished? Energy Policy 37(1):181–189

Shul'ga I, Zelenskii O, Vikhlyaev A (2012) Gasification of wood chips. Coke Chem 55(8):324–327

Son Y-I, Yoon SJ, Kim YK, Lee J-G (2011) Gasification and power generation characteristics of woody biomass utilizing a downdraft gasifier. Biomass Bioenergy 35(10):4215–4220. doi:10.1016/j.biombioe.2011.07.008

Warren TJB, Poulter R, Parfitt RI (1995) Converting biomass to electricity on a farm-sized scale using downdraft gasification and a spark-ignition engine. Bioresour Technol 52(1):95–98. doi:10.1016/0960-8524(95)00022-7

Wei L (2010) Technical and economic evaluation of small-scale biomass gasification facilities in Mississippi. PhD Dissertation, Mississippi State University, USA

Yoon H, Cooper T, Steinfeld A (2011) Non-catalytic autothermal gasification of woody biomass. Int J Hydrog Energy 36(13):7852–7860

Zainal ZA, Rifau A, Quadir GA, Seetharamu KN (2002) Experimental investigation of a downdraft biomass gasifier. Biomass Bioenergy 23(4):283–289. doi:10.1016/s0961-9534(02)00059-4

Paper II

Characterization and pilot-scale fluidized bed gasification of herbaceous biomass: A case study on alfalfa pellets

Shiplu Sarker, Fernando Bimbela, José Luis Sánchez, Henrik Kofoed Nielsen

Published in **Energy Conversion and Management**, 2015, 91: 451-458

Journal information (ISI web of science):

Publisher: **Elsevier**
Impact factor: **4.38** (2014)
Rank: **14/88** (Energy & Fuels)

Energy Conversion and Management xxx (2014) xxx–xxx

Contents lists available at ScienceDirect

Energy Conversion and Management

journal homepage: www.elsevier.com/locate/enconman

Characterization and pilot scale fluidized bed gasification of herbaceous biomass: A case study on alfalfa pellets

Shiplu Sarker[a,*], Fernando Bimbela[b], José Luis Sánchez[b], Henrik Kofoed Nielsen[a]

[a] University of Agder, Faculty of Engineering and Science, Serviceboks 509, 4898 Grimstad, Norway
[b] Universidad Zaragoza, Thermochemical Processes Group (GPT), Aragon Institute of Engineering Research (I3A), I+D+i building, C/Mariano Esquillor s/n, E-50018 Zaragoza, Spain

ARTICLE INFO

Article history:
Received 26 August 2014
Accepted 13 December 2014
Available online xxxx

Keywords:
Alfalfa pellets
Pilot scale fluidized bed
Gasification
Equivalence ratio
Temperature

ABSTRACT

Pilot-scale bubbling fluidized bed gasification tests of alfalfa pellets were performed at two different operational periods ranged on the basis of two given equivalence ratio (ER) (the ratio between actual air and the stoichiometric air) namely as 0.25 and 0.30. During the test, the solid feeding rate was kept constant at 4.7 kg/h while the air input was varied and thus the ER. Increasing air from 4.16 to 4.99 N m^3/h contributed to the evolution pattern of several parameters such as the rise in gas lower heating value (LHV) and gas yield, the average maximum of which were 4.2 MJ/N m^3 and 1.5 N m^3/kg respectively. Gas composition was mainly boosted by the concentration of CO, as the rest of the combustible components stayed rather unaffected due to the modified air flow rate. The steady state bed temperature agreed with the trend of air flow and ranged between 720 and 780 °C, despite gasification start-up occurred at 800 °C. Total char (~282 g/kg) and tar yield (~1.1 g/N m^3) showed reasonable values while tar composition was predominantly led by the amount of phenols.

1. Introduction

In the spectrum of renewable energy, biomass poses as one of the most important alternatives to fossil fuels [1], accounting as the fourth largest energy source [2] in the world after coal, petroleum and natural gas, and offering substantial advantages including no net [3] and even negative CO_2 emissions [4,5], depending on the use of CO_2 capture technologies. In fact, it is the only renewable source that can feasibly be transformed into various forms of fuels, i.e.: solids, liquids and gases, through different conversion pathways: thermo-chemical, bio-chemical and biological [2,6]. Within the thermochemical conversion routes [7] gasification is attractive owing to its flexibility and simplicity. The gas produced from biomass gasification is a clean (once it is adequately conditioned) combustible fuel typically consisting of CO, H_2, CO_2, CH_4 and C_2H_n, [8,9] which is viably used for a number of applications including heat, electricity or as a synthesis gas (or syngas) that can serve as raw-material in the manufacture of other value added products [10]. To achieve gasification, a series of reactors may be implemented, such as fixed-bed, moving bed, fluidized-bed and entrained flow gasifier [6]. For a suitable energy output and operational ranges each of these gasifiers has its own advantages and disadvantages. Fluidized bed (FB) gasifiers for instance are relatively less complex, flexible and efficient [11,12] and thus are used in numbers in medium and small scale applications [13].

In addition to the types of the gasifiers, various gasifying agents such as air, steam, steam–oxygen and CO_2 can significantly influence the output quality and performance of gasification [11,14]. The choice of gasification hence is not only a choice of a gasifier but also a choice of the gasifying medium. Air as a gasifying agent despite yielding a low heating value gas, has certain advantages over others [11]. Air is easily available everywhere and its introduction to gasification does not incur additional costs for its production, thus as a medium invariably emerges as cheap, easy and readily available option for various scales of operations, as does this study.

Although a great deal of biomass feedstocks have already been explored in fluidized bed gasification, the work in regards to herbaceous biomass especially to alfalfa (*Medicago sativa* L.) is potentially scarce. The majority of efforts for this biomass to date have only been paid to pyrolysis [15,16] and characterization [17] with a noted investigation primarily toward fixed-bed downdraft gasification [18]. But considering the potential of environmental and financial advantages [19] including with lignocellulosic properties, alfalfa could be an attractive fuel for distributed power generation where the possibility of fluidized bed gasification is enormous [20]. The focus of the present study thus is to utilize alfalfa pellets (that does not compete with the animal feeding) for a pilot-scale fluidized bed gasification, which can serve as a means of producing

* Corresponding author. Tel.: +47 37233144.
E-mail address: shiplu.sarker@uia.no (S. Sarker).

http://dx.doi.org/10.1016/j.enconman.2014.12.034
0196-8904/

renewable energy to the areas de-centralized from the national electricity grid.

As a local biomass, alfalfa has vast potential around the Ebro valley area in the Northeast (NE) Spain, constituting the regions of Aragon and Catalunya, with available lands of 107,000 and 42,500 ha respectively. Of the total available land for the alfalfa in Spain, 58% is covered by these regions, with average dry matter (DM) yields of about 17 t ha^{-1} y^{-1} [19] The majority of this yield is primarily realized through pelletization [21] which in terms of energy production is also interesting, as pellets are easy-to-handle, superior than to other forms of biomass. Alfalfa pellets are thus utilized in the present context of gasification.

Research in regards to pilot-scale fluidized bed gasifier is extensive [13,22–26] and has been conducted for a number of feedstocks operating with a number of experimental conditions. In a recent work by Campoy et al. [13] for example a pilot-scale BFB (Bubbling fluidized bed) gasifier was involved to process five different biomass: wood pellets, orujillo, meat and bone meal (MBM), dried sewage sludge (DSS) and municipal solid waste (MSW) for a number of operating conditions, i.e.; bed temperatures (770–870 °C) and ERs (0.23–0.43) for which gasification performance was compared among the feedstocks. A comprehensive other research [22] furthermore included ten biomass (ranging from woody to agricultural) to test simultaneous gasification and energy conversion by a pilot scale air-blown fixed-bed downdraft gasification power plant unit for which operational parameters was observed as against different syngas flow rates (105–211 N m^3/h). Documented researches [27,28] also considered co-gasification of a wide range of biomass for the pilot-scale studies, utilizing different modes of gasification system.

In line with these efforts, the preliminary work presented here introduces alfalfa pellets to a pilot-scale bubbling FB reactor with a purpose of evaluating gasification for a range of bed temperatures (720–780 °C) and ER (0.25–0.30).

2. Materials and methods

2.1. Feedstock

Herbaceous biomass alfalfa pellets (average dimensions: approximately 6 mm Ø and 25 mm length) were used as feedstock for this study. Approximately 100 kg of alfalfa pellets with 100% purity from the first harvest (April 2013) were manufactured by Cooperativa Campo San Gregorio and kindly supplied by Molinos Afau S.L., both established on Pina de Ebro (Spain).

Alfalfa was grown and harvested around the Ebro valley, in the surroundings of Pina de Ebro, a village located 40 km southeast from Zaragoza (capital of Aragón, a region in the Northeast of Spain, coordinates: 41°39′0″N, 0°53′0″W). Generally, alfalfa grown in this region is harvested two/three times per season in the rainfed areas or six/seven times per season under irrigation [29] areas. To produce pellets, harvested alfalfa was first dried to approximately 10% of moisture by employing a rotary drum dryer, using flue gas as the drying medium. Dried biomass was then sent to a hammer mill equipped with a screen size of 3.2–6.4 mm, grinding the biomass to particles suitable for pelletization. As soon as the alfalfa was ground, it was delivered to the press mill consisting of a roller and heated die drilled with a series of perforated holes (~6 mm) through which biomass was squeezed. No external binders or stabilizing agents were used in the pelletizing process. The raw pellets exiting from the die were hot which was cooled to an ambient temperature of about 5 °C in the cooler and conveyed for further storage. A blade was typically used to cut the pellets to a predefined length, as those proceeded to the exit.

2.2. Characterization of feedstock

Alfalfa pellets were characterized in terms of moisture, ash, volatiles, fixed carbon, calorific values and of elemental compositions to examine the possibilities for gasification.

Moisture content of the alfalfa pellets was analyzed per triplicate as according to the standard ASTM D-871-82. Volatile matter was measured per triplicate based on the protocol suggested by EN 15148 while the protocol EN 15403:2011 was used for determining the ash content. Before the analyses of volatile matter and ash, biomass pellets were milled to an average particle size of <5 mm by using a lab-scale hammer mill (Mercanofil.Mateu y Solè, Spain). The calorific value of the alfalfa pellets was determined per triplicate using a calorimetric bomb (IKA C2000, Germany) complying with the standard ASTM D 4809-95.

Finally, the ultimate analysis was performed by using an elemental analyzer (Leco TruSpec Micro, USA) by which a simultaneous determination of C, H, N and S was obtained. As oxygen content cannot be analyzed directly by the present instrument, it was calculated by-difference.

In addition to the ultimate and proximate analyses, structural analysis in terms of cellulose, hemicellulose and lignin content of different sections of alfalfa crop are presented in Table 1 as according to the Refs. [30,16].

2.3. Pilot scale fluidized bed gasification

Gasification experiments were carried out by a pilot-scale bubbling fluidized bed gasifier located at Universidad Zaragoza, rated with an approximate maximum throughput capacity of 10 kg/h and operating at autothermal regime once that the temperature inside the reactor rises high enough to maintain gasification conditions. A global view of the gasifier, along with the associated components is illustrated by Fig. 1while the following sub-sections discuss their working principles, as found during the operation of the plant.

2.3.1. Feeding system

The feeding system is composed of two hoppers of approximately 40 kg of capacity each, with their corresponding screw feeders that can be regulated independently with variable frequency drivers, discharging the solids into a third screw feeder (from now on, named as shuttle). One of the hoppers contains the raw material and the other is filled with silica sand, which is used as coadjutant material to aid feeding the raw material into the reactor, as well as to constitute the reaction bed.

Biomass and sand as contained in the hoppers were continuously introduced at the bottom of the reactor by means of the shuttle. The motion of the shuttle is expressed by the revolution per minute (rpm) and controlled by a variable frequency driver, adjusted to the necessary set-point in order to achieve the desired solids feeding rate. Prior to the tests, a calibration of the screw feeders from the hoppers was done.

2.3.2. Fluidizing agent and preheating

Air that used for gasification was preheated during the start-up by a ~15 kW electric heater (Tellsa, Spain). The fluidizing agent is

Table 1
Structural composition of alfalfa.

	Cellulose	Hemicellulose	Lignin	References
Alfalfa hay, matured, % (DM)	29.6	14	14	[30]
Alfalfa hay, weathered, % (DM)	30	13	15	[30]
Alfalfa, early bud (g/kg DM)	265	122	141[a]	[16]
Alfalfa, full flower (g/kg DM)	285	123	169[a]	[16]

[a] Klason lignin.

Please cite this article in press as: Sarker S et al. Characterization and pilot scale fluidized bed gasification of herbaceous biomass: A case study on alfalfa pellets. Energy Convers Manage (2014), http://dx.doi.org/10.1016/j.enconman.2014.12.034

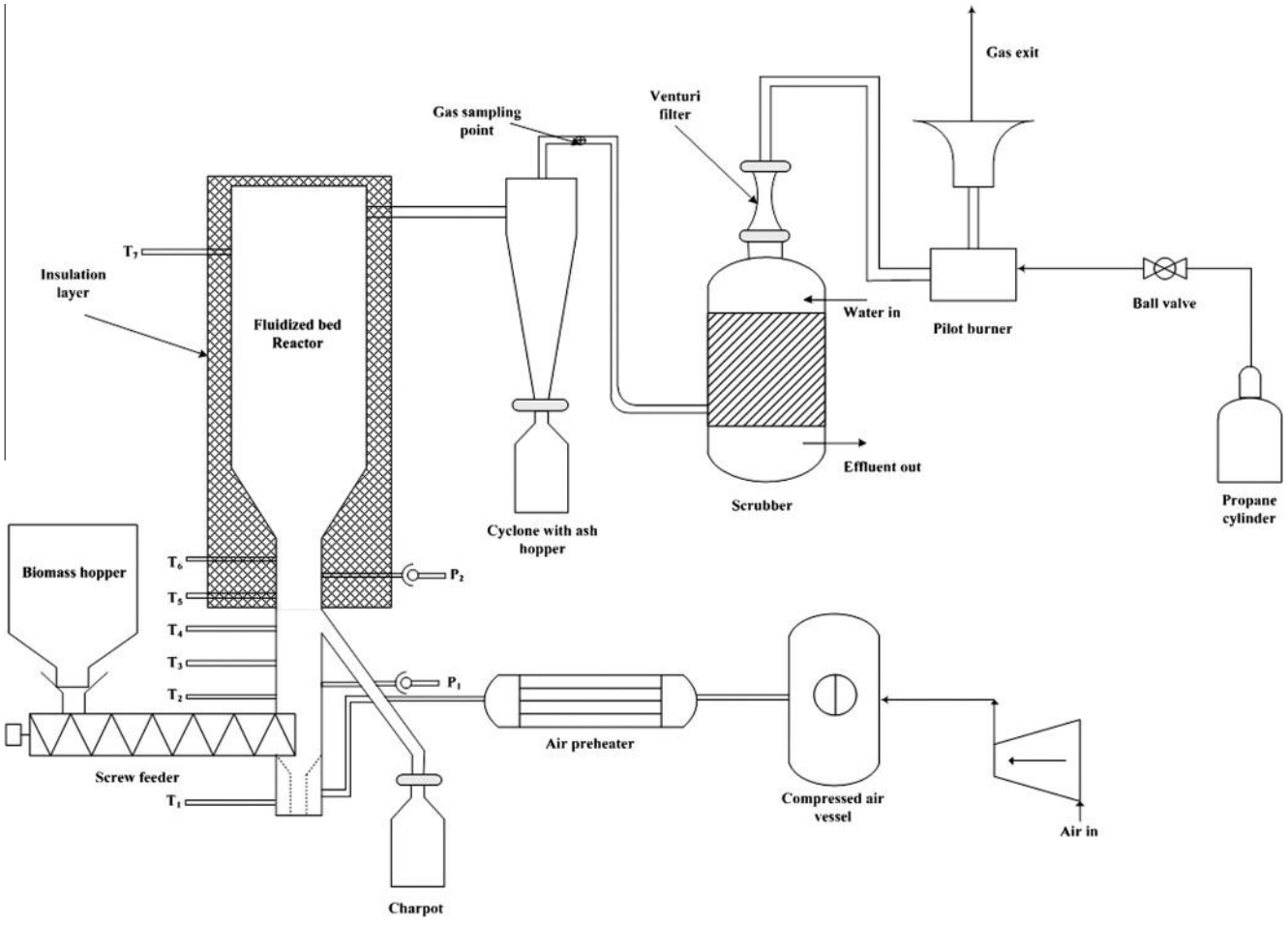

Fig. 1. Schematic diagram of the process flow.

entered into the reactor through the nozzles located at the bottom of the reactor and is regulated by a thermal mass flow controller operating within the range between 0.5 and 100 N m^3/h (Bronkhorst HIGH-TECH, the Netherlands).

2.3.3. Reactor and the measurement sensors

The body of the reactor is made of AISI 310 refractory stainless steel with a diameter and total height of 0.36 m and 3.5 m respectively. The total height is split into two sections, i.e., bed and freeboard with the latter slightly bigger in circumferential area (0.23 m), located above the main body of the gasifier. Insulation layers composed of 0.3 m thick insulating blankets (Unifrax Insulfrax S, Spain) cover the entire reactor from top to the bottom, minimizing heat transfer to the surroundings. Seven thermocouples (T_1–T_7) (bottom-up) as shown in Fig. 1 monitor temperature at various heights of the reactor. Temperature probe T_1 measures temperature at the inlet of the reactor while equidistant thermocouples T_2 through T_6 register temperature variations occurring in and around the bed. Probe T_7 is the uppermost sensor located at the freeboard of the reactor, determining the temperature of the gas exit. Besides the temperature sensors, pressure sensors P_1 and P_2 (Fig. 1) are positioned at the side of the reactor to monitor the fluidization condition of the bed.

2.3.4. Gas cleaning and conditioning

Immediately after the production, gas was cleaned and conditioned by means of a series of devices composed of cyclone, ash hopper and scrubber. First of all, gas leaving from the reactor circulated through a cyclone stripping entrained particles and then through a scrubber removing condensable tars. Char, ash and inactive bed materials were collected in the bins (ash hopper and char pot) located at the bottom of the cyclone and side of the reactor respectively. After each operation the bins were emptied to analyze residue quality and further to account mass balance.

2.3.5. Gas sampling

Part of the gas coming out from the main gas exit to flare (located outside the gasification unit to avoid hazard), was sampled in a sampling train consisting of two tar condensers, a particle filter, a flow meter and a gas analysis system. The entry of the sampling train was continuously heated by an electrical resistance at 450 ± 5 °C to avoid undesired condensation of condensable products in the producer gas before the condensers. As passing through the sampling line, producer gas was first cooled in the two ice condensers (~0.75 L each) and being washed out of the majority of the tars. Cooled gas was then cleaned by a cotton filter before being analyzed for permanent gases by the gas analyzer. The quantity of the gas used for sampling was measured by a gas flow meter, situated in between cotton filter and the analyzer while the quantity of the tar deposited on the condensers was manually recovered at the end of the each gasification test. An estimation of the amount of tar produced was done based on the manual volumetric measurement of the collected liquids in the sampling line while its composition was evaluated by a GC–MS (Gas chromatography-mass spectrometry) (Agilent 7890 A, USA).

Please cite this article in press as: Sarker S et al. Characterization and pilot scale fluidized bed gasification of herbaceous biomass: A case study on alfalfa pellets. Energy Convers Manage (2014), http://dx.doi.org/10.1016/j.enconman.2014.12.034

2.3.6. Gas analysis equipment

Located furthest to the sampling train, a micro-gas chromatograph (Agilent 3000A μGC, Model G2801A, USA) equipped with two analysis modules (Plot U and Molsieve 5A) and thermal conductivity detectors were used to analyze the permanent gases of the sample taken from the producer gas line. Measurement was conducted real-time (once in every two min) based on the calibration of CO_2, C_2H_4, C_2H_6, C_2H_2 and H_2S for Plot U module, and H_2, N_2, CH_4, CO and O_2 for MolSieve 5A module respectively. The gas composition data continuously produced by the μGC was stored in a computerized data acquisition system for further interpretation.

2.4. Experimental protocols

During start up, the sand constituting the initial reactor bed was heated by the air delivered from the preheater in order to heat up the reactor until the temperatures of around 450–500 °C. The heating up process using the electric heater generally takes around 3 h because of the size of the reactor and the air flow rate necessary to maintain a bubbling fluidized bed regime inside the reactor.

After about 3 h of preheating, bed temperature rose to around 500 °C, at which a small amount of biomass was combusted and rapidly increased the bed temperature to a desired level of ca. 750–800 °C, high enough to initially sustain autothermal conditions during the gasification step. The heat released in the autothermal conditions, with the exception of energy losses, was utilized in the endothermic reactions allowing pyrolysis and gasification reactions to endure.

The initial gasification temperature in this set of experiments was targeted at 800 ± 10 °C, achieved after some 20 min of combustion. Changeover from combustion to gasification conditions and, subsequently, the modification of the ER were obtained by increasing the air flow but keeping the constant biomass feeding rate. For this set of experiments the solids feeding rate was kept stable at 4.7 kg/h whereas air flow rate was varied between 4.16 and 4.99 N m^3/h such that the corresponding ER could be fixed at 0.25 and 0.30 respectively. The ER was calculated by obeying the relationship as follows:

$$ER = \frac{Q_{air}}{Q_{alfalfa} \times 3.54} \quad (1)$$

The stoichiometric amount of air required for complete combustion of alfalfa pellets was found to be 3.54 N $m^3/kg_{feedstock}$ based on the elemental composition of the pellets and hence given at the denominator of the Eq. (1). The terms Q_{air} and $Q_{alfalfa}$ in Eq. (1) additionally represent the air and feed flow rates in N m^3/h and kg/h respectively.

As gasification conditions were reached and the gasification step was initiated, steady state condition could be achieved in about 20 min of time-on-stream, beyond which further data collection was continued to evaluate the evolution profiles of temperature, gas composition, lower heating value, gas yield and cold gas efficiency as an effect of varied ER. The calculation of the producer gas heating value (in MJ/N m^3), gas yield and cold gas efficiency (CGE) were performed by employing the Eqs. (2)–(4) [31] while the development of temperature, pressure and air flow rate were registered in a data logger, later transferred to a computer for further interpretation.

$$LHV_{producer\ gas} = ((25.7 \times H_2) + (30.0 \times CO) + (85.4 \times CH_4) + (151.3 \times (C_2H_2 + C_2H_4 + C_2H_6))) \times \left(\frac{4.2}{1000}\right) \quad (2)$$

$$V_{producer\ gas} = \frac{Q_{air} \times 79}{N_2 \times m_{feedstock}} \quad (3)$$

$$CGE = \frac{LHV_{producer\ gas} \times V_{producer\ gas}}{LHV_{feedstock}} \times 100\% \quad (4)$$

where $LHV_{producer\ gas}$ is the dry base lower heating value of producer gas in MJ/N m^3; $V_{producer\ gas}$ is the dry gas yield in N m^3/kg_feedstock; Q_{air} is the air supply in N m^3/h; $m_{feedstock}$ is the biomass input in kg/h, $LHV_{feedstock}$ is the dry base calorific value of the pellets in MJ/kg and CGE is the cold gas efficiency in percent.

During the test, the gasifier ran through a transition stint of some 20 min after which temperature stabilization was achieved and continued for about 3 h, followed by the plant shut-down. The steady state was mainly divided into two periods based on the imposed ER ratios, the effect of which was investigated on various operational parameters, i.e., gas composition, LHV, efficiency, gas yield, char yield and tar yield, which are described in the following sub-sections.

3. Results and discussions

3.1. Biomass characterization

Table 2 presents the results obtained from the feedstock characterization.

With regards to moisture, the level found in alfalfa pellets was at ~8.7% (m/m) which compared to a previous work [32] is lower in range. Some amount of moisture helps thermal conversion [33] while too much brings negative consequences, such as the reduction in fuel energy content and process temperature. The value revealed from the present study, as lying below 10%, is expected to avoid the issues related to high moisture content and thus making the raw-material suitable for gasification [34].

Volatiles contents were in the range of 74% (dry fuel basis) which albeit a little lower than that from the study by Sharma [18] in harmony with another work carried out by Boateng and the co-authors [16]. As of ash content, alfalfa pellets displayed an average level of ~15% (dry basis) which is higher than the past study conducted by Boateng et al. [16]. However, since the gasification temperature for the present study did not exceed the melting point of ash, the plant operation was not influenced by its high quantity.

Average lower calorific value after analysis amounted as ~16 MJ/kg (dry base) which can be considered lower than the typical for most of the herbaceous biomass including alfalfa as according to the study by Domalski et al. [35]. The LHV value obtained has been compared to the theoretical LHV that could be calculated according to the empirical correlation proposed by Gaur and Reed

Table 2
Physical and chemical properties of alfalfa pellets.

Proximate and ultimate analyses of alfalfa pellets (n = 3)	
Proximate analysis (%)	
Moisture	8.73 ± 0.64
Volatile matter	74.4 ± 1.29
Ash	15.5 ± 0.44
Ultimate analysis (dry base, %)	
Carbon	41.60 ± 0.44
Hydrogen	4.90 ± 0.07
Oxygen[a]	33.94 ± 0.48
Nitrogen	2.39 ± 0.15
Sulfur	0.25 ± 0.02
Lower heating value (dry basis, kJ/kg)	
Analytical	16097.63 ± 98
Theoretical[b]	15378.01 ± 10

[a] Calculated by difference.
[b] Gaur and Reed [36].

Please cite this article in press as: Sarker S et al. Characterization and pilot scale fluidized bed gasification of herbaceous biomass: A case study on alfalfa pellets. Energy Convers Manage (2014), http://dx.doi.org/10.1016/j.enconman.2014.12.034

[36]. The value found from the measurements in the bomb calorimeter is in good concordance to the value obtained using the abovementioned empirical correlation (~15.4 MJ/kg). The ultimate analysis revealed the mean percentages of C, H, O, N and S in the pellets as 41.6, 4.9, 33.9, 2.4 and 0.25% respectively (Table 2). Except the percentage composition of carbon, this finding showed a good agreement with the literature [32]. Moreover, the low sulfur, high hydrogen and reasonably acceptable oxygen level make this biomass attractive in the context of gasification.

As per structural composition of alfalfa, results obtained from the literatures vary with the maturity and the different forms of the crops [16,30]. In general, the cellulose content constituted the major composition followed by the lignin and hemicellulose (Table 1). The level of lignin in comparison with other similar feedstocks was found lower in alfalfa [37] which is probably because of high level of nitrogen and low level of carbon containing in its chemical composition. Besides low lignin, the simultaneous variation in cellulose and lignin proportion of different maturities of alfalfa was reported to affect the quality of the oil produced from the pyrolysis of alfalfa in a study conducted by Boateng et al. [16]. Due to the uniformity of the feedstock, corresponding effect of such nevertheless was not observed in the present gasification work.

3.2. Pilot scale fluidized bed gasification

3.2.1. Effect of ER on gasification of alfalfa pellets

The effect of ER on the quality of the producer gas was investigated for 0.25 and 0.30. The producer gas was composed of series of gas species CO, CO_2, H_2, CH_4, C_2H_4, C_2H_6 and N_2 the evolution of which over time is depicted by Fig. 2.

As shown, the increase in ER from 0.25 to 0.30 had little effect on the product gas composition where most of the combustible and incombustible components kept stable or reduced. The concentration of CO_2, for example, slightly declined and reached to an average of 19.8 ± 0.2 vol.% at ER = 0.3 compared to the average of 20.2 ± 0.2 vol.% at ER = 0.25 (Figs. 2a and 3h).

This was in contrast with that of the CO, which increased from 8.4 ± 0.01 to 9.1 ± 0.05 vol.%, mainly at the expense of CO_2 and CH_4 (Table 3).

The inverse relationship between CO and CO_2, as observed, is a typical phenomenon of the Boudouard reaction ($C + CO_2 \overset{+heat}{\Longleftrightarrow} 2CO$), evidenced by the many past studies such as the one by Aznar et al. [25]. The extent of such reaction, nonetheless, is not critical in the present findings as the variation of those gas components was rather insignificant for varied ER.

Investigating the concentration of other gas species between the two successive ER, the following results were revealed: H_2 decreased from 13.3 ± 0.3 to 12.8 ± 0.1 vol.%, CH_4 decreased from 2.73 ± 0.04 to 2.66 ± 0.02 vol.%, C_2H_4 decreased from 0.88 ± 0.1 to 0.87 ± 0.03 vol.% and C_2H_6 decreased from 0.26 ± 0.03 to 0.25 ± 0.02 vol.% respectively (Table 3, Figs. 2 and 3h).

As of gas LHV, a positive effect of increasing the ER was observed, displaying an average value of 4.21 ± 0.02 MJ/N m^3 (dry base) for the higher ER compared to an average of 4.19 ± 0.08 MJ/N m^3 (dry base) for the ER = 0.25 (Figs. 2 and 3g). The LHV is a direct function of the combustible quantity which in the present case rose (from 25.3% to 26.0%) as ER rose, and thus accordingly the LHV. As a rule of thumb, the gas LHV at minimum 4.2 MJ/N m^3 (dry base) suits the operation of an internal combustion (IC) engine [38], yielding simultaneous heat and electricity. Based on gas LHV, the present experiments at ER = 0.30 favors that application and hence promising in terms of fluidized bed gasification.

In terms of gas yield, which is an important parameter to determine the productivity of gasification, a similar pattern to that of LHV was observed where the increase in ER from 0.25 to 0.30

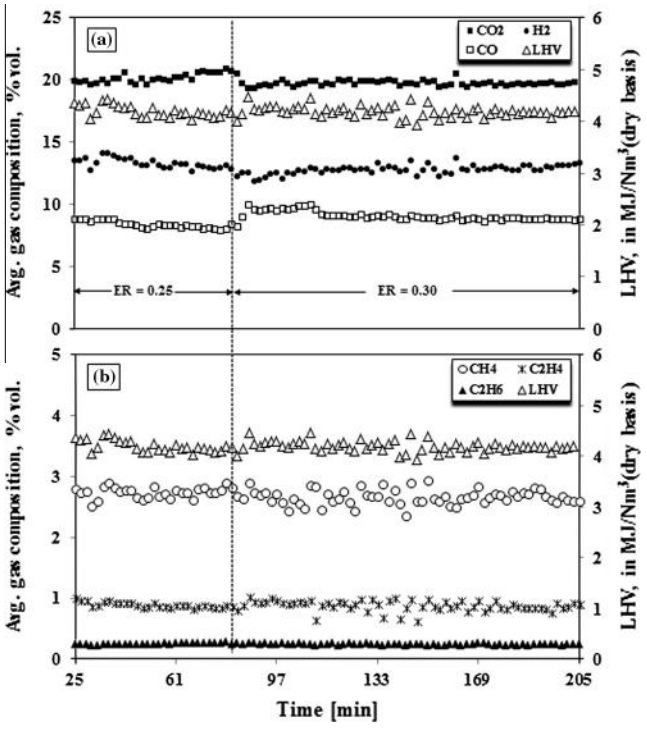

Fig. 2. Continuous evolution of gas composition and its lower heating value as a function of ER.

caused the gas yield to rise from 1.36 ± 0.00 to 1.52 ± 0.02 N m^3/kg (Fig. 3g). This trend is in agreement with several past studies that dealt with similar gasification investigations [25,39]. The prime reason of this gas yield behavior is possibly related to the high rate of devolatilization [24] which was successively greater as a result of the higher ER. Several endothermic reactions such as char gasification, steam reforming and tar cracking are also significantly favored when air supply is increased and thus contribute to augment gas production [25].

Unlike preceding parameters, the effect of each ER change on char and tar yields were impossible to examine as the ER varied on-line and the measurement (of tar and char) conducted off-line. However, the total char and tar yield for the whole ER range at the end of each experiment was analyzed and found as 281.7 ± 28.0 g/kg and 1.12 ± 0.04 g/N m^3 respectively (Fig. 3i, Table 3), closely coinciding with the previous studies dealing with the downdraft gasification of alfalfa and fluidized bed co-gasification of coal, biomass and plastic waste respectively [18,25].

As a direct function of LHV and producer gas quantity, the cold gas efficiency (CGE) exhibited a higher value (38.5 ± 5%) for the higher ER, with a difference as much as 10% (Table 3 and Fig. 3g) for that of lower ER. Definitely, efficiency in the range of 60% or less suggests low productivity which perhaps was associated with the lower yield of the combustible gases, i.e.; the yield of CO, H_2, CH_4 etc., and the development of lower gasification temperature, that peaked slightly below 800 °C at the present investigations. Similar phenomenon with regards to the low CGE was also observed by Gómez-Barea et al. [24].

3.2.2. Effect of the equivalence ratio on operational temperatures

Fig. 3 illustrates the temperature profiles of various sensors (T_1–T_7) and their corresponding effect on ER.

As observed (Fig. 3f), T_7 exhibited the lowest of all the temperatures due to its location close to the gas exit, in vicinity to the top of the reactor. This sensor was assigned to record the temperature

Please cite this article in press as: Sarker S et al. Characterization and pilot scale fluidized bed gasification of herbaceous biomass: A case study on alfalfa pellets. Energy Convers Manage (2014), http://dx.doi.org/10.1016/j.enconman.2014.12.034

Table 3
Summary of the operational parameters obtained from the gasification of alfalfa pellets.

Operational parameters	Run 1		Run 2	
	ER = 0.25	ER = 0.3	ER = 0.25	ER = 0.3
Air input (N m^3/h)	4.16	4.99	4.16	4.99
Biomass feed (kg/h)	4.7		4.7	
CO (vol.%)	8.43 ± 0.31	9.08 ± 0.03	8.42 ± 0.35	9.15 ± 0.48
H_2 (vol.%)	13.02 ± 0.45	12.91 ± 0.31	13.50 ± 0.60	12.73 ± 0.53
CH_4 (vol.%)	2.77 ± 0.11	2.67 ± 0.14	2.70 ± 0.15	2.65 ± 0.27
C_2H_4 (vol.%)	0.81 ± 0.05	0.89 ± 0.07	0.95 ± 0.07	0.85 ± 0.16
C_2H_6 (vol.%)	0.25 ± 0.02	0.23 ± 0.02	0.25 ± 0.01	0.26 ± 0.01
CO_2 (vol.%)	20.31 ± 0.41	19.6 ± 0.28	20.04 ± 0.48	19.9 ± 0.29
N_2 (vol.%)	51.5 ± 0.74	50.6 ± 1.0	54.14 ± 0.96	54.45 ± 0.84
Lower heating value (MJ/N m^3)	4.13 ± 0.13	4.21 ± 0.15	4.25 ± 0.17	4.19 ± 0.16
Specific gas yield (N m^3/kg_fuel)	1.36 ± 0.02	1.66 ± 0.03	1.35 ± 0.19	1.38 ± 0.03
Cold gas efficiency (%)	33.8 ± 1.05	42.14 ± 1.26	34.76 ± 1.4	34.85 ± 1.56
Char yield (g/kg)	301.52		261.92	
Tar yield (g/N m^3)	1.15		1.09	

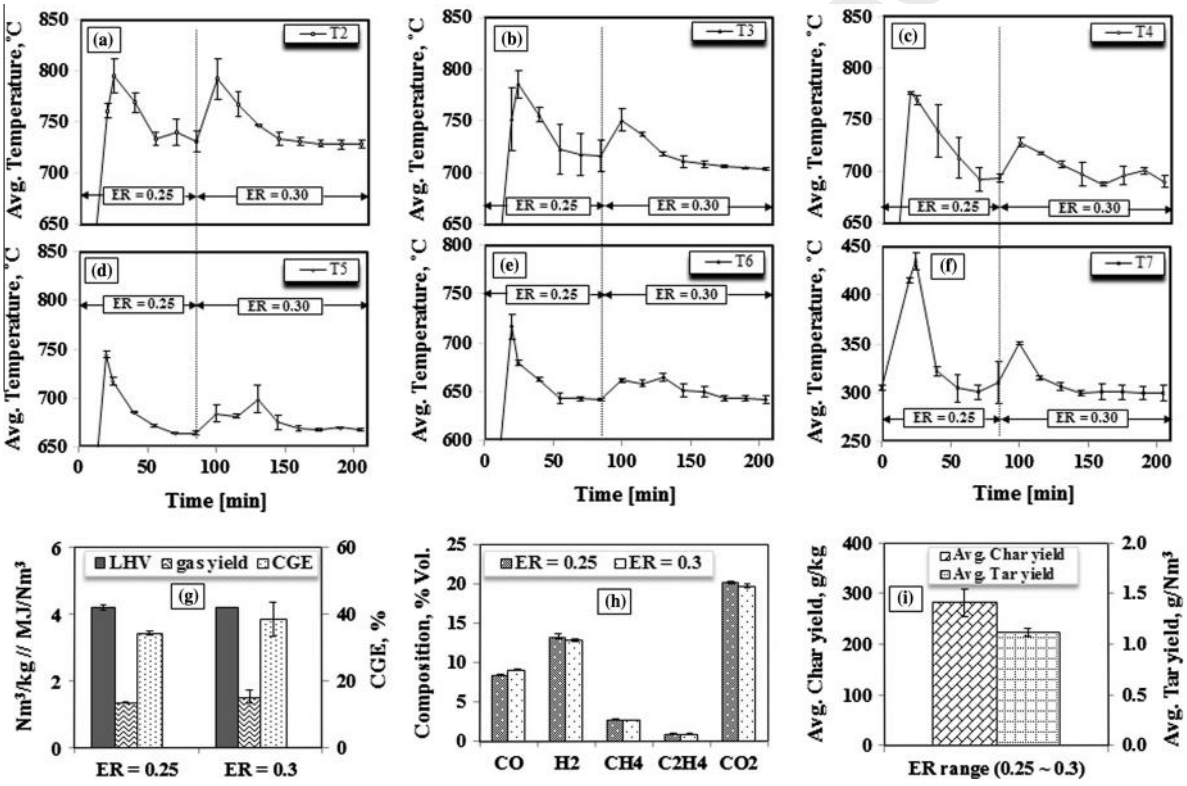

Fig. 3. Effect of ER on various operational variables.

of the freeboard. Temperatures registered by T_3 (Fig. 3b) may be associated with gasification due to its operating range situating nearest to the temperature of combustion, which was likely to be detected by sensor T_2 (Fig. 3a). The combustion temperature may also be defined as the temperature of bed. Among all the probes, thermocouple T_4 (Fig. 3d) showed the temperature variation in proximity to the overflow – collecting the unburned char and ash, and hence may be assigned to reduction. Being the closest neighbors to the freeboard, pyrolysis may be recognized by thermocouples T_5 and T_6 (Fig. 3d and e) as showing a lower temperature than those of combustion, gasification and reduction.

In general, temperatures developed in all the sensors increased with ER and maintained distinctive differences between themselves (Fig. 3a–f). This is somewhat logical as the energy available to the bed improves with the quantity of oxygen available more heat is supplied to the reactor as a result of enhanced combustion. In addition to the rise in temperature, increased oxygen also influenced the several operational variables, the relations of which with the bed temperature are presented in Fig. 4.

As for gas composition (Fig. 4a–e), CO content increased with bed temperature and H_2 decreased. This was in contrast with the study by Hanping et al. [39] according to which both CO and H_2 increased as the bed temperature increased. However, the increasing extent of these gases was reported to be tender for the bed temperature lower than 800 °C. The development of low bed temperature in the present study agrees with the past work and hence indicates why the effect of temperature was less pronounced in the evolution profile of CO and H_2. The tendency of variation among the other combustible gases (such as, CH_4, C_2H_4 and C_2H_6) was not so significant, although slight increasing and decreasing trends were noticed. Theoretically, the severity of several reforming and cracking reactions increase as a result of a higher bed temperature

Please cite this article in press as: Sarker S et al. Characterization and pilot scale fluidized bed gasification of herbaceous biomass: A case study on alfalfa pellets. Energy Convers Manage (2014), http://dx.doi.org/10.1016/j.enconman.2014.12.034

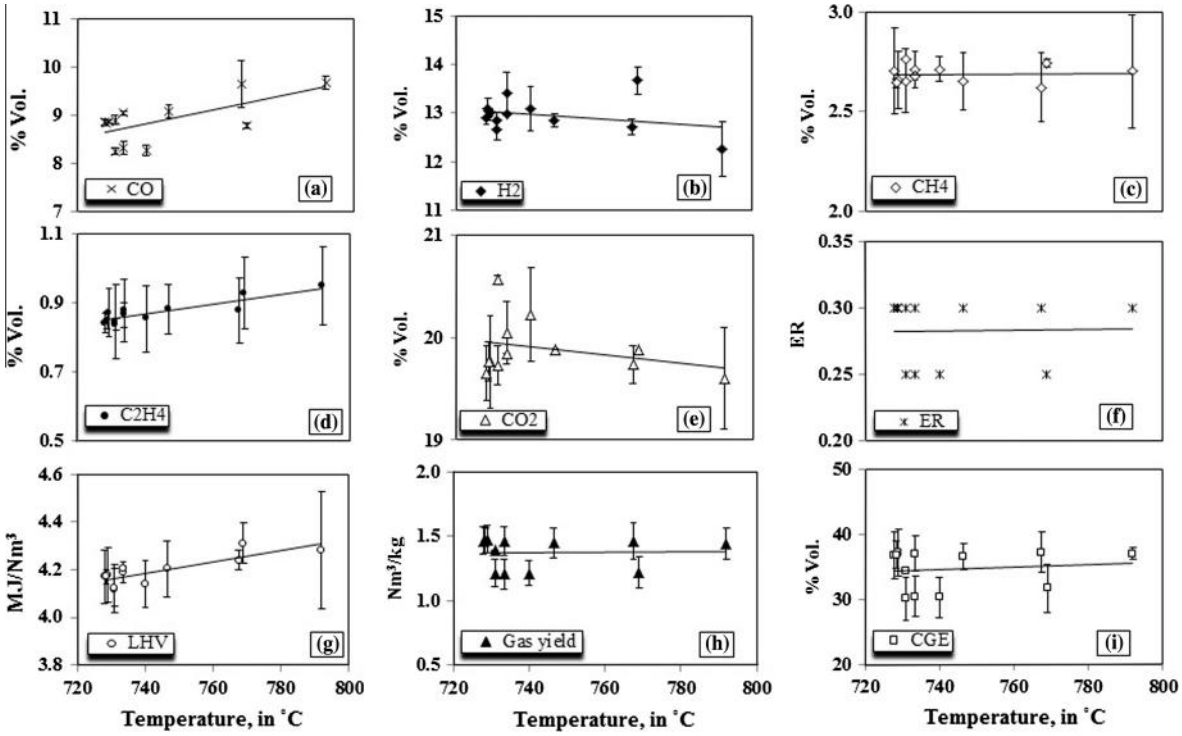

Fig. 4. Influence of bed temperature on the production trend of several operational variables.

Table 4
Identification of the tar components deposited in the condensers.

Run 1				Run 2			
Condenser 1		Condenser 2		Condenser 1		Condenser 2	
Peaks	Compounds	Peaks	Compounds	Peaks	Compounds	Peaks	Compounds
11.548	3-methyl-Pyridine	11.791	3-methyl-Pyridine	11.782	3-methyl-Pyridine	11.801	3-methyl-Pyridine
17.310	Phenol	17.333	Phenol	17.399	Phenol	17.453	Phenol
20.902	2-methyl-Phenol	19.244	Benzonitrile	19.244	Benzonitrile	20.905	2-methyl-Phenol
21.188	2-Aminopyridine	21.825	3-methyl-Phenol	20.886	2-methyl-Phenol	21.335	2-Aminopyridine
21.826	3-methyl-Phenol	24.368	4-ethyle Benzenamine	21.245	2-Aminopyridine	21.897	3-methyl-Phenol
24.379	4-ethyle-Benzenamine	30.076	N-2-propenyl-Benzenamine	21.866	3-methyl-Phenol	23.569	4-ethyle Benzenamine
						23.949	2.5-dimethyl-2-Hexane
						24.423	4-ethenyl Benzenamine
				31.958	Isoquinoline	30.89	N-dimethyl-N Phenylenediamine
36.013	Indole	32.876	Quinoline	36.038	Indole	32.927	Quinoline

and thus participate in the production of higher amounts of H_2 and CO. In the present case, the involvement of reforming and cracking reactions are only implied by the trend of CO, but rather unnoticed by H_2 as the latter slightly dropped throughout (Fig. 4b).

Despite the insignificant effect on individual gas species, the total combustible quantity slightly rose (from 25.3 to 26 vol.%) with temperature and reflected to the gas LHV as shown in Fig. 4g. As the bed temperature rose, the total CO as well as the CH_4 content increased, in spite of reduced H_2, and thus contributed to a net rise in gas calorific value. Likewise LHV, the average gas yield and the CGE also peaked with a rise in the bed temperature (Fig. 4h and i). The reason of the improved gas yield may be explained by the rate of solid–gas reactions, which increased as a result of the heightened bed temperature.

3.3. Tar characterization

Although a direct relationship between each ER change and tar yield could not be established, the total tar yield after gasification was measured both for volume and composition. The volumetric tar yield data has already been presented in the preceding section. This section only discusses compositional tar.

As already mentioned, GC–MS was employed for evaluating tar composition which was grouped as according to the point of sampling: such as upstream (condenser close to the sample entrance – condenser 1) and downstream (condenser further to the sample entrance – condenser 2). The tar abundances and their corresponding peaks with identifications for two sampling points are demonstrated by Table 4.

As observed, the abundance of tar compounds varied with the sampling locations. Peaks were in general found more frequent and higher for condenser 2 as compared to that of condenser 1. Among the twelve identified components, phenol, 3-methyl-phenol and 3-methyl pyridine were common between the two condensers. Tar of these types, especially the phenols, are the organic compounds of 6 carbons, yielded due to pyrolytic degradation of lignin [40]. Another reason of the high availability of phenols in the tar spectra is the low gasification temperature, the increase of which contributes to convert those into gaseous products. Apart from the phenols, the other detected compounds

Please cite this article in press as: Sarker S et al. Characterization and pilot scale fluidized bed gasification of herbaceous biomass: A case study on alfalfa pellets. Energy Convers Manage (2014), http://dx.doi.org/10.1016/j.enconman.2014.12.034

were predominantly the nitrogen containing tars specified as 2-aminopiridyne and indole found in condenser 1, and benzonitrile, N-2-propenyl-benzenamine, 2.5 dimethyl – 2-Hexane, N-dimethyl-N-phenylenediamine and quinolone found in condenser 2 respectively (Table 4). The presence of nitrogen in the tar sample is perhaps originated from fuel N, the degradation of which in general increases with the increase in operation temperature [40]. High gasification temperature also contributes to the production of PAHs (Poly aromatic hydrocarbons: naphthalene, acenaphthene, anthracene, phenanthrene etc.) which logically was not detected in the present analysis. Among the aromatic compounds identified, quinoline was by far the heaviest (~129 g/mol) molecule potentially caused the stringent odor to the nearby environment while indole, a medium sized heterocyclic aromatic compound, appeared to be a major source of fragrances as the analysis revealed.

4. Conclusions

This work examined the performance of pilot scale bubbling fluidized bed gasification of alfalfa pellets at varied ER. Most of the important parameters including bed temperature demonstrated an increasing trend as the quantity of input air improved. The average gas LHV for instance reached to a level > 4.2 MJ/N m^3 which is interesting in-terms of energy conversion via gas engine. Additionally, the cold gas efficiency and the gas yield peaked at ~39% and ~1.6 N m^3/kg (dry basis) respectively as an impact of increased ER. Good gasification properties including with the lignocellulosic nature, which suits for distributed energy, make alfalfa a promising biomass to introduce for FB processing, as the preliminary study thus far revealed.

Acknowledgements

This study was conducted at Thermochemical Process Group (GPT) from the Universidad Zaragoza (UNIZAR), Spain, financed jointly by the University of Agder (UiA), Norway and BRISK (Biofuel Research Infrastructure for Sharing Knowledge), EU, under the framework of UZR2-22-04-13 BRISK TNA. The authors wish to thank both of these funding bodies. The lab facility and the assistance from a number of scientific personnel offered by UNIZAR are regarded core of this work and therefore are highly noted.

References

[1] Kirkels AF, Verbong GPJ. Biomass gasification: Still promising? A 30-year global overview. Renew Sustain Energy Rev 2011;15:471–81.
[2] Saxena R, Adhikari D, Goyal H. Biomass-based energy fuel through biochemical routes: a review. Renew Sustain Energy Rev 2009;13:167–78.
[3] Caliandro P, Tock L, Ensinas AV, Marechal F. Thermo-economic optimization of a solid oxide fuel cell–gas turbine system fuelled with gasified lignocellulosic biomass. Energy Convers Manage 2014.
[4] Barnes D, Froese RE, Mannes RG, Warner B. Combined sustainable biomass feedstock combustion, CO_2/EOR, and saline reservoir geological carbon sequestration in Northern Lower Michigan, USA: towards negative CO_2 emissions. Energy Procedia 2011;4:2955–62.
[5] Möllersten K, Yan J, Moreira JR. Potential market niches for biomass energy with CO_2 capture and storage—opportunities for energy supply with negative CO_2 emissions. Biomass Bioenergy 2003;25:273–85.
[6] Alauddin ZABZ, Lahijani P, Mohammadi M, Mohamed AR. Gasification of lignocellulosic biomass in fluidized beds for renewable energy development: a review. Renew Sustain Energy Rev 2010;14:2852–62.
[7] Zhang K, Chang J, Guan Y, Chen H, Yang Y, Jiang J. Lignocellulosic biomass gasification technology in China. Renewable Energy 2013;49:175–84.
[8] Barman NS, Ghosh S, De S. Gasification of biomass in a fixed bed downdraft gasifier–A realistic model including tar. Bioresour Technol 2012;107:505–11.
[9] Sarker S, Nielsen H. Preliminary fixed-bed downdraft gasification of birch woodchips. Int J Environ Sci Technol. 1–8.
[10] Bimbela F, Oliva M, Ruiz J, García L, Arauzo J. Steam reforming of bio-oil aqueous fractions for syngas production and energy. Environ Eng Sci 2011;28:757–63.
[11] Wang L, Weller CL, Jones DD, Hanna MA. Contemporary issues in thermal gasification of biomass and its application to electricity and fuel production. Biomass Bioenergy 2008;32:573–81.
[12] Alipour Moghadam R, Yusup S, Azlina W, Nehzati S, Tavasoli A. Investigation on syngas production via biomass conversion through the integration of pyrolysis and air–steam gasification processes. Energy Convers Manage 2014;87:670–5.
[13] Campoy M, Gómez-Barea A, Ollero P, Nilsson S. Gasification of wastes in a pilot fluidized bed gasifier. Fuel Process Technol 2014;121:63–9.
[14] Gil J, Corella J, Aznar MaP, Caballero MA. Biomass gasification in atmospheric and bubbling fluidized bed: effect of the type of gasifying agent on the product distribution. Biomass Bioenergy 1999;17:389–403.
[15] Boateng A, Jung H, Adler P. Pyrolysis of energy crops including alfalfa stems, reed canarygrass, and eastern gamagrass. Fuel 2006;85:2450–7.
[16] Boateng AA, Mullen CA, Goldberg N, Hicks KB, Jung H-JG, Lamb JF. Production of bio-oil from alfalfa stems by fluidized-bed fast pyrolysis†. Ind Eng Chem Res 2008;47:4115–22.
[17] Butterman HC, Castaldi MJ. Influence of CO_2 injection on biomass gasification. Ind Eng Chem Res 2007;46:8875–86.
[18] Sharma A. Assessing the suitability of various feedstocks for biomass gasification. Louisiana State University; 2011.
[19] González-García S, Moreira MT, Feijoo G. Environmental performance of lignocellulosic bioethanol production from Alfalfa stems. Biofuels Bioprod Biorefin 2010;4:118–31.
[20] Buragohain B, Mahanta P, Moholkar VS. Biomass gasification for decentralized power generation: the Indian perspective. Renew Sustain Energy Rev 2010;14:73–92.
[21] Mani S, Sokhansanj S, Bi X, Turhollow A. Economics of producing fuel pellets from biomass. Appl Eng Agri 2006;22:421.
[22] Arjharn W, Hinsui T, Liplap P, Raghavan G. Evaluation of electricity production from different biomass feedstocks using a pilot-scale downdraft gasifier. J Biobased Mater Bioenergy 2012;6:309–18.
[23] Elder T, Groom LH. Pilot-scale gasification of woody biomass. Biomass Bioenergy 2011;35:3522–8.
[24] Gómez-Barea A, Arjona R, Ollero P. Pilot-plant gasification of olive stone: a technical assessment. Energy Fuels 2005;19:598–605.
[25] Aznar MP, Caballero MA, Sancho JA, Francés E. Plastic waste elimination by co-gasification with coal and biomass in fluidized bed with air in pilot plant. Fuel Process Technol 2006;87:409–20.
[26] Kim YD, Yang CW, Kim BJ, Kim KS, Lee JW, Moon JH, et al. Air-blown gasification of woody biomass in a bubbling fluidized bed gasifier. Appl Energy 2013;112:414–20.
[27] Narobe M, Golob J, Klinar D, Francetič V, Likozar B. Co-gasification of biomass and plastics: pyrolysis kinetics studies, experiments on 100 kW dual fluidized bed pilot plant and development of thermodynamic equilibrium model and balances. Bioresour Technol 2014;162:21–9.
[28] Yu MM, Masnadi MS, Grace JR, Bi X, Lim CJ, Li Y. Co-gasification of biosolids with biomass: thermogravimetric analysis and pilot scale study in a bubbling fluidized bed reactor. Bioresour Technol 2014.
[29] Fanlo R, Chocarro C, Lloveras J, Ferran X, Serra J, Salvia J, et al. Alfalfa production and quality in Northeast Spain. Grassland Sci Europe 2006;11:261–3.
[30] Phyllis2. ECN, The Netherlands.
[31] Sarkar M, Kumar A, Tumuluru JS, Patil KN, Bellmer DD. Gasification performance of switchgrass pretreated with torrefaction and densification. Appl Energy 2014;127:194–201.
[32] Jenkins B, Baxter L, Miles Jr T, Miles T. Combustion properties of biomass. Fuel Process Technol 1998;54:17–46.
[33] Acharjee TC, Coronella CJ, Vasquez VR. Effect of thermal pretreatment on equilibrium moisture content of lignocellulosic biomass. Bioresour Technol 2011;102:4849–54.
[34] García R, Pizarro C, Lavín AG, Bueno JL. Characterization of Spanish biomass wastes for energy use. Bioresour Technol 2012;103:249–58.
[35] Domalski ES, Jobe Jr TL, Milne TA. Thermodynamic data for biomass conversion and waste incineration. National Bureau of Standards, Washington, DC (US); Solar Energy Research Inst., Golden, CO (US); 1986.
[36] Gaur S, Reed TB. An atlas of thermal data for biomass and other fuels. Golden, (CO, (United States): National Renewable Energy Lab.; 1995.
[37] Demirbas A. Combustion characteristics of different biomass fuels. Prog Energy Combust Sci 2004;30:219–30.
[38] P. Quakk, H. Knoef, H. Stassen. Energy from biomass: a review of combustion and gasification technology. World Bank Technical Paper; 1999.
[39] Hanping C, Bin L, Haiping Y, Guolai Y, Shihong Z. Experimental investigation of biomass gasification in a fluidized bed reactor. Energy Fuels 2008;22:3493–8.
[40] Li L, Huang S, Wu S, Wu Y, Gao J, Gu J, et al. Fuel properties and chemical compositions of the tar produced from a 5 MW industrial biomass gasification power generation plant. J Energy Inst 2014.

Paper III

Semi-continuous feeding and gasification of alfalfa and wheat straw pellets in a lab-scale fluidized bed reactor

Shiplu Sarker, Jesús Arauzo, Henrik Kofoed Nielsen

Published in **Energy Conversion and Management**, 2015, 99: 50-61

Journal information (ISI web of science):

Publisher: **Elsevier**
Impact factor: **4.38** (2014)
Rank: **14/88** (Energy & Fuels)

Energy Conversion and Management xxx (2015) xxx–xxx

Contents lists available at ScienceDirect

Energy Conversion and Management

journal homepage: www.elsevier.com/locate/enconman

Semi-continuous feeding and gasification of alfalfa and wheat straw pellets in a lab-scale fluidized bed reactor

Shiplu Sarker[a,*], Jesús Arauzo[b], Henrik Kofoed Nielsen[a]

[a] University of Agder, Faculty of Engineering and Science, Jon Lilletuns vei 9, Service boks, 4898 Grimstad, Norway
[b] University of Zaragoza, Thermochemical Process Group, Aaragon Institute of Engineering Research (I3A), I+D building, C/Mariano Esquillor s/n, E-50018 Zaragoza, Spain

ARTICLE INFO

Article history:
Received 1 February 2015
Accepted 7 April 2015
Available online xxxx

Keywords:
Fluidized-bed
Alfalfa
Wheat straw
Pellets
Gasification
Equivalence ratio

ABSTRACT

Small scale air-blown fluidized bed gasification of alfalfa and wheat straw pellets were conducted for semi-continuous solid feeding and range of operating conditions varied due to the modifications in equivalence ratio (ER) (0.20–0.35) achieved both by varying solid and air input. Alfalfa pellets displayed an improvement in several gasification variables such as gas lower heating value (~4.1 MJ/Nm^3), specific gas yield (1.66 Nm^3/kg), cold gas efficiency (~42%) and carbon conversion efficiency (~72%) as ER maximized to 0.35 which was found optimum for this feedstock for the present course of experiments. Gasification parameters of wheat straw pellets on the other hand were characterized by a great degree of variation as the ER progressively increased. The optimum performance of this biomass was likely to achieve at ER = 0.30 when gas lower heating value and cold gas efficiency maximized to ~4 MJ/Nm^3 and ~37% respectively. Moreover, a substantial drop in tar yield (58.7 g/Nm^3) at this ER was also indicative to the optimal thermal conversion at this point of operation. Overall, both the feedstocks presented promising alternatives for utilization into the small-scale fluidized bed gasification which is increasingly emerging as a sustainable solution towards processing lignocellulosic biomass.

1. Introduction

In the worldwide energy policy, renewable energy is of interest based on the fact that fossil fuel is rapidly diminishing and the energy demand is exorbitantly rising due to the imminent surge in population [1]. There is thus an urgent need to integrate all categories of renewable energy where the contribution of biomass is ever increasing. Biomass resource is abundant and covers a wide range, starting from terrestrial to marine, all of which bearing huge potential to get converted into renewable energy by means of the prevailing technologies such as: biological, thermal, and biochemical [2]. Producing liquid biofuel from straw, starch and oil seed crops, one example of biomass utilization, has been a popular approach for the last few decades which however recently brought into a serious attention as a result of controversy towards competition to agricultural lands for feed rather than for food, or the dilemma of "Food vs. Fuel" [3]. This therefore shifted a deeper attention towards lignocellulosic biomass, or the biomass deriving from the agricultural wastes and energy crops to contribute to the liquid biofuels as well as to the gases. In line with that, the focus of the present study deals with the gases that can be produced by utilizing lignocellulosic biomass, particularly by alfalfa and wheat straw pellets, via a process called gasification.

Gasification basically is a thermochemical process, occurring at oxygen (oxidizing agent) suppressed condition, typically transforming solid biomass into producer gas that subsequently being utilized into further energy applications and value added products. The emanating gas once dried in general composed of CO, H_2, CO_2, CH_4, C_2H_4, C_nH_n and minor amounts of tar and particulates [4,5], which as a part of renewable energy exploited into the downstream units. Existing gasification technologies (fixed-bed, fluid-bed, entrained flow, etc.) differ widely according to the availability, type, and form of the fuel, and to the amount of energy that can be produced. Among these, fluidized bed gasification is commonly utilized because of its flexibility in dealing with a range of biomass including difficult fuels such as wastes [6], straw [7], husk [8] and bagasse [9], and high conversion efficiency due to the greater solid gas contact reactions [10]. This technology also suits operation for diverse gasifying agents (air, steam, O_2, CO_2, etc.) and results higher efficiency than a Rankine cycle (a cycle that models the performance of a steam turbine system), once integrated with I.C. (internal combustion) engine for small to medium scale (0.5–5 MW_e) applications [11].

As a herbaceous crop, the availability of alfalfa (*Medicago sativa* L.) is primarily dependent on the geographic and climatic conditions with a high dry matter yield exhibited in the temperate regions

* Corresponding author. Tel.: +47 37233144.
E-mail address: Shiplu.sarker@uia.no (S. Sarker).

http://dx.doi.org/10.1016/j.enconman.2015.04.015
0196-8904/

[12], such as around the Ebro valley areas in Spain [13], and many places in the USA [14]. This feedstock has historically been used for livestock feed because of the less cell wall carbohydrates and abundant protein on its leaves which are suitable for animals' digestion [15]. However, the stems of alfalfa, sharing as much as 50% of the total biomass, are mostly comparable with the conventional lignocellulosic structure – composing mainly of cellulose and hemicellulose, and thus least applied as animal diet [16]. This leaves opportunity for this feedstock to exploit into the energy conversion, besides as a fodder crop. In fact, many literatures have already evaluated the potential of lignocellulosic alfalfa in several areas, especially towards production of second generation (2G) biofuel [17] in respect to the environmental [15] and to the economic aspects [18], and characterization [19], and scarcely to gasification using fixed bed downdraft gasifier [20] and recently through pilot-scale bubbling fluidized bed gasifier [21]. The motivation of using alfalfa as a feedstock for biofuel production favors predominantly due to the agro-ecological conditions, i.e.; requirement of less N fertilizer, better conversion economics, etc. allowing crop rotation with corn and hence higher final yields [18]. However, the inevitable byproducts from the bioethanol industries together with the insignificant net savings from the greenhouse gas emission and the unattractive economic competitiveness with the fossil fuel based oil are still a major concern [22], hindering the rapid expansion of this technology. These all therefore lead gasification, especially the small scale technology that can be readily integrated on farm operation [7], a feasible option for thermochemical conversion of alfalfa, resulting producer gas with an upgrading possibility to heat, electricity chemicals, bio-oil, etc. and the residual ash potentially be recycled as fertilizer.

Wheat straw is another biomass examined in the present work. Unlike alfalfa, wheat (*Triticum aestivum* L.) straw has been extensively studied in many literatures with diverse investigations in several areas, such as: [23–30]. In regards to gasification, this crop residue is interesting as a result of its increasing availability [31], less impact to land use changes since no additional agricultural land is required for its production [32], and superior environmental performances [33]. However, implications such as high tar content, ash agglomeration, and ash slagging [34], are still major drawbacks towards using this feedstock for gasification. Overcoming some of these issues to effectively achieve gasification, significant efforts have already been paid in which modifications of the reactors [35] and pretreatment of feedstock were suggested [36]. This study does not report any modifications of such to the existing technologies, however, proposes to utilize a small scale fluidized bed gasification system which potentially is economically attractive due its easy access to the fuel source together with the opportunity to effectively enhance biomass utilization.

Number of documented researches [37,38] has already demonstrated the fluidized bed gasification of lignocellulosic biomass for various operating conditions, i.e.; effect of air ER (Equivalence ratio), effect of bed temperature, etc. but low density, complex fuel handling, feeding, etc. has been a challenge to apply these feedstocks for gasification as these studies concluded. So far successful utilization of various forms of lignocellulosic biomass starting from raw straw [8] to milled straw [39] has been mentioned. The effect of several feeding locations has also been inspected [40]. Nevertheless, direct feeding of biomass pellets to a lab-scale (<10 g/min throughput) reactor and to evaluate the corresponding gasification performance at varying operating conditions has been hardly reported, as far as authors know. Considering this, the present study focuses on comparing the gasification performance on direct pellet feeding of two different lignocellulosic biomasses (alfalfa and wheat straw) at numerous ER that varies between the range of 0.20 and 0.35 for which corresponding effect in-terms of temperature and other major parameters are also examined.

2. Materials and methods

2.1. Biomass feedstock

Alfalfa and wheat straw pellets with average dimensions of ∅6 mm × 25 mm length and ∅8 mm× 20 mm length respectively were used as feedstocks for the gasification tests conducted in this work.

Alfalfa was grown and harvested around the Ebro valley, in the surroundings of the village Pina de Ebro, located 40 km southeast from Zaragoza (capital of Aragon, a region in the Northeast of Spain). Approximately 100 kg of alfalfa pellets with 100% purity (no additives) from the first harvest (April 2013) were manufactured by Cooperativa Campo San Gregorio and kindly supplied by Molinos Afau S.L. (Pina de Ebro, Spain).

Wheat straw on the other hand was harvested from Castilla y Leon fields, in the surroundings of the village Valladolid and Tordesillas, located 70 km south from Valladolid (capital of Castilla y León, a region in the West of Spain). Pellets of approximate amount of 100 kg with 100% purity (no additives) were manufactured by Pitesa (on Tordesillas, Spain) and kindly supplied by Molinos Afau S.L. (Pina de Ebro, Spain).

2.2. Assessing physiochemical quality of the feedstock

Prior to the gasification tests, the pellets were assessed in terms of physical and chemical quality by means of proximate and ultimate analysis. By proximate analysis, several physical variables such as moisture, volatiles, ash and lower heating value (LHV) were determined for which following standards were used: moisture as according to EN 14774-3:2009, volatile matter as according to EN 15148:2009 and ash as according to EN 14775:2009 respectively. To analyze calorific value, an in-situ bomb calorimeter (IKA C2000, Germany) set to comply with the protocol ASTM D 4809-95 was used. Additionally, theoretical LHV was also determined based on the empirical correlation (developed from the ultimate analysis) proposed by Gaur and Reed [41].

Ultimate analysis determined the chemical composition in-terms of the percent amount of C, H, O, Cl, N and S by using an in-situ elemental analyzer (Leco TruSpec Micro, USA). C, H and N was evaluated based on the standard EN 15104:2011, while S was determined following the protocol EN 15289:2011. Oxygen was calculated by difference, as direct measurement by the present instrument was not possible.

Prior to the above analyses, the samples were prepared by grinding to an average size of <5 mm by using an in-situ hammer mill manufactured by Mercanofil.Mateu y Solè, Spain.

2.3. Determining ash fusion temperature

Ash fusion temperature of the feedstocks was determined by using a Rhodium ash fusion furnace (EM 201-17, Hesse instruments, Germany) featured with a camera and image processing software, capturing images at predefined intervals of temperature. For the analysis, the sample ash was first prepared into paste by adding a few drops of distilled water to improve stability. Afterwards, it was molded into compact cylinder of 3 mm (height) and 3 mm (Ø) by using a die and allowed to dry. The cylindrical sample was then placed on a Al_2O_3 slab located inside the furnace heated in an oxidizing environment (air) at two steps constant heating rate of 30 °C/min between 0 °C (or, the room temperature) and 550 °C and 5 °C/min between 550 °C and 1750 °C respectively. A thermocouple positioning underneath the slab enabled to trace the progress of temperature while a digital probe fitted inside the furnace displayed the evolutions of images at every 5 °C rise

Please cite this article in press as: Sarker S et al. Semi-continuous feeding and gasification of alfalfa and wheat straw pellets in a lab-scale fluidized bed reactor. Energy Convers Manage (2015), http://dx.doi.org/10.1016/j.enconman.2015.04.015

in temperature. The sample condition for other important temperatures at any point within the 5 °C rise in temperature was also recorded as images. The various phases of the sample such as onset of deformation to the flow were evaluated as according to the European Standard CEN/TS 15370-1:2006. The list of temperatures that can be evaluated by analysis are: sintering temperature (SST), shrinkage temperature (ST), deformation temperature (DT), sphere temperature (ST), hemispherical temperature (HT) and the flow temperature (FT). Here, only the relevant temperatures are presented.

2.4. Thermo-gravimetric analysis (TGA)

Thermo-gravimetric study of the pellets was conducted by using a thermal analyzer (NETZSCH STA 449 F3 Jupiter, Germany). During experiments, samples between 5 and 10 mg was heated to a maximum temperature of 950 °C, for a constant heating rate of 10 °C/min. The final temperature was achieved after three steps of heating holding for a particular length of time. To this end, sample was first heated up to 110 °C and kept at that temperature for 30 min to remove moisture. Subsequently, it was pyrolized until 600 °C and dwelled at that temperature for 60 min to allow volatiles to be released. Sample was then combusted and heated up to 950 °C in N_2/O_2 (79/21%) environment and kept at that temperature for 20 min to allow char to be converted into ashes. Nitrogen was used as carrier gas, flowed at a rate of 100 normal mL/min to sweep the produced gas away from the instrument. To ensure repeatability, each experiment in each condition was performed in duplicate.

2.5. Gasification experimental set-up

The gasification tests were carried out by means of a lab-scale bubbling fluidized bed reactor, operating at atmospheric pressure and air as a gasifying medium for a fuel throughput capacity up to 10 g/min. Besides gasifier, the gasification system also includes: feeding system, gas cleaning devices (cyclone, ash hopper, etc.), temperature sensors, tar sampling unit and gas analysis components, providing the required measurement facilities for R&D. A generalized scheme of the gasifier including with the associated components are depicted by Fig. 1.

2.5.1. Gasifier and the bed material

The gasifier itself is made of an AISI 310 refractory austenitic stainless steel tubular pipe with an inner diameter and height of 0.040 m and 1.5 m respectively. The entire reactor together with the cyclone and ash hopper are enclosed to an electrical furnace (~5 kW, 1000 °C) heated by the PID (Proportional-integral-derivative) controllers positioned in the bed and cyclone respectively. The temperature developed in the PID zones (reactor bed and cyclone) is monitored by a couple of K-type thermocouples. The bed in the reactor is made of silica sand (avg. particle size: ~367 μm, density: 2200 kg/m^3, minimum fluidization velocity: 0.016 m/s) and kept at around 150 mm of static depth, which was achieved by pouring sand particles from the top of the reactor via a concentric pipe running through the air distributor plate. The bed material overflows and subsequently deposited in the char pot located at the bottom of the reactor if the corresponding sand filling (typically ~40 g) exceeds the level of ~150 mm. The residual char, ash and bed-material (Fig. 2) as produced during gasification are also deposited in the char pot. The operation flow of the fluidizing agent through the bed was kept three to seven times of the minimum fluidization velocity (U_{mf}) which is consistent as according to the study by Mastral et al. [42].

2.5.2. Feeding system

Feeding system for biomass is comprised of two mechanisms with a provision of either continuous or, semi-continuous input. Typically for a continuous feeding, a screw feeder connected to the side of the reactor by a sloping pipe, operating with a feeding range of 0.5–10 g/min, is used. Continuous feeding while tested resulted feeder clogging due to the handling difficulties of pellets, as the current feeder was meant to feasibly operate with ground biomass only. Present work thus opted for semi-continuous feeding (manual batch feeding – once in every three minutes) provided through a two valve assembly (Fig. 3), the steps of which can be described as follows.

Firstly, ahead of a gasification test a number of batches of pellets consisting of 9–15 g (depending on operational ER) were prepared. Then for a given interval, which is three minutes in this case, each batch of fuel was introduced manually through the two valve assembly: during feeding, first the top valve was opened and the bottom valve kept closed and then the valves were alternated and finally both valves were kept closed. This procedure was repeated until the end of the each experiment.

It is to note that there were some minor variations (±10 s) in feeding interval, caused due to the operation of the manual valves and inspection of the data. This nevertheless did not influence the evolution pattern of the operational parameters. In general, thermal conversion of biomass pellets is affected by several operational factors including with the conditions applied during pelletizing. Biswas et al. [43] reported that conversion time of a single pellet (oven dried) can extend to as much as >200 s when pelletizing temperature exceeds 200 °C with average 150–180 s for pelletizing temperature at around 200 °C. Based on this fact and considering the feeding of multiple pellets at a time the feeding interval of three minutes has been chosen for this study.

2.5.3. Gas conditioning and tar recovery

Producer gas, as leaving from the reactor, first came in contact with a hot cyclone separating dust particles and then with a hot cartridge filter, removing further impurities. Subsequently, the gas was stripped of tar by the two cold condensers placed in series on the gas exit train. The majority of the tar present in the gas was condensed in the condensers and quantified off-line for determining volumes. After passing through the tar condensers, the gas was further cleaned by a cotton filter, located at the far end of the exit train. Finally the gas headed to a gas analysis system – composing of a gas meter and a μGC, facilitating volumetric and compositional analysis of the permanent gases. After each gasifier operation, ash hopper and char bin were cleaned and emptied while the cartridge (for the cartridge filter) and cotton (for the cotton filter) were replaced. The gas train starting from the cartridge filter until the condenser was covered by a 0.050 m thick insulation blanket (Unifrax Insulfrax S, Spain) to reduce heat loss to the surrounding environment.

2.5.4. Analytical methods

During test runs, several operational variables were monitored and analyzed. For example, temperature in the reactor, cyclone and gas exit was measured real-time by means of K-type thermocouples and displayed in a control panel.

Flow of fluidizing agent (air) was monitored and controlled by a flow controller (operating range: 0.5–100 Nm^3/h, Bronkhorst HIGH-TECH, the Netherlands) and was introduced through the distributor plate to the bottom of the reactor.

Char and ash amount was measured from the solid residues collected after each operation complying with the procedure as follows: first to collect all the solid residues from all the possible locations, then to subtract the known amount of bed-material from the total collected residues, afterwards to incorporate muffling at

Please cite this article in press as: Sarker S et al. Semi-continuous feeding and gasification of alfalfa and wheat straw pellets in a lab-scale fluidized bed reactor. Energy Convers Manage (2015), http://dx.doi.org/10.1016/j.enconman.2015.04.015

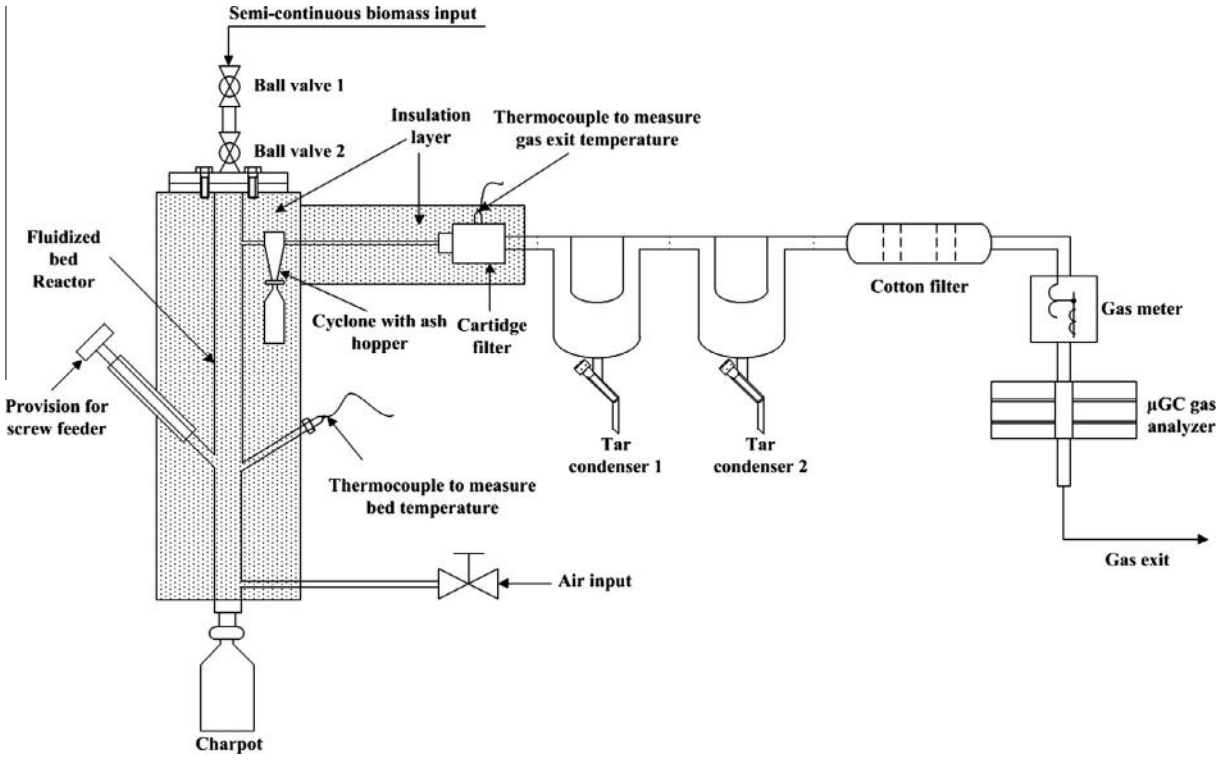

Fig. 1. A generalized scheme of the lab-scale gasification system.

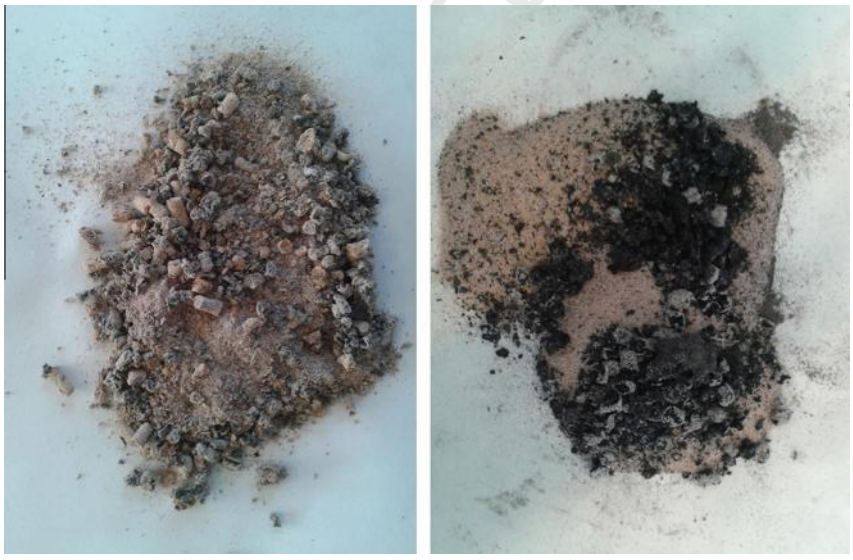

Fig. 2. Residual char, ash and bed-material from the gasification tests (left: alfalfa, right: wheat straw).

550 °C (according to the standard CEN/TS 15403:2006) for discounting the percent amount of ash, and finally to employ by difference for determining the fraction of each material (typically char, ash and sand) contributing the total residues.

Producer gas analysis was conducted by a series of equipment composed of a gas flow meter (domestic diaphragm gas meter, operating range: 0.01–10 m^3/h) and a micro-GC (Agilent 3000A µGC, Model G2801A, USA) itself equipped with two analyses modules (Plot U and Molsieve 5A) and thermal conductivity detectors. By the gas flow meter, volumetric flow of the gas was measured real-time and recorded manually once in every two/three minutes while the compositional analysis was carried out once in every two minutes of operation by the two µGC module calibrated for measuring CO_2, C_2H_4, C_2H_6, C_2H_2 and H_2S (Plot U module), and H_2, N_2, CH_4, CO and O_2 (MolSieve 5A module) respectively. The continuous measurement performed by the µGC was acquired to a computer facilitating the data analysis.

2.5.5. Experimental protocol and gasification conditions

Before initiating the experiment, the reactor was electrically pre-heated by the PID controllers. The heating of the reactor bed up to the gasification temperature of ~850 °C took approximately 3–4 h. Air supply was started as soon as the pre-heating initiated so that necessary fluidization bubbling (in the bed) was

Please cite this article in press as: Sarker S et al. Semi-continuous feeding and gasification of alfalfa and wheat straw pellets in a lab-scale fluidized bed reactor. Energy Convers Manage (2015), http://dx.doi.org/10.1016/j.enconman.2015.04.015

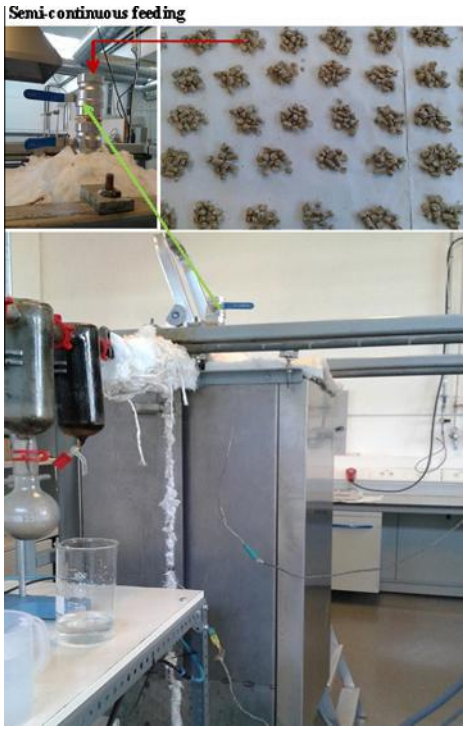

Fig. 3. Semi-continuous feeding with two valve assembly.

maintained both during gasification and pre-gasification stages. As soon as the gasification condition was achieved, the biomass feeding was introduced and given once in every three minutes. After the solid feeding was commenced, the gasifier reached to a stationary state in about 10 min of time-on-stream, as indicated by the evolution of stable temperature (±10 °C variation) and producer gas energy content (±0.5 MJ/Nm^3 variation), which continued for further 45–60 min to facilitate steady state measurement of several parameters such as temperature, gas quantity, composition, lower heating (LHV), cold gas efficiency (CGE), and carbon conversion efficiency (CCE). The expressions used to calculate some of these variables are given as follows:

$$LHV_{gas} = ((25.7 \times H_2) + (30.0 \times CO) + (85.4 \times CH_4) + (151.3 \times (C_2H_2 + C_2H_4 + C_2H_6))) \times \left(\frac{4.2}{1000}\right) \text{ [MJ/Nm}^3\text{]} \quad (1)$$

$$CGE = \frac{LHV_{gas} \times V_{gas}}{LHV_{feedstock}} \quad (2)$$

$$CCE = \frac{Y \times 1000(CO\% + CH_4\% + CO_2\% + 2(C_2H_4\% + C_2H_6\% + C_2H_2\%)) \times 12}{m \times (1 - X_{ash}) \times 22.4 \times C\%} \quad (3)$$

where V_{gas} is the dry gas yield in Nm^3/kg_feedstock; Q_{air} is the air supply in Nm^3/h; m is the biomass input in kg/h; LHV_{gas} is the lower heating value of dry producer gas in MJ/Nm^3; $LHV_{feedstock}$ is the dry base calorific value of the pellets in MJ/kg; Y is the producer gas output in Nm^3/h; Xash is the ash content of the feed biomass and C% is the elemental carbon percentage of feedstock.

Except the bed temperature, which was aimed at ~850 °C for both the feedstocks, the experimental conditions in respect to ER range was kept slightly different between the two feedstocks to compensate the difference in size influencing the manual feeding; for example ER = 0.23 could not be achieved for wheat straw pellets. The ER change was generally achieved either by varying the air flow, which was done for alfalfa pellets, or, by varying both the air and the solid flow, which was done for the wheat straw pellets respectively. The reason of such ER change scheme was purely based on the convenience of feeding as well as on keeping the gasification operation within the limit of minimum fluidization velocity (see Section 2.5.1 and Table 3). In case of alfalfa pellets, the ER varied in the range between 0.23 and 0.35 by adjusting the air flow rate between 0.16 Nm^3/h and 0.25 Nm^3/h at a constant solid flow rate of 0.20 kg/h. On the other hand, wheat straw pellets saw the ER modification between the range of 0.20 and 0.35 as a result of simultaneous modification in air and biomass input between 0.21 and 0.25 Nm^3/h, and 0.18 and 0.30 kg/h respectively. The ER values for this study were chosen from among the ranges found in the relevant literatures [8,22,44–46] and calculated by using Eq. (5).

$$ER = \frac{Actual\ weight\ oxygen\ from\ air / weight\ dry\ biomass}{stoichiometric\ air / biomass} \quad (4)$$

3. Results and discussions

3.1. Feedstock physiochemical properties

The results of the physical and chemical properties of alfalfa and wheat straw pellets in-terms of proximate, ultimate and other analyses are illustrated in Table 1.

As found, the average specific density of individual pellets for each feedstock varied between the range of ~1000 and 1200 kg/m^3 which are fairly typical for most of the biomass [47] and desirable for gasification [20].

As far as the proximate analysis is considered, the variation in amount of moisture and volatiles between the two feedstocks were not so substantial (Table 1) as opposed to the amount of ash which was remarkably different with a level exceeding 15% (dry basis) for alfalfa pellets (Table 1). The higher ash content in alfalfa was presumably because of the higher level of phosphorous, potassium and nitrogen, as found in its chemical composition (Table 1). Although higher level of ash, earlier pilot scale experiments on the same feedstock (alfalfa pellets) did not encounter operational difficulties [21] in regards to agglomeration, sintering, etc. and hence provided the motivation to extend the investigation in-regards to the small scale application, such as the investigation in the context of the present study.

Table 1
Physiochemical properties of alfalfa and wheat straw pellets.

Properties of the feedstocks	Alfalfa pellets	Wheat straw pellets
Proximate analysis (%)		
Moisture	8	7.5
Volatile Matter, dry base	74.4	78.8
Ash, dry base	15.5	5.2
Ultimate analysis (dry base, %)		
Carbon	41.6	46.2
Hydrogen	4.9	5.4
Oxygen[a]	33.9	42.6
Chlorine	1.43	0.15
Nitrogen	2.39	0.38
Sulfur	0.25	0.06
Lower heating value (dry basis, MJ/kg)		
Analytical	16.7	18.41
Theoretical[b]	17.62	19.45
Specific pellet density, kg/m^3	1198	1015

[a] Calculated by difference.
[b] Gaur and Reed, Ref. [41].

In terms of the measured average lower heating value, the amount found in wheat straw pellets (~18 MJ/kg) was superior than that of alfalfa pellets (~17 MJ/kg) (Table 1). This was presumably because of the effect of ash and of the amount of carbon which is approximately 12% lower in alfalfa, as compare to that of wheat straw (Table 1). Theoretical LHV calculation based on the empirical correlation revealed the similar results agreeing with the measurements with a maximum deviation of ~±5%.

As for ultimate analysis, both feedstocks showed varied compositions in regards to the percent amount of C, H, O, Cl, N and S (Table 1). C, H and O composition of alfalfa amounted to 41.6%, 4.9% and 33.9% respectively which compared to the corresponding amount of wheat straw pellets (46.2%, 5.4% and 42.6% respectively) were lower (Table 1) and less than the average for the similar biomass investigated in the past [48]. Conversely, in regards to the level of Cl, N and S, higher values were obtained from alfalfa than those from the wheat straw as a result of the difference in the amount of ash.

3.2. Thermo-gravimetric analysis

Fig. 4(a and b) depicts the TGA and DTG (Differential thermo-gravimetric) plots of alfalfa and wheat straw pellets for a constant heating rate of 10 °C/min. As observed (red and green curves for alfalfa and wheat straw respectively), pyrolysis (until 600 °C) followed by combustion (600–950 °C) led to a greater mass loss from wheat straw than that of alfalfa. This is in agreement with the proximate analysis results, particularly, those in-terms of volatiles and ash (Table 1). Lower ash and higher volatiles are the desirable properties for gasification which perhaps would favor wheat straw over alfalfa, as the TGA study in this work revealed.

3.3. Ash fusion temperature

Table 2 demonstrates three important temperatures during the period of melting biomass ash. Melting temperature may be used to roughly predict the characteristics of ash which is mainly composed of the inorganic metals and their oxides.

One important element indicating the melting properties of ash is K. In general, the increasing amount of K contributes to decrease the melting temperature liable to cause several operational difficulties such as agglomeration, melting, and slagging. Analyzing the ash melting results from the present study, alfalfa exhibited lower temperature than that of wheat straw (Table 2) which possibly indicating higher K in its (alfalfa) ash content. This however could not be confirmed from the obtained analysis. Hence, a pertinent literature survey based on the available dataset provided by Phyllis2 [49] was conducted and contradictory results were obtained. Despite the higher flow temperature, the average amount of K in alfalfa (~34%) was found higher than that of wheat straw (~18%) which basically opposes the hypothesis as developed on the basis of the theoretical correlation between the level of K and ash melting temperature. Similar phenomenon was observed in an earlier work conducted by Rizvi et al. [50]. It can thus be concluded that besides K, ash melting temperature is also influenced by the presence of other metals whose combined effect should

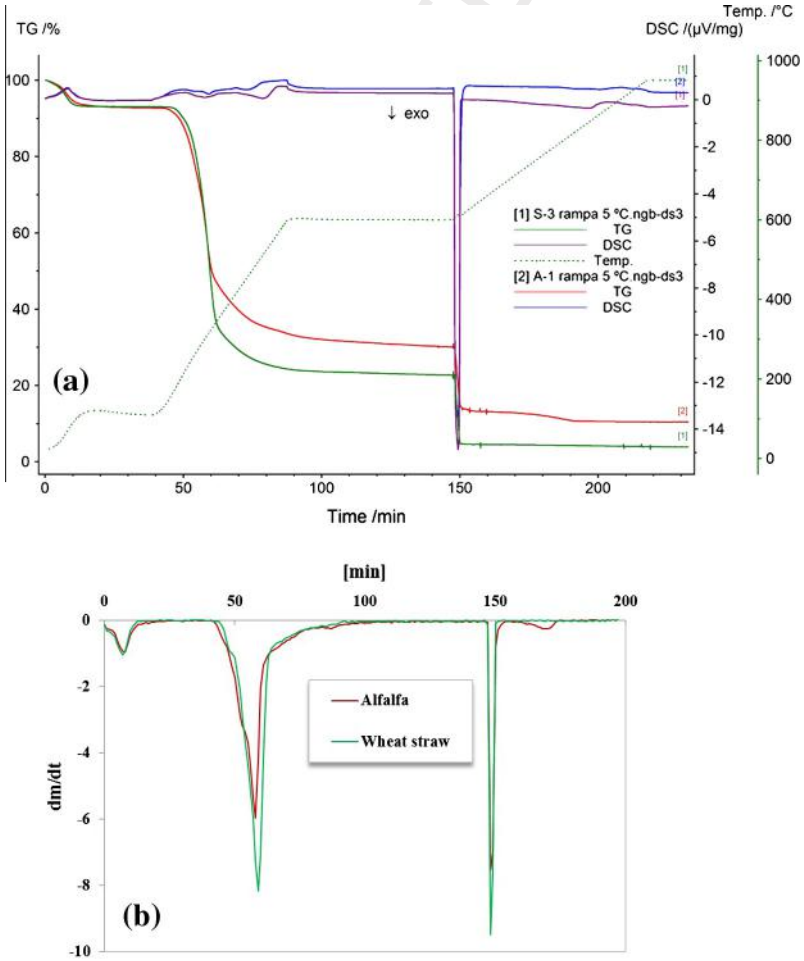

Fig. 4. TG and DTG diagram of alfalfa and wheat straw in nitrogen environment (heating rate: 10 °C/min); (a) TGA plots and (b) DTG plots.

Please cite this article in press as: Sarker S et al. Semi-continuous feeding and gasification of alfalfa and wheat straw pellets in a lab-scale fluidized bed reactor. Energy Convers Manage (2015), http://dx.doi.org/10.1016/j.enconman.2015.04.015

Table 2
Analysis of ash fusion temperatures.

Ash fusion temperatures				
	Present analysis		Phyllis 2[a]	
	Alfalfa	Wheat straw	Alfalfa[b]	Wheat straw[c]
DT (°C)	1173	941	870	932
HT (°C)	1178	1067	1323	1106
FT (°C)	1201	1273	1514	1298

[a] Ref. [49].
[b] Average of 20 samples.
[c] Average of 94 samples.

be thoroughly considered while predicting the melting temperature of biomass ash.

3.4. Impact of ER on product gas composition

ER in general affects several gasification properties including producer gas quality. In the present study, the producer gas composition as a result of varied ER in the range of 0.20–0.35 was investigated for alfalfa and wheat straw pellets; the average results of some of which are depicted by Fig. 5(a–d); where error bars representing the deviation of the average values for each run.

As observed, the stepwise increase in ER for alfalfa pellets contributed to improve most of the combustible gas quantities (H_2, CH_4, C_2H_6, C_2H_2) which maximized while ER peaked at 0.35 (Fig. 5a and b). Conversely, the concentration of CO first increased from 14.30% to 15.03% between ER 0.23 and 0.30 then decreased to 14.4% when ER climbed to 0.35 (Fig. 5a). The individual gas concentration which rose between the ER 0.23 and 0.35 are listed as: CO_2 from 13.56% to 15.0%, H_2 from 2.89% to 3.77%, CH_4 from 1.70% to 2.62%, C_2H_6 from 0.16% to 0.245% and C_2H_2 from 0.09% to 0.17% respectively (Fig. 5a and b). Increasing ER definitely favored the net effect of gasification reactions and as a result enhanced product gas compositions in-terms of H_2, CH_4, C_2H_6, C_2H_2, and partly to CO up to the value at 0.30. The rising trend of CO within ER 0.23–0.30 was likely to be prompted by the extent of endothermic Boudouard (Eq. (5)) and exothermic carbon partial oxidation (Eq. (7)) which agree with the recent pilot-scale study [21] conducted for the same feedstock. However, ER > 0.30 perhaps concurrently decreased the severity of Boudouard reaction (Eq. (5)) and increased the rate of combustion (Eq. (6)) as a result yielded lower CO and higher CO_2 in the product gas composition (Fig. 5a). The set of pertinent reactions involve in gasification is given below:

$$\textit{Boudouard reaction}: \quad C + CO_2 = 2CO; \quad \Delta H = +172 \text{ kJ} \tag{5}$$

$$\textit{Combustion reaction}: \quad C + O_2 = CO_2; \quad \Delta H = -408.8 \text{ kJ} \tag{6}$$

$$\textit{Carbon partial reaction}: \quad 2C + O_2 = 2CO; \quad \Delta H = -246.4 \text{ kJ} \tag{7}$$

$$\textit{Water gas shift reaction}: \quad CO + H_2O = CO_2 + H_2; \quad \Delta H = +41.98 \text{ kJ} \tag{8}$$

$$\textit{Water gas reaction}: \quad C + H_2O = CO + H_2; \quad \Delta H = +131 \text{ kJ} \tag{9}$$

Unlike alfalfa pellets, the mean producer gas compositions obtained from the gasification of wheat straw pellets exhibited no clear trend, except the concentration of CO_2 which rose throughout (Fig. 5c). As for combustible components particularly there was a significant decrease in the amount of H_2, dropping from 4.1% to 3.0% as the ER varied between the range of 0.20 and 0.35. CO likewise declined too until ER = 0.25 then followed the similar increasing and decreasing pattern that of alfalfa pellets within the ER between 0.25 and 0.35 (Fig. 5c). The simultaneous decrease in H_2 and CO along with the increase in CO_2 perhaps implies the combustion reactions to dictate over gasification as long as the supply oxygen is enhanced. In regards to the hydrocarbon products, the concentration of CH_4 and C_2H_4 displayed a rising tendency up until ER = 0.30, peaked at 2.97% and 1.08% respectively (Fig. 5d). This phenomenon is perhaps attributed to the reforming reactions that improved as the input oxygen rose [51]. Such reactions however weakened as those two gas species declined rapidly with further rise in ER at highest 0.35. At this point perhaps the combustion reaction (Eq. (6)) became stronger and hence escalating CO_2 in the average product gas together with the reduction in CH_4 and C_2H_4 content (Fig. 5c and d). The trend of C_2H_2 meanwhile increased in contrast to that of C_2H_6 which decreased as the level of ER gradually

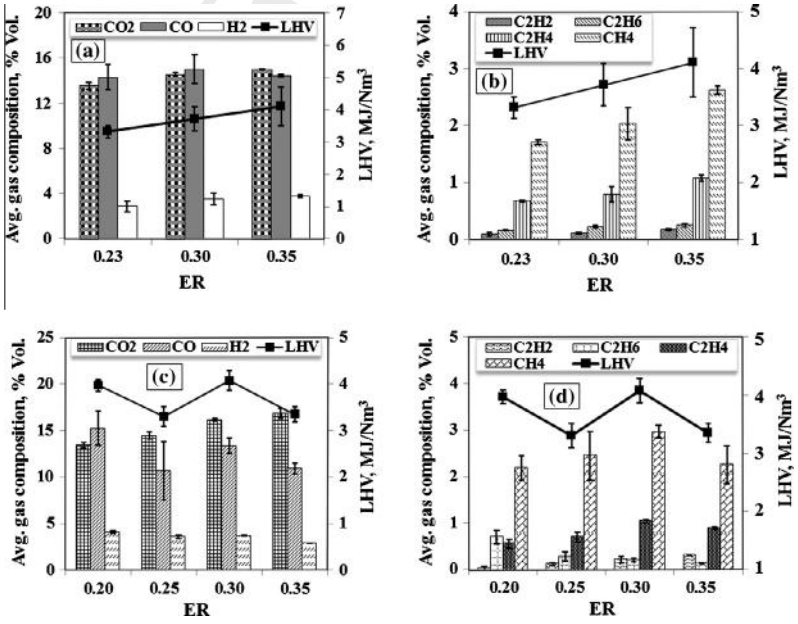

Fig. 5. Influence of ER on product gas composition of alfalfa and wheat straw pellets gasification; (a) syngas composition of alfalfa, (b) light hydrocarbon composition of alfalfa, (c) syngas composition of wheat straw, (d) light hydrocarbon composition of wheat straw.

Please cite this article in press as: Sarker S et al. Semi-continuous feeding and gasification of alfalfa and wheat straw pellets in a lab-scale fluidized bed reactor. Energy Convers Manage (2015), http://dx.doi.org/10.1016/j.enconman.2015.04.015

rose (Fig. 5d). The C_2H_6 trend obtained from this study complies with the past research by Xue et al. [45] while the concurrent effect of both (C_2H_2 and C_2H_6) perhaps be explained by the effect of inverse hydrogenation, expressed as:

$$C_2H_2 + H_2 \leftrightarrow C_2H_6; \quad \Delta H > 0 \tag{10}$$

3.5. Impact of ER on the performance of gasification

Effect of ER on several aspects of gasification such as lower heating value (LHV), gas yield, tar yield, cold gas efficiency (CGE) and carbon conversion efficiency (CCE) are illustrated by Fig. 6(a–f), whereas Table 3 demonstrates the average results as obtained from the individual gasification experiments. It should be noted that the error bars in Fig. 6 representing the deviation of the average values for each run.

In regards to alfalfa pellets, average LHV increased as ER increased (Fig. 6a). The strength of reforming reactions perhaps enhanced as ER rose and hence the increase in light hydrocarbons and consequently the improved gas LHV. This was also confirmed by the yielding pattern of tar, as induced by the cracking reactions, declined from mean 53 g/Nm^3 to 34 g/Nm^3 corresponding to the ER at 0.30 and 0.35 respectively (Fig. 6c). Likewise LHV, the gas yield (Nm^3/kg) showed an upward trend (Fig. 6b) and hence the increase in CGE and CCE, peaking to average 42% and 72% respectively for the ER reaching highest at 0.35 (Fig. 6e and f). Char yield (g/kg) meanwhile dropped significantly with a difference as much as 50% between the lowest and the highest ER (Fig. 6d). Decrease in char yield together with the impact of other parameters (as already explained) was likely to improve the performance of alfalfa gasification for the level of ER augmented up to 0.35 which appears to be optimum for the present case of experiments.

As far as wheat straw pellets are concerned, the performance of gasification varied to a great degree as ER varied. For instance, when ER slightly increased from 0.20 to 0.25 the dry gas LHV (in MJ/Nm^3, dry basis) decreased (Fig. 6a) as a result of the reduction in combustible gases such as the drop in the amount of CO, H_2, CH_4 and C_2H_4. Conversely, the specific gas yield (Nm^3/kg biomass) rose (Fig. 6b) likely due to the enhancement of the rate of devolatilization [44]. This however did not reflect to the percent yield of CGE and CCE which kept fairly constant (Fig. 6e and f) presumably due to the development of higher char (Fig. 6d). Similar phenomenon was observed by the past work conducted by Xue et al. [45]. Further rise in ER at 0.30 positively contributed to several parameters such as gas LHV, specific gas yield, CGE and CCE while decreased the value of tar and char (Fig. 6(a–f)). At higher ER, the yield of CH_4 and other hydrocarbons (C_2H_6, C_2H_2) increased, despite the lower CO, resulting the obvious rise in total gas LHV (Fig. 6c and d). Moreover, the rate of several endothermic reactions such as cracking and reforming increased; leading to improvement in efficiencies in-terms of CCE and CGE (Fig. 6e and f). The trend of most of these parameters however declined as ER further increased to the highest 0.35, except the amount of tar, which rose to ~71 g/Nm^3 from the level of ~59 g/Nm^3 (at ER = 0.30) (Fig. 6c), and the gas yield, which jumped to all time maximum at 1.74 Nm^3/kg (dry basis) (Fig. 6b). As the combustible quantities diminished, this gas yield was mainly boosted by the increased amount of CO_2 contributed due to the rise in combustion reactions (Eqs. (6) and (7)). The enhanced CO_2 also resulted improved CCE despite the deterioration of the other major parameters such as the amount of gas LHV and CGE.

3.6. Impact of ER on bed temperature and gasification parameters

Increase in ER in general leads to improve the bed temperature influencing several gasification parameters the corresponding relation of which is demonstrated by Fig. 7(a–h).

For alfalfa pellets it was observed that the bed temperature varied to a narrow margin of 869–873 °C for the ER varied between the range of 0.23 and 0.35 (Fig. 7(a–d)). The maximum temperature was achieved corresponding to the ER at max. 0.35. When bed temperature peaked, the quantity of LHV, gas yield, CCE and CGE rose and the tar and char yield fell mainly due to the enhanced water gas shift reaction (Eq. (8)), combustion (Eq. (6)), tar reforming (refer Ref. [52] for equations) and water gas reaction (Eq. (9)). These observations coincide with the earlier works reported by

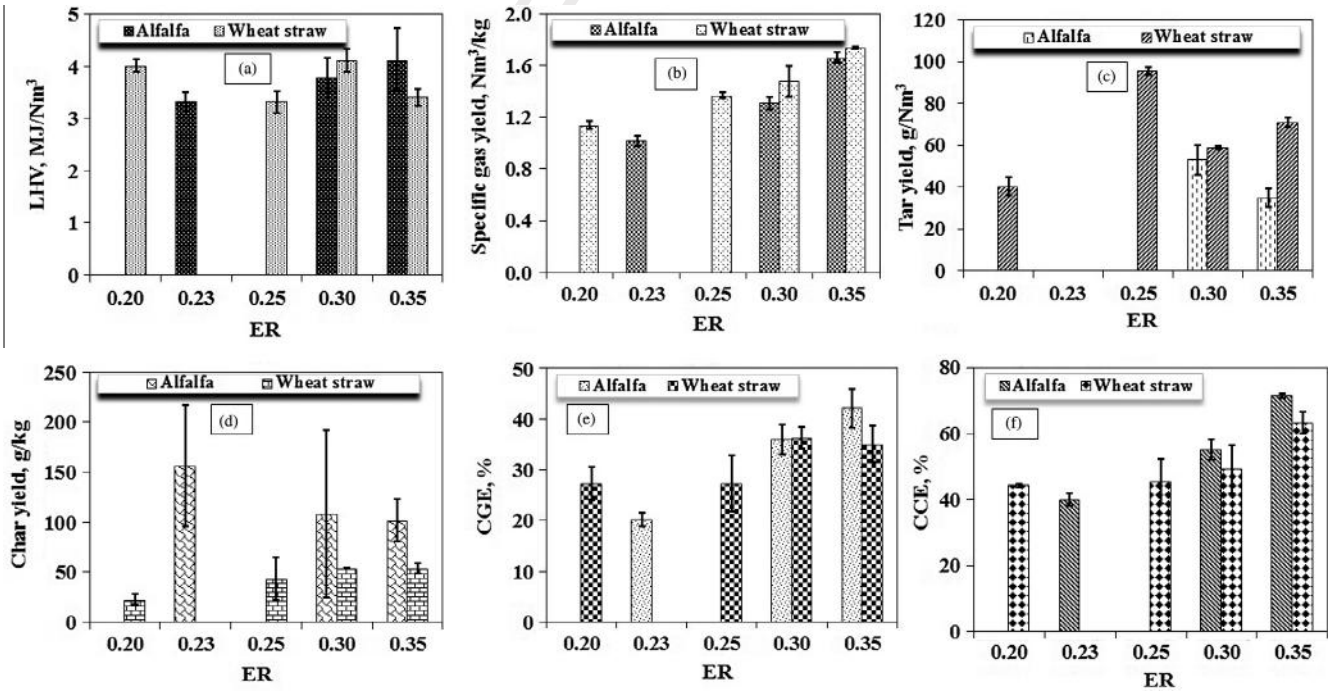

Fig. 6. Gasification performance of alfalfa and wheat straw pellets; (a) comparison of producer gas LHV between alfalfa and wheat straw, (b) comparison of producer gas yield, (c) comparison of tar yield, (d) comparison of char yield, (e) comparison of CGE, (f) comparison of CCE.

Please cite this article in press as: Sarker S et al. Semi-continuous feeding and gasification of alfalfa and wheat straw pellets in a lab-scale fluidized bed reactor. Energy Convers Manage (2015), http://dx.doi.org/10.1016/j.enconman.2015.04.015

Table 3
Average results of the gasification tests.

Operating parameters	Alfalfa pellets							Wheat straw pellets							
	Run 1	Run 2	Run 3	Run 4	Run 5	Run 6	Run 7	Run 8	Run 9	Run 10	Run 11	Run 12	Run 13	Run 14	Run 15
Biomass flow rate, kg/h	0.20	0.20	0.20	0.20	0.20	0.20	0.20	0.30	0.30	0.24	0.24	0.18	0.18	0.18	0.18
Air flow rate, Nm^3/h	0.16	0.16	0.21	0.21	0.21	0.25	0.25	0.24	0.24	0.24	0.24	0.21	0.21	0.25	0.25
Bed temperature, °C (at start)	850	850	850	850	850	850	850	850	850	850	850	850	850	850	850
Bed temperature, °C (steady condition)	871.6 ± 5.4	872.1 ± 3.6	876.0 ± 5.5	874.0 ± 1.7	868.8 ± 2.8	874.0 ± 3.6	874.1 ± 4.0	869.2 ± 1.7	870.1 ± 3.3	872.0 ± 1.1	872.0 ± 1.9	873.0 ± 1.0	872.0 ± 1.1	873.0 ± 2.7	873.8 ± 1.8
Equivalence ratio (ER)	0.23	0.23	0.30	0.30	0.30	0.35	0.35	0.20	0.20	0.25	0.25	0.30	0.30	0.35	0.35
U_f/U_{mf}	3.06	3.06	4.01	4.01	4.01	4.78	4.78	4.59	4.59	4.59	4.59	4.01	4.01	4.78	4.78
CO (% vol. dry base)	15.09 ± 1.04	13.50 ± 1.07	13.77 ± 1.17	16.28 ± 1.75	15.03 ± 2.17	14.31 ± 1.5	14.48 ± 1.29	13.96 ± 0.97	16.52 ± 0.94	8.48 ± 1.13	12.89 ± 1.09	13.93 ± 0.77	12.76 ± 0.77	11.33 ± 1.15	10.48 ± 1.35
H_2 (% vol. dry base)	3.23 ± 0.34	2.55 ± 0.29	3.20 ± 0.98	4.12 ± 0.42	3.31 ± 0.84	3.84 ± 0.52	3.71 ± 0.81	4.21 ± 0.57	4.00 ± 0.38	3.72 ± 0.82	3.39 ± 0.71	3.69 ± 0.27	3.72 ± 0.25	2.88 ± 0.47	2.85 ± 0.45
CO_2 (% vol. dry base)	13.79 ± 0.57	13.34 ± 0.87	14.47 ± 1.63	14.78 ± 1.16	14.46 ± 1.21	14.98 ± 0.89	15.03 ± 0.96	13.66 ± 1.07	13.23 ± 1.17	14.19 ± 0.72	14.73 ± 0.95	16.10 ± 0.39	16.30 ± 0.33	16.46 ± 0.61	17.24 ± 0.51
CH_4 (% vol. dry base)	1.72 ± 0.14	1.67 ± 0.09	1.9 ± 0.28	2.36 ± 0.37	1.84 ± 0.15	2.67 ± 0.19	2.57 ± 0.21	2.37 ± 0.40	2.01 ± 0.25	2.81 ± 0.07	2.08 ± 0.40	3.07 ± 0.15	2.88 ± 0.10	2.55 ± 0.27	1.97 ± 0.21
Lower heating value, MJ/Nm^3	3.45 ± 0.51	3.19 ± 0.43	3.42 ± 0.27	4.16 ± 0.18	3.76 ± 0.12	4.12 ± 0.44	3.27 ± 0.63	3.92 ± 0.32	4.09 ± 0.41	3.17 ± 0.53	3.46 ± 0.48	4.26 ± 0.27	3.96 ± 0.22	3.52 ± 0.39	3.29 ± 0.28
Specific gas yield (Nm^3/kg_fuel)	0.99 ± 0.59	1.05 ± 0.81	1.25 ± 0.73	1.35 ± 0.35	1.33 ± 0.24	1.69 ± 0.18	1.63 ± 0.43	1.15 ± 0.24	1.12 ± 0.21	1.35 ± 0.11	1.39 ± 0.30	1.39 ± 0.14	1.56 ± 0.18	1.73 ± 0.20	1.75 ± 0.18
Cold gas efficiency (%)	21.26 ± 1.20	20.86 ± 2.00	28.96 ± 1.50	34.96 ± 2.05	31.19 ± 1.70	43.42 ± 1.91	41.58 ± 2.23	25.78 ± 1.50	25.94 ± 1.03	24.41 ± 1.36	27.22 ± 2.31	27.22 ± 2.25	35.14 ± 1.61	34.54 ± 0.94	32.62 ± 1.53
Char yield (g/kg)	199.47	113.14	N.D.	49.50	167.21	116.60	86.82	19.60	26.89	58.89	28.92	54.50	53.20	50.30	57.63
Tar yield (g/Nm^3)	N.D.	N.D.	59.40	45.30	54.50	37.90	31.70	37.30	43.40	97.10	94.30	58.20	59.20	72.70	69.50
Ash yield, (g/kg)	163.20	158.50	N.D.	169.8	173.2	157.5	155.3	65.30	71.0	46.4	77.8	56.3	57.1	58.50	60.7

N.D.: Not determined; U_f: fluidization velocity, cm/s; U_{mf}: minimum fluidization velocity, cm/s (1.6).

Refs.[7,52]. Among the parameters investigated, it is also interesting to note that the yield of char corresponding to lower ER value (0.23–0.30) differed to a great degree amongst the trial runs, causing high standard deviation of the obtained results (Fig. 7c). These however were likely to stabilize at higher ER (namely at 0.35) indicating improved thermal conversion as a result of improved supply of air.

Likewise alfalfa pellets, maximum bed temperature was achieved when ER reached maximum at 0.35. The bed temperature for this feedstock varied to a range between 868 and 873 °C corresponding to the ER at 0.20–0.35 (Fig. 7(e–h)). The trend of gas yield and CCE followed with the increase in ER and thus with the temperature (Fig. 7h). Conversely, in-terms of quality (for example, gas LHV) and CGE the trend of the producer gas appeared to degrade, especially beyond the temperature of ~869 °C when ER exceeded the level of 0.30 (Fig. 7e). This is consistent with the theoretical correlation as logically the higher the air supply, the higher the bed temperature, and higher the extent of combustion (Eq. (6)), resulting lower the energy from the producer gas and ultimately lower the efficiency in-terms of CGE. As for tar yield on the other hand the level rose and amounted to ~71 g/Nm^3 at bed temperature of 873 °C (Fig. 7f) potentially due to the development of heavy tar molecules (such as naphthalene and quinolone) in its total composition at the expense of light tars. It is worthwhile here to note that the heavy tar, especially the content of naphthalene and similar is potentially stable over a wide range of temperature and thus can continue to develop for temperature that exceeds 850 °C, as evidenced by the Refs. [28,53] for the similar feedstock. The compositional analysis of tar nevertheless was not in the scope of the present work and thus that literature results cannot be precisely compared. In regards to the un-combusted char yield, this feedstock did not exhibit a high standard deviation above bed temperature of 869 °C unlike alfalfa pellets and tended to stabilize at higher temperature corresponding to the ER range between 0.30 and 0.35 (Fig. 7g). This clearly indicates the stable char conversion as a consequence of elevated temperature in the fluid bed. Based on the present discussion it can thus be concluded that the parameters such as LHV, CGE and tar established as optimum at ER = 0.30 when the corresponding bed temperature reached to a level of ca. 869 °C (Fig. 7e, f and h). This ER value is reasonably close as far the as the past study [39] is concerned, indicating operating parameters to be optimum at ER = 0.25.

3.7. Comparison with the relevant literature results

The results obtained from the present gasification tests have been compared to the existing literature (Table 4) dedicated to the similar investigation in the past.

As can be seen (Table 4), the studies ranged from small scale to pilot scale fluidized bed and fixed bed gasification. The literature work entirely devoted to the gasification of alfalfa is scarce, and thus not many relevant data are available. Hence just the two important recent works [20,21] including the present work are considered for comparison. As clearly shown in Table 4, significant differences in-terms of gas compositions and other parameters are established among these studies. Particularly, pronounced difference in-terms of the level of tar, char, H_2 and CO are observed between the pilot-plant study [21] and this study, despite the gas LHV which is fairly similar. This perhaps is attributed due to the contrasting solid feeding mechanism; being continuous for pilot-scale and semi-continuous for lab-scale (this study) respectively. As it appeared, semi-continuous feeding caused a dramatic impact in the H_2 production which reduced to approximately four times than that of the pilot-scale experiments. Among the various char conversion reactions governing the evolution of product gas composition, char oxidation is the fastest [54] and hence requires

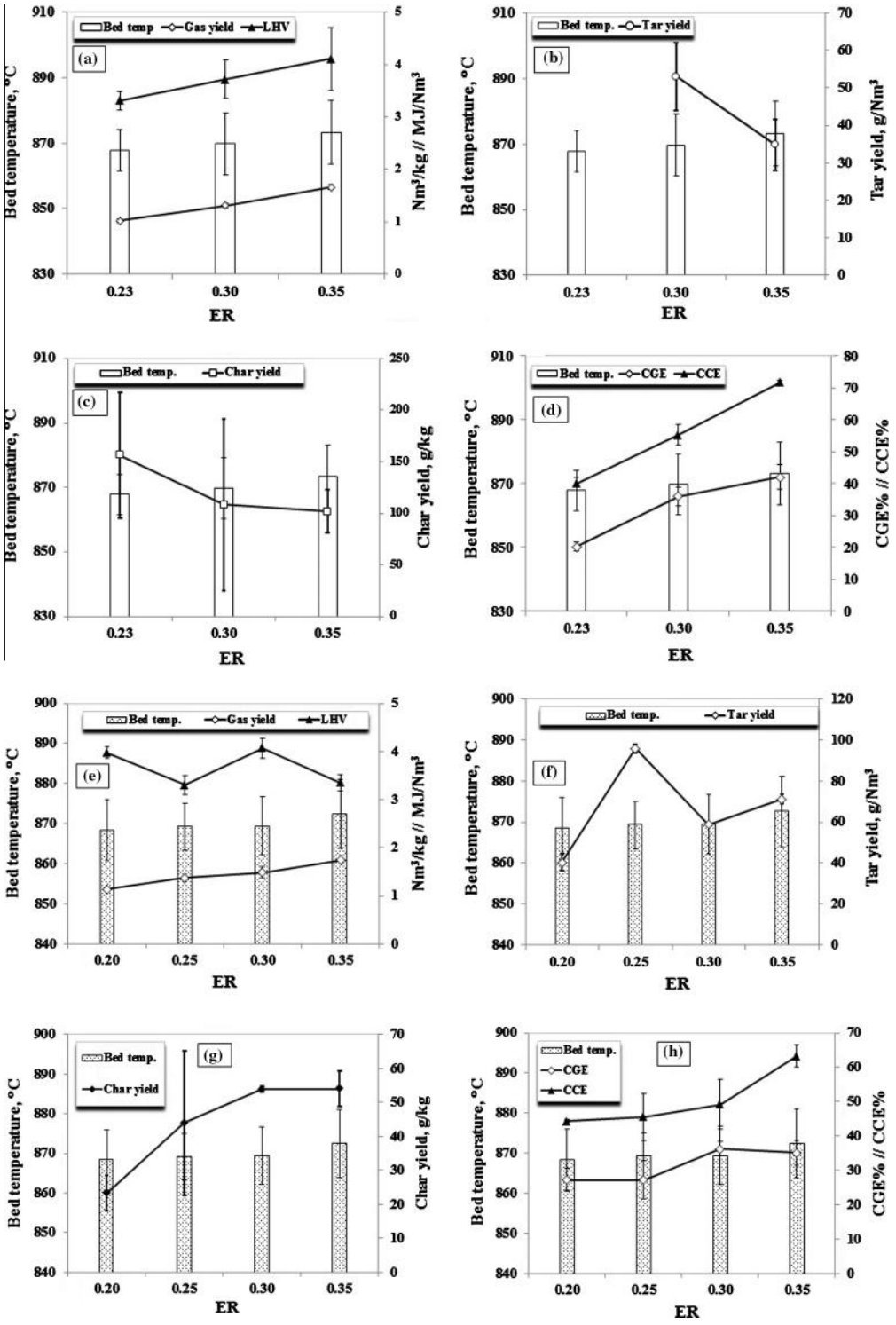

Fig. 7. Simultaneous effect of ER and bed temperature on gasification performance of alfalfa and wheat straw pellets; (a) producer gas LHV or, gas yield from alfalfa (b) tar yield from alfalfa (c) char yield from alfalfa (d) CGE or, CCE from gasification of alfalfa (d) producer gas LHV or, gas yield from wheat straw (b) tar yield from wheat straw (c) char yield from wheat straw (d) CGE or, CCE from gasification of wheat straw.

least residence time, whereas, char steam gasification (water–gas reaction), which contributes to boost product gas with H_2 is three to five orders of magnitude slower [54] than that of char oxidation and hence higher residence time is required to allow this reaction to occur. Maintaining an optimal residence time balancing the interactions of various reactions is important to improve the gasification phenomenon as well as the overall efficiency which appeared to be established by the process itself in case of continuous reactor. While for semi-continuous feeding, this parameter might be optimized by carrying out experiments for number of residence time which however was not in the scope of the present study and hence effect of such cannot be discussed here. It is however can be hypothesized that the residence time required to achieve efficient water–gas reaction could not be matched by the

Please cite this article in press as: Sarker S et al. Semi-continuous feeding and gasification of alfalfa and wheat straw pellets in a lab-scale fluidized bed reactor. Energy Convers Manage (2015), http://dx.doi.org/10.1016/j.enconman.2015.04.015

Table 4
Comparison of alfalfa and wheat straw gasification among the similar literature studies.

Reference	Alfalfa			Wheat straw	
	This work	[20]	[21]	This work	[53]
Gasifier specifications (air as gasifying agent)	Lab-scale BFB, 0.5–10 g/min. biomass feed	Pilot scale Fixed-bed downdraft, 18–23 kg/h	Pilot-scale BFB, 10 kg/h	Lab-scale BFB, 0.5–10 g/min. biomass feed	BFB, ~2.37 kg/h
ER	0.23–0.35	Not given	0.25–0.30	0.20–0.35	0.15–0.35
Average gas composition (% vol., dry base)					
H_2	3.4	7.88	13.05	3.57	9[b]
CO	14.58	11.36	8.75	12.55	7[b]
CH_4	2.12	1.39	2.7	2.47	3[b]
CO_2	14.38	16.89	20	15.24	Not given
LHV, MJ/Nm^3	3.71	2.78	4.2	3.67	2.93[b]
Bed temp. °C (at start)	~850	~700	~780	~850	800[b]
Freeboard temp.					
Gas yield, Nm^3/kg	1.33	Not given	1.44	1.43	Not given
Cold gas efficiency	32.78	Not given	36.39	31.48	Not given
Carbon conversion efficiency	55.65	Not given	N.D.	50.59	Not given
Tar yield, g/Nm^3	43.96	0.5	1.12	66.46	7.69[a]
Char yield, g/kg	122.13	Not given	281.72	43.75	Not given

present semi-continuous feeding and thus the lower H_2 in the product gas composition. Worthwhile also to note that the difference in the size of the operating plants might also result dissimilarity in the product gas composition in spite of the similarity in residence time and thereby the results obtained among the various scales of plants are not completely exchangeable. Generally, small scale plants are less efficient compared to pilot or, commercial scale plants [55].

Meanwhile, as compare to semi-continuous feeding, continuous feeding to pilot-plant [21] resulted higher char yield as a result of the lower operating temperature (~780 °C) which concurrently negatively affected the product gas composition in terms of CO. Conversely, despite the lower bed temperature, in-terms of CO_2, the level in the pilot-plant was higher which might due to the effect of several endothermic reactions namely water–gas shift reaction (Eq. (8)) and the reverse Boudouard reaction (Eq. (5)) contributing to the indirect production of CO_2 at the expense of temperature. As of tar, on the other hand, current work exhibited significantly higher yield than that of pilot-plant [21], implying the presence of weaker cracking reactions unable to convert liquids into useful gases.

Opposed to the fixed-bed gasification study [20], the present work revealed higher gas LHV due to the high level of methane in the product gas composition, but exhibited lower H_2 which probably because of the poor water–gas shift reaction (Eq. (8)). The rate of water–gas shift reaction in general increases with temperature, but the conversion of reactants to products (CO_2 and H_2) decreases [56]. Higher operating temperature is thus the reason why hydrogen yield from the present study was lower in contrast to the study by Sharma [20]. Fixed-bed downdraft gasifier inherently results less tar than the fluidized bed gasifier, and thus logically yielded the lowest tar among all the technologies compared here.

Likewise alfalfa, the study solely dedicated to air gasification of wheat straw is limited. This is mainly because of the physical and chemical properties of this feedstock causing several operational difficulties in terms of ash agglomeration, slagging, etc. Knowing the process difficulties, thus a common approach to treat this biomass is to use either steam or, CO_2 as gasifying agent, and catalyst as the reducer to minimize tar and ash content. In this regard, thus, study by Ref. [53] dealing with air gasification of wheat straw in BFB gasifier has been selected to allow comparison. As observed (Table 4), the gas composition substantially differs in-terms of the level of H_2 and CO, in spite of a fairly comparable LHV. Particularly for the earlier work [53], H_2 is found higher, which is perhaps due to the increased water gas shift reaction (Eq. (8)), and CO is found lower which is probably due to the weaker Boudouard reaction (Eq. (5)) as a result of the lower bed temperature (~850 °C) compared to that (>850 °C) from this study. Comparison in regards to other parameters cannot be made due to the lack of the available data.

4. Conclusions

After the series of gasification trial runs of alfalfa and wheat straw pellets following conclusions can be drawn. Over the range of the test conditions investigated, the gasification performance of alfalfa pellets maximized at ER = 0.35 which reflected to the gas LHV peaking to ~4.1 MJ/Nm^3, gas yield to ~1.7 Nm^3/kg, CGE to ~42% and CCE to ~72% respectively. The gasification performance of wheat straw pellets on the other hand erratically varied as the operating conditions varied with optimized performance apparently achieved at ER = 0.30 corresponding to the bed temperature of ~870 °C. At this ER, the level of important parameters such as gas LHV, tar yield, CGE and CCE reached to ~4 MJ/Nm^3, 58.7 g/Nm^3, ~39% and 49% respectively which however tended to degrade as the ER rose further.

In general, the average hydrogen content in the producer gas composition of the two biomasses was low and thus these feedstocks may not be suitable to utilize for hydrogen production. The average CGE and CCE values were also low to recommend the present technology for a commercial scale application. Process characteristics such as low combustible quantity in the producer gas, low char conversion, carbon losses with tar, particulates in cyclone, and particulate and carbon in hot filters, appeared to contribute to decrease these efficiencies. However, owing to the fairly attractive gas LHV, the producer gas may be recommended to utilize in a small scale combined heat and power (CHP) plant application where heat and electricity are simultaneously generated by the direct firing of gas through engine or, turbine.

Acknowledgement

Special thanks go to the people of the Thermochemical Process Group (GPT) from the Universidada Zaragoza (UNIZAR), Spain for

their relentless support during the course of this work. Universitetet i Agder is also acknowledged for providing finance.

References

[1] Rahman MM, Mostafiz SB, Paatero JV, Lahdelma R. Extension of energy crops on surplus agricultural lands: a potentially viable option in developing countries while fossil fuel reserves are diminishing. Renew Sustain Energy Rev 2014;29:108–19.
[2] McKendry P. Energy production from biomass (part 2): conversion technologies. Bioresour Technol 2002;83:47–54.
[3] Lim JS, Abdul Manan Z, Wan Alwi SR, Hashim H. A review on utilisation of biomass from rice industry as a source of renewable energy. Renew Sustain Energy Rev 2012;16:3084–94.
[4] Balat M, Balat M, Kırtay E, Balat H. Main routes for the thermo-conversion of biomass into fuels and chemicals. Part 2: Gasification systems. Energy Convers Manage 2009;50:3158–68.
[5] Sarker S, Nielsen H. Preliminary fixed-bed downdraft gasification of birch woodchips. Int J Environ Sci Technol. p. 1–8.
[6] Xiao R, Jin B, Zhou H, Zhong Z, Zhang M. Air gasification of polypropylene plastic waste in fluidized bed gasifier. Energy Convers Manage 2007;48:778–86.
[7] Boateng AA, Banowetz GM, Steiner JJ, Barton TF, Taylor DG, Hicks KB, et al. Gasification of Kentucky bluegrass (*Poa pratensis* l.) straw in a farm-scale reactor. Biomass Bioenergy 2007;31:153–61.
[8] Makwana J, Joshi AK, Athawale G, Singh D, Mohanty P. Air gasification of rice husk in bubbling fluidized bed reactor with bed heating by conventional charcoal. Bioresour Technol 2015;178:45–52.
[9] Gómez EO, Augusto Barbosa Cortez LS, Lora ES, Sanchez CG, Bauen A. Preliminary tests with a sugarcane bagasse fueled fluidized-bed air gasifier. Energy Convers Manage 1999;40:205–14.
[10] Arena U, Di Gregorio F, De Troia G, Saponaro A. A techno-economic evaluation of a small-scale fluidized bed gasifier for solid recovered fuel. Fuel Process Technol 2015;131:69–77.
[11] Kurkela E, Nieminen M, Simell P. Development and commercialization of biomass and waste gasification technologies from reliable and robust co-firing plants towards synthesis gas production and advanced power cycles. In: Proc of second world biomass conference; 2004. p. 10–5.
[12] Lamb JF, Sheaffer CC, Samac DA. Population density and harvest maturity effects on leaf and stem yield in alfalfa. Agron J 2003;95:635–41.
[13] Fanlo R, Chocarro C, Lloveras J, Ferran X, Serra J, Salvia J, et al. Alfalfa production and quality in Northeast Spain. Grassland Sci Eur 2006;11:261–3.
[14] Moore K, Moser LE, Vogel KP, Waller SS, Johnson B, Pedersen JF. Describing and quantifying growth stages of perennial forage grasses. Agron J 1991;83:1073–7.
[15] González-García S, Moreira MT, Feijoo G. Environmental performance of lignocellulosic bioethanol production from Alfalfa stems. Biofuels, Bioprod Biorefin 2010;4:118–31.
[16] Boateng A, Jung H, Adler P. Pyrolysis of energy crops including alfalfa stems, reed canarygrass, and eastern gamagrass. Fuel 2006;85:2450–7.
[17] Boateng AA, Mullen CA, Goldberg N, Hicks KB, Jung H-JG, Lamb JF. Production of bio-oil from alfalfa stems by fluidized-bed fast pyrolysis†. Ind Eng Chem Res 2008;47:4115–22.
[18] Vadas P, Barnett K, Undersander D. Economics and energy of ethanol production from alfalfa, corn, and switchgrass in the Upper Midwest, USA. BioEnergy Res 2008;1:44–55.
[19] Butterman HC, Castaldi MJ. Influence of CO_2 injection on biomass gasification. Ind Eng Chem Res 2007;46:8875–86.
[20] Sharma A. Assessing the suitability of various feedstocks for biomass gasification. Louisiana State University; 2011.
[21] Sarker S, Bimbela F, Sánchez JL, Nielsen HK. Characterization and pilot scale fluidized bed gasification of herbaceous biomass: a case study on alfalfa pellets. Energy Convers Manage 2015;91:451–8.
[22] Zabaniotou A, Bitou P, Kanellis T, Manara P, Stavropoulos G. Investigating Cynara C. biomass gasification producer gas suitability for CHP, second generation biofuels, and H_2 production. Ind Crops Prod 2014;61:308–16.
[23] Ji W, Shen Z, Wen Y. Hydrolysis of wheat straw by dilute sulfuric acid in a continuous mode. Chem Eng J 2015;260:20–7.
[24] Shang L, Ahrenfeldt J, Holm JK, Sanadi AR, Barsberg S, Thomsen T, et al. Changes of chemical and mechanical behavior of torrefied wheat straw. Biomass Bioenergy 2012;40:63–70.
[25] Jenkins B, Baxter L, Miles Jr T, Miles T. Combustion properties of biomass. Fuel Process Technol 1998;54:17–46.
[26] Li X, Wang S, Duan L, Hao J, Li C, Chen Y, et al. Particulate and trace gas emissions from open burning of wheat straw and corn stover in China. Environ Sci Technol 2007;41:6052–8.
[27] Sun R, Fang J, Rowlands P, Bolton J. Physicochemical and thermal characterization of wheat straw hemicelluloses and cellulose. J Agri Food Chem 1998;46:2804–9.
[28] Carpenter DL, Bain RL, Davis RE, Dutta A, Feik CJ, Gaston KR, et al. Pilot-scale gasification of corn stover, switchgrass, wheat straw, and wood: 1. Parametric study and comparison with literature. Ind Eng Chem Res 2010;49:1859–71.
[29] Mahinpey N, Murugan P, Mani T, Raina R. Analysis of bio-oil, biogas, and biochar from pressurized pyrolysis of wheat straw using a tubular reactor. Energy Fuels 2009;23:2736–42.
[30] Zheng Y, Jensen PA, Jensen AD, Sander B, Junker H. Ash transformation during co-firing coal and straw. Fuel 2007;86:1008–20.
[31] Lal R. World crop residues production and implications of its use as a biofuel. Environ Int 2005;31:575–84.
[32] Nguyen TLT, Hermansen JE, Mogensen L. Environmental performance of crop residues as an energy source for electricity production: the case of wheat straw in Denmark. Appl Energy 2013;104:633–41.
[33] Nguyen TLT, Hermansen JE, Nielsen RG. Environmental assessment of gasification technology for biomass conversion to energy in comparison with other alternatives: the case of wheat straw. J Cleaner Prod 2013;53:138–48.
[34] Nutalapati D, Gupta R, Moghtaderi B, Wall TF. Assessing slagging and fouling during biomass combustion: a thermodynamic approach allowing for alkali/ash reactions. Fuel Process Technol 2007;88:1044–52.
[35] Lv P, Xiong Z, Chang J, Wu C, Chen Y, Zhu J. An experimental study on biomass air–steam gasification in a fluidized bed. Bioresour Technol 2004;95:95–101.
[36] Prins MJ, Ptasinski KJ, Janssen FJ. More efficient biomass gasification via torrefaction. Energy 2006;31:3458–70.
[37] Zhang K, Chang J, Guan Y, Chen H, Yang Y, Jiang J. Lignocellulosic biomass gasification technology in China. Renewable Energy 2013;49:175–84.
[38] Lucia LA. Lignocellulosic biomass: A potential feedstock to replace petroleum. BioResources 2008;3:981–2.
[39] Ergudenler A, Ghaly A. Quality of gas produced from wheat straw in a dual-distributor type fluidized bed gasifier. Biomass Bioenergy 1992;3:419–30.
[40] Armesto L, Bahillo A, Veijonen K, Cabanillas A, Otero J. Combustion behaviour of rice husk in a bubbling fluidised bed. Biomass Bioenergy 2002;23:171–9.
[41] Gaur S, Reed TB. An atlas of thermal data for biomass and other fuels. National Renewable Energy Lab., Golden, CO (United States); 1995.
[42] Mastral FJ, Esperanza E, Berrueco C, Juste M, Ceamanos J. Fluidized bed thermal degradation products of HDPE in an inert atmosphere and in air–nitrogen mixtures. J Anal Appl Pyrol 2003;70:1–17.
[43] Biswas AK, Rudolfsson M, Broström M, Umeki K. Effect of pelletizing conditions on combustion behaviour of single wood pellet. Appl Energy 2014;119:79–84.
[44] Gómez-Barea A, Arjona R, Ollero P. Pilot-plant gasification of olive stone: a technical assessment. Energy Fuels 2005;19:598–605.
[45] Xue G, Kwapinska M, Horvat A, Kwapinski W, Rabou L, Dooley S, et al. Gasification of torrefied Miscanthus × giganteus in an air-blown bubbling fluidized bed gasifier. Bioresour Technol 2014;159:397–403.
[46] Mohammed M, Salmiaton A, Wan Azlina W, Mohammad Amran M, Fakhru'l-Razi A. Air gasification of empty fruit bunch for hydrogen-rich gas production in a fluidized-bed reactor. Energy Convers Manage 2011;52:1555–61.
[47] Mani S, Sokhansanj S, Bi X, Turhollow A. Economics of producing fuel pellets from biomass. Appl Eng Agric 2006;22:421.
[48] Tillman DA. Biomass cofiring: the technology, the experience, the combustion consequences. Biomass Bioenergy 2000;19:365–84.
[49] Phyllis2. Database for biomass and waste, ECN, The Netherlands. <https://www.ecn.nl/phyllis2>. [accessed 25.01.15].
[50] Rizvi T, Xing P, Pourkashanian M, Darvell LI, Jones JM, Nimmo W. Prediction of biomass ash fusion behaviour by the use of detailed characterisation methods coupled with thermodynamic analysis. Fuel 2015;141:275–84.
[51] Aznar MP, Caballero MA, Sancho JA, Francés E. Plastic waste elimination by co-gasification with coal and biomass in fluidized bed with air in pilot plant. Fuel Process Technol 2006;87:409–20.
[52] Lahijani P, Zainal ZA. Gasification of palm empty fruit bunch in a bubbling fluidized bed: a performance and agglomeration study. Bioresour Technol 2011;102:2068–76.
[53] Hanping C, Bin L, Haiping Y, Guolai Y, Shihong Z. Experimental investigation of biomass gasification in a fluidized bed reactor. Energy Fuels 2008;22:3493–8.
[54] Basu P. Biomass gasification and pyrolysis: practical design and theory. Academic press; 2010.
[55] Dornburg V, Faaij APC. Efficiency and economy of wood-fired biomass energy systems in relation to scale regarding heat and power generation using combustion and gasification technologies. Biomass Bioenergy 2001;21:91–108.
[56] Ratnasamy C, Wagner JP. Water gas shift catalysis. Catal Rev 2009;51:325–440.

Paper IV

Assessing the gasification potential of five woodchips species by employing a lab-scale fixed-bed downdraft reactor

Shiplu Sarker, Henrik Kofoed Nielsen

Published in **Energy Conversion and Management**, 2015, 103: 801-813

Journal information (ISI web of science):

Publisher: **Elsevier**
Impact factor: **4.38** (2014)
Rank: **14/88** (Energy & Fuels)

Assessing gasification potential of five woodchips species by employing a lab-scale fixed-bed downdraft reactor

Shiplu Sarker*, Henrik Kofoed Nielsen

University of Agder, Faculty of Engineering and Science, Serviceboks 509, 4898 Grimstad, Norway

Abstract

This paper is aimed to assess the performance of air blown fixed-bed downdraft gasification of local lignocellulosic biomasses which in perspective of Southern Norway are both available and sustainable. Long rotation forest crops birch, oak and spruce, coupled with energy crops poplar and willow were used as feedstocks. The gasification conditions undertaken were widely varied in-terms of air (~3.20 to 4.20 Nm^3/h) and fuel flow (~1.70 to 2.10 kg/h) so that the corresponding equivalence ratio (ER) differed (0.19 to 0.80) and ultimately reflected to other operational parameters such as bed temperature (~550 °C to 760 °C maximum), producer gas yield (~1.50 Nm^3/kg to 2.30 Nm^3/kg, wet base), cold gas efficiency (~35% to 51 %), carbon conversion efficiency (~61% to 76%) and so on. An emphasis was also placed on evaluating material balance by accounting the by-products (such as tar, char) of gasification so that the system reliability is identified. Overall, the gasification performance of different woody biomass was found viable over a broad range of operating condition which is appealing in contributing this technology in the context of regional bioenergy and thus towards the renewable energy.

Keywords: Fixed-bed downdraft gasification, Forest crops, Energy crops, Southern Norway, Equivalence ratio, Operating parameters.

*Corresponding author
Email: shiplu.sarker@uia.no
Phone: +4737233144

1. Introduction

The post oil era is approaching and there is an urgent need to achieve energy reliability and sustainability. This therefore results biomass, one of the most abundant and renewable sources, to consider as fuel for today and for the coming days in future. Technology towards biomass conversion is advanced and transformation into range of fuels such as solids, liquids and gases are successfully achieved through various conversion pathways (thermochemical, biochemical and biological) (Zhang et al., 2013). Bio-based feedstocks are furthermore CO_2 neutral (Albertazzi et al., 2005), environmentally beneficial and economically advantageous, allowing to continuously increase (3.7%/yr until 2030 (2015)) their usage worldwide. At present, biomass accounts over 10% of the total global primary energy supply (2014) and more is expected to appear in the near future.

As a part of thermochemical conversion, gasification has been practiced since World War II (Kirkels & Verbong, 2011) and offers substantial advantages in efficiently converting bio-materials into useful products. Contrary to combustion, gasification (Grover & Mishra, 1996) takes place at a reduced oxidant environment and thus allows to greatly reduce the emission precursors from the emanating gases. Technologies propelling gasification are numerous and can broadly be classified as fluidized bed, fixed-bed, entrained-bed and plasma gasifiers (Heidenreich & Foscolo, 2015). As far as operational performance, total product yield and type of feedstocks are concerned, these technologies are inherently different. Mainly, fluidized-bed gasifiers suit for small size feedstocks and operate with high temperature while fixed bed gasifiers operate with lower temperature and suit for coarse size feedstock as feeding materials (McKendry, 2002). Although high quality gas can be produced from any of the prevailing configurations, fixed-bed downdraft reactors offer additional advantages of yielding less tar and lenient requirements for producer gas cleaning and thus economically and technically more sound and attractive (Warnecke, 2000). Considering these, present paper focuses on fixed-bed downdraft gasification that

processed five different woody biomasses (birch, oak, spruce, poplar and willow) collected from the local areas of Southern Norway.

Likewise most other Scandinavian countries, woody biomass are abundant in Norway. Thanks to its large productive forest resource which covers approximately 24% of the total land area (Bright et al., 2010) from where a vast supply of woody-materials is guaranteed primarily through harvest and standing stocks. Among the woody species available in the Southern Norwegian forests: birch, pine, spruce and oak are dominating and have been attractive for multiple uses including space heating. Space heating by utilizing biomass resources is one of the priorities in Norwegian future target for bioenergy expansion (Trømborg et al., 2011). However, the progress in bio-based space heating is hindered owing to the low electricity price and thus the widespread utilization of electrical heaters; over 75% households in Norway are for example currently relying on electricity for meeting their space heating demand, and the use of fossil oil in the heating burners (Trømborg et al., 2011). . Hence, to meet the future target of bioenergy increase, a sustainable approach is necessary where gasification can be a promising alternative which not only offers to direct utilization of producer gas for heat production but also provides opportunity to use liquid bio-oil as a readily available fuel to the existing infrastructures, for example, to the oil-burners that are used as space heating options. Besides, gasification can also be directed towards various other applications, for instance, to produce steam for the process industries or, to provide raw gas to FT (Fischer-Tropsch) conversion unit for upgrading gas into easily handled liquids and chemicals (Bridgwater, 2003). The gasification potential thus is huge and versatile and to gain full advantage of which integration of different feedstocks with many different suitable characteristics are necessary.

Present paper is an effort towards that direction investigating the feasibility of several woody (e.g. woodchips) biomass including forest trees and energy crops (poplar and willow) as feedstocks for fixed-bed downdraft gasification which under the local scenario can emerge as a viable alternative for combustion and for other potential applications. Further, to examine the sensitivity of the proposed gasification, the operating conditions especially the equivalence ratio (ER) is widely varied (0.19 - 0.80) so that the operational margin and the

threshold is determined which in turn may provide a good basis under which operational conditions for the real-life applications within the local perspective can be chosen.

Thus far studies devoted to examine the effect of several operational parameters on fixed-bed gasification performance (qualitative and quantitative analysis of producer gas) of various woodchips include but not limited to are (Balu & Chung, 2012; Lenis et al., 2013; Sheth & Babu, 2009; Zainal et al., 2002). However, a single study evaluating the fixed-bed gasification potential of both forest biomass and energy crops is scarce. Additionally, such investigation within the context of local area of Southern Norway is none and therefore the purpose of this work is unique as far as local bioenergy research is concerned.

2. Materials and methods

2.1. *Woodchips feedstock*

Five local tree species namely: birch (*Betula pendula*), oak (*Quercus petraea*), spruce (*Picea abies*), poplar ('Spirit' *Populous trichocarpa*) and willow short rotation coppice, SRC (*Salix* Sp.) was considered as feedstocks for this study. Birch, oak and spruce was harvested from the local forest at Dømmesmoen, Grimstad (coordinate: 58° 21' 8.6" N, 8° 34' 32.78" E) whereas willow and poplar SRC were cultivated and harvested from a dedicated agricultural land (area: ca. 0.30 ha), located around the same place as that of forest biomass. The harvesting of the feedstocks ranged at various periods between the year 2012 and 2015 (refer to Table 1). To produce woodchips (size ~1-10 mm thick.) from the forest crops, trees were cut by a chain saw and then chipped by a disc chipper (NHS 720 IE 4, Denmark). The chips were afterwards dried either by indoor air drying or by an in-situ batch dryer, using hot air as a drying medium. For the energy crops on the other hand, two steps drying was undertaken. First, after harvesting, trees were left outdoor for sun drying and then wood chips were

made by employing a bush saw. Afterwards, the woodchips were dried by following the same procedure as that of the forest crops. After drying, equilibrium moisture in the woodchips upon storage is strongly affected by the relative humidity than to the air temperature. Hence, the moisture content in the woodchips was re-assessed before utilizing to any gasification tests, so that precise estimation can be made. Table 1 lists the average moisture content of the woodchips using for gasification and the different properties associated with the biomass harvest, drying and pre-treatment. The images of the different wood chips are shown in Figure 1.

Figure 1: Photographs of the woodchips used in this study

2.2. *Physiochemical analysis*

Physiochemical properties in-terms of moisture, volatiles, ash, lower heating value (LHV) and of chemical elements were carried out by the external lab Eurofins Environmental Testing Sweden AB, Gothenburg, Sweden. Each individual properties reported in the proximate analysis was evaluated based on the standards given in Table 2.

Ultimate analysis determined the percent composition of carbon (C), hydrogen (H), nitrogen (N) sulfur (S), chlorine (Cl) and Oxygen (O) complying with the protocols stated in Table 2.

Table 1: Tree harvesting period and pre-treatment

Tree species	Tree type	Age [yrs]	Bulk density, kg/m^3 (n=3)	Harvest period	Drying method	Moisture, % (after drying)*
Birch (*Betula pendula*)	Forest crop (hardwood)	N.D.	252 ± 3.5	Summer, 2013	Open air (wood chips)	9.15
Oak (*Quercus petraea*)	Forest crop (hardwood)	N.D.	208 ± 3.2	Summer, 2014	Batch dryer (wood chips)	8.47
Spruce (*Picea abies*)	Forest crop (hardwood)	~ 47	133 ± 4.4	Winter, 2015	Batch dryer (wood chips)	9.05
Poplar (*Populous tremula*)	Energy crop (softwood)	3	138 ± 4.2	Spring, 2012	Open air (stem), in-door (wood chips)	11.38
Willow (*Salix* Sp.)	Energy crop (softwood)	2 or, 3	145 ± 2.6	Spring, 2012	Open air (stem), in-door (wood chips)	8.60

N.D.: Not determined; *: Analysis standard EN 14774-1:2009

2.3. *Experimental facility*

Fixed-bed downdraft gasification system

A schematic of fixed-bed downdraft gasifier including gasification system is presented by Figure 2. The gasification system comprised of a fixed-bed downdraft gasifier (Victory Gasworks, Vancouver, Washington, USA), a hopper, producer gas cooling and cleaning units (cooling water line, settling chamber and dry filter), a reciprocating grate, a weighing scale, a shaker, gas flaring line, a blower, producer gas sampling unit (hot filter, pump, cooler and gas analyzers) and a gas engine (Kubota, USA, 14.5 kW max.). Hopper is a conical shape (0.13 m^3) stainless steel (0.5 m Ø; AISI 304 & 316) double-walled structure, through which biomass was fed. An electrical shaker is attached at the side wall of the hopper, giving periodic vibrations (15 sec/min) so as to reduce bridging and channeling (Gai & Dong, 2012). A condensate drain valve is also found at the bottom of the hopper between the two walls to manually drain any collected moisture; drain valve is normally closed and made open after each gasification test.

The reactor itself is made of AISI 304 & AISI 316 stainless steel cylinder with an internal diameter of 0.26 m and a height of 0.60 m assembled below the hopper by a coupling consisting of a gasket and a series of nuts and bolts (bolt size: 5 × 13 mm). At the mid-height (0.30 m height) of the reactor a constriction is found which is made of an exchangeable restriction ring of 100 mm Ø (5 mm). Air supply system is consisted of six equidistant nozzles of ~5 mm Ø, located at 0.2 m height (from top) of the reactor and a speed control induced draft fan placed at the end of the gas exit. With suction from the fan, air is introduced to the reactor through an air-diaphragm meter (0.04 – 6 m^3/h; BK-G4, Elster, Germany), registering the flow into the gasifier.

Below the reactor there is a circular perforated grate, oscillating reciprocally (30 sec/min) to ensure flow of the material from the top and dispose of ash to the bottom. A weighing scale (DINI ARGEO, Italy, 1500 kg max.) placed

underneath the gasifier assembly monitors fuel mass loss during gasification. Throughout the reactor there are provisions for several measuring ports allowing the access of different sensors. Using these ports, five K-type thermocouples and two differential pressure sensors (Smart DCM/SN Diff, Fema, Germany) were installed (Figure 2).

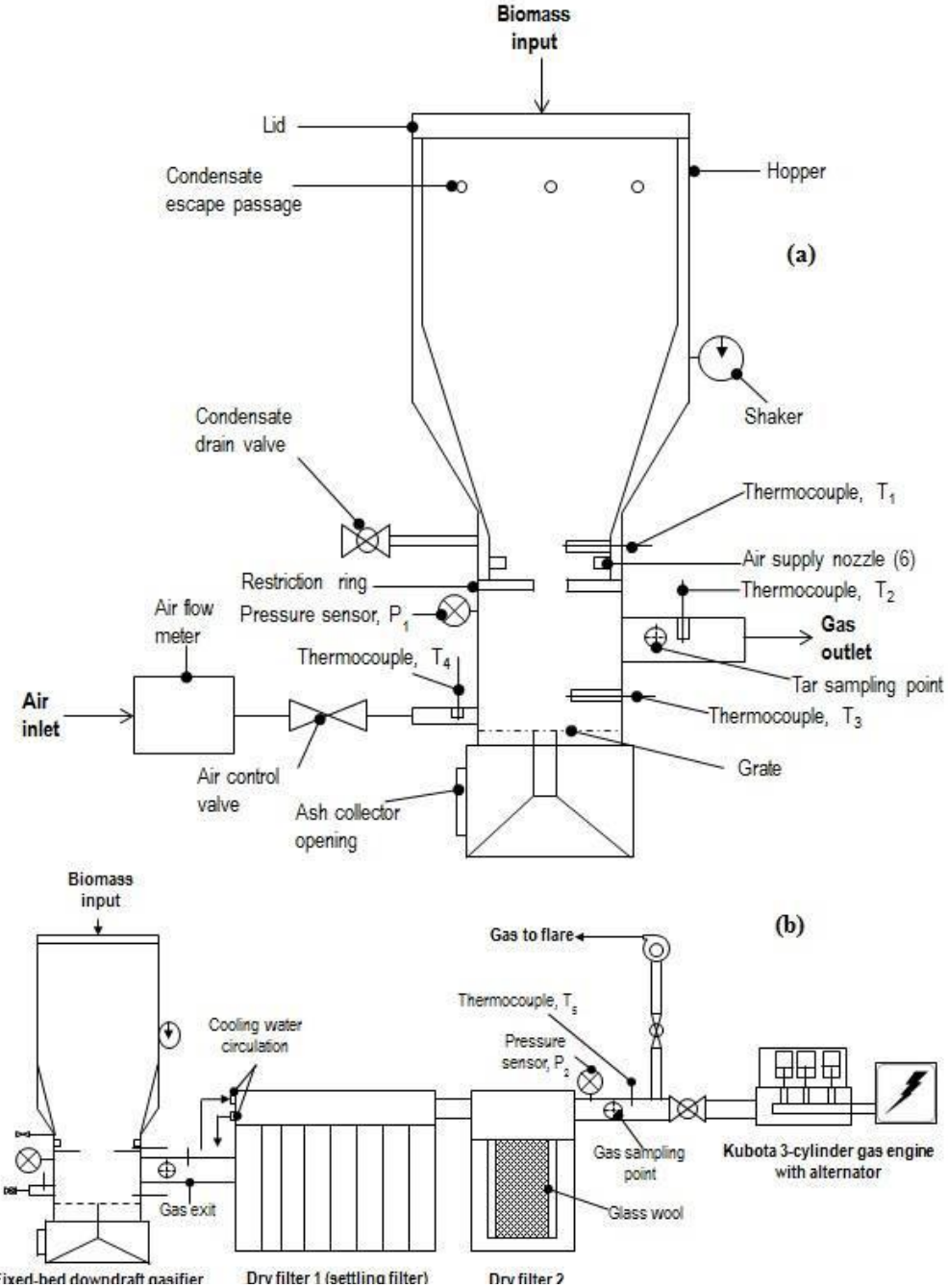

Figure 2: Experimental facility using fixed-bed downdraft gasification system (Top: fixed bed downdraft gasifier; bottom: gasification system)

Three thermocouples are equidistantly (150 mm apart) located around the bed and one each is placed at the air input and at the sampling line respectively (Figure 2). It is worthwhile to note that the temperatures measured by the sensors located close to the bed might experience discrepancies from the real temperature due to the position of the sensor tips which were kept slightly away from the bed to avoid bending and wear and tear. During gasification, as the woodchips thermally degraded, the producer gas exited from the reactor and cooled, cleaned and conditioned via a gas-water heat exchanger, and two series of filters: settling chamber (dry filter with hanging ribbons) and dry filter (comprised of standard glass wool for insulation). The relatively cleaned and conditioned gas subsequently was either diverted to the engine or to the flare depending on the gas quality and needs. Focusing on the objective of the present study (which is qualitative and quantitative analysis of producer gas), engine tests was not considered and produced gas was only flared and continuously analyzed real time by analyzers located at the downstream of the gas sampling train (described in section 2.2.3). The analyzers, air diaphragm meter, pressure and temperature sensors, scale, all are connected to a data acquisition module (LabView, National Instruments, USA), transferring real time continuous data to a stand-alone PC for further analysis and record.

Test procedure

In gasification start up, reactor was initially filled with barbeque charcoal until above the height of air supply nozzles. This corresponded to about 2 kg of charcoal with minor variation of ± 0.1 kg. After charcoal input, woodchips were fed from the top of the hopper between the amount 7 - 12 kg, depending on the density and type of the fuel. Once fed, hopper was closed by a lid and inspected for air leakages. Gasifier was then ignited and simultaneously air supply valve and sampling line was opened and data logger was also started. Generally, the heat required to develop gasification condition is established by the combustion of charcoal (exothermic reaction). Hence, the ignition started up with charcoal, which gradually transferred to woodchips, as the process stabilized (in respect to temperature and fuel flow) in about half an hour. The stationary condition

continued for another 5-6 h until the complete conversion of the given biomass was achieved. Throughout each experiment, air supply was manually varied by adjusting the range 3-8 m^3/h to attain optimization in terms of equivalence ratio (ER) and temperature. In some cases, air supply was also regulated by the process itself attributed due to the transition of conversion from charcoal to fresh biomass, bridging, variation in the quantity of flow of solid mass (fuel, charcoal, ash), etc. The woodchips in the gasifier was flown downward by gravity which was mainly influenced by the rate of conversions and the quantity of input air. Typically, process optimization was achieved for biomass flow rate of ~1.7- 2.4 kg/h and the resulting ER was determined from the following expression (Eq. 1):

$$ER = \frac{Actual\ air\ fuel\ ratio}{Stoichometric\ air\ fuel\ ratio} \quad (1)$$

where the actual air fuel ratio was calculated from the ratio of air and fuel supply rate used during gasification tests and the stoichiometric air fuel ratio was determined based on the chemical formula (m/m) (Eq. 2), as follows:

$$C_aH_bO_c + \text{x}\ (O_2 + 3.25\ N_2) = yH_2O + zCO_2 \quad (2)$$

where a, b and c are the values calculated by using the ultimate analysis results and the corresponding molecular weight of the elements C, H and O. It is to be noted that the ER calculation did not account unconverted residual carbon resulted after gasification test run.

The other parameters relevant to gasification such as producer gas yield, lower heating value (LHV), cold gas efficiency (CGE) and carbon conversion efficiency (CCE) were evaluated based on the relevant equations given elsewhere in the study (Sarker et al., 2015b).

After any given test, the gasifier was emptied from residual char and condensate that were deposited along the main and sampling line and quantified to account mass balance. Residual char was additionally analyzed for determining fractional ash through muffling (Muffling furnace, Nabertherm P330, Germany) at 550 °C

according to the standard CEN/TS 15403:2006. Afterwards, char fraction contributing to the solid residue was determined by-difference.

Producer gas analysis

To perform quantitative and qualitative analysis, the part of the producer gas was sampled in a gas sampling line consisting of hot filter, cotton filter, dew-point analyzer, cooler, pump and gas analyzers. The gas was first cleaned from particles by using a ceramic hot filter (FE2, ABB, Germany) electrically heated to a temperature of about 150 ˚C. Gas was further cleaned from aerosols and suspended particles by a cotton filter before passing through a dew-point analyzer (Omega, RHB-1500, USA) measuring the dew point of the produced gas, further used to determine the gas moisture content (Petersson, 2004). Gas was then circulated through a cooler (SCC-C Sample gas cooler, ABB, Germany) which reduces the sample gas temperature to ~3 ˚C. The flow throughout the entire sampling unit was provided by a membrane pump (4N, ABB, France), operated between the range of 0 and 50 L/h. The cleaned and conditioned gas after the filters and the cooler was finally directed to gas analyzers (Advance optima, AO2020; ABB, Germany), quantifying the gas in-terms of CO, CO_2 , H_2, O_2 and CH_4. Gas analyzer URAS 26 (non-dispersive infrared sensor) evaluates CO, CO_2 and CH_4; CALDOS 27 (thermal conductivity detector) determines H_2; and MAGNOS 206 (paramagnetic analyzer) measures the composition in terms of O_2 respectively. To provide real-time data, gas was continuously sampled throughout the period of gasification and the analyzers' values were transferred to a LabView acquisition module.

2.4. *Tar sampling*

After each gasification test, condensates deposited at various gas cooling locations (bottom of the gas cooler and between the hopper walls) were measured for determining weight and collectively called as gravimetric tar. Tar composition on the other hand was determined as according to the Solid Phase Adsorption (SPA) method developed by KTH (The Royal Institute of Technology, Sweden). To this end, first of all, sampling of the gas was conducted during the stable period of gasification through a sampling point

located in the vicinity of the hot gas exit. Sampling apparatus was consisted of two series of syringes and a needle. First syringe (SUPELCO, USA) was packed with 3-mL solid phase extraction (SPE) adsorption cartridge with 500 mg of aminopropyl-bonded silica adsorbent and connected with a needle (11.5 mm length, 1.09 mm Ø) the tip of which passed through a septum located at the entry of the sampling point. The second syringe (100 mL, BD Plastipak, USA) was fitted at the back of the first syringe, drawing the air through the assembly. During sampling, approximately 100 mL of air was manually drawn by the second syringe, allowing tar vapors to trap and adsorb on the bed of aminopropyl silica adsorbent. The tar laden cartridge syringe was then sealed from the both ends by stoppers, wrapped by aluminium foil papers and stored in a refrigerator (< 4 °C) before carrying out for compositional analysis. During the compositional analysis, first the sampled cartridges were desorbed into aromatic and phenol fractions and then undergone for gas chromatographic (GC) measurement according to the protocol as described elsewhere by (Brage et al., 1997). External lab Verdant chemical technologies affiliated to KTH, Sweden performed this analysis and kindly provided the results afterwards which have been reported in this paper.

3. Results and discussions

3.1. *Biomass characterization*

Dry base proximate and ultimate analysis of the feedstocks in-terms of volatiles, ash and the chemical elements are depicted in Table 2.

As expected, the level of volatiles irrespective of the type of woody biomass by and large was similar, except for willow (80.7 %) which was slightly different. Volatiles within the margin of 80 % are typical for most of the woody biomass, as documented in the comprehensive database (Phyllis2). Unlike volatiles, ash

Table 2: Physical and chemical properties of the different biomass

	Birch	Oak	Spruce	Poplar	Willow	Test standard
Proximate analysis (dry basis)						
Volatile matter, %	82.2	82.9	82.6	83.9	80.7	EN 15148 : 2009
Ash, %	0.5	1.4	0.7	0.9	1.3	EN 14775 : 2009
Ultimate analysis (dry basis)						
Carbon, %	50.4	48.9	50.7	49.4	49.9	EN 15104 : 2011
Hydrogen, %	5.6	6.0	6.0	6.0	5.9	EN 15104 : 2011
Oxygen, %	43.4	43.5	42.4	43.5	42.4	EN 14918 : 2010
Nitrogen, %	0.12	0.20	0.14	0.22	0.53	EN 15104 : 2011
Sulphur, %	0.017	0.018	0.011	0.019	0.038	SS 187177: 1991
Chlorine, %	0.019	<0.011	<0.011	<0.011	<0.011	EN 15289/15408
Lower heating value, MJ/kg	20.005	18.896	20.271	19.673	19.803	SS EN 14918
Structural analysis (dry basis)*	[a]	[b]	[c]	[d]	[e]	
Cellulose, %	40.6	38.1	44.5	46.2	38.5	[N/A]
Hemicellulose, %	29.6	26.1	20.6	24.4	17.6	[N/A]
Lignin, %	26.3	25.9	27.8	24.5	26.3	[N/A]

[*]: Ref (Gai & Dong, 2012); [a]: avg. 7 samples; [b]: avg. 3 samples; [c]: avg. 4 samples; [d]: avg. 5 samples; [e]: avg. 1 sample; [N/A]: not applicable

amount among the woody fuels was dissimilar and ranged between 0.5 % and 1.4 % with the highest from oak and willow, and the lowest from birch respectively (Table 2). Besides oak, energy crops (poplar and willow) in general presents higher ash than those of the forest crops due to relatively more bark content compared to the older trees. For oak this perhaps can be attributed due to several factors such as fertilization, soil quality, environmental conditions, high bark in wood and so on (Serapiglia et al., 2013). The LHV on the other hand seemed to present an inverse relationship with ash being highest and lowest for spruce and oak respectively (Table 2). In general, the LHV for all the biomass ranged between ~19 MJ/kg and ~20 MJ/kg (Table 2).

Observing elemental analysis results, no clear difference among carbon, hydrogen and oxygen composition was noticed the average of which more or less kept at ~50 %, ~ 6 % and ~ 43 % respectively, with a slightly lower amount of C for oak. Unlike, the percent amount in-terms of N and S varied and the highest values for both the elements were observed from willow. The N and S content in the fuel is normally influenced by the fertilization and by the increased fraction of bark in the wood (Adler et al., 2005; Klasnja et al., 2002). However, as the energy crops poplar and willow underwent similar fertilization, the difference in N and S might have occurred due to the higher amount of bark. Among the energy crops willow in general has higher bark to wood ratio than that of the forest biomass (Adler et al., 2005).

In regards to the structural composition as obtained from the Phyllis database, no clear trend of cellulose, hemicellulose and lignin were observed between the two classes of biomass (forest crops and energy crops). Noticeably, cellulose was the highest components found across the feedstocks in contrast to that of lignin for the higher density biomass birch and oak. Nevertheless, for the lower density woodchips (spruce, poplar and willow) the content of hemicellulose was found lower than that of lignin (Table 2).

3.2. *Gasification of woodchips*

Fixed-bed downdraft gasification on five different woody biomasses (three long rotation and two short rotation crops) was carried out to examine the evolution of operational parameters in regards to product gas composition, LHV, cold gas efficiency, carbon conversion efficiency and temperature the effect of which as a result of varied ER, temperature and time are presented in Figure 3 through 8. Further, the results are discussed in the following sub-sections.

Effect of ER on gas composition

The producer gas resulted from the gasification of woodchips was mainly composed of CO, CO_2, O_2, N_2, H_2, H_2O and CH_4. The distribution of these gas species varied according to the type of the fuel and to the operating conditions such as ER the effect of which is illustrated by Figure 3. Moreover, linear regression results as an effect of ER on various gasification characteristics are included in Table 3.

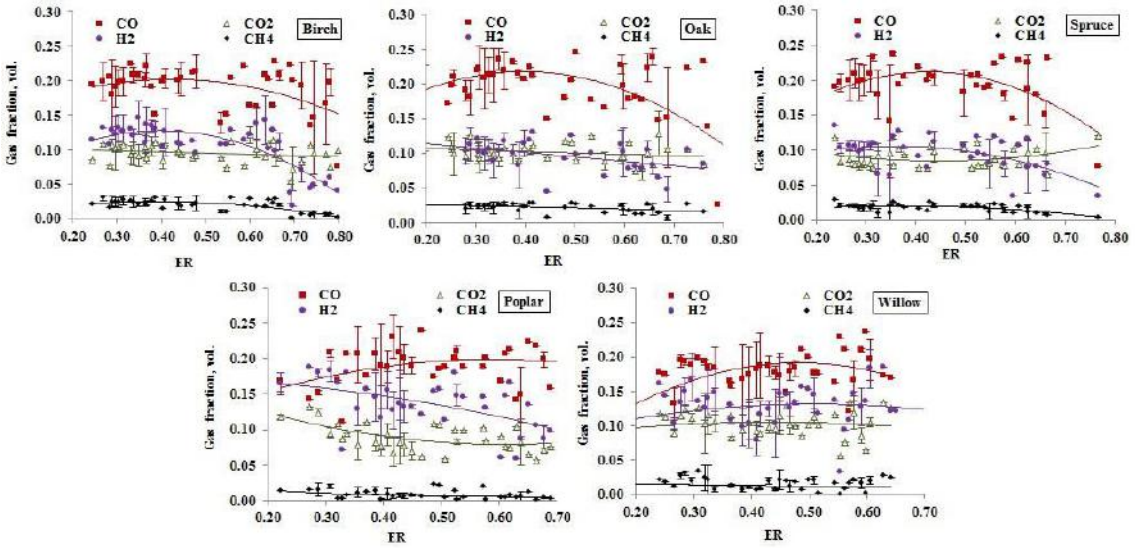

Figure 3: Variation in gas compositions as an effect of ER

As for combustible gas species, increasing ER contributed to increase CO up to a certain level of ER and then decreased for birch, oak, spruce and willow (Figure 3). This trend of CO coincides with the similar study by (Zainal et al., 2002) and was presumably attributed due to the combined effect of Boudouard (Eq. 3) and combustion reactions (Eqs. 4 & 5). At higher ER theoretically the strength of combustion reactions (Eqs. 4 & 5) increase which results the increased conversion of CO into CO_2 while at lower ER the extent of Boudouard (Eq. 3) reaction increase as a result contributing the enhanced production of CO at an expense of CO_2 (Sarker et al., 2015a).

Boudouard reaction: $C + CO_2 \leftrightarrow 2CO;\ \Delta H = +172\,kJ/mol$ (3)

Combustion reaction: $C + O_2 \leftrightarrow CO_2;\ \Delta H = -408.8\,kJ/mol$ (4)

Carbon partial reaction: $2C + O_2 \leftrightarrow 2CO;\ \Delta H = -246.4\,kJ/mol$ (5)

Dry reforming : $CH_4 + CO_2 \leftrightarrow 2CO + 2H_2;\ \Delta H = -793\,kJ/mol$ (6)

Hydrogasification: $C + 2H_2 \leftrightarrow CH_4;\ \Delta H = +75\,kJ/mol$ (7)

Methanation: $CO + 3H_2 \leftrightarrow CH_4 + H_2O;\ \Delta H = -227\,kJ/mol$ (8)

Steam reforming: $CH_4 + H_2O \leftrightarrow CO + 3H_2;\ \Delta H = +206\,kJ/mol$ (9)

Water-gas reaction: $C + H_2O \leftrightarrow CO + H_2;\ \Delta H = +131\,kJ/mol$ (10)

Water-gas shift : $CO + H_2O \leftrightarrow CO_2 + H_2;\ \Delta H = +41.98\,kJ/mol$ (11)

The CO trend for poplar unlike other biomasses was increasing as the ER rose. This trend however was statistically insignificant (p = 0.05) (Table 3).

In regards to CH_4, the trend of birch and spruce was increasing and decreasing in contrast to that of oak, poplar and willow which were decreasing. The pattern of H_2 followed the similar trend of CH_4 for birch, oak, spruce and poplar, except for willow for which the tendency was increasing and decreasing; this trend however was statistically insignificant (p = 0.31) (Table 3). In general, energy crops willow and poplar yielded less CH_4 and higher H_2 than that of the forest biomass (Figure 5). This perhaps can be due to the higher level of inherent moisture (Table 4) strengthening the reforming reactions to enhance the production of H_2 at an expense of CH_4 (Ni et al., 2006).

Table 3: Regression analysis of gasification performance (all runs)

	Birch		Oak		Spruce		Poplar		Willow	
	R^2	**p**	**R^2**	**p**	**R^2**	**p**	**R^2**	**p**	**R^2**	**p**
CO fraction, vol.	0.21	0.02	0.41	< 0.01	0.30	0.04	0.11	0.05	0.30	0.02
CO_2 fraction, vol.	0.09	0.07	0.04	0.01	0.10	0.18	0.31	< 0.01	0.08	0.05
H_2 fraction, vol.	0.63	< 0.01	0.19	0.01	0.38	< 0.01	0.14	< 0.01	0.14	0.31
CH_4 fraction, vol.	0.50	< 0.01	0.20	0.01	0.29	< 0.01	0.28	< 0.01	0.06	0.03
Gas LHV, MJ/Nm^3	0.63	< 0.01	0.27	< 0.01	0.36	< 0.01	0.20	0.04	0.17	0.19
Vg, Nm^3/kg	0.13	0.03	0.12	0.02	0.07	0.02	0.03	0.07	0.09	0.09
CGE fraction	0.43	< 0.01	0.24	0.03	0.14	0.04	0.15	0.03	0.06	0.05
CCE fraction	0.31	< 0.01	0.13	0.06	0.09	0.06	0.13	0.05	0.15	0.04

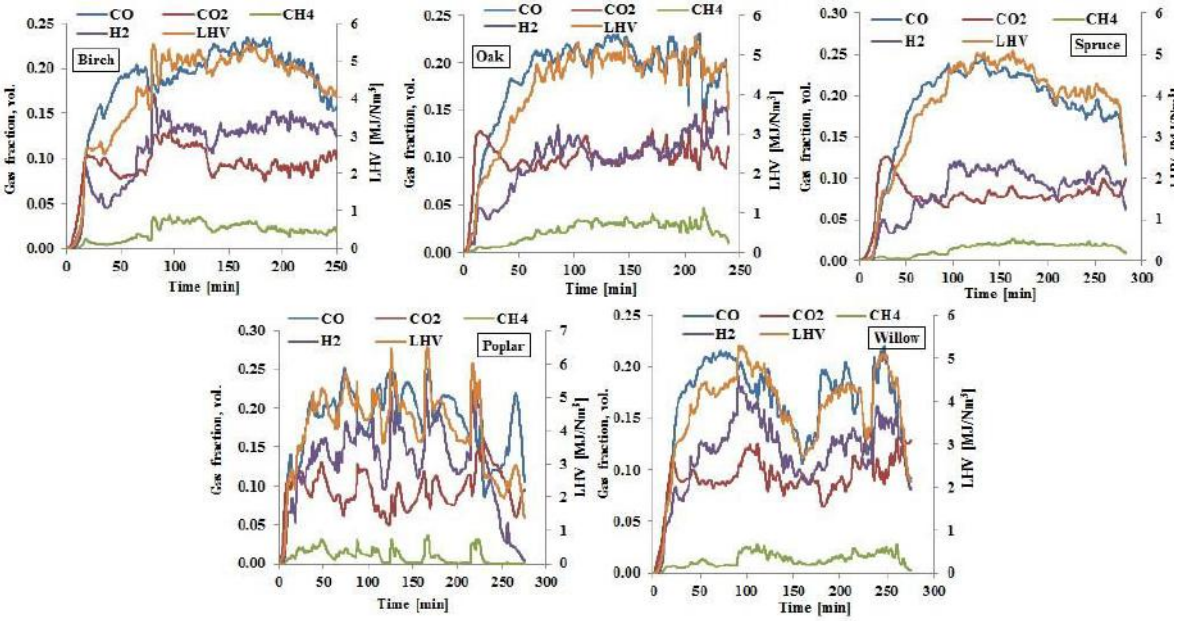

Figure 4: Real-time evolution of producer gas composition from a representative test run on each feedstock

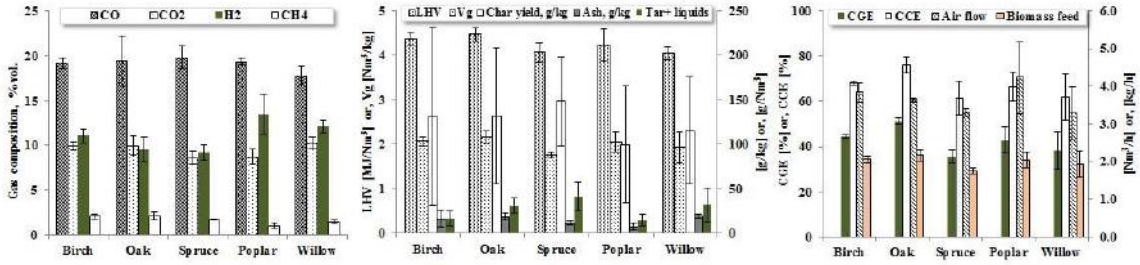

Figure 5: Average performance of gasification for all runs (three tests per woodchips species)

As of incombustible species in the producer gas CO_2, O_2 and H_2O was measured and only the evolution of CO_2 is discussed. Expectedly, the CO_2 trend for most of the biomass was found inverse to that of CO except for birch and poplar which was decreasing. The trend of birch however was not statistically significant ($p > 0.05$) (Table 3) while the trend of poplar showed a large statistical deviation at higher value of ER, believed to be caused due to the bridging evidenced in Figure

4. Bridging has been one of the challenges in the present gasification tests, encountered for number of instances. Zainal et al.(Zainal et al., 2002) termed bridging as a normal phenomenon in fixed bed downdraft gasification likely to be prompted due to the variation in wood chips size,air flow and temperature, etc.. In another study (Purdon, 2010), wood chips size less than ~19 mm was considered vulnerable to cause process difficulties in-terms of bridging and such. As the present work used wood chips of 1-10 mm size, bridging formation was expected and eventually experienced which however did not reportedly cause a complete process failure.

Noticeably, the H_2 yield from all the tests conducted on spruce was by far the lowest (Figure 5) which perhaps indicates that the water-gas reaction (Eq. 10) compromised to other endothermic reactions aiding to sustain gasification. A similar phenomenon for low density softwoods alike spruce was also observed by the past study (Purdon, 2010).

Effect of ER on performance of gasification

As ER varied (0.19 – 0.80), several gasification parameters such as gas LHV, specific gas yield (Vg, Nm^3/kg, wet base), CGE and CCE also varied, the evolution of which corresponding to each woody feedstock was illustrated by the Figure 6 while the summary results obtained from each gasification test are given in Table 4.

In regards to birch, increase in ER between the range 0.15 and 0.41 contributed to increase the average gas LHV which however decreased as the ER rose further to the end (0.80). As observed from the Figure 3, lower ER contributed to increase the trend of the combustible gas species (CO, CH_4 and H_2) and therefore the obvious increase in LHV which however logically decreased in case of higher ER, as the contributing gas species fell. Noticeably, peak LHV for this feedstock reached to ~5.2 MJ/Nm^3 (wet base) corresponding to the ER at 0.33. The peak and the average LHV (~4.37 MJ/Nm^3, wet base) saw a dramatic improvement in this work since the last work by the same authors (Sarker & Nielsen, 2015) due mainly to the improvement in operational parameters in

regards to the ER, air flow and temperature (Table 4). As for Vg (wet base), the similar pattern of LHV was observed which increased and decreased as the ER gradually increased. The Vg averaged at ~2.06 Nm^3/kg (wet base) (Table 4 & Figure 5) with maximum at ~2.65 Nm^3/kg (wet base) corresponding to the ER = 0.38. Increased gas yield during the lower ER was perhaps due to the enhanced volatilization (Gómez-Barea et al., 2005) during the state of gasification while the decreased gas yield during the higher ER was due to the dilution caused by the proportional increase in N_2 as an effect of proportional rise in air supply. Since the similar increasing and decreasing trend was obtained both from LHV and gas yield, the simultaneous effect of these has been reflected to the evolution of CGE and CCE, averaging to ~45% and ~68% that further maximized at ~63% and ~90% corresponding to the ER at 0.37 and 0.38 respectively (Table 4).

Likewise birch, the trend of LHV for oak was also increasing and decreasing and peaked to ~5.1 MJ/Nm^3 corresponding to the ER = 0.41 (T = ~546 °C) (Fig.6).

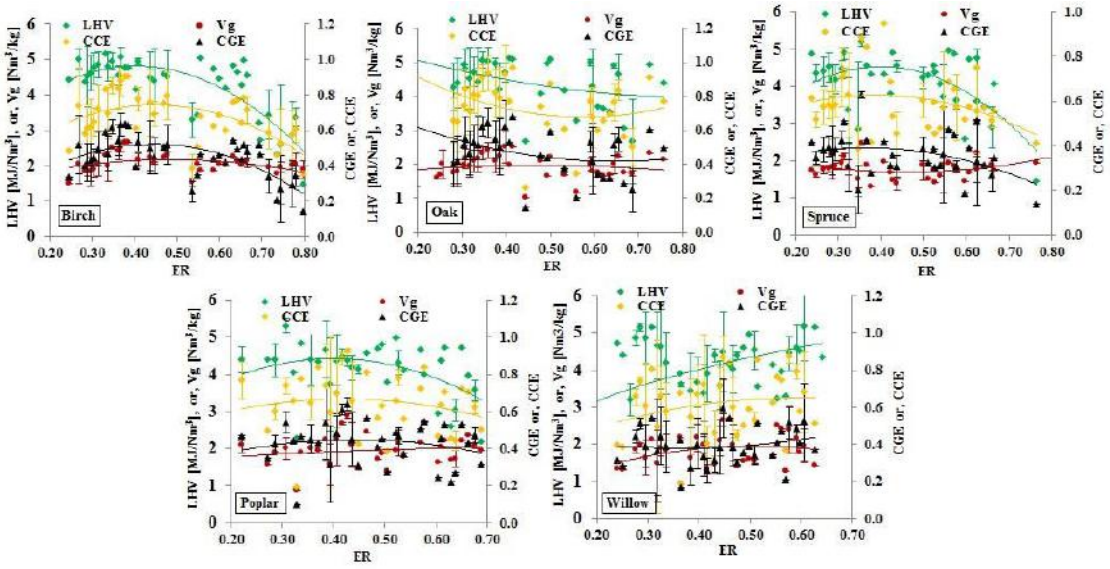

Figure 6: Average performance of gasification for all runs in relation to ER

Table 4: Operational conditions and summary results from the gasifier test runs

Biomass type	**Birch**			**Oak**			**Spruce**			**Poplar**			**Willow**		
Run ID	R1	R2	R3	R4	R5	R6	R7	R8	R9	R10	R11	R12	R13	R14	R15
Test date	19.12.2014	20.02.2015	25.02.2015	03.12.2014	09.12.2014	30.01.2015	10.01.2015	13.01.2015	04.03.2015	05.02.2015	06.02.2015	10.02.2015	20.11.2014	24.11.2014	16.02.2015
Avg. Air flow rate, Nm^3/h	3.53 ± 0.40	3.95 ± 0.72	4.00 ± 1.22	3.59 ± 0.67	3.64 ± 0.43	3.70 ± 0.48	3.18 ± 0.57	3.31 ± 0.25	3.22 ± 0.52	4.06 ± 0.77	3.37 ± 0.61	5.26 ± 0.95	2.91 ± 0.7 7	2.82 ± 0.82	4.09 ± 0.82
Air density, kg/m^3	1.22	1.21	1.21	1.22	1.22	1.21	1.22	1.22	1.22	1.23	1.23	1.20	1.22	1.21	1.21
Avg. Room temp., °C	16.4 ± 0.7	18.4 ± 0.7	18.0 ± 0.6	16.1 ± 0.7	16.0 ± 0.9	17.8 ± 1.1	16.1 ± 1.1	17.1 ± 1.1	17.0 ± 0.6	15.0 ± 0.3	19.2 ± 0.6	20.6 ± 0.7	17.3 ± 1.4	19.1 ± 0.8	17.4 ± 0.8
Biomass feed rate, kg/h	2.52 ± 0.51	2.80 ± 0.91	2.50 ± 0.49	2.38 ± 0.53	2.61 ± 0.65	2.36 ± 0.60	2.47 ± 0.45	2.43 ± 0.18	2.49 ± 0.25	2.50 ± 0.55	2.26 ± 0.34	4.49 ± 0.63	2.69 ± 0.7 4	2.70 ± 0.97	2.51 ± 0.41
Biomass moisture content, %	6.6	8.6	8.3	7.4	6.7	6.7	6.3	6.6	11.0	9.8	10.0	10.5	6.9	7.7	9.8
Total biomass+charcoal feed, kg	6.39	10.615	12.29	9.837	9.602	13.1	9.251	8.643	7.217	11.923	7.366	12.902	9.272	6.5	10.9
Total biomass + charcoal converted, kg	4.67	9.37	11.59	8.76	8.65	9.90	8.21	7.33	5.66	11.11	5.99	12.05	8.54	5.70	8.70
Tar + condensate output (hopper),g	130	N.D.	120	115.8	162	N.D.	122	160	11	126.29	85	22	115	146	0
Tar + liquid output (cooler), g	120	250	130	302	535	710	416	636	262	174	171	200	417	275	265
Total operational time, min.	255	366	336	282	250	347	250	283	241	403	297	275	325	275	346
Avg. Room temp., °C	16.4	18.4	18.0	16.1	16.0	18.0	16.1	17.1	17.0	15.0	19.2	20.6	17.3	19.1	17.4
CO composition (producer gas), wt.%	19.7 ± 1.7	19.4 ± 3.8	18.5 ± 3.7	21.7 ± 5.1	20.3 ± 3.4	16.4 ± 4.7	18.3 ± 4.3	20.6 ± 2.4	20.5 ± 2.4	19.0 ± 3.3	19.5 ± 3.8	19.7 ± 2.6	19.0 ± 2.7	16.9 ± 3.8	17.3 ± 3.0
CO_2 composition (producer gas), wt.%	10.0 ± 2.1	10.3 ± 1.1	9.5 ± 1.6	9.1 ± 1.8	11.1 ± 1.3	9.73 ± 2.2	9.4 ± 1.5	7.9 ± 0.6	8.6 ± 1.1	8.8 ± 2.4	7.90 ± 1.8	9.6 ± 2.4	10.2 ± 2.2	9.6 ± 1.6	11.0 ± 2.3
H_2 composition (producer gas), wt.%	11.9 ± 2.3	10.3 ± 3.3	11.0 ± 4.3	9.0 ± 2.3	11.1 ± 2.3	8.5 ± 4.5	9.2 ± 3.2	10.0 ± 1.5	8.4 ± 3.0	14.2 ± 3.0	10.9 ± 3.0	15.3 ± 2.8	12.9 ± 4.2	12.1 ± 3.5	11.4 ± 3.6
CH_4 composition (producer gas), wt.%	2.1 ± 0.8	2.3 ± 1.0	1.8 ± 1.1	2.2 ± 0.8	2.5 ± 0.6	1.6 ± 1.2	1.7 ± 0.8	1.8 ± 0.5	1.6 ± 0.4	0.8 ± 0.5	0.9 ± 0.7	1.3 ± 0.9	1.2 ± 1.0	1.5 ± 0.6	1.6 ± 1.2
LHV, MJ/Nm^3 (wet basis)	4.5 ± 0.4	4.4 ± 1.1	4.2 ± 1.1	4.5 ± 1.1	4.6 ± 0.9	4.3 ± 1.0	3.9 ± 1.1	4.3 ± 0.5	4.0 ± 0.7	4.2 ± 0.5	3.9 ± 0.8	4.6 ± 0.5	4.2 ± 0.7	3.95 ± 1.0	3.97 ± 0.9
Avg gas yield, Nm^3/kg (wet basis)	2.00 ± 0.29	2.02 ± 0.42	2.17 ± 0.54	2.13 ± 0.32	2.05 ± 0.38	2.32 ± 0.86	1.89 ± 0.30	1.81 ± 0.23	1.67 ± 0.26	2.30 ± 0.45	1.91 ± 0.38	1.93 ± 0.25	2.03 ± 0.4 6	1.45 ± 0.40	2.22 ± 0.38
CGE, % (wet basis)	45.1 ± 7.8	44.1 ± 14.8	44.3 ± 14.1	52.5 ± 13.4	50.9 ± 15.1	50.0 ± 14.1	34.9 ± 12.6	38.6 ± 7.8	32.8 ± 8.2	49.3 ± 12.2	39.0 ± 12.6	40.3 ± 6.3	42.9 ± 11.2	28.9 ± 11. 2	43.1 ± 10.4
CCE, % (wet basis)	67.3 ± 11.0	68.5 ± 16.6	68.5 ± 18.4	79.5 ± 17.4	76.5 ± 17.5	72.3 ± 14.2	56.0 ± 13.4	58.2 ± 10.0	70.0 ± 20.5	71.6 ± 16.4	59.2 ± 15.8	68.6 ± 18.1	65.8 ± 14. 7	50.4 ± 26.4	69.6 ± 11.6
Avergae producer gas dew point, °C	11.3 ± 0.5	13.6 ± 0.4	13.0 ± 0.2	11.7 ± 0.7	11.4 ± 0.5	11.8 ± 0.4	10.7 ± 0.5	11.3 ± 0.6	12.3 ± 0.9	13.2 ± 0.6	14.3 ± 0.5	16.1 ± 0.8	11.5 ± 0.8	14.5 ± 0.4	12.0 ± 0.8
ER range	0.20-0.78	0.20-0.77	0.20-0.80	0.25-0.79	0.19-75	0.19-0.64	0.20-0.77	0.25-0.67	0.25-0.60	0.22-0.83	0.25-0.71	0.22-0.64	0.25-0.81	0.14-0.58	0.23-0.81
Bed temperature, °C	594	684	625	647	600	575	565	602	553	711	620	668	609	667	755
[a]Moisture, producer gas %	10.21	11.78	11.35	10.47	10.28	11.35	9.83	10.21	10.87	11.49	12.30	13.72	10.34	12.45	10.67
Char yield, g/kg (wet basis)	242.25	104.15	48.41	93.06	82.99	220.34	102.74	140.07	201.72	63.41	175.43	60.32	62.37	102.15	180.64
Ash yield, g/kg (wet basis)	26.92	13.14	8.54	16.42	16.16	23.94	9.79	11.85	14.02	4.77	11.60	5.75	16.58	20.92	21.19
Tar+liquid yield, g/Nm^3 (wet basis)	26.77	13.21	9.94	22.41	39.32	30.91	34.67	60.00	28.88	11.75	22.38	9.55	30.68	50.95	13.72

N.D.: Not detected; [a]: determined based on Ref. (Phyllis 2) by using a correlation between dew point and gas moisture

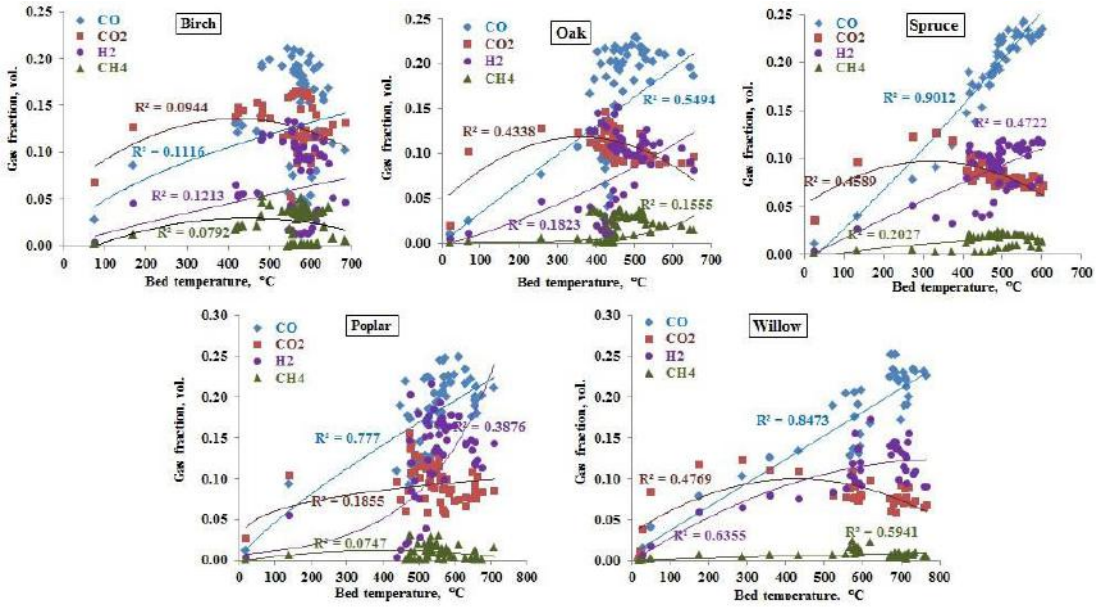

Figure 7: Variation in gasification compositions as an effect of bed temperature

The peak LHV for this biomass seemed to establish at a higher ER than that of birch while the average (~4.47 MJ/Nm3, wet base) kept little higher (Figure 5). This perhaps can be explained by the effect of bulk density (Table 1) the lower the value of which typically contributes to increase the supply air to the reactor and thus the increased operational ER (Purdon, 2010). The Vg meanwhile showed the similar trend as of birch and averaged at ~2.17 Nm^3/kg (wet base) with a peak reaching to ~2.52 Nm^3/kg (wet base) corresponding to the ER = 0.42 (Figure 6); these values (average and peak) however are little inferior than those of birch. With the concurrent effect of the trend of LHV and gas yield, the CGE and CCE showed obvious increasing and decreasing tendencies averaging to 46% and 72% respectively, maximized at 68% and 97% corresponding to the same ER at 0.42 (Figure 6).

As far as gasification performance of spruce is concerned, the gas LHV demonstrated a similar trend to that of birch and oak. This value however

averaged a little lower at ~4.1 MJ/Nm^3 (wet base) and peaking to ~5.2 MJ/Nm^3 (wet base) corresponding to the ER = 0.36. By and large, the trend of gasification properties of this wood chips is pretty comparable to that of birch, expect the pattern of Vg showing a decreasing and increasing tendency throughout. Noticeably, the average specific gas yield for this crop reached to ~1.76 Nm^3/kg (wet base) which maximized at ~2.45 Nm^3/kg (wet base) corresponding to the ER = 0.36. These yields however were lower than those of birch and oak and attributed due to the presence of less H_2 in its product gas (Figure 6). As a consequence of less average H_2, the CGE of this biomass was also lower and reached to ~35% which maximized to ~63% corresponding to the ER = 0.36 (Table 4, Figures 6 & 7). CCE on the other hand averaged to ~61% and maximized to 95% corresponding to the ER = 0.41. Likewise CGE, this yield was also found lower which presumably due to the presence of less amount of carbonaceous gas in the producer gas components. It is worthwhile to note that unlike CGE, the level of CCE is essentially affected by the amount of carbon containing species in the producer gas and thus in spite of the presence of less amount of combustible quantities, greater CCE value can be achieved due to the higher abundance of CO_2.

In addition to the forest biomass, gasification performance of energy crops poplar and willow has also been investigated where the performance in-regards to the former was found superior than that of the latter. For instance, the average gas LHV, Vg, CGE and CCE obtained from poplar were: ~4.2 MJ/Nm^3 (wet base), ~2.05 Nm^3/kg (wet base), ~43% and ~66% respectively, in contrast to those obtained from willow as: ~4.0 MJ/Nm^3 (wet base), ~1.93 Nm^3/kg (wet base), ~38% and ~62% respectively (Table 4 & Figure 5). The peak LHV and Vg for poplar was by far the highest among all the wood chips tested here, reaching to ~5.3 MJ/Nm^3 (wet base) (at ER = 0.31) and ~2.68 Nm^3/kg (wet base) (at ER=0.42) respectively (Figure 6). In regards to willow on the other hand, the peak LHV amounted to ~5.1 MJ/Nm^3 (wet base) corresponding to the ER = 0.29 which was the lowest among all the feedstocks discussed here (Figure 6). The Vg on the other hand appeared to maximize at ER = 0.45 to 2.66 Nm^3/kg (wet base) which is comparable to that of poplar. However, owing to the lower average Vg

and LHV, the CGE and CCE of this biomass demonstrated lower average values as compared to those of birch, oak and poplar (Figure 5, Table 4).

From the above discussion, it can thus be concluded that optimum gasification on studied wood chips was achieved when the ER operated between the range 0.29 and 0.42.

3.3. *Effect of bed temperature*

The gasification performance of the woodchips were affected by the variation in bed temperature and reflected to the major operational parameters such as gas composition, gas yield, LHV, CGE and CCE the corresponding relationship of which are depicted by Figures 7 & 8.

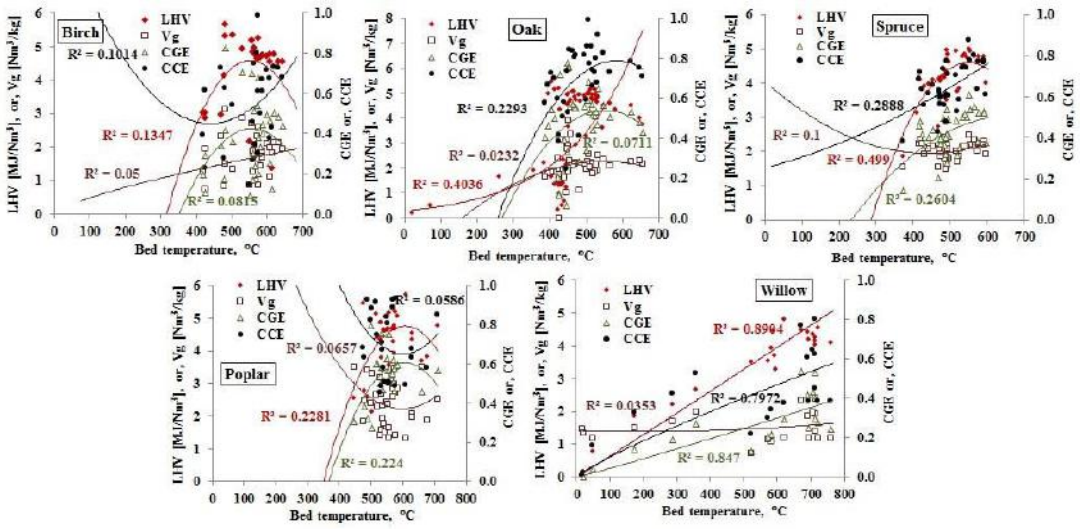

Figure 8: Performance of gasification as an effect of bed temperature

Among the several biomass investigated, two extreme peak temperatures - being highest (~770°C) and lowest (~600°C), were observed from willow and spruce respectively. The other crops achieved maximum temperature of around 700°C,

with a slightly higher value attained from poplar. For a given biomass, bed temperature is a direct function of air and typically high air flow leads to high bed temperature. However, for a given air flow rate, the bed temperature is a function of type of fuel (its physical and chemical characteristics) and the type of gasification reactors. As the chemical composition among the woodchips used in this study did not present much of a variation and the controlling parameter (such as air flow) kept fairly stable, the difference in maximum bed temperature was likely to occur due to the variation in physical properties (Lenis et al., 2013), i.e.; the size of woodchips, the ratio between bark and wood, density etc. Lower density fuel typically contributes higher bed temperature as more air is drawn into the reactor resulting enhanced combustion (Purdon, 2010). This seemed to be established in case of willow and poplar. However, despite the lower density fuel, the lower bed temperature from the gasification of spruce is surprising. One possible reason for this could be the higher extent of endothermic reactions contributing gasification to sustain at an expense of heat. The lower gasification temperature of this biomass directly impacted the thermal conversion and as a result the highest yield of char and tar (Figure 5). Conversely, the higher temperature contributed to enhance the extent of cracking char and tar and hence the lower production of these substances in case of gasification of willow and poplar (Figure 5). On the other hand, birch and oak although yielded reasonable char and tar (Figure 5), showed better performance in terms of gasification efficiencies (i.e.; CGE, CCE), as the gas LHV and specific yield from these fuels kept higher.

Meanwhile, observing Figure 7, with the rise in bed temperature the gas compositions among the wood chips birch, oak, spruce, poplar and willow exhibited the following tendencies: CO and H_2 increased, CO_2 increased and decreased except for poplar for which only increased, CH_4 increased except for poplar and birch for which both increased and decreased. As already mentioned, the phenomenon of increasing CO and decreasing CO_2 at higher bed temperature could probably be attributed due to the enhanced Boudouard (Eq. 3) reaction, while the increasing hydrogen might be prompted due to the increased water-gas (Eq. 10) or, water-gas shift reaction (Eq. 11) (Cao et al., 2006). The decreased methane at higher bed temperature was on the other hand likely influenced

through steam reforming (Eq. 9) (Pinto et al., 2002) which tended to establish in case of birch and poplar. However, in case of other biomass this trend was perhaps inversed and associated with the reverse reforming or, dry reforming (Eq. 6).

Along with the gas compositions, the other parameters influencing the gasification performance established the following tendencies (Figure 8): gas LHV increased and decreased except for oak and willow for which only increased; Vg increased except for poplar and spruce for which decreased and increased; CGE increased except for birch, oak and poplar for which increased and decreased; CCE increased except for birch and poplar for which decreased and increased and for oak increased and decreased respectively. For birch and most other crops, expectedly, the increasing and decreasing tendency of LHV were resulted due to the similar tendency of CH_4, the minor variation of which greatly affects the magnitude of LHV (Xue et al., 2014). For the rest of the feedstock, the trend of LHV was increasing which was mainly because of the greater contribution of CO that linearly rose as the bed temperature rose. In regards to the specific gas yield theoretically the yield enhances as the bed temperature rises since the extent of tar cracking and combustion reactions (Eqs. 4 & 5) strengthen. This appeared to establish for all the crops but for poplar and spruce for which the gas yield gradually decreased and increased as the bed temperature augmented. The decreased gas yield during the higher bed temperature was likely to be caused due to the dilution of product gas with N_2 when the air supply increased while the higher product gas at higher bed temperature was due to the increased combustion leading to escalate CO_2 and as a result the enhanced level of specific gas. The combined effect of gas LHV and Vg reflected to the evolution of CGE, the patter of which was either increasing or, increasing and decreasing. The maximum CGE ranged between ~53% and ~82%, achieved between the corresponding temperature of ~483°C and ~670°C respectively. Noticeably, the highest CGE was obtained from birch at ~82% corresponding to the bed temperature of 483°C in contrast to the lowest from willow at ~53% corresponding to the bed temperature of ~670°C. In general, the excessive bed temperature led to decrease the CGE, as the product gas composition was degraded by the higher amount of incombustible components

such as the enhanced amount of CO_2. In contrary, the level of CCE increases as the level of bed temperature rises, since this efficiency is positively affected by the enhanced amount of carbonaceous gas, for example, the increased concentration of CO, CH_4, CO_2 and so on. Thus the peak CCE for all the biomass was achieved at a relatively higher temperature despite the evolution trend demonstrated different pattern as the type of the feedstocks differed.

Concluding from the above discussion, the gasification performance in-terms of LHV, Vg, CGE and CCE of the studied biomass can decisively be ranked as: oak > birch > poplar > willow > spruce, which can be also confirmed by the data presented in Figure 5.

3.4. *Tar recovery and composition*

Tar is a complex mixture of chemical compounds consisting of series of aromatic hydrocarbons which can remain stable over a wide range of gasification temperatures and thus to some extent their presence in the producer gas is unavoidable. In the present study, the gravimetric tar was sampled in combination with water and analyzed for the evaluation of gasification performance and mass balance as shown in Tables 6 & Figure 5.

As observed, among all the biomass investigated, spruce resulted the highest amount of tar + liquids at ~41 g/Nm^3 in contrast to poplar at ~12 g/Nm^3. Spruce by far achieved the lowest gasification temperature which might be the reason why this biomass yielded the highest tar. In general, the lower temperature leads to yield higher amount of primary tar (Basu, 2010) as opposed to secondary and tertiary tar and therefore the majority of the tar in this feedstock might have been the primary tar. In contrary, due to the higher gasification temperature, a substantial fraction of primary tar convert into gas and other form of tars and thus less total tar from the gasification of poplar. In regards to oak and willow on the other hand the level of gravimetric tar were found fairly similar (at ~30 g/Nm^3) although the gasification temperature between these two biomasses were different being willow to be higher than that of oak (Figures 7 & 8). This perhaps could be due to the variation in the amount of liquid condensates between the

two samples rather than the tar itself since these two components were collectively called tar.

Table 5: Tar composition results obtained from the SPA tests conducted for the sample of oak (Run R5)

Tar components	Chemical formula	Amount [μg]
Aromatics		
Benzene	C_6H_6	25.60
Toluene	C_7H_8	13.78
m/p-Xylene	C_8H_{10}	1.67
o-Xylene	C_8H_{10}	2.39
tert-Butylcyclohexane	$C_{10}H_{20}$	N.D.
Indan	C_9H_{10}	N.D.
Indene	C_9H_8	N.D.
Naphthalene	$C_{10}H_8$	N.D.
Phenolics		
Phenol	C_6H_6O	10.59
o-Cresol	C_7H_8O	4.44
m-Cresol	C_7H_8O	5.97
p-Cresol	C_7H_8O	2.42
2,4-Xylenol	$C_8H_{10}O$	1.23
2,5/3,5-Xylenol	$C_8H_{10}O$	1.92
2,6-Xylenol	$C_8H_{10}O$	0
2,3-Xylenol	$C_8H_{10}O$	0.95

In addition to the gravimetric tar, the compositional tar exclusively for oak was measured as according to the SPA protocol and the results are illustrated in Table 5. The tar samples collected for other feedstocks did not produce representative results due to the technical and analytical constraints and hence is not reported here. As observed in Table 5, aromatics such as benzene, toluene and xylene are the most abundant tars detected from the present analysis followed by the

phenolics such as phenols, cresols and xylenols. These spectra of tar are predominantly originated from the structural composition of biomass (Li et al., 2014) and can appear over a broad range of operating conditions, particularly, when the gasification temperature is low (between the range 400 and 850 °C) (Hernández et al., 2013; Morf et al., 2002). However, when the gasification temperature is higher, the pattern of tar may differ and mainly dominated by the presence of secondary and tertiary tar, i.e.; the PAHs (Siedlecki & De Jong, 2011), at an expense of primary tar (Carpenter et al., 2010). Nevertheless, owing to the low gasification temperature this tar was not logically identified in the current analysis.

3.5. *Mass balance*

The mass balance calculation by incorporating the plant inputs (fuel flow and air flow) and outputs (gas, char, tar, liquids and particulates) for runs R3, R5, R7, R12 and R13 corresponding to the woody biomass birch, oak, spruce, poplar and willow are presented in Table 6. As can be seen, the lowest magnitude of error was found from the gasification of oak followed by spruce, birch, poplar and willow. By and large, the balance closure gave over 95% accuracy for all the cases which coincide with the existing literature (Li et al., 2004) and hence can be considered acceptable.

However, the resulted minor errors might have been occurred due to the several factors such as: minor gas leakages – possibly encountered from the circumference of the temperature sensors, gasifer lid and from several joints in piping; systematic and precision errors– discrepancies resulted by the instruments incorporated for acquiring data; analytical errors during calculations – the values which were instead obtained from the instruments, analytically determined by using the formulas and based on some assumptions (Siedlecki & De Jong, 2011); rounding-off errors during data analysis; mass losses during sampling and feeding; uncaptured tar and accumulation of particulates, etc.

4. Conclusions

Long rotation forest crops (birch, oak and spruce) and short rotation energy crops (poplar and willow) exhibited a great potential for being converted into useful gas via fixed-bed downdraft gasification. In terms of most of the operational parameters, the gasification performance of birch and oak closely agreed with oak giving the highest average LHV (~4.5 MJ/Nm^3, wet base), CGE (~51%) and Vg (~2.2 Nm^3/kg, wet base). These biomasses nevertheless yielded higher char than that from their counterpart others. Energy crops poplar and willow on the

Table 6: Estimation of mass balance for the selected gasification tests

	Mass balance				
Test date	25.02.2015	09.12.2014	10.01.2015	10.02.2015	20.11.2014
Test ID	R3	R5	R7	R12	R13
Feedstock type	Birch	Oak	Spruce	Poplar	Willow
Total solid (biomass+charcoal) input, kg	12.29	9.60	9.25	12.90	9.27
Air input, kg	22.40	15.47	13.25	19.53	15.71
Producer gas output, kg	32.70	23.05	20.17	30.23	22.54
Char output, kg	0.70	0.95	1.04	0.85	0.73
Liquid, tar and particulates output, kg	0.25	0.70	0.54	0.22	0.53
Error, kg	1.04	0.37	0.75	1.12	1.18
Error, %	3.01	1.48	3.33	3.45	4.72

other hand displayed higher bed temperature, being willow to be the highest, which favored to reduce tar, char and ash, and to greatly enhance H_2 content. On an average, the results obtained from the above biomasses (birch, oak, poplar and willow) are interesting in aspects of utilizing product gas to transform into H_2, liquid biofuel and heat and electricity through arrays of downstream conversion units. Meanwhile, the performance of spruce in various aspects of gasification was revealed poor, although this fuel provided the highest average CO (vol.) and higher average CH_4 (vol.) than that of the energy crops. The degraded performance of spruce may be associated with its physical properties such as low bulk density andlow bark to wood ratio, etc. Worthwhile also to note, unlike other crops, spruce was the only softwood in this study presumably contributed to develop thermal conversion inherently different than that of the hardwoods. Nonetheless, the mean gas quality (LHV: ~4.1 MJ/Nm^3, Vg: ~1.8 Nm^3/kg, wet base) and the process performance obtained from this feedstock still in the acceptable range to meet the requirement of the downstream applications such as energy production via gas engine or, turbine. All in all, considering the overall performance, the wood species examined in this study may be ranked as: oak > birch > poplar > willow > spruce for which the optimized ER appeared to establish between the range 0.29 and 0.42.

Acknowledgement

The authors largely thank J.B. Ugland AS for providing funding for the gasification installation. People involved in pre-treatment and processing of biomass are also acknowledged. For crucial technical assistance, Lab Engineers Steve Schading & Johan Olav Brakestad (UiA, Grimstad) are appreciated. Additionally, the first author of this paper thanks University of Agder (Norway) for providing PhD funding during the course of this research.

References

Annual Energy Outlook 2015. <http://www.eia.gov/forecasts/aeo/pdf/0383(2015).pdf>, Accessed: [07.07.2015]

Adler, A., Verwijst, T., Aronsson, P. 2005. Estimation and relevance of bark proportion in a willow stand. *Biomass and Bioenergy*, **29**(2), 102-113.

Albertazzi, S., Basile, F., Brandin, J., Einvall, J., Hulteberg, C., Fornasari, G., Rosetti, V., Sanati, M., Trifirò, F., Vaccari, A. 2005. The technical feasibility of biomass gasification for hydrogen production. *Catalysis Today*, **106**(1–4), 297-300.

Balu, E., Chung, J.N. 2012. System characteristics and performance evaluation of a trailer-scale downdraft gasifier with different feedstock. *Bioresource Technology*, **108**(0), 264-273.

Basu, P. 2010. *Biomass gasification and pyrolysis: practical design and theory*. Academic press.

Brage, C., Yu, Q., Chen, G., Sjöström, K. 1997. Use of amino phase adsorbent for biomass tar sampling and separation. *Fuel*, **76**(2), 137-142.

Bridgwater, A.V. 2003. Renewable fuels and chemicals by thermal processing of biomass. *Chemical Engineering Journal*, **91**(2–3), 87-102.

Bright, R.M., Strømman, A.H., Hawkins, T.R. 2010. Environmental Assessment of Wood-Based Biofuel Production and Consumption Scenarios in Norway. *Journal of Industrial Ecology*, **14**(3), 422-439.

Cao, Y., Wang, Y., Riley, J.T., Pan, W.-P. 2006. A novel biomass air gasification process for producing tar-free higher heating value fuel gas. *Fuel Processing Technology*, **87**(4), 343-353.

Carpenter, D.L., Bain, R.L., Davis, R.E., Dutta, A., Feik, C.J., Gaston, K.R., Jablonski, W., Phillips, S.D., Nimlos, M.R. 2010. Pilot-scale gasification of corn stover, switchgrass, wheat straw, and wood: 1. Parametric study and comparison with literature. *Industrial & Engineering Chemistry Research*, **49**(4), 1859-1871.

Gai, C., Dong, Y. 2012. Experimental study on non-woody biomass gasification in a downdraft gasifier. *International Journal of Hydrogen Energy*, **37**(6), 4935-4944.

Gómez-Barea, A., Arjona, R., Ollero, P. 2005. Pilot-plant gasification of olive stone: a technical assessment. *Energy & fuels*, **19**(2), 598-605.

Grover, P., Mishra, S. 1996. *Biomass briquetting: technology and practices*. Food and Agriculture Organization of the United Nations.

Heidenreich, S., Foscolo, P.U. 2015. New concepts in biomass gasification. *Progress in Energy and Combustion Science*, **46**, 72-95.

Hernández, J.J., Ballesteros, R., Aranda, G. 2013. Characterisation of tars from biomass gasification: Effect of the operating conditions. *Energy*, **50**(0), 333-342.

Kirkels, A.F., Verbong, G.P.J. 2011. Biomass gasification: Still promising? A 30-year global overview. *Renewable and Sustainable Energy Reviews*, **15**(1), 471-481.

Klasnja, B., Kopitovic, S., Orlovic, S. 2002. Wood and bark of some poplar and willow clones as fuelwood. *Biomass and Bioenergy*, **23**(6), 427-432.

Lenis, Y., Osorio, L., Pérez, J. 2013. Fixed bed gasification of wood species with potential as energy crops in Colombia: the effect of the physicochemical properties. *Energy Sources, Part A: Recovery, Utilization, and Environmental Effects*, **35**(17), 1608-1617.

Li, L., Huang, S., Wu, S., Wu, Y., Gao, J., Gu, J., Qin, X. 2014. Fuel properties and chemical compositions of the tar produced from a 5 MW industrial biomass gasification power generation plant. *Journal of the Energy Institute*.

Li, X.T., Grace, J.R., Lim, C.J., Watkinson, A.P., Chen, H.P., Kim, J.R. 2004. Biomass gasification in a circulating fluidized bed. *Biomass and Bioenergy*, **26**(2), 171-193.

McKendry, P. 2002. Energy production from biomass (part 3): gasification technologies. *Bioresource technology*, **83**(1), 55-63.

Morf, P., Hasler, P., Nussbaumer, T. 2002. Mechanisms and kinetics of homogeneous secondary reactions of tar from continuous pyrolysis of wood chips. *Fuel*, **81**(7), 843-853.

Ni, M., Leung, D.Y.C., Leung, M.K.H., Sumathy, K. 2006. An overview of hydrogen production from biomass. *Fuel Processing Technology*, **87**(5), 461-472.

Petersson, B.Å. 2004. *Tillämpad byggnadsfysik*. Studentlitteratur.

Phyllis2. ECN, The Netherlands.

Pinto, F., Franco, C., André, R.N., Miranda, M., Gulyurtlu, I., Cabrita, I. 2002. Co-gasification study of biomass mixed with plastic wastes. *Fuel*, **81**(3), 291-297.

Purdon, M.J. 2010. Softwood gasification in a small scale downdraft gasifier, Humboldt State University. <http://humboldt-dspace.calstate.edu/bitstream/handle/2148/665/Thesis-MichaelJoePurdon-FinalFinalDraft.pdf?sequence=1>, Accessed: [10.07.2015]

Renewables 2013 global status report. REN21. <http://www.ren21.net/Portals/0/documents/Resources/GSR/2013/GSR2013_lowres.pdf>, Accessed: [07.07.2015]

Sarker, S., Arauzo, J., Nielsen, H.K. 2015a. Semi-continuous feeding and gasification of alfalfa and wheat straw pellets in a lab-scale fluidized bed reactor. *Energy Conversion and Management*, **99**, 50-61.

Sarker, S., Bimbela, F., Sánchez, J.L., Nielsen, H.K. 2015b. Characterization and pilot scale fluidized bed gasification of herbaceous biomass: A case study on alfalfa pellets. *Energy Conversion and Management*, **91**, 451-458.

Sarker, S., Nielsen, H.K. 2015. Preliminary fixed-bed downdraft gasification of birch woodchips. *International Journal of Environmental Science and Technology*, **12**(7), 2119-2126.

Serapiglia, M., Cameron, K., Stipanovic, A., Abrahamson, L., Volk, T., Smart, L. 2013. Yield and Woody Biomass Traits of Novel Shrub Willow Hybrids at Two Contrasting Sites. *BioEnergy Research*, **6**(2), 533-546.

Sheth, P.N., Babu, B.V. 2009. Experimental studies on producer gas generation from wood waste in a downdraft biomass gasifier. *Bioresource Technology*, **100**(12), 3127-3133.

Siedlecki, M., De Jong, W. 2011. Biomass gasification as the first hot step in clean syngas production process–gas quality optimization and primary tar reduction measures in a 100 kW thermal input steam–oxygen blown CFB gasifier. *biomass and bioenergy*, **35**, S40-S62.

Trømborg, E., Havskjold, M., Lislebø, O., Rørstad, P.K. 2011. Projecting demand and supply of forest biomass for heating in Norway. *Energy Policy*, **39**(11), 7049-7058.

Warnecke, R. 2000. Gasification of biomass: comparison of fixed bed and fluidized bed gasifier. *Biomass and Bioenergy*, **18**(6), 489-497.

Xue, G., Kwapinska, M., Horvat, A., Kwapinski, W., Rabou, L., Dooley, S., Czajka, K., Leahy, J. 2014. Gasification of torrefied Miscanthus× giganteus in an air-blown bubbling fluidized bed gasifier. *Bioresource technology*, **159**, 397-403.

Zainal, Z.A., Rifau, A., Quadir, G.A., Seetharamu, K.N. 2002. Experimental investigation of a downdraft biomass gasifier. *Biomass and Bioenergy*, **23**(4), 283-289.

Zhang, K., Chang, J., Guan, Y., Chen, H., Yang, Y., Jiang, J. 2013. Lignocellulosic biomass gasification technology in China. *Renewable Energy*, **49**(0), 175-184.

Paper V

Feasibility analysis of a renewable hybrid energy system with a producer gas generator fulfilling remote household electricity demand in Southern Norway

Shiplu Sarker

Published in **Renewable Energy**, 2016, 87: 772-781

Journal information (ISI web of science):

Publisher: **Elsevier**
Impact factor: **3.476** (2014)
Rank: **20/89** (Energy & Fuels)

Renewable Energy xxx (2015) 1–10

Contents lists available at ScienceDirect

Renewable Energy

journal homepage: www.elsevier.com/locate/renene

Feasibility analysis of a renewable hybrid energy system with producer gas generator fulfilling remote household electricity demand in Southern Norway

Shiplu Sarker

University of Agder, Faculty of Engineering and Science, Serviceboks 509, 4898, Grimstad, Norway

ARTICLE INFO

Article history:
Received 3 August 2015
Received in revised form
1 November 2015
Accepted 3 November 2015
Available online xxx

Keywords:
Hybrid energy
Techno-economic
Optimum solution
Sensitivity analysis

ABSTRACT

Hybrid energy system is increasingly emerging as an option to produce energy for the remote areas. This paper presented an economic feasibility analysis of a single standalone house operating with a hybrid power plant consisting of a fixed capacity producer gas generator (2 kWe) and other renewable energy sources (Photovoltaic and wind). The National Renewable Energy Laboratory's Hybrid Optimization Model for Electric Renewable (HOMER) model was employed which evaluated the techno-economic analysis based on the criteria of net present cost and levelized cost of electricity. Taking the site specific daily average solar radiation, average wind speed and load data into account, renewable hybrid model consisting of Bio/PV (Photovoltaic)/wind/battery/capacitor was found feasible giving 19,866 kWh/year of energy with a levelized cost of electricity of 0.306 kWh/yr. While comparing the hybrid system with a diesel or, natural gas generator alone, the maximum savings from CO_2 emissions worth 22,626 kg/yr. was achieved. The sensitivity analysis over a range of diesel/natural/producer gas price (0.1 $/L to 1 $/L or, 0.1 $/m^3 to 1.0 $/m^3) showed that in addition to the environmental benefits hybrid energy configuration could result economic advantages when the producer gas price does not exceed the threshold of 0.1 $/m^3.

1. Introduction

Energy is a single most commodity mankind deals every day. Yet, its ceaseless availability is not always guaranteed and the production is often associated with familiar issues like carbon footprint, low efficiency and resource depletion. To reverse these challenges and to enhance reliability, energy needs be produced from alternative sources such as from wind, solar and biomass and the access should be achieved through viable pathways so that demands both at centralized and decentralized levels are feasibly met.

As a country, Norway has an exemplary share of renewable energy worth ~95% of the total production capacity due thanks to its wealth of hydroelectricity [1]. Although hydropower is one of the most promising sectors of renewable energy, the nation is also blessed with other potential sources such as wind and biomass [2]. With the availability of blend of renewable resources, Norway as a Kyoto ratified country is nicely shaped to fulfill its commitment towards reducing 30% CO_2 emissions by the year 2020 [3]. The drive towards meeting the targeted CO_2 reduction could be directed in multiple areas at several scales and levels where the integration of various forms of renewable energy would be the key.

In-terms of the availability of various forms renewable energy, Southern Norway, especially Grimstad (58° 20′ 25″ N, 8° 35′ 36″ E) is particularly attractive. Due to the preferential geographical locations, this area is heavily endowed with high solar irradiation with annual horizontal insolation of around 900 kW h/m^2 [4]. It also has wide range of forest resources [5] as well as abundant wind [6]. However, the electricity production from solar energy in Grimstad, likewise entire Norway, is not significant [7]. Total electricity generation from wind is also far too small compare to the demand because of the lack of initiative and investment. Although solar and wind contain a huge potential to be converted into energy, the major constraints regarding these sources are unreliability and unpredictability [8]. A stand-alone renewable energy plant operating 100% with solar energy may be unrealistic, as power cannot be produced during the cloudy days when sunlight is unavailable. Alternatively, a stand-alone system operating solely with wind turbine is also infeasible throughout the year due to the

E-mail address: shiplu.sarker@uia.no.

http://dx.doi.org/10.1016/j.renene.2015.11.013
0960-1481/

unusable production of power when wind speed goes below 3 m/s or, above 20 m/s (for the wide range of wind turbine capacity) [9]. Thus, to avoid this problem, hybrid energy system can offer a valuable alternative which involves two or, more sources of energy for fulfilling a particular demand. Typical hybrid energy system for instance can combine a fossil fuel generator either with solar or, wind energy or, both. A number of documented researches have demonstrated that hybrid energy systems are more suitable than single source energy systems in-terms of economic feasibility and reliability. In fact, renewable hybrid energy systems have been a topic of investigation in many contemporary works. For example, a Biomass gasification/PV hybrid energy system was modeled and validated by Ref. [10] for power supply to a decentralized section of a renewable energy research building in Congo for which the optimum size and cost of the power plant units were determined. The results indicated that hybrid energy system as an isolated unit is feasible to satisfy the power demand of an independent research center in Congo. In another work [11], a standalone hybrid system consisting of wind/PV/fuel cell (FC) was modeled to determine the power demand management of a remote area in a Pacific Northwest region in the USA using real climatic data both for winter and summer scenarios. The results showed that the proposed hybrid system is effective for regulating round the year power demand of the remote municipalities. In addition to the small scale plants, hybrid energy systems of large scale capacity providing power for a remote hotel located in subtropical coastal area of Queensland, Australia, was assessed in a study by Ref. [12] for several combinations of renewable energy system. Feasibility analysis revealed that hybrid plant based on wind energy conversion system (WECS) exhibited potential long-term advantages in terms of Net Present Cost (NPC) for tourist resorts requiring stand-alone electricity. Further, Ashok K [13] modeled and analyzed the several configurations of renewable hybrid systems capable to provide electricity demand of a remote village in south Kerala, India. The main objective of the study was to find an optimum combination of energy sources which are attractive in-terms of least life cycle cost. It was concluded that micro-hydro-wind was optimum in terms of both economics and environments, provide electrification to the rural remote community at a unit cost of 6.5 R s/kWh. Lately, Khan et al. [14] proposed a technique where renewable hybrid configuration featuring PV/biogas digester/membrane distillation (MD) was considered for a purpose of producing energy as well as of supplying pure drinking water to the inhabitants of a remote village (Panipara) located in Bangladesh. After feasibility analysis it has been concluded that hybrid energy plant offers a clear economic advantage in a case when including with the utilization of renewable electricity the by-products from the biogas digester is used as fertilizers for on-farm application.

Based on these facts, techno-economic analysis of a renewable hybrid energy system meeting energy demand of a standalone house in Southern Norway is proposed in this paper which, to the best of the author's knowledge, has not been investigated in the past. The other aspect of this work which is the addition of wood gas generator in the hybrid system has been scarcely explored in the previous literature and hence making the context of this study interesting both in regard to the local bioenergy as well as to the standalone renewable electricity.

2. Methods

To evaluate the suitability of producer gas (PG) generator in meeting a single household electricity demand, first an energy system comprised of a fossil fuel generator was designed followed by analysis in-terms of cost, energy and emissions. Subsequently, a series of hybrid configurations consisting of producer gas generator and one or, two other renewable energy options was developed and the techno-economic parameters were evaluated. The results obtained from all the configurations afterwards were compared and the optimum solution was identified.

The average consumption of electricity for a typical household in Norway was assumed as according to the data provided by the study [15] and presented in Fig. 1 while the demographic and the energy data as relevant to calculation were used from a reliable statistical reference such as Statistics Norway [16] and the cost of energy devices were carefully estimated as according to the current market prices and pertinent literature sources. The design, simulation and optimization of the energy systems were carried out by using a simulation tool HOMER (Hybrid Optimization Model for Electric Renewables) developed by the National Renewable Energy Laboratory (NREL) which allowing free access to the users over a definitive period. HOMER analyzes feasible energy system configurations from among number of possibilities based on the ascending net present cost (NPC).

The details of the energy systems including cost and other parameters as considered in this study are given in the following subsections.

2.1. System architecture

2.1.1. Mono energy system

Mono energy system model was developed based on the conventional energy devices such as diesel or, natural gas generator capable of supplying the entire household electricity demand round the year. One configuration for each fuel with a generator (2.5 kW), battery (2 units, 2.16 kW h each) and a converter (1 kW) was designed and corresponding simulation was performed. The simulation results were subsequently optimized based on the least plant cost and best match energy supply scenarios.

The sensitivity analysis was additionally performed as against the range of diesel and natural gas prices between 0.1 and 1.0 $/kWh with a step of 0.1 $ increase. The design of mono-energy system in the HOMER platform is presented by Fig. 2.

2.1.2. Hybrid energy system

Hybrid energy model for several combinations was formulated by keeping producer gas generator as a mandatory option. The producer gas generator was assumed to be integrated with an existing gasification plant capable to produce minimum 2 kW of electricity. In this case, the gasification facility available in the University of Agder was considered as a model gasification plant

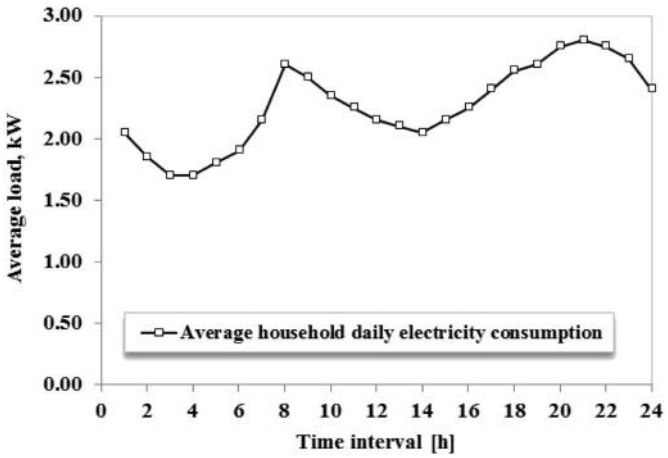

Fig. 1. Average electricity consumption of a typical household in Southern Norway.

Please cite this article in press as: S. Sarker, Feasibility analysis of a renewable hybrid energy system with producer gas generator fulfilling remote household electricity demand in Southern Norway, Renewable Energy (2015), http://dx.doi.org/10.1016/j.renene.2015.11.013

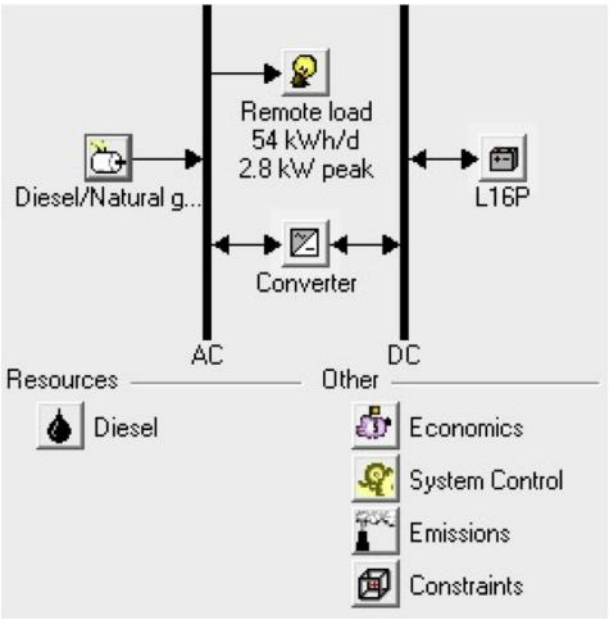

Fig. 2. Mono energy system design in HOMER.

which can produce maximum 5 kW of electricity.

Besides producer gas generator, the other components added to the hybrid systems include PV arrays, wind turbine, diesel generator, natural gas generator, battery and capacitor, an example of which is demonstrated by Fig. 3. The several hybrid systems used for present modeling is listed in Table 1. After system design was accomplished, the hybrid models were simulated and afterwards the results were optimized as an effect of the sensitivity of fuel cost, i.e., the variable price of diesel, natural gas and wood gas.

2.2. Input resources

2.2.1. Load data

Based on the open access data [16], it is reported that the total private annual household electricity consumption at Grimstad, Norway was 153.8 GW h/yr. in 2013. The total number of private houses in Grimstad is 9995 [16] and hence per household electricity consumption can be determined as 15387.67 kW h/yr. which in-terms of daily consumption corresponds to 42.16 kW h/d. The

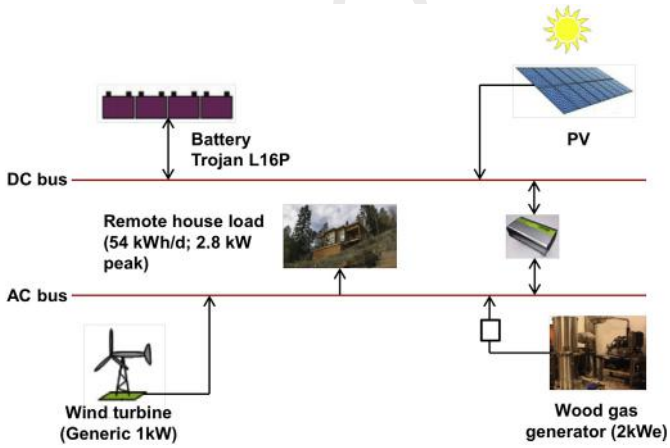

Fig. 3. System architecture of a hybrid energy plant.

Table 1
Hybrid plants used for HOMER simulation.

Total components	Hybrid plant type
4	Bio/PV/battery/converter
4	Bio/Wind/battery/converter
4	Diesel/PV/battery/converter
4	NG/PV/battery/converter
4	NG/wind/battery/converter
5	Bio/PV/wind/battery/converter
5	Bio/Diesel/PV/battery/converter
5	Bio/NG/PV/battery/converter
5	Bio/NG/wind/battery/converter

Bio: Producer gas generator.
PV: Photo voltaic arrays.
NG: Natural gas generator.

estimated distribution of electricity consumption during the workdays for an average household in Norway is illustrated by Fig. 1 [15]. According to the segment-base end-user demand, domestic electricity consumption is mostly contributed by the space heating (45%) followed by the demand for residual (19%), hot water (12%), lighting (5%) and other appliances (19%). Space heating together with the consumption for lighting and entertaining devices is maximized when people return from work and hence the load curve hit to peak during the evening (Fig. 1). There is also high space heating and lighting demand during the morning resulting a short peak of electricity consumption at that particular time of the day (Fig. 1).

The present techno-economic evaluation is carried out based on the assumption that the average electricity requirement for a particular household is 54 kW h/d with a load factor of 80%, meaning that the possible peak load electricity is 2.8 kW.

2.2.2. Generator fuels

Both natural and wood gas is proposed as generator fuel for this study. Since the wood gas is assumed to be produced and delivered by the in-situ fixed-bed downdraft gasification combined heat and power plant (CHP), the cost associated with the production of wood gas is considered as the cost at which wood gas is available. Hence, the total wood gas price is expected to be influenced by the price of woodchips, capital cost and the operation and maintenance cost of the gasification CHP facility, calculated based on the equation (1) through (5) [17].

Table 2 shows the technical data used in calculating the producer gas price ($/m^3).

$$G_c = NPV + C_F + C_p \quad (1)$$

$$NPV = \frac{I}{A_{t,r}} \quad (2)$$

Table 2
Gasification plant data.

	Specifications
Capital cost	$ 1500/kWe
Interest	5%
Life time	20 yrs.
Unit cost of biomass	$ 0.20/kg
Biomass consumption	2.4 kg/h
Gas production	5 m^3/h
Gas density	1.3 kg/m^3
Internal energy requirement	1.3 kW
Unit electricity price	$ 0.14/kWh

$$A_{t,r} = \frac{1 - \frac{1}{(1+r)^t}}{r} \quad (3)$$

$$C_F = C_u * C_f \quad (4)$$

$$C_p = \textit{internal plant consumption}(kWh) * \textit{unit electricity cost}(\$/kWh) \quad (5)$$

where NPV is the annual cost of the plant in $/yr., r is the annual interest rate in %, t is the plant life time in years, C_F is the total cost of the biomass in $/yr., C_u is the unit cost of biomass in $/kg, C_f is the total biomass consumption in kg/yr. and C_p is the cost due to the internal power consumption in $/yr.

Unlike producer gas, natural gas or, diesel is expected to be supplied from the local market and thus is likely to be affected by the market constraints such as international price fluctuations, sudden spike in production cost etc. To account such changes into investigations sensitivity analysis as an effect of varied natural gas price was conducted. The range of natural gas/diesel price considered for assessment varied between 0.10 $/m^3 and 1.0 $/m^3 in the interval of 0.10 $ each. Wood gas price is also foreseen to be varied depending on the technology and the type of wood used for gasification. Hence, sensitivity effect for range of wood gas price at the same price interval of fossil fuels was also evaluated.

2.2.3. Solar irradiation and ambient temperature

The selected site is known for its high availability of solar irradiation and hence attractive for the application of solar energy.

The monthly solar radiation data of this site were acquired through NASA [18] for 22 years average and presented by Fig. 4. As observed, available global solar radiation exhibits seasonal as well as monthly variation with average maximum for June (5.78 kW h/m^2/day) and average minimum for December (0.31 kW h/m^2/day) respectively. Likewise solar radiation, clearness index peaks close to the mid of the year in the month of May (0.532) and then reaches plateau by the end of the year in the month of December (0.363). The average daily solar radiation and clearness index for Grimstad is expected to 2.84 kW h/m^2/day and 0.489 respectively.

In addition to the solar radiation, the ambient temperature was also considered for this work. The temperature data was obtained from NASA database [18] and presented in Fig. 5. As expected, due to the geographic location, the average temperature in Grimstad peaks during the month of July and diminishes in December. By and large the annual temperature varies between the range 1.2 °C and 19.6 °C.

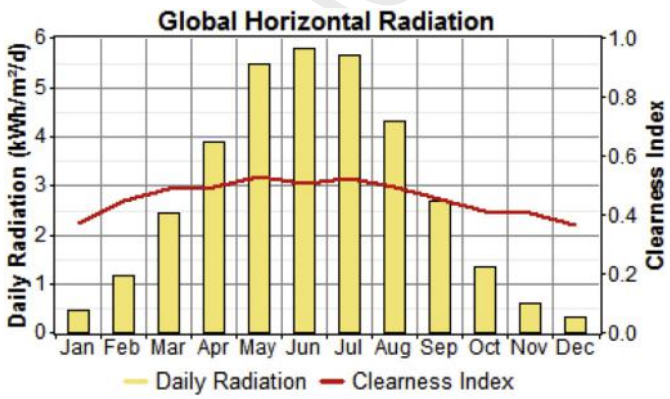

Fig. 4. Annual global horizontal solar radiation at Grimstad.

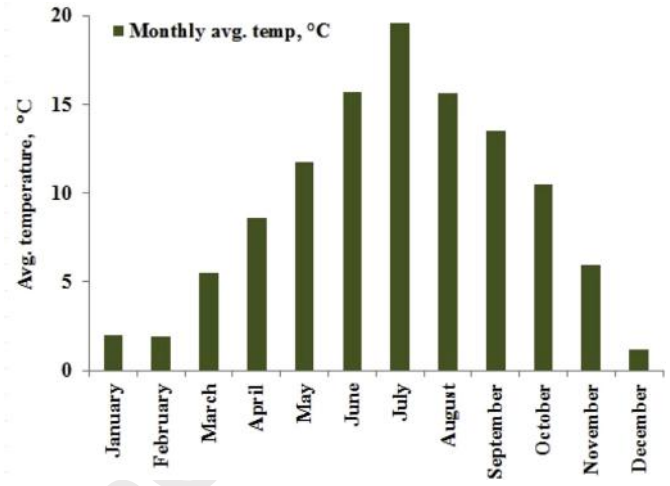

Fig. 5. Monthly average temperature profile at Grimstad.

2.2.4. Average wind speed

The annual wind speed variation for Grimstad is presented by Fig. 6. This data is based on the statistics of NASA database [18] which reports average monthly wind speed for the last 10 years.

The wind speed was measured in 3 h intervals at 10 m height of the earth's surface varied between the range 2.664 and 7.195 m/s. Generally, higher wind speed is available at the later part of the year between the month October and December. Overall, wind has a high potential in the proposed location.

2.3. Energy components

2.3.1. Generator

Three types of fuel namely diesel, natural gas and producer gas were used for the configurations modeled in this work. Thus, an existing generator available in the international market capable of operating both with liquid and gaseous fuel were selected, the specification of which along with the cost data is presented in Table 3.

Performance of the generator is generally evaluated based on its efficiency expressed by the ratio between output power and input fuel consumption.

Corresponding to each fuel, this efficiency was calculated by following the equation (6) and displayed as an example in Fig. 7.

$$\eta_g = \frac{3600\,P_e}{\rho_f\,(P_{gen}F_0 + P_eF_1)} \quad (6)$$

where η_g is the generator efficiency in %, P_e is the output power in kW, ρ_f is the density of the fuel in kg/m^3, P_{gen} is the rated generator power in kW, F_o is the generator fuel curve intercept co-efficient in L/h/rated kW or, m^3/h/rated kW and F_1 is the fuel curve slope in L/h/output kW or, m^3/h/output kW respectively.

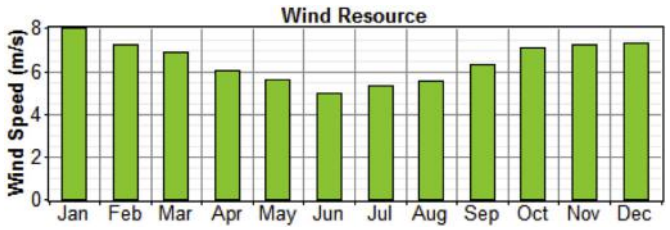

Fig. 6. Seasonal variation in wind resources at Grimstad.

Please cite this article in press as: S. Sarker, Feasibility analysis of a renewable hybrid energy system with producer gas generator fulfilling remote household electricity demand in Southern Norway, Renewable Energy (2015), http://dx.doi.org/10.1016/j.renene.2015.11.013

Table 3
Generator technical sheet [19].

	Specifications
Rated power	2.8 kW
Investment	$ 1200
Cost of replacement	$ 1000
Cost of operation and maintenance	$ 0.05/h
Operating hours	15,000
Minimum load ratio	30%
Fuel lower heating value & density	
Diesel	43.2 MJ/kg, 820 kg/m^3
Natural gas	45 MJ/kg, 0.79 kg/m^3
Producer gas	3.52 MJ/kg, 1.3 kg/m^3
Fuel consumption	
Gasoline: 1/2, 3/4 & full load	0.25,0.32 & 0.39 gal/h
LP gas: 1/2, 3/4 & full load	0.19,0.26 & 0.31 gal/h
Natural gas: 1/2, 3/4 & full load	29, 32 & 42 cu. ft/h

The DG/NG/PG fuel intercept co-efficient and slope, as required for efficiency calculation, were determined from the performance data given in the specifications (Table 3), resulted the corresponding values as: 0.1494 L/h/rated kW & 0.2643 L/h/output kW for diesel; 0.0525 m^3/h/rated kW & 0.44 m^3/h/output kW for natural gas and 0.02823 m^3/h/rated kW & 2.857 m^3/h/output kW for producer gas respectively.

2.3.2. PV array

PV modules in the hybrid configuration were set for meeting the peak load demand that cannot be achieved by the PG generator alone (operating at a rate of 2 kWe output). While simulating, the sizes of the PV arrays were allowed to vary within the given range (1–3 kW) so that an optimum configuration depending on fulfilling the electricity demand at low energy costs can be attained. Design of PV array in HOMER is influenced by the two parameters such as solar radiation and atmosphere temperature which primarily is the user defined parameters adjusted according to the location and time. By default, HOMER considers PV power to be directly proportional to the solar radiation and as a result uses the equation (7) for power calculation. However, apart from solar radiation, temperature can also affect the PV output; for example to reduce the PV efficiency at a corresponding rise in atmosphere temperature. Thus the PV module in this work accounted both radiation and temperature and accordingly below equation (8) was used for calculation. Additionally, the annual solar radiation profile for the studied location (Grimstad, Norway) found from HOMER is depicted by Fig. 4.

$$P_{PV} = P_{PVS} f_{PV} \frac{G_I}{G_{IS}} \quad (7)$$

Table 4
PV cell technical data.

	Specifications
Rated power	1–3 kW
Investment	$ 1750/kW
Cost of replacement	$ 1200/kW
Cost of operation and maintenance	$ 20/year
Life time	30 years
Derating factor	90%
Temperature co-efficient of power	−0.5%/°C
Nominal operating cell temperature	47 °C
Efficiency at standard test condition	13%

$$P_{PV} = P_{PVS} f_{PV} \frac{G_I}{G_{IS}} \left[1 + \alpha_p (T_c - T_s) \right] \quad (8)$$

where, P_{PV} is the power output from the module in kW, P_{PVS} is the rated power output at test condition, in kW, f_{PV} is the PV derating factor (%), G_I is the solar radiance incident on the PV array in current hour in kW/m^2, G_{IS} is the solar radiance incident on the PV array in the test condition, in kW/m^2, α_p is the temperature co-efficient in %/°C, T_c is the PV module temperature in current hour, in °C and T_s is the PV module temperature in the test condition, in °C.

The technical specification of PV module considered in this simulation study is provided in Table 4.

2.3.3. Wind turbine

Wind turbine is one of the renewable energy options included in the hybrid energy configuration of this work. Power producing capacity of wind turbine is generally characterized by the power curve displaying relationship between wind speed and rated power and hence highly dependent on the studied location. In the present site, the available average annual wind speed is 6.445 m/s which is potentially suitable to generate sufficient power for meeting single household electricity demand.

Hence wind turbine could be an attractive alternative in the present combined energy system. The detail of the turbine as proposed here can be viewed in Table 5.

2.3.4. Storage battery

To ensure reliable supply of power in the case when no wind, solar or, producer gas energy is available, battery storage is required.

Current study thus considers a battery (Trojan L16P, 6 V) both for mono and hybrid energy configurations. The technical data of the battery is given in Table 6.

2.3.5. Converter

Hybrid system often needs a power converter to exchange energy between AC and DC devices that allow matching the final load in its type of requirement.

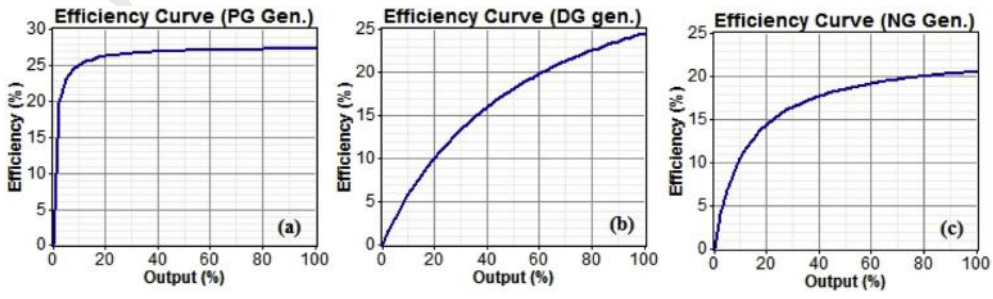

Fig. 7. Modeled efficiency of generators: (a) Producer gas (b) Diesel (c) Natural gas.

Please cite this article in press as: S. Sarker, Feasibility analysis of a renewable hybrid energy system with producer gas generator fulfilling remote household electricity demand in Southern Norway, Renewable Energy (2015), http://dx.doi.org/10.1016/j.renene.2015.11.013

Table 5
Wind turbine technical data.

	Specifications
Rated power	1 kW
Investment	$ 1000/kW
Cost of replacement	$ 800/kW
Cost of operation and maintenance	$ 10/year
Life time	15 years
Hub height	25 m
Rotor diameter	2.5 m
Number of rotor blades	3
Cut-in wind speed	2.5 m/s
Cut-out wind speed	none
Furling wind speed	13 m/s

Table 6
Battery technical specification.

	Specifications
Type	L16P
Nominal voltage	6 V
Nominal capacity	360 A h (2.16 kW h)
Investment	$ 300/quantity
Cost of replacement	$ 300/quantity
Cost of operation and maintenance	$ 20/year
Float life	10 years
Round trip efficiency	85%
Maximum charge rate	1 A/Ah
Maximum charge current	18 A

Due to the presence of several AC and DC components, the current hybrid set-up is designed with a converter the technical specifications of which are illustrated by Table 7.

2.4. Output power, economics and emissions calculation

For techno-economic assessment HOMER uses two steps. First it evaluates technical feasibility of a model based on the best possible energy demand that can be fulfilled. Then it ranks the range of obtained solutions according to the ascending order of the net present cost (NPC) [20,21]. NPC is the determination of the plant costs present value minus all profits gained over the expected life time. The annual value of the NPC is determined from the value of total annual cost which is expressed by the eq. (9)

$$C_{ann,tot} = CRF(i, R_{proj}) C_{NPC,tot} \tag{9}$$

where $C_{NPC,\ tot}$ is the total net present cost, i is the annual real interest rate (%), R_{proj} is the project life time and CRF (i, N) is the capital recovery factor.

The annual real interest rate, and the capital recovery factor are further calculated by the equations (10) and (11).

$$i = \frac{i' - f}{1 + f} \tag{10}$$

Table 7
Converter technical data.

	Specifications
Rated power	1 kW
Investment	$ 300/kW
Cost of replacement	$ 300/kW
Cost of operation and maintenance	$ 10/Kw/year
Life time	15 years
Efficiency	90%

$$CRF(i, N) = \frac{i(1+i)^N}{(1+i)^N - 1} \tag{11}$$

where i′ is the nominal interest rate, f is the annual inflation rate and N is the number of years.

Coupled with NPC, HOMER also calculates cost of energy (COE) as a part of economic analysis. COE is defined as a ratio between annual electricity cost and the total electricity load served by the system, expressed by the eq. (12) below:

$$COE = \frac{C_{ann,tot}}{E_{served}} \tag{12}$$

where E_{served} is the total electrical load served (kWh/yr.)

Levelized cost of energy (LCOE) incorporates capital costs, depreciation, operation, maintenance, management etc. into account and allows a direct comparison of the costs of all forms of energy system.

Emissions are the important criteria under which environmental feasibility of an energy system can be assessed. For emissions calculation HOMER takes six pollutants CO_2, CO, unburned hydrocarbon (UHC), particulate matter (PM), SO_2 and NO_X into account and tabulates their annual emissions per kilogram of fuel input. In this case the quantity of emissions among the studied configurations was evaluated and compared to justify environmental performance.

3. Results and discussions

To perform feasibility and economic analysis, first HOMER simulation was conducted for a standalone household in the Southern area of Norway by using a mono energy system comprising of diesel or, natural gas resource. Then hybrid system comprising with various combinations of energy components were used to perform another set of simulation from which an optimum solution comprising only of renewable options was identified. The results from the both case was compared and finally the sensitivity analysis in regard to the variable fuel cost was performed. The forthcoming sub-sections discuss the various aspects of these results in perspective of energy, economics and environment.

3.1. Mono-energy system

An optimized mono-energy system obtained from the simulation of HOMER consisted of diesel or, natural gas generator of 2.5 kW, two batteries of 2.16 kW h and one capacitor of 1 kW capacities respectively.

The economic viability of the energy plant is sensitive to the fuel cost and based on current diesel and natural gas price of 0.8 $/L and 0.6 $/m^3, the optimized solutions of the two plants are presented in Table 8. As observed, initial investment of both the plants was found similar as the similar generator cost data was used for simulation. In-terms of NPC and LCOE on the other hand, natural gas system was found economically more suitable than diesel generator system although both the plants were able to produce same amount of electricity throughout the year. In regard to the emissions, expectedly, NG system produced less amount of CO_2 than DG system. However, corresponding to the other pollutants (CO, UHC, PM, SO_2 and NO_X) the emissions from the NG system was found little higher than that of DG. This difference in emission properties was likely to be caused due to the difference in fuel properties, type of conversion generator and consumption of fuel. NG used for modeling was assumed to have lower percentage content of carbon than that of diesel which possibly was the reason

Please cite this article in press as: S. Sarker, Feasibility analysis of a renewable hybrid energy system with producer gas generator fulfilling remote household electricity demand in Southern Norway, Renewable Energy (2015), http://dx.doi.org/10.1016/j.renene.2015.11.013

Table 8
Optimized mono-energy system for the diesel price of 0.8 $/L and natural gas price of 0.6 $/m.[3].

Generator (kW)	Battery	Converter (kW)	Initial capital ($)	Operating cost ($/yr)	Total NPC ($)	COE ($/kWh)	Renewable fraction	Diesel (L)	Natural gas (m^3)	Operation (hrs)	Emissions (CO_2), kWh/y
2.5	2	1	1971	7967	101,254	0.408	0	8592	–	8760	22,626
2.5	2	1	1971	7097	90,420	0.365	0	–	10,007	8760	19,302

why completely burned pollutant (i.e., CO_2) from this fuel was found less than the unburned pollutants than those of diesel.

In addition to find an optimum solution based on fixed fuel price, the sensitivity of the plant was determined for the diesel price between the range 0.1 $/L and 1 $/L and natural gas price between the range 0.1 $/$m^3$ and 1 $/$m^3$ respectively. As the Fig. 8 shows, LCOE varied almost linearly with the price of the diesel. The LCOE value ranged between 0.106 $/kWh and 0.495 $/kWh and the NPC ranged between $26,300 and $122,669, as the fuel price increased from 0.1 $/L to 1 $/L. Both LCOE and NPC reaches to breakeven corresponding to the unit fuel cost of ca ~0.52 $/L beyond which LCOE increases faster than NPC. Likewise diesel system, LCOE for NG system also showed linear relationship with the cost of fuel. The LCOE and NPC for this configuration ranged between 0.113 $/kWh and 0.566 $/kWh, and $28,063 and $140,312 which compared to diesel operating system is a bit higher. Since the simulation and sensitivity analysis condition for both the systems were kept identical, the difference in LCOE and NPC was likely to be caused due to the difference in the generator efficiencies. The efficiency of the diesel and NG generator as per HOMER simulation was found as 20.4% and 23.8% respectively.

3.2. Hybrid energy system

3.2.1. Optimum solutions

With the given parameters and assumptions based on the average solar radiation of 2.84 kW h/m^2/day, wind speed of 6.445 m/s, primary load of 54 kW h/d, natural gas, wood gas and diesel price of 0.6 $/$m^3$, 0.1 $/$m^3$ and 0.8 $/L respectively, eight power plant configurations were simulated the categorical optimized solution of which is tabulated in Table 9 and the variation in LCOE vs. NPC is depicted in Fig. 9.

As observed, based on NPC, Bio/PV/Diesel is the least suitable solution while Bio/PV/Wind is the most economic. In total three renewable hybrid energy plants were identified and among the renewable/fossil hybrid configurations, contribution of renewable energy varied from 11% to 78% with the highest for Bio/NG/Wind and lowest for PV/NG respectively. The LCOE varied between 0.106 and 2.526 with the lowest for diesel and highest for the case of Bio/PV. Since the present standalone house is expected to be self-sufficient by utilizing all the available power from the producer gas generator and the rest from the other renewable sources, the forthcoming discussion only considers the hybrid energy systems comprised solely of the renewable sources.

As already mentioned, among the renewable energy options three optimized hybrid plants were identified namely Bio/PV/wind, Bio/PV and Bio/wind where the hybrid plant Bio/wind/PV/battery/capacitor system with 1 kW of PV arrays (5.1% PV penetration), one wind turbine of 1 kW (14.5% wind penetration), 4 unit batteries each of 2.16 kW h each, and 1 kW sized power converter was appeared to be optimum for the household. Compare to Bio/PV and Bio/Wind the optimum configuration contributed to reduce the NPC of about 10% and 8% respectively with a similar impact for LCOE. This system was also found to have an initial capital cost of $ 4,207, an annual operating cost of $ 5459/year, a total NPC of $ 72,232 and a LCOE of 0.306 $/kWh. The monthly average electric production from the optimized hybrid wind/PV/battery power system is depicted by Fig. 10. It can be observed that the wood gas generator serves most of the electricity demand followed by the wind turbine and the PV array. This implies that the wood gas generator satisfies the base load. The contribution from other small capacity units such as battery storage however did not reflect to Fig. 10 [22]. In general, the monthly average electricity production matches with the monthly load with higher production between

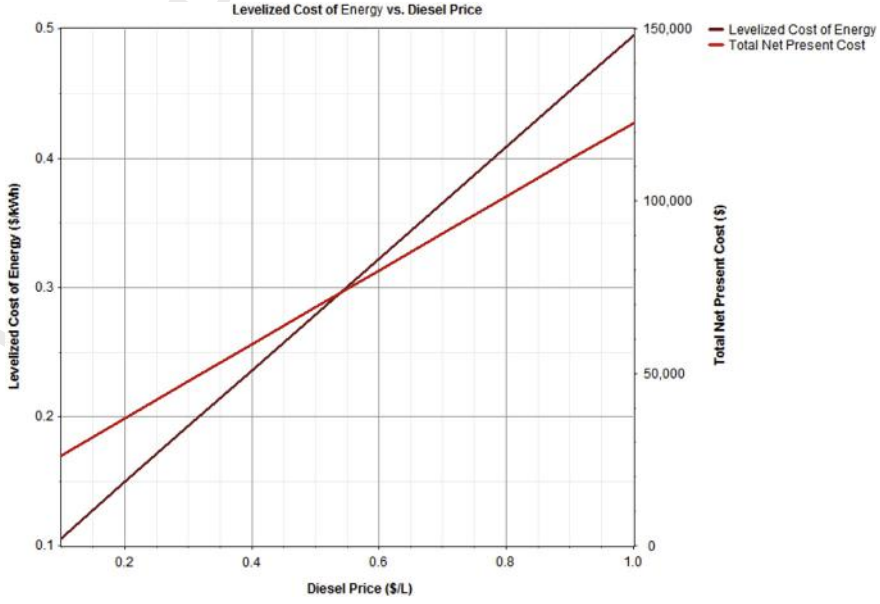

Fig. 8. Effect of diesel price on NPC and LCOE.

Please cite this article in press as: S. Sarker, Feasibility analysis of a renewable hybrid energy system with producer gas generator fulfilling remote household electricity demand in Southern Norway, Renewable Energy (2015), http://dx.doi.org/10.1016/j.renene.2015.11.013

Table 9
Optimized hybrid energy system for the diesel price of 0.8 $/L, natural gas price of 0.6 $/m^3 and wood gas price of 0.1 $/m^3.

PV (kW)	Wind turbine (kW)	Generator (kW)			Battery (Unit)	Converter (kW)	Initial capital ($)	Operating cost ($/yr)	Total NPC ($)	COE ($/kWh)	Ren. fraction	Diesel (L)	Natural gas (m^3)	Wood gas (m^3)	Operation (hrs) G1/G2	Emissions (CO_2), kg/yr
		Wood gas	Natural gas	Diesel												
1	1	2			1	1	4207	5459	72,232	0.306	1.00			45,142	8760	26,894
	3	2			4	3	5957	5777	77,949	0.332	1.00			45,974	8345	27,390
2.5		2			3	1	6432	5870	79,589	0.341	1.00			47,758	8760	28,453
1		2		1	2	1	3636	6385	83,210	0.336	0.74	1726		39,915	8760/5230	28,325
2.5			2			1	6425	5739	77,947	0.334	0.11		7004		8760	13,509
1		2	1		1	1	3636	5905	77,230	0.312	0.73		2199	39,190	8760/5315	27,589
	1		2.5		1	1	2671	5754	74,382	0.300	0.13		7862		8760	15,164
	1	2	1		1	1	2886	5795	75,101	0.303	0.78		1810	37,408	8589/4381	25,778

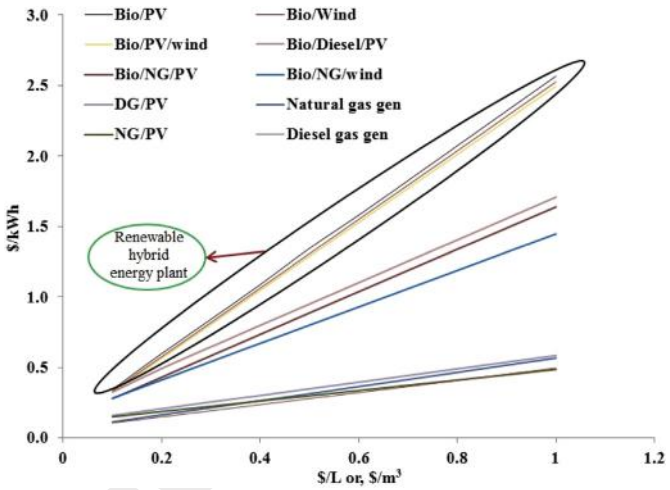

Fig. 9. Variation in levelized cost of energy as an effect of fuel price.

September and March (Fig. 10). The total annual electricity generation from the optimized system is 19,866 kWh/yr. in which 15,628 kW h/year (~79%) was contributed from the producer gas generator, 2886 kW h/yr. (~15%) comes from the wind turbine while the rest (1366 kW h/year) was met by the PV arrays respectively. The optimized system produced an unmet electric load of 6 kW h/year (~0%) and excess electricity, which is the surplus electricity, of ~48 kW h/year (0.2%). Typically, the excess electricity produced by the hybrid system is always expected, which can further be reutilized as heating or cooling load for the household [23].

3.2.2. Economic and emission analysis

The cash flow summary of the various equipment in the hybrid Bio/PV/wind/battery power system, including the power converters with the breakup of capital, replacement, O &M, fuel, and salvage costs is illustrated by Fig. 11. As found, the majority of the total NPC is incurred for the producer gas generator and the least of the NPC is resulted for the power converters.

The capital cost of the suggested hybrid power system (54 kW h/day of primary load, 2.84 kW h/m^2/day of global solar radiation, 6.445 m/s of wind speed, 1 kW of PV capacity, one 1 kW of wind turbine, 1 unit of battery and 1 kW of power converter capacity) is worth $ 72,232 with a replacement cost of $ 7093 and O&M cost of $ 5145 respectively.

The cost of the optimum system was further analyzed in regard to the variation in the size of some energy components such as the variation in the amount of batteries and capacitors. Fig. 12 shows the NPC and LCOE values against the number of batteries and capacitors in the optimal hybrid Bio/PV/wind/battery system. It can be seen that the NPC values of the system increase from $ 72,000 to $ 80,000 with an increase in number of batteries with the lowest and highest for 1 and 5 unit batteries respectively. The LCOE values followed the similar trend that of NPC and noticeably these values increase from 0.306 $/kWh to 0.326 $/kWh with the increase in the number of batteries. The lowest and highest LCOE values are found corresponding to the battery units of 1 and 5 respectively. Likewise variation in the number of batteries, Fig. 12 shows the NPC and LCOE values against the number of power converters in the optimal system. As observed, the NPC and LCOE values of the system increase with the increasing number of converters. The NPC values range between $ 72,232 and $ 75,886, while the LCOE values range between $ 0.306 and $ 0.321 corresponding to the converter amounts varying from 1 to 5 units respectively. The economics of

Please cite this article in press as: S. Sarker, Feasibility analysis of a renewable hybrid energy system with producer gas generator fulfilling remote household electricity demand in Southern Norway, Renewable Energy (2015), http://dx.doi.org/10.1016/j.renene.2015.11.013

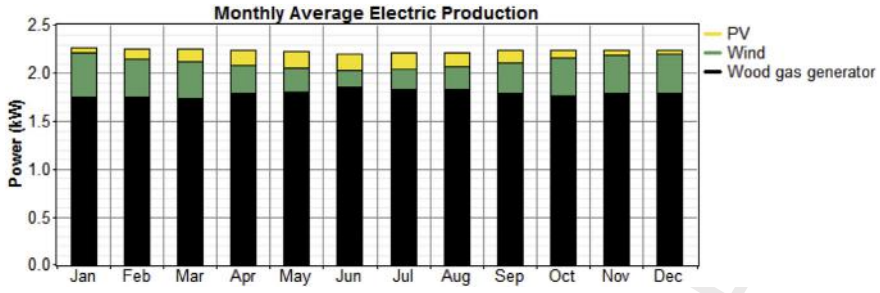

Fig. 10. Monthly average electricity production from the optimum hybrid plant.

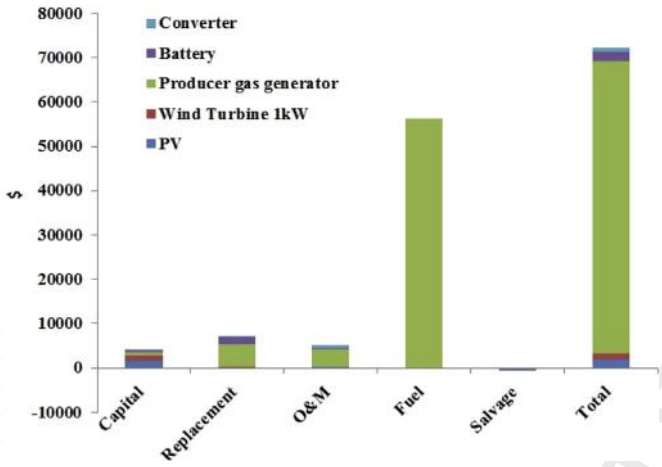

Fig. 11. Summary of component specific cash flow in hybrid system.

optimum hybrid system configurations is clearly sensitive to the variation in the size of the power plant components, particularly, in terms of the numbers of batteries or, converters.

From the emission analysis it can be seen that the total CO_2 emissions resulted at 26,894 kg/yr. which corresponding to that of the diesel only plant was somewhat higher (Table 8). However, it is to be noted that the CO_2 emission from the hybrid energy plant since resulted from the biomass fueled generator will not contribute to the net GHG emissions, as biomass is renewable. A study by Ref. [24] mentioned that the biomass energy crops can potentially fix 5992 kg/ha of annual CO_2 emission, if used for energy conversion.

3.2.3. *Sensitivity analysis*

In the present HOMER simulation, the effect of different fuel cost such as diesel, natural gas and wood gas are used as sensitivity variables.

Since the optimum renewable energy solution was not comprised of the option of diesel or, natural gas generator, the effect of diesel and natural cost will not be discussed. Fig. 13 shows the NPC and LCOE values of the optimized configuration as against the variable wood gas price ranged between 0.1 \$/m^3 and 1 \$/m^3. Clearly, the higher the wood gas price, the higher the NPC and LCOE values. The NPC of the optimized plant varied between the range of \$72,232 and \$ 577,378 while LCOE ranged between 0.306 \$/kWh and 2.444 \$/kWh. Noticeably, each 0.1 \$/m^3 increase in fuel price greatly affected the value of both NPC and LCOE. Overall, nine steps increase in wood gas price contributed to about eight times increase in both NPC and LCOE. It is thus important that the cost of producer gas keeps as low as possible so that the proposed hybrid plant stays competitive in comparison to the plants operating only with fossil or, with the combination of fossils and renewables.

4. Conclusions

This study examined the techno-economic viability of using producer gas generator (2 kWe) in a hybrid energy system for a distributed power generation suitable for a single household in Norway. Assuming the average solar radiation and wind data from NASA [18] and the cost of equipment based on the standard literature values, the HOMER modeling revealed eight economically feasible hybrid configurations, out of which three were completely renewables. From the renewable hybrid configurations, hybrid plant consisting of Bio/PV/wind/battery/capacitor with annual daily average global solar radiation of as 2.84 kW h/m^2/day and annual average wind speed of 6.445 m/s was found optimum. The total annual electricity produced by the optimum hybrid system resulted to 19866 kW h/yr. with NPC and LCOE as \$ 72,232 and 0.306 \$/kWh respectively. Comparing to the mono diesel or, natural gas configuration, the hybrid system was in generally not found cost effective. However, the net emissions savings worth 22,626 kg/yr. was potentially achieved while fossil fuel sources was replaced with producer gas generator and other renewable sources.

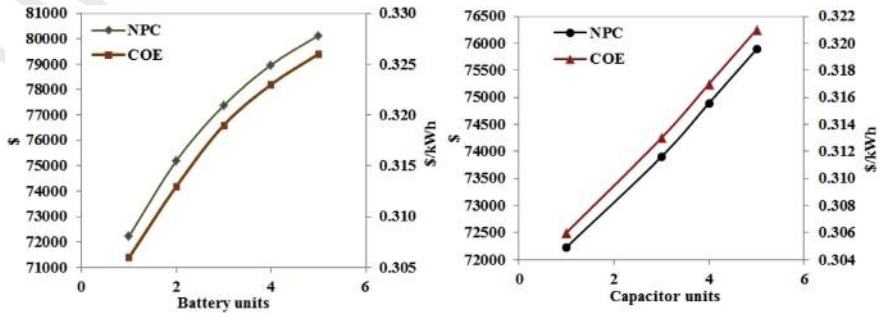

Fig. 12. Effect of the battery and capacitor units on NPC and LCOE of hybrid system.

Please cite this article in press as: S. Sarker, Feasibility analysis of a renewable hybrid energy system with producer gas generator fulfilling remote household electricity demand in Southern Norway, Renewable Energy (2015), http://dx.doi.org/10.1016/j.renene.2015.11.013

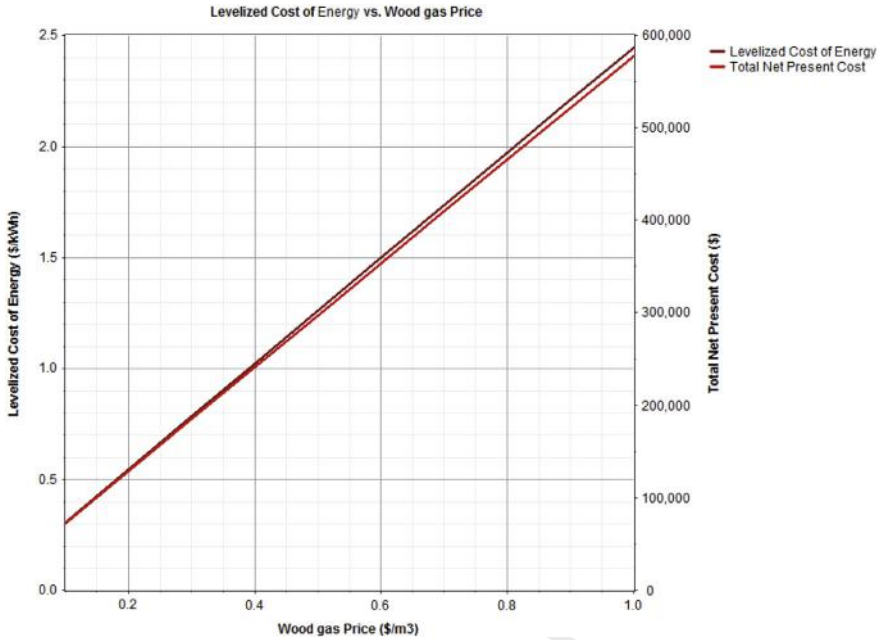

Fig. 13. Effect of wood gas price on NPC and LCOE of hybrid system.

The sensitivity analysis as an effect of change in diesel/NG/producer gas price showed that hybrid energy configuration Bio/PV/wind can appear as economically feasible solution compare to diesel only/NG only when producer gas price does not exceed the limit of 0.1 $/m^3. With the global tension over fossil fuel sources and the ever vacillating gasoline price, the arrival of expensive fossil fuel scenario is more than likely in the coming years when renewable hybrid energy configuration is expected to be an instrumental option in ensuring energy security and reliability.

Acknowledgments

The author wishes to thank University of Agder, Norway for providing grants & facilities to conduct this work.

References

[1] D.A. Hagos, A. Gebremedhin, B. Zethraeus, Towards a flexible energy system – a case study for Inland Norway, Appl. Energy 130 (2014) 41–50.
[2] M. Odenberger, T. Unger, F. Johnsson, Pathways for the North European electricity supply, Energy Policy 37 (2009) 1660–1677.
[3] S.G. Bekken, K. Schöffel, S. Aakenes, T. Hatlen, Å. Slagtern, L.E. Øi, The CLIMIT program and its strategy for Norwegian research, development and demonstration of CCS technology, Energy Procedia 37 (2013) 6508–6519.
[4] A. Imenes, G. Yordanov, O. Midtgård, T. Saetre, Development of a test station for accurate in situ IV curve measurements of photovoltaic modules in Southern Norway, in: Photovoltaic Specialists Conference (PVSC), 2011 37th IEEE, IEEE, 2011, pp. 003153–003158.
[5] R.M. Bright, A.H. Strømman, T.R. Hawkins, Environmental assessment of wood-based biofuel production and consumption scenarios in Norway, J. Industrial Ecol. 14 (2010) 422–439.
[6] I. Barstad, S. Grønås, Southwesterly flows over Southern Norway – mesoscale sensitivity to large-scale wind direction and speed, Tellus A 57 (2005) 136–152.
[7] H. Åm, The sun also rises in Norway: Solar scientists as transition actors, Environ. Innovation Soc. Transitions (2015), http://dx.doi.org/10.1016/j.eist.2015.01.002.
[8] M.S. Adaramola, M. Agelin-Chaab, S.S. Paul, Analysis of hybrid energy systems for application in southern Ghana, Energy Convers. Manag. 88 (2014) 284–295.
[9] L.C. Pagnini, M. Burlando, M.P. Repetto, Experimental power curve of small-size wind turbines in turbulent urban environment, Appl. Energy 154 (2015) 112–121.
[10] E. Hurtado, E. Peñalvo-López, Á. Pérez-Navarro, C. Vargas, D. Alfonso, Optimization of a hybrid renewable system for high feasibility application in non-connected zones, Appl. Energy 155 (2015) 308–314.
[11] C. Wang, M.H. Nehrir, Power management of a stand-alone wind/photovoltaic/fuel cell energy system, Energy Convers. IEEE Trans. 23 (2008) 957–967.
[12] G.J. Dalton, D.A. Lockington, T.E. Baldock, Feasibility analysis of stand-alone renewable energy supply options for a large hotel, Renew. Energy 33 (2008) 1475–1490.
[13] S. Ashok, Optimised model for community-based hybrid energy system, Renew. Energy 32 (2007) 1155–1164.
[14] E.U. Khan, A.R. Martin, Hybrid renewable energy with membrane distillation polygeneration for rural households in Bangladesh: Pani Para Village case study, in: Renewable Energy Research and Application (ICRERA), 2014 International Conference on. IEEE, 2014, pp. 365–368.
[15] Andrei Z. Morch, Nicolai Feilberg, Hanne Sæle, Karen Byskov Lindberg, Method for development and segmentation of load profiles for different final customers and appliances, in: Eceee Summer Study Proceedings. ECEEE, Belambra Les Criques, France, 1–6 June, 2013, pp. 1927–1933.
[16] S. Norway. Statistik sentralbyrå. 2015 ed. https://www.ssb.no (Last accessed: 19.07.15.).
[17] T.W. Jones, J.D. Smith, An historical perspective of net present value and equivalent annual cost, Account. Hist. J. (1982) 103–110.
[18] NASA. Surface Meteorology and Solar Energy. https://eosweb.larc.nasa.gov/cgi-bin/sse/grid.cgi (Last accessed 19.07.15.).
[19] C.M. Diesel. Triple fuel generator. http://www.centralmainediesel.com/order/03352.asp?page=3352 (Last accessed:19.07.15.).
[20] S.K. Nandi, H.R. Ghosh, Prospect of wind–PV-battery hybrid power system as an alternative to grid extension in Bangladesh, Energy 35 (2010) 3040–3047.
[21] M.A.M. Ramli, A. Hiendro, S. Twaha, Economic analysis of PV/diesel hybrid system with flywheel energy storage, Renew. Energy 78 (2015) 398–405.
[22] K.Y. Lau, M.F.M. Yousof, S.N.M. Arshad, M. Anwari, A.H.M. Yatim, Performance analysis of hybrid photovoltaic/diesel energy system under Malaysian conditions, Energy 35 (2010) 3245–3255.
[23] M. Beccali, S. Brunone, M. Cellura, V. Franzitta, Energy, economic and environmental analysis on RET-hydrogen systems in residential buildings, Renew. Energy 33 (2008) 366–382.
[24] M. Carvajal, Investigation into CO_2 absorption of the most representative agricultural crops of the region of murcia, in: CSIC (Consejo Superior de Investigaciones Cientificas), Madrid, Spain, 2010. http://www.lessco2.es/pdfs/noticias/ponencia_cisc_ingles.pdf (Last accessed: 19.07.15.).

Please cite this article in press as: S. Sarker, Feasibility analysis of a renewable hybrid energy system with producer gas generator fulfilling remote household electricity demand in Southern Norway, Renewable Energy (2015), http://dx.doi.org/10.1016/j.renene.2015.11.013